Mechanisms of molecular switching in the Wnt signal transduction pathway

Joshua E. Flack

Emmanuel College, University of Cambridge

This dissertation is submitted for the degree of Doctor of Philosophy

July 2018

Supervisor: Dr. Mariann Bienz

MRC Laboratory of Molecular Biology

Mechanisms of molecular switching in the Wnt signal transduction pathway

Joshua E. Flack

Summary

Wnt signalling is a critical cellular communication pathway controlling cell fate in all metazoan organisms. Timely activation of this pathway is crucial to coordinate development, control homeostasis of adult tissues, and to avoid cancer.

Wnt signal transduction depends primarily on the activities of three multiprotein complexes; the 'degradasome', which targets the central effector β-catenin for degradation in the absence of Wnt; the 'signalosome', which is assembled by Dishevelled upon Wnt-receptor binding to inactivate the degradasome, thus allowing β-catenin to accumulate; and the 'enhanceosome', which captures β-catenin, granting it access to target genes and relieving their transcriptional repression by Gro/TLE. Many of the components of these complexes have now been identified, but details of their regulation, and in particular the mechanisms by which they are switched on and off, remain poorly understood.

The majority of this thesis is concerned with the mechanism by which β-catenin relieves the transcriptional repression imposed upon Wnt target genes, and thereby activates the Wnt 'transcriptional switch'. In Chapter 2, I present data showing that apposition of Gro/TLE and UBR5, a HECT E3 ubiquitin ligase, by β-catenin promotes Gro/TLE ubiquitylation, earmarking it for extraction by the VCP/p97 ATPase and ultimately leading to inactivation of its repressive function. In Chapter 3, I present the results of a different, ongoing study to identify the mechanism by which a cytoplasmic negative regulator, Naked, acts to interfere with the function of Dishevelled, promoting the switching of signalosomes and the termination of canonical Wnt signalling.

These findings advance our understanding of the mechanisms by which the Wnt signalling pathway is switched on and off, and suggest new targets for therapeutic intervention in Wnt-driven cancers.

Declaration

This dissertation is the result of my own work, and includes nothing which is the outcome of work done in collaboration except where specified in the text. In addition, I declare that it is not substantially the same as any that I have submitted, or, is being concurrently submitted for a degree or diploma or other qualification at the University of Cambridge or any other University or similar institution. It does not exceed the prescribed word limit.

Joshua E. Flack

11th July, 2018

Summary

Wnt signalling is a critical cellular communication pathway controlling cell fate in all metazoan organisms. Timely activation of this pathway is crucial to coordinate development, control homeostasis of adult tissues, and to avoid cancer.

Wnt signal transduction depends primarily on the activities of three multiprotein complexes; the 'degradasome', which targets the central effector β-catenin for degradation in the absence of Wnt; the 'signalosome', which is assembled by Dishevelled upon Wnt-receptor binding to inactivate the degradasome, thus allowing β-catenin to accumulate; and the 'enhanceosome', which captures β-catenin, granting it access to target genes and relieving their transcriptional repression by Gro/TLE. Many of the components of these complexes have now been identified, but details of their regulation, and in particular the mechanisms by which they are switched on and off, remain poorly understood.

The majority of this thesis is concerned with the mechanism by which β-catenin relieves the transcriptional repression imposed upon Wnt target genes, and thereby activates the Wnt 'transcriptional switch'. In Chapter 2, I present data showing that apposition of Gro/TLE and UBR5, a HECT E3 ubiquitin ligase, by β-catenin promotes Gro/TLE ubiquitylation, earmarking it for extraction by the VCP/p97 ATPase and ultimately leading to inactivation of its repressive function. In Chapter 3, I present the results of a different, ongoing study to identify the mechanism by which a cytoplasmic negative regulator, Naked, acts to interfere with the function of Dishevelled, promoting the switching of signalosomes and the termination of canonical Wnt signalling.

These findings advance our understanding of the mechanisms by which the Wnt signalling pathway is switched on and off, and suggest new targets for therapeutic intervention in Wnt-driven cancers.

Acknowledgements

My three and half years as a PhD student at the LMB have been filled with so many highlights that it will always be a time I look back on extremely fondly. An enormous part of this has been down to the supervision of Mariann Bienz. Having first taken me on as a wide-eyed second year undergraduate, my development as a scientist owes much to her supportive, relaxed style of supervision. She encouraged me to work hard on projects that interested me, whilst always allowing time for adventures (scientifically or in life!) on the side.

I would also like to mention all of the other past and present members of the Bienz Lab, who always created a fun environment for science during my time in the lab: Gonzalo Beitia, Marc Fiedler, Melissa Gammons, Lisa Heinke, Janic le Pen, Ben Moore, Miha Renko, Moore van Tienen and Trevor Rutherford. I would especially like to thank Nikola Novčić and Juliusz Mieszczanek, whose efforts provided much of the insight detailed in Chapter 2 of this thesis. I would also like to extend my gratitude to everyone else at the LMB who helped me with experiments, reagents or discussions throughout my time as a student, particularly my examiners, David Barford and Barry Thompson.

I would like to thank my family and friends for their continued support throughout my studies. Sailing with past and present members of the Cambridge University Sailing Team has probably caused me more stress than any of my experiments, providing a hugely welcome distraction from the lab. My parents have always been there to offer home comforts and an escape from the student lifestyle, and tried their hardest to follow along with tales of Wnt and ubiquitin. My housemates, Laurence and Arden, were a delight to live with, despite my wacky sleep schedule and fondness for washing up. Finally my girlfriend, Tebbs, for putting up with me – you're a legend.

Table of Contents

List of Figures

Chapter 3: Wnt signalosome switching by Naked

Abbreviations

ABC	active β-catenin
ADP	adenosine diphosphate
APC	adenomatous polyposis coli
ARD	armadillo repeat domain
ATP	adenosine triphosphate
BCL9	B-cell CLL/lymphoma 9 protein
B9L	BCL9-like protein
BioID	identification of proteins by biotin proximity labelling
BioIP	immunoprecipiation of proteins by biotin proximity labelling
BirA*	biotin ligase (R118G mutant)
BMP	bone morphogenetic protein
β-TrCP	β-transducin repeat containing protein
ChiLS	Chip/LDB1-SSDP
ChIP	chromatin immunoprecipitation
CHX	cycloheximide
CID	(β-)catenin inhibitory domain
CK1	casein kinase 1
coIP	co-immunoprecipiation
COS-7	CV-1 in origin, SV40 cell line 7
CRD	cysteine-rich domain
CRISPR	clustered regularly interspersed short palindromic repeats
CYLD	cylindromatosis protein
DAPI	4'-6-diamidino-2-phenylindole
DEP	(domain of) Dishevelled/Egl-10/Pleckstrin
DIX	(domain of) Dishevelled/Axin
DMEM	Dulbecco's modified eagle medium
DMSO	dimethyl sulfoxide
DUB	deubiquitylase
Dsh	Dishevelled (fly)
Dvl	Dishevelled (mammalian)
EDD1	E3 identified by differential display 1
EDTA	ethylenediaminetetraacetic acid
EMT	epithelial to mesenchymal transition
FAP	familial adenomatous polyposis
FBS	foetal bovine serum
FBXW7	F-box/WD repeat-containing protein 7

Fz	Frizzled
GFP	green fluorescent protein
GPCR	G-protein coupled receptor
Gro	Groucho
GSK	glycogen synthase kinase
HA	haemagglutinin
HDAC	histone deacetylase
HECT	homologous to E6-AP C terminus
HECTD1	HECT E3 ubiquitin protein ligase D1
HEK293(T)	human embryonic kidney cell line 293 (T antigen)
HES1	hairy and enhancer-of-split 1
HRD	histidine-rich domain
HUWE1	HECT, UBA and WWE domain-containing protein 1
HMW	high molecular weight
Hyd	Hyperplastic discs
IP	immunoprecipitation
kDa	kilodalton
KO	knock-out
LC-MS/MS	liquid chromatography tandem mass spectrometry
LDB1	LIM-domain binding protein 1
LDS	lithium dodecyl sulphate
LEF	lymphoid enhancer factor
LGR5	leucine-rich repeat-containing G-protein coupled receptor 5
LiCl	lithium chloride
LRP	low-density lipoprotein receptor-related protein
Luc	luciferase
MBP	maltose-binding protein
MLLE	MLLE motif containing (domain)
MMTV	mouse mammary tumour virus
N4BP1	NEDD4-binding protein 1
NBR1	next to BRCA1 protein 1
NEDD4	neuronal precursor cell-expressed developmentally downregulated 4
Nkd	Naked
NLS	nuclear localisation sequence
NMR	nuclear magnetic resonance
NPC	nuclear pore complex
PBS	phosphate-buffered saline
PCP	planar cell polarity
PDZ	domain in (PSD95, Discs-large 1, ZO-1)

PI3K	phosphoinositide 3-kinase
polyUb	polyubiquitin
p62/SQSTM1	protein of 62 kDa/sequestosome-1
RBR	RING-Between-RING
RFP	red fluorescent protein
RGS	regulator of G-protein signalling (domain)
RING	really interesting new gene
RNF43	RING finger protein 43
RT-qPCR	reverse-transcriptase quantitative polymerase chain reaction
SCF	Skp, Cullin, F-box containing
SEC-MALS	size exclusion chromatography multi-angle light scattering
SEM	standard error of the mean
Sens	Senseless
sgRNA	single guide RNA
SNP	single nucleotide polymorphism
SSDP	single stranded DNA-binding protein
SUMO	small ubiquitin-like modifier
TCF	T-cell factor
TGF-β	transforming growth factor β
TLE	transducin-like enhancer of split
TRIP12	thyroid hormone receptor interacting protein 12
VCP/p97	valosin-containing protein/protein of 97 kDa
Ub	ubiquitin
Ub-TLE	ubiquitylated TLE
UBA	ubiquitin-associated domain
UBD	ubiquitin-binding domain
UBE3C	ubiquitin-protein ligase E3C
UbiCRest	ubiquitin chain restriction analysis
UBR5	UBR domain containing E3 ubiquitin-protein ligase 5
UPS	ubiquitin-proteasome system
Vg	Vestigial
WD40	tryptophan-aspartate repeat containing (domain)
Wg	Wingless
Wnt/STOP	Wnt-dependent stabilisation of proteins
wt	wild-type
XIAP	X-linked inhibitor of apoptosis protein
ZNRF3	Zinc RING finger protein 3

1. Introduction

The development of a zygote into a multicellular organism with defined axes, polarity, form and function is an intricate process that is exquisitely dependent upon intercellular communication. The Wnt signalling cascade represents one of a small number of widespread and evolutionarily conserved signalling pathways that direct and control these developmental processes through the operation of transcriptional switches. These same pathways, which also include Notch, Hedgehog and BMP/TGF-β (bone morphogenetic protein/transforming growth factor-β), are later deployed to specify stem and progenitor cell populations necessary for homeostasis in adult tissues. Mutations in components of these pathways are therefore, perhaps unsurprisingly, often causative to growth-related pathologies and cancer.

Compared to other signalling molecules, a unique aspect of Wnt is its ability to act as a directional growth factor, shaping a growing tissue whilst inducing cells to proliferate and divide (Nusse & Clevers, 2017). These signals can thus direct new cells to be allocated such that intricately organised structures are formed (Goldstein *et al*., 2006). The Wnt pathway was first identified in *Drosophila* when a mutagenesis screen yielded a mutant lacking wings, named *wingless* for its striking phenotype (Sharma, 1973). Seminal work in Heidelberg subsequently demonstrated that *wingless* was in fact one of a number of segment polarity genes crucial for patterning the developing embryo (Nüsslein-Volhard & Wieschaus, 1980), in the process identifying several mutations that were later traced to other components of the Wnt pathway (Siegfried *et al*., 1992; Siegfried *et al*., 1994). The pathway was discovered independently in mammals, when work in mice identified a proto-oncogene (termed integration 1 or *Int-1*) whose activation was responsible for the characteristic tumours induced by pro-viral insertion of the mouse mammary tumour virus (MMTV; Nusse & Varmus, 1982). The name ‘Wnt’ was derived as a portmanteau of ‘wingless’ and ‘Int-1’ when the two genes were subsequently shown to encode orthologous secreted proteins (Rijsewijk *et al*., 1987).

Much of the early work focused on understanding Wnt signalling in developmental contexts. A role for Wnt in vertebrate development was first demonstrated with the finding that injection of *Int1* mRNA causes axis duplication in *Xenopus* embryos (McMahon & Moon, 1989). However, it was not until the 1990s that a connection was made between the Wnt pathway and human disease. Mutations in the adenomatous polyposis coli (*APC*) gene were identified in patients with a hereditary colon cancer syndrome termed familial adenomatous polyposis (FAP; Groden *et al*., 1991; Kinzler *et al*., 1991; Nishisho *et al*., 1991). The APC protein was shown soon after to interact with β-catenin (Rubinfeld *et al*., 1993; Su *et al*., 1993), known as Armadillo in *Drosophila* (Peifer *et al*., 1992; Peifer, 1995) and now understood to be the central effector of the ‘canonical’ Wnt pathway.

Through a huge amount of meticulous study over the last three decades, the core components of this canonical Wnt signalling pathway have been identified, and the effects of pathway disruption studied in numerous systems. Despite this, many of the cellular mechanisms underlying signal transduction remain unclear, and certain details of these mechanisms constitute the focus of this thesis.

1.1. The canonical Wnt signalling pathway

Wnts are secreted, cysteine-rich proteins of approximately 40 kilodaltons (kDa), which fall into 13 conserved subfamilies (Loh *et al.*, 2016). All act by binding to receptors on the surface of nearby cells and initiating cytoplasmic signal transduction pathways. Most of this signalling occurs via the canonical pathway, in which β-catenin is the central effector. Different, though overlapping, suites of receptors, co-receptors (in particular) and cytoplasmic effectors permit the transduction of alternative, β-catenin-independent Wnt signals via two 'non-canonical' pathways: the planar cell polarity (PCP; Strutt, 2003; Peng & Axelrod, 2012) and Wnt/Ca^{2+} pathways (Kohn & Moon, 2005).

The canonical Wnt pathway (often termed Wnt/β-catenin signalling) is controlled by the opposing activities of three highly dynamic multiprotein complexes (**Fig. 1.1**). In the off state, β-catenin is constitutively phosphorylated and thereby earmarked for degradation by the 'destruction complex' or 'degradasome' (Stamos & Weis, 2013). The core degradasome contains two kinases, glycogen synthase kinase 3 (GSK3) and casein kinase 1α (CK1α), scaffolded by the key tumour suppressors Axin and APC.

Upon Wnt binding to Frizzled (Fz) and LRP5/6 (low-density lipoprotein receptor-related protein 5/6), the 'signalosome' complex is assembled upon the cytoplasmic domains of these receptors. The signalosome is assembled by the Fz-binding protein Dishevelled (Dvl; Bilic *et al.*, 2007), whose dynamic polymerization increases its avidity for Axin (Bienz, 2014). The whole degradasome is recruited, via Axin, to the membrane, where the intracellular tail of LRP5/6 becomes phosphorylated at specific residues and thus serves as a competitive inhibitor of GSK3 (Tamai *et al.*, 2004; Stamos *et al.*, 2013). Inactivation of GSK3 allows unphosphorylated β-catenin to accumulate and translocate into the nucleus (Peifer *et al.*, 1994).

Transcriptional activation requires binding of this stabilised β-catenin to TCF/LEF (T-cell factor/lymphoid enhancer factor) proteins that are tethered at enhancers of Wnt target genes. Access to these transcription factors is blocked by Gro/TLE (Groucho/transducin-like enhancer of split), a TCF-binding transcriptional co-repressor that acts through a combination of chromatin compaction and histone deacetylation (Sekiya & Zaret, 2007). Gro/TLE is the

key repressive component of the 'Wnt enhanceosome' complex (Fiedler *et al.*, 2015; van Tienen *et al.*, 2017), which earmarks repressed target genes for inducibility and, upon capture of β-catenin by BCL9 (B-cell CLL/lymphoma 9 protein), switches on their transcription.

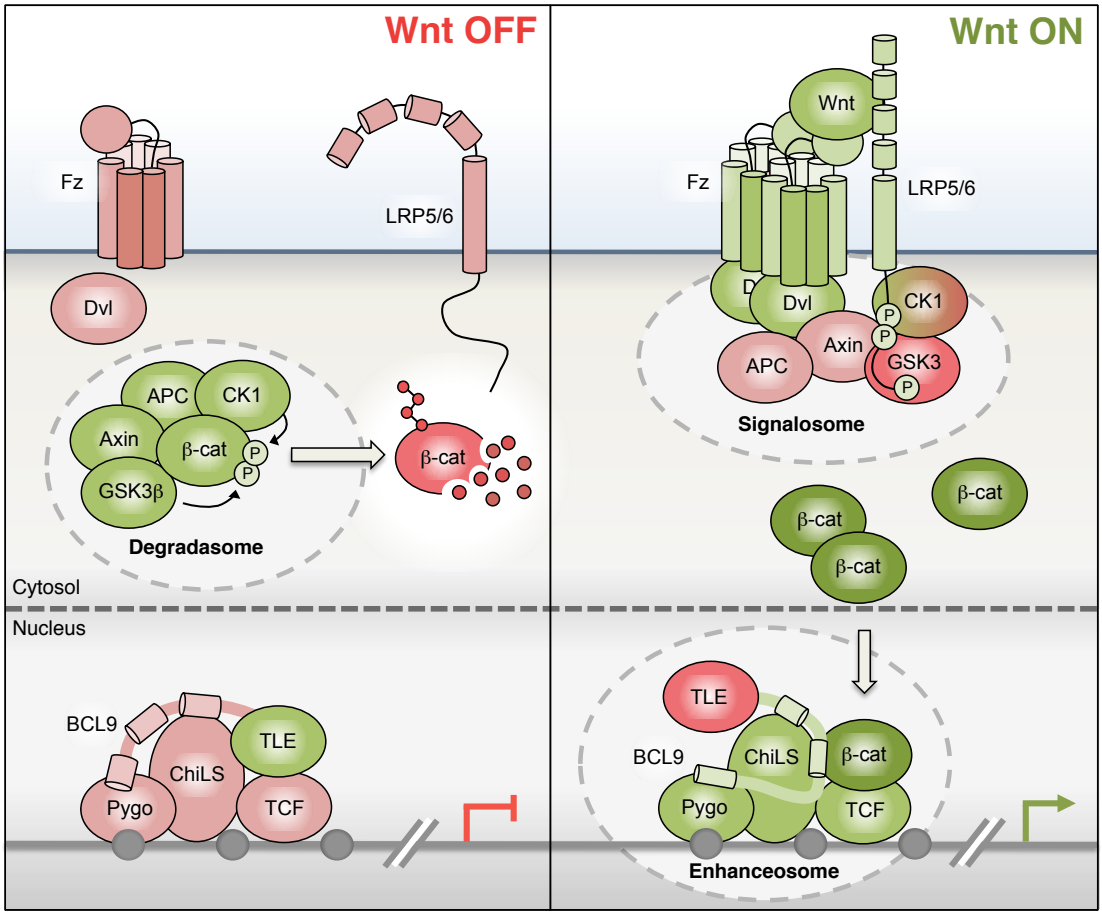

Figure 1.1 Overview of the canonical Wnt signalling pathway.
Three multiprotein complexes are primarily responsible for the transduction of Wnt signals. In the absence of Wnt (left), β-catenin is constitutively earmarked for degradation via phosphorylation by kinases of the degradasome. Wnt triggers assembly of signalosomes (right), inhibiting the degradasome and allowing β-catenin to accumulate and translocate into the nucleus, whereupon it is captured by the enhanceosome and triggers transcriptional activation. See text for more details. Active components are shown in green, inactive components in red. Adapted from Gammons & Bienz, 2017.

1.1.1. The degradasome

Although it is the central effector of Wnt signalling, most β-catenin is actually found in complex with E-cadherin and α-catenin in adherens junctions; stable structures formed at the contact points of cells that facilitate their close physical interaction (Peifer *et al.*, 1992). A distinct, more dynamic pool of β-catenin is responsible for transducing the Wnt signal through the cytosol. These pools operate independently, and indeed in some species, including *C. elegans*, these functions are carried out by distinct homologs (Korswagen *et al.*, 2000).

In the 'Wnt off' state, β-catenin is sequentially phosphorylated by the two constitutively active kinases of the degradasome at a series of N-terminal serine/threonine residues (**Fig. 1.2A**; Liu *et al.*, 2002). A 'priming' phosphorylation of Ser-45 by CK1α triggers subsequent modification of three residues by GSK3 (Amit *et al.*, 2002), which render N-terminal lysine residues of β-catenin substrates of the F-box containing E3 ubiquitin ligase β-TrCP (β-transducin repeat containing protein), targeting it for proteasomal degradation (Aberle *et al.*, 1997; Kitigawa *et al.*, 1999; Wu *et al.*, 2003).

The degradasome depends on a plethora of multivalent and partially redundant interactions between multiple components for its ordered assembly (**Fig. 1.2B**; Gammons & Bienz, 2017). The central and limiting component is Axin, which binds to β-catenin via a small central helix, as well as to APC, GSK3 and CK1α via separate domains (Hart *et al.*, 1998; Faux *et al.*, 2008), coordinating these components in a spatial fashion. Mutations that destabilise the N-terminal RGS (Regulator of G-protein signalling) domain, blocking the interaction with APC, exhibit dominant-negative activity, triggering formation of aberrant Axin aggregates that interfere with normal degradasome formation (Anvarian *et al.*, 2016). Axin can also undergo reversible head-to-tail homopolymerization via its C-terminal DIX (Dishevelled/Axin) domain to generate short filaments (Fiedler *et al.*, 2011), although Axin concentrations are usually maintained at a low level (preventing weak DIX-DIX interactions from occurring) by RNF146, a RING E3 ubiquitin ligase that targets it for proteasomal degradation (Lee *et al.*, 2003; Zhang *et al.*, 2011). Indeed, Axin degradasomes (unlike Dvl signalosomes) only become visible as cytoplasmic puncta when tankyrase, a polyADP-ribosyltransferase that activates RNF146, is inhibited, leading to a large increase in Axin levels (DaRosa *et al.*, 2015; Huang *et al.*, 2009).

The other key protein involved in degradasome assembly is APC, which interacts directly with Axin through multiple conserved motifs (Spink *et al.*, 2000), but also indirectly, possibly through β-catenin (Pronobis *et al.*, 2015). Although it is clearly essential for degradasome function, the specific molecular functions of APC remain poorly understood. Like Axin, APC is able to self-associate (via mutual interaction between N-terminal regions), a feature required

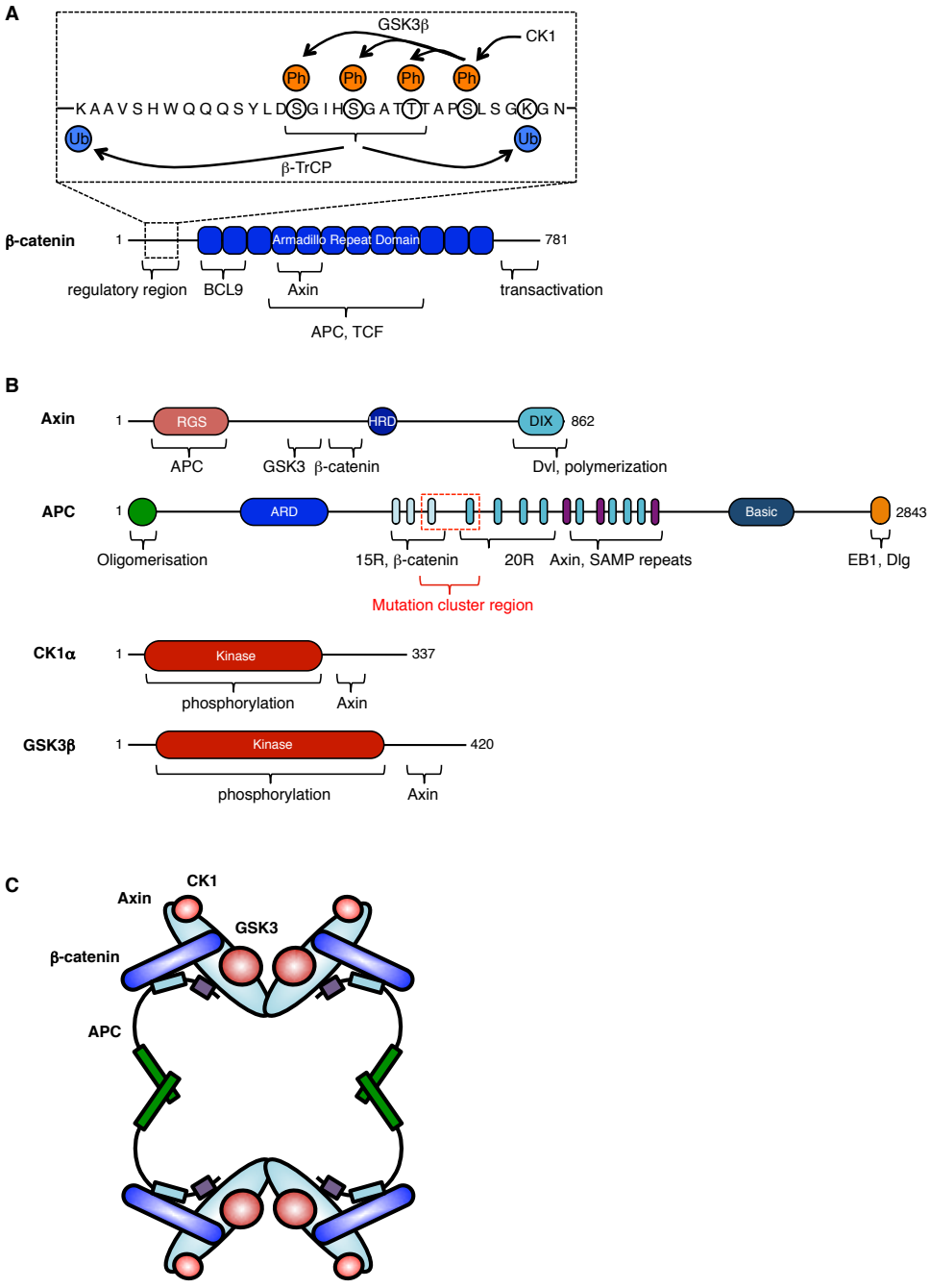

Figure 1.2 Structure and interactions of the degradasome.

(A) Domain architecture, interactions and regulation of β-catenin. Priming phosphorylation of Ser-45 by CK1 triggers sequential phosphorylation of Thr-41, Ser-37 and Ser-33, which subsequently promotes polyubiquitylation of Lys-19 and Lys-49 by β-TrCP.

(B) Domain architecture and key interactions of other core degradasome components.

(C) Proposed model for the degradasome. Multimerization of both Axin and APC contributes to the assembly of these multiprotein complexes. See text for more details. Adapted from Kunttas-Tatli *et al.*, 2014.

for degradasome assembly (**Fig. 1.2C**; Mendoza-Topaz *et al*., 2011; Kunttas-Tatli *et al*., 2014; Pronobis *et al*., 2017). APC may therefore facilitate Axin homopolymerization by increasing its local concentration to levels permissive for DIX-DIX interaction, and/or could provide cross-links between Axin filaments, potentially providing an explanation for the three-dimensional structures of degradasomes that have been observed (Thorvaldsen *et al*., 2015). APC also interacts with the central region of β-catenin through two separate repeat regions termed 15R and 20R (Rubinfeld *et al*., 1993; Spink *et al*., 2001), in a fashion that is enhanced by GSK3- and CK1α-mediated phosphorylation of the third 20R repeat (Tickenbrock *et al*., 2003). A large majority of colorectal cancer-causing mutations in APC are truncations clustering around a small region termed the β-catenin inhibitory domain (CID), located between the second and third 20R repeats, demonstrating the importance of the APC/β-catenin interaction (Kohler *et al*., 2009). Why full deletions of APC are rarely observed in cancer is unclear, although retention of partial β-catenin binding seems to promote tumourigenesis (Albuquerque *et al*., 2002), or it may be related to a separate role of APC in cell adhesion (Bienz & Hamada, 2004).

In the absence of a Wnt signal, Axin and APC thus function to appose β-catenin with the kinases that earmark it for degradation, although the exact biochemical roles of these proteins remain somewhat elusive. Full understanding may require a complete *in vitro* reconstitution of a functional degradasome complex, and the determination of its structure, a goal that several labs are now working towards.

1.1.2. The signalosome

Wnt proteins are lipid modified during synthesis on a single serine residue by a palmitoyltransferase termed Porcupine (Willert *et al*., 2003; Rios-Esteves & Resh, 2013). This single lipid moiety is crucial for Wnt export (through binding to Wntless/Evi; Bartscherer *et al*., 2006) and receptor binding (Janda *et al*., 2012), but it also renders the protein hydrophobic. The lipid may therefore tether Wnt to cell membranes, restricting its spread, and activity, to cells that directly contact each other. Indeed, recent evidence suggests that the role of Wingless in *Drosophila* can be largely fulfilled by a membrane-tethered form of the protein that cannot diffuse (Alexandre *et al*., 2014), though it could still be transported over longer distances on vesicles or filopodia (Stanganello *et al*., 2015).

All Wnt proteins bind to heterodimeric receptor complexes, which in the canonical pathway consist of a Fz receptor and an LRP5/6 co-receptor (**Fig 1.3A**). Fz proteins, of which there are 10 in mammals, are the archetypal members of the Frizzled ('F') class of G-protein coupled receptors (GPCRs; Hanlon & Andrew, 2015), although the importance of Fz signalling via heterotrimeric G-proteins remains a point of contention (see for example Nichols *et al*., 2013).

All Fzs have a large N-terminal extracellular cysteine-rich domain (CRD; Bhanot *et al*., 1996) that constitutes the primary binding site for Wnt (Dann *et al*., 2001). A crystal structure of the complex shows that Wnt 'grasps' the CRD via two distinct binding interfaces, one of them involving the palmitoylate moiety of Wnt sitting in a hydrophobic groove of the CRD (Janda *et al*., 2012). Removal of the lipid by the Wnt antagonist Notum completely blocks signalling, highlighting the importance of this interaction (Kakugawa *et al*., 2015). There is extensive Wnt/Fz cross-reactivity, with a single Wnt able to bind multiple Fzs, and vice versa (Dijksterhuis *et al*., 2015). Furthermore, Wnts are not the only ligands of Fz receptors: the cysteine-knot protein Norrin (Xu *et al*., 2004) and, intriguingly, *Clostridium difficile* toxin B (TcdB) can also bind and signal via Fz (Tao *et al*., 2016).

During signalling, Fz cooperates with the single-transmembrane proteins LRP5/6 (known as Arrow in *Drosophila*; Wehrli *et al*., 2000), such that Wnt binding leads to coupling of the two receptors (**Fig 1.3B**; Janda *et al*., 2017). This mechanism leads to a conformational change in the receptors and triggers formation of Wnt 'signalosome' complexes on the cytoplasmic face of the active receptors, a process that is dependent on dynamic polymerization of Dvl via its DIX domain (Bilic *et al*., 2007; Schwarz-Romond *et al*., 2007a). This increases the avidity of Dvl for Axin, enabling it to recruit Axin (and with it, the degradasome) through mutual DIX interactions (Schwarz-Romond *et al*., 2007b; Fiedler *et al*., 2011). Dvl polymerisation also triggers phosphorylation of LRP5/6 by GSK3 (and subsequently CK1γ) on specific PPPSP motifs in the cytoplasmic tail (Bilic *et al*., 2007; Davidson *et al*., 2005), which become binding sites for Axin, reinforcing the interaction between the degradasome and the LRP5/6 tail (Tamai *et al*., 2004; Metcalfe *et al*., 2010). This proximity allows the phosphorylated motifs to bind the active site of GSK3 and competitively inhibit its catalytic activity, preventing phosphorylation of β-catenin (Stamos *et al*., 2014), although it has also been proposed that β-catenin ubiquitylation is the key step that is inhibited (Li *et al*., 2012). Alternative mechanisms for GSK3 inhibition have also been suggested, including the sequestration of GSK3 and LRP5/6 away from β-catenin in multivesicular bodies (Taelman *et al*., 2010), although the physiological relevance of this model is dubious (Metcalfe & Bienz, 2011). As well as the key stabilisation of β-catenin, GSK3 inhibition has a marked effect on other Wnt components, including Axin itself, which is rapidly dephosphorylated and subsequently degraded during signalling (Willert *et al*., 1999; Ji *et al*., 2017).

Whilst the role of LRP5/6 is now relatively well understood, the function of Fz in signal transduction is somewhat more obscure. The cytoplasmic face of Fz can bind directly to the Dvl DEP (Dishevelled/Egl-10/Pleckstrin) domain (Tauriello *et al*., 2012), potentially creating the high local concentration of Dvl molecules required for polymerization to occur. Intriguingly,

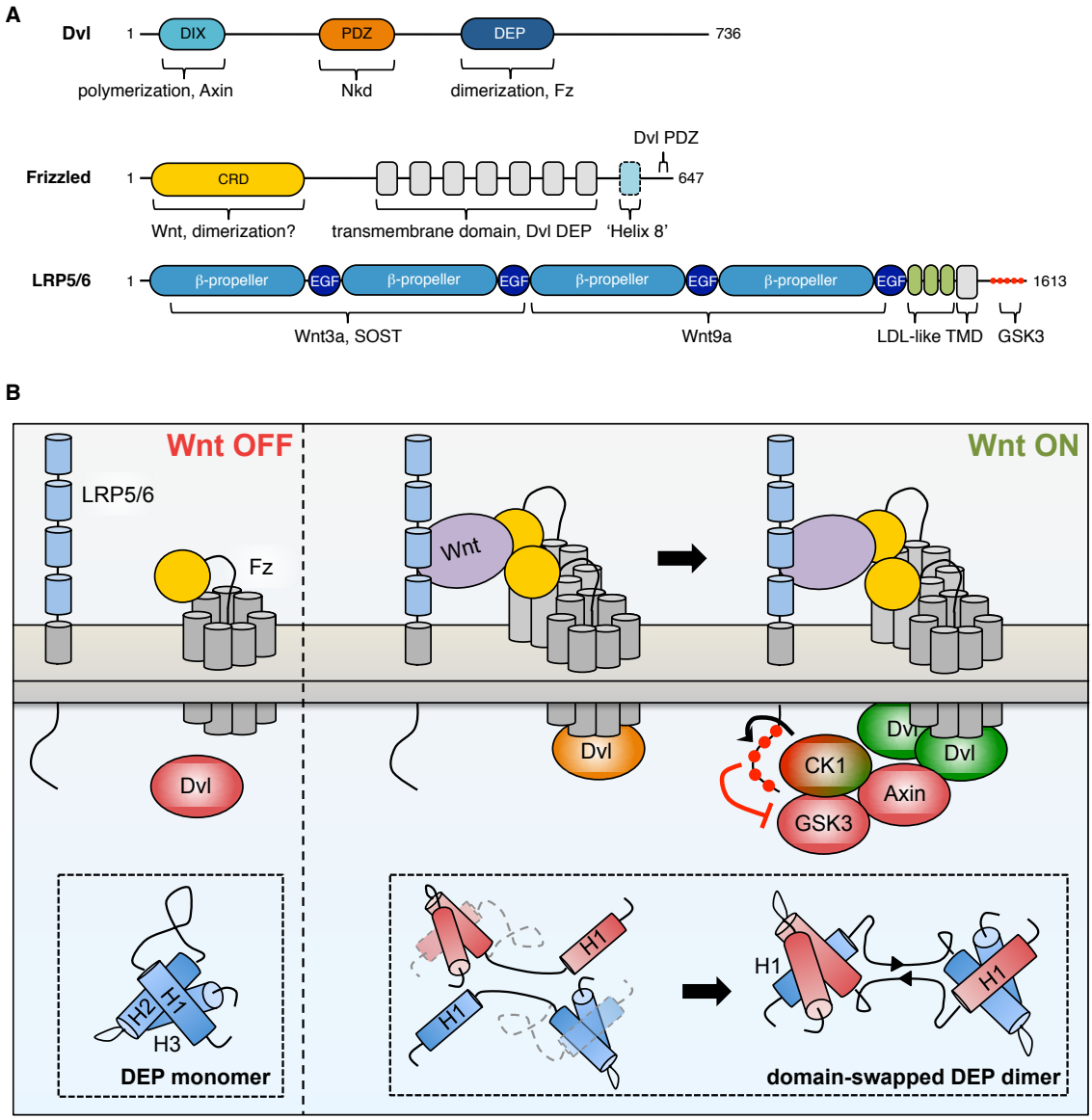

Figure 1.3 Mechanisms of signalosome formation.

(A) Domain architecture and key interactions of Dvl and Wnt receptors.

(B) Model for Wnt-triggered signalosome formation. Fz and LRP5/6 are coupled upon Wnt binding, creating a high local concentration of Dvl on the cytoplasmic faces of these receptors and triggering signalosome assembly through polymerization of the Dvl DIX domain. This also requires DEP domain-swap dimerization (see inset panels), and may be potentiated by multimerization of Fz. LRP6 becomes phosphorylated on five C-terminal residues (depicted as red dots), subsequently acting to competitively inhibit GSK3. See text for more details. Adapted from Gammons & Bienz, 2017.

as well as DIX-DIX interactions, dimerization of the DEP domain through 'swapping' of an N-terminal helix has recently been shown to be essential for Dvl polymerization (**Fig 1.3B;** Gammons *et al.*, 2016a). The role of Fz may thus be to bring together Dvl molecules together to sufficient levels to trigger DEP dimerization, catalyzing an initial rate-limiting step of signalosome formation that is thermodynamically unfavourable to reverse (Gammons & Bienz, 2017). Recent work has suggested several mechanisms by which Fz itself may be

clustered so as to further potentiate this effect: LRP5/6 is reportedly associated with clathrin-coated pits, potentially relocating Fz to these small membrane regions upon signalling (Hagemann *et al.*, 2014; Gammons *et al.*, 2016a). Alternatively, Fz multimerization could occur via binding of two CRDs to a single palmitoleic acid moiety on Wnt (Nile *et al.*, 2017; DeBruine *et al.*, 2017), or even directly through its transmembrane region (Petersen *et al.*, 2017).

Like the degradasome, Wnt signalosomes represent highly complex and dynamic protein assemblies, reflecting the molecular properties of the constituent proteins (Gammons & Bienz, 2017). Many details of signalosome assembly and, in particular, disassembly, are the subject of current research, and aspects of these processes constitute the subject of **Chapter 3** of this thesis.

1.1.3. The enhanceosome

The key condition for canonical Wnt signal transduction to be executed is that β-catenin is stabilised and enters the nucleus. The exact details of how β-catenin traverses the nuclear pore complex (NPC) are unclear, given that it lacks an obvious nuclear localisation sequence (NLS), and its transport appears to be independent of the small GTPase Ran (Fagotto *et al.*, 1998; Yokoya *et al.*, 1999), although the C-terminal armadillo repeat domain (ARD) of β-catenin structurally resemble the HEAT repeats of importin-β, and can mediate direct interaction with nucleoporins (Lee *et al.*, 2000; Sharma *et al.*, 2012). It is also possible that a binding partner of β-catenin (perhaps APC or BCL9) may chaperone it through the NPC, although this has not been conclusively demonstrated (Rosin-Arbesfeld *et al.*, 2000), and there is also evidence for a role of microtubular transport in some instances (Sugioka *et al.*, 2011). Fold change in β-catenin, rather than absolute concentration, is the critical determinant for transcription activation, implying that even low levels are sufficient for induction of target gene expression (Goentoro & Kirschner, 2009).

Once it is has entered the nucleus, β-catenin effects a context-dependent cellular response through the transcriptional activation of TCF-bound target genes. This process occurs within the context of a large multiprotein complex termed the 'Wnt enhanceosome' (**Fig 1.4**). This complex consists of a core 'ChiLS' module (made up of a dimer of Chip/LIM-domain binding protein 1 (LBD1) and a tetramer of SSDP (single stranded DNA-binding protein)), which binds to Pygo, BCL9 (or its homolog BCL9-like (B9L)) and Gro/TLE, which links the complex to TCF and represses target genes in the absence of β-catenin (Fiedler *et al.*, 2015; van Tienen *et al.*, 2017; Cavallo *et al.*, 1998). The enhanceosome can be tethered to DNA by lineage-determining proteins, such as homeodomain, bHLH (basic helix-loop-helix) and GATA-binding

transcription factors, serving to integrate Wnt signalling with other positional information (Bronstein & Segal, 2011).

TCF/LEF proteins are key transcription factors that employ sequence-specific DNA binding, as well as context-dependent interactions, to specify genes that are regulated by the Wnt pathway (Cadigan & Waterman, 2012). These factors are anchored on DNA via a highly conserved C-terminal HMG box (Giese *et al*., 1991), and bind directly to the central ARD of β-catenin with high affinity (Knapp *et al*., 2001). Known as dTCF/Pangolin in *Drosophila* (van de Wetering *et al*., 1997; Schweizer *et al*., 2003), there are four TCF orthologs in mammals, all of which are extensively regulated by alternative splicing (van de Wetering *et al*., 1996; Cadigan & Waterman, 2012). Although several non-TCF proteins have been described as alternative transcriptional effectors of Wnt signalling, recent genome-wide approaches in mammalian cells and *Drosophila* imply that all direct activation of β-catenin target genes involves TCF (Schuijers *et al*., 2014; Franz *et al*., 2017).

Two opposing models for the function of the essential proteins Pygo and BCL9/B9L have been proposed. The first of these suggests that these components are recruited to the enhanceosome by β-catenin only upon active Wnt signalling, during which Pygo serves to recruit transcriptional co-activator proteins via an NPF motif (Städeli & Basler, 2005). More recent evidence suggests that Pygo and BCL9 are constitutively associated with the enhanceosome (de la Roche & Bienz, 2007), via the concomitant interaction of Pygo with methylated histone tails and the ChiLS complex (Fiedler *et al*., 2008; Fiedler *et al*., 2015). BCL9 then interacts with multiple enhanceosome components, stabilising and scaffolding their assembly. Furthermore, whilst the interaction of β-catenin with TCF and APC is mutually exclusive, the binding site on β-catenin for BCL9 does not overlap with that for TCF (Hoffmans & Basler, 2004), permitting a model in which BCL9 serves to capture β-catenin and 'load' it onto TCF (**Fig. 1.4B;** Mieszczanek *et al*., 2008; Fiedler *et al*., 2015).

Once loaded onto TCF, β-catenin recruits transcriptional activators through its C-terminal-most armadillo repeats and flexible C-terminal tail (Vleminckx *et al*., 1999; Mosimann *et al*., 2009). These consist largely of histone acetyltransferases, including CBP/p300 (Takemaru & Moon, 2000; Hecht *et al*., 2000), and chromatin remodeling complexes such as SWI/SNF (Switch/Sucrose Non-Fermentable; Barker *et al*., 2001), which serve to reverse the repression exerted upon target genes by Gro/TLE. Although the exact nature of this repression is not fully clear, it likely involves chromatin condensation (dependent upon Gro/TLE tetramerization through an N-terminal Q domain), as well as histone deacetylation (Chen *et al*., 2000; Song *et al*., 2004; Sekiya *et al*., 2007; Chodaparambil *et al*., 2014; see also **Section**

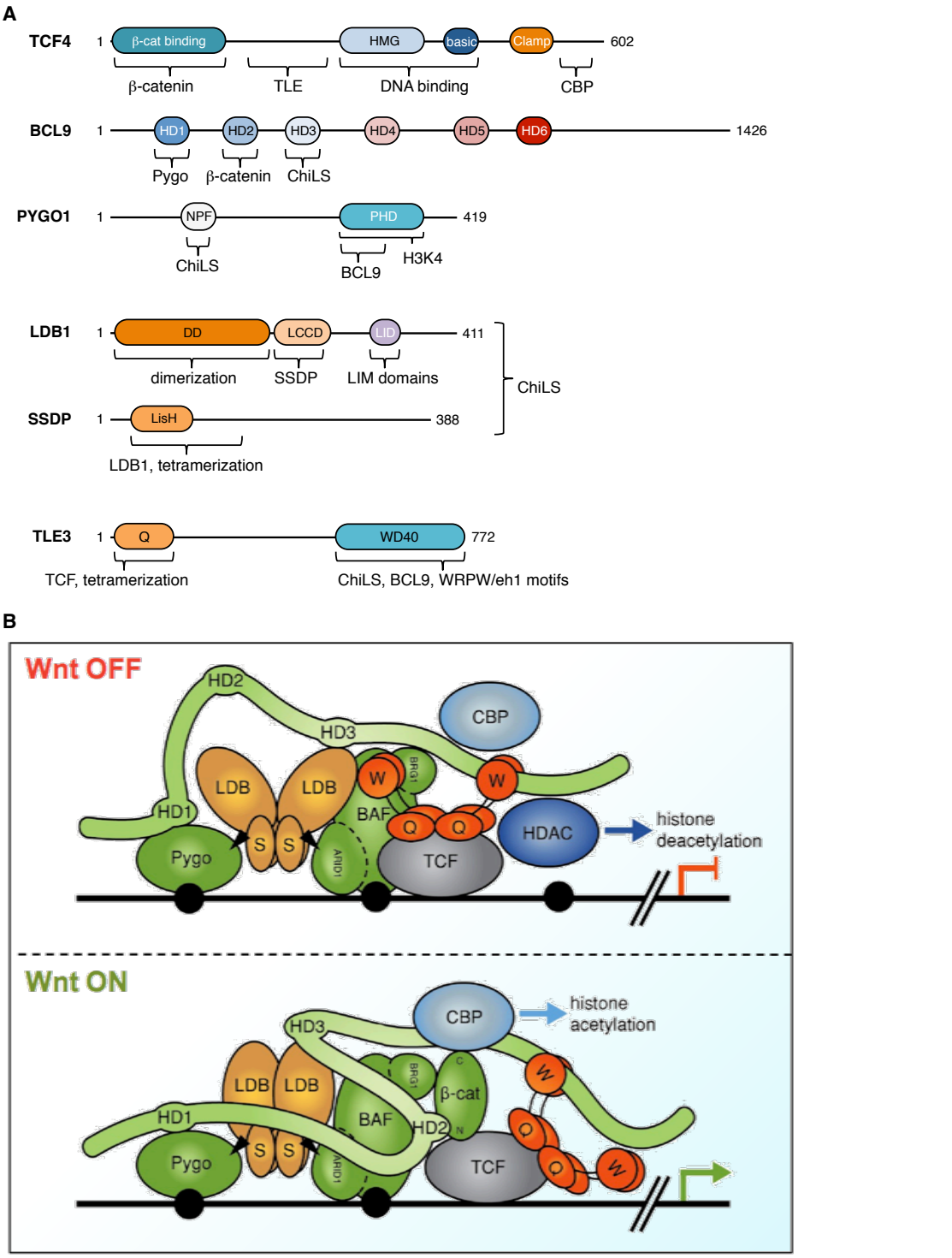

Figure 1.4 Overview of the Wnt enhanceosome.

(A) Domain architecture and key interactions of core Wnt enhanceosome components.

(B) Model of transcriptional switching by the Wnt enhanceosome. The repressed state (top) is conferred by tetramerization of Gro/TLE via its Q domain (Q). Capture of β-catenin by BCL9 (bottom) induces a rearrangement of enhanceosome components into an active state permissive for transcription. The mechanism(s) by which Gro/TLE is inactivated is unclear. See text for more details. Adapted from van Tienen *et al.*, 2017.

2.1.5). The mechanism by which Gro/TLE is inactivated, such that transcriptional activation can occur is a further mystery, and is the principal subject of **Chapter 2** of this thesis. Counterintuitively, β-catenin can also recruit transcriptional repressors, such as ICAT (which functions to displace both TCF and CBP/p300 from β-catenin through competitive binding), in order to terminate transcription in a timely fashion (Daniels & Weis, 2002).

Just like the degradasome and signalosome, the Wnt enhanceosome depends on numerous multivalent and redundant interactions between individual components for its assembly and function. A recent study from the Bienz lab, based on proximity-labelling of endogenous proteins, provided evidence that the composition of the enhanceosome is not altered significantly during signalling, suggesting that changes in transcriptional activity are instead dependent on conformational rearrangements triggered by the binding of β-catenin (van Tienen *et al*., 2017). Further studies are required to decipher the intricacies of these rearrangements and the mechanisms by which they control the activity of this enigmatic complex.

1.2. Wnt signalling controls development and self-renewal of adult tissues

Wnt-operated transcriptional switches are conserved from placozoa (primitive animals lacking body axes and tissues) to humans, and regulate numerous aspects of development (Wodarz & Nusse, 1998; Ringrose *et al*., 2013). Cell fate specification in the *C. elegans* embryo, *Drosophila* larval patterning and *Xenopus* axes establishment have all been used as models for studying Wnt signalling in developmental contexts. Such complex processes invariably require the integration of multiple inputs, from both Wnt and other key signalling pathways (van Amerongen & Nusse, 2009). In particular, Wnt and Hedgehog are often secreted by adjacent groups of cells, for example at segment boundaries in *Drosophila*, where they establish reciprocal signalling systems in which they are mutually dependent (Ingham & McMahon, 2001).

In addition to its key role in development, Wnt signalling persists in adult organisms and is a key regulator of homeostasis in self-renewing tissues such as the intestinal epithelium. The mammalian intestine is covered by a single sheet of epithelial cells, which is invaginated into a series of alternating crypts and villi (**Fig. 1.5**). The base of each crypt houses a stem cell compartment, from which proliferative ‘transit-amplifying’ cells migrate upwards towards the apex of the villi, terminally differentiating into specialised cell types in the process, before being shed into the gut lumen (van der Flier & Clevers, 2009). The rate of proliferation of the transit-amplifying cells is extraordinary (such that the entire epithelium is renewed

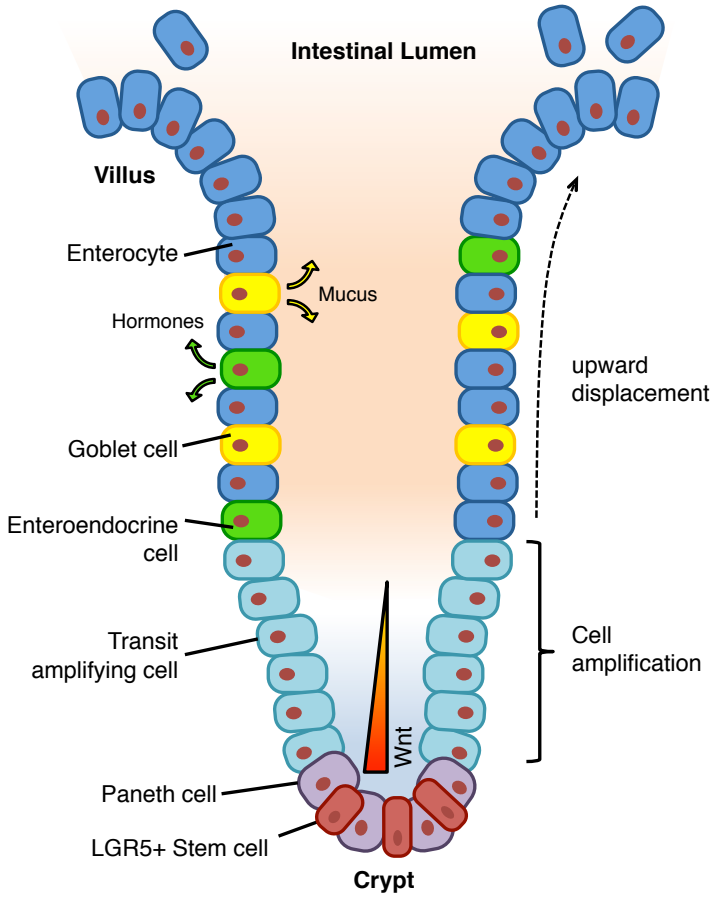

Figure 1.5 Wnt signalling in the intestinal epithelium. Long-lived Wnt-receptive stem cells, marked by LGR5, give rise to transit-amplifying cells which are displaced upwards, differentiating in the process into specialised lineages before being shed into the intestinal lumen. The entire epithelium is renewed approximately every 120 hours. Wnt is expressed in a gradient, highest at the base of the crypt and decreasing along the crypt-villus axis.

approximately every 120 hours), in contrast to the extremely long-lived and slowly dividing stem cells. This proliferation, and the acquisition of cell fate, is coordinated by a small number of signalling pathways, principally Wnt and Notch (Tian *et al.*, 2015).

The defining characteristic of stem cells is their capacity to self-renew, while also producing specialised cells. This behaviour is primarily dictated by short-range signals, which typically originate from a defined stem cell 'niche' (Losick *et al.*, 2011). Wnt was first implicated in intestinal homeostasis when it was shown that TCF4 knockout lead to loss of intestinal stem cells and catastrophic breakdown of the epithelium in mice (Korinek *et al.*, 1998), and signalling was subsequently observed to be highest at the base of each crypt, decreasing gradually along the crypt-villus axis (van de Wetering *et al.*, 2002). Conditional knockout of β-catenin in the proliferative compartment confirmed the requirement for Wnt signalling in maintenance of intestinal cell proliferation (Ireland *et al.*, 2004). Wnt is now known to be required for the maintenance of most, if not all, types of stem cell: indeed, pluripotent embryonic stem cells can be maintained in culture with the addition of just two small molecules, one of which (termed CHIR) potently activates Wnt signalling through inhibition of GSK3 (Silva *et al.*, 2008).

The exact identity of the key stem cells has historically been a matter of some contention. However, lineage-tracing experiments identified a small population of cycling cells, marked by surface expression of LGR5 (leucine-rich repeat-containing G-protein coupled receptor 5), as long-lived, multipotent stem cells (Barker *et al.*, 2007). LGR5 promotes cell surface expression of Fz, potentiating the reception of Wnt signals by these stem cells (de Lau *et al.*, 2011). LGR5 has subsequently been demonstrated to mark stem cells in many other organs, including hair follicles, where Wnt is also known to play multiple roles (Jaks *et al.*, 2008; DasGupta & Fuchs, 1999). The outcome of Wnt signalling in different tissues seems to depend on the developmental history of the receiving cell. For example, it promotes self-renewal and proliferation of intestinal and haematopoietic stem cells, but dictates specific cell fate decisions in neural crest stem cells (Reya *et al.*, 2003; Lee *et al.*, 2004).

More recently, organotypic cell culture has been used to study the role of Wnt signalling in intestinal self-renewal. These cultures (termed 'organoids') are self-organizing, three-dimensional structures that contain multiple organ-specific cell types arranged in an organ-like fashion, and can be genetically and phenotypically stable on a timescale of years. Epithelial organoids (or "mini-guts") can be grown from a single LGR5+ stem cell (Sato *et al.*, 2009), and as such are amenable to manipulation by a number of cutting-edge techniques, such as CRISPR/cas9-mediated genome editing (Schwank & Clevers, 2016).

Despite these advances, it is still unclear whether there is a common mechanism by which Wnt signals maintain the 'stemness' of their target cells (Clevers & Nusse, 2012). Stem cells are destined to differentiate by default, and it seems likely that Wnt signals block this intrinsic step, probably by suppressing the expression of differentiation-specific genes, and various model systems are now being employed to test this hypothesis.

1.3. Inappropriate or hyperactive Wnt signalling drives tumourigenesis

The specific behaviours of stem cells, which characterise development and homeostasis, often mirror those that characterise cancer cells. Aberrations in fundamental signalling pathways are regularly, therefore, associated with tumourigenesis. Although frequently hyperactivated in numerous cancers, the Wnt pathway it is best known for its causative role in intestinal tumourigenesis. Colorectal cancers are amongst the most common neoplasms in humans, with approximately 5% of Western populations expected to develop some form of colorectal malignancy during their lifetime (Bienz & Clevers, 2000).

A small fraction of colorectal cancers occur in an inherited fashion, giving clues as to the underlying molecular causes. The APC gene was first characterised as a tumour suppressor when it was identified as being mutated in familial adenomatous polyposis (FAP), a rare hereditary colon cancer syndrome characterised by the development of numerous

adenomatous polyps during early adulthood, which invariably develop into carcinomas (Kinzler *et al*., 1991; Nishisho *et al*., 1991). FAP patients typically inherit one mutant copy of *APC*, and polyps develop upon spontaneous mutation of the second copy. The vast majority of these mutations are truncations, located in the mutation cluster region (MCR) between the second and third 20R repeats, which preclude binding of APC to Axin and thus prevent formation of the degradasome, leading to massive stabilisation of β-catenin (Nagase & Makamura, 1993; Kohler *et al*., 2009). Colorectal cancers that are *APC* wt (i.e. do not carry *APC* mutations) often carry inactivating mutations in Axin, or point mutations of β-catenin that prevent its phosphorylation by GSK3 or CK1α (Morin *et al*., 1997; Liu *et al*., 2000). Interestingly, over 10% of colorectal adenocarcinomas have mutations in FBXW7 (F-box/WD repeat-containing protein 7), a component of an E3 ubiquitin ligase complex that is not required for Wnt-dependent transcriptional activation by β-catenin, but is central to a novel arm of Wnt-signalling termed Wnt-dependent stabilisation of proteins (Wnt/STOP), whose targets include prominent oncogenes such as c-Myc (Acebron *et al*., 2014; Zhan *et al*., 2017).

As well as the core pathway components, several regulators that 'fine-tune' Wnt signalling have also been implicated in cancer. For example, inactivating mutations in the RNF43 (RING finger protein 43) and ZNRF3 (Zinc RING finger protein 3) E3 ubiquitin ligases (negative regulators of Wnt signalling which promote endocytosis and hence limit cell-surface levels of Fz; Hao *et al*., 2012; Koo *et al*., 2012) have been identified in pancreatic cancer and adrenocortical carcinoma, respectively (Wu *et al*., 2011; Assié *et al*., 2014), whilst chromosomal fusions involving R-spondin can be found in colon cancer (Seshagiri *et al*., 2012). Several studies have also suggested a link between Wnt and non-coding RNAs; microRNA-146a can stabilise β-catenin, leading to maintenance of Wnt signalling and symmetric division of colorectal cancer stem cells (Hwang *et al*., 2014).

Polyp formation occurs at the boundary between crypts and villi, where cells from the proliferative zone grow into a neighbouring villus to form a microadenoma **(Fig. 1.6A)**. This process is dependent upon *APC* mutation, but is only an early step towards malignancy (Powell *et al*., 1992). Development from a benign polyp into a severely dysplastic carcinoma requires additional mutations which drive aggressive tumour formation, often in well-characterised oncogenes or tumour suppressors such as K-RAS, SMAD4 and/or p53 (**Fig. 1.6B**; Kinzler & Vogelstein, 1996). Wnt signalling is also thought to contribute to metastasis of colorectal cancer cells through the activation of genes that promote the epithelial to mesenchymal transition (EMT; the process by which polarised epithelial cells transform into migratory cells with invasive capacity) such as SNAI2 (Wu *et al*., 2012). Indeed, overexpression of B9L results in morphological changes, accompanied by increased migratory properties, in epithelial cells, suggestive of a role in EMT (Brembeck *et al*., 2004).

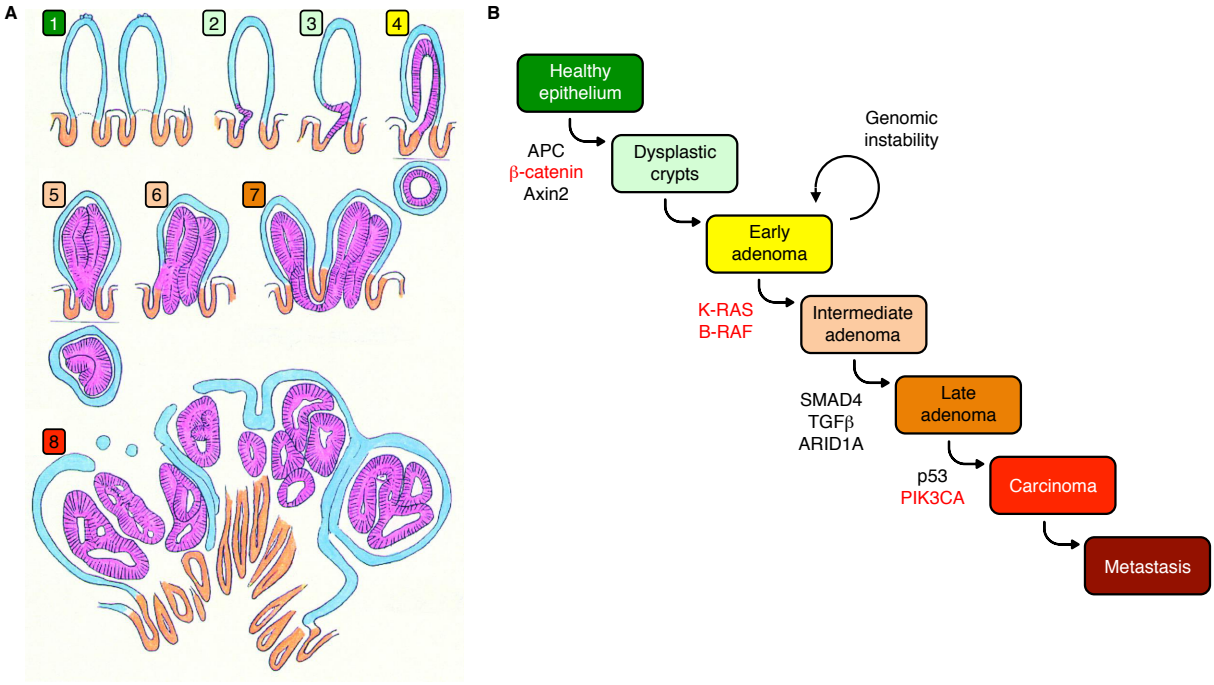

Figure 1.6 Multistep models of intestinal tumourigenesis.

(A) Adenomatous polyp formation in the intestinal epithelium. Cells expand from the crypt into a villus, forming a microadenoma (2-4). This microadenoma can expand into multiple neighbouring villi, eventually forming a large adenomatous polyp (5-8). Adapted from Oshima *et al.*, 1997.

(B) Genetic progression of colorectal cancer tumourigenesis. Neoplastic development is initiated by activating mutations in Wnt pathway components (e.g. in APC), which can be inherited or spontaneous. This is followed by various mutations that drive the progression from an early adenoma to a malignant carcinoma. Components commonly mutated in a gain-of-function fashion are shown in red, loss-of-function in black. Adapted from Pinto & Clevers, 2005.

Although less common, Wnt-related pathology is not restricted to cancer. Mutations in Wnt signalling components, either inherited or spontaneous, are known to also contribute to the development of numerous degenerative diseases. Well-characterised mutations in LRP6 or SOST (an LRP6-binding Wnt antagonist; Semënov *et al.*, 2005) cause sclerosteosis and hereditary osteoporosis (Baron and Kneissel, 2013), whilst diseases such as familial exudative vitreoretinopathy can be caused by mutation of LRP5, Fz4, or Norrin (Nusse & Clevers, 2017). Furthermore, increased risk for type 2 diabetes has been linked to single nucleotide polymorphisms (SNPs) in gene coding for Wnt5b, Wnt10b and TCF4, suggesting a link between Wnt signalling and metabolic disease (Grant *et al.*, 2006; Clevers & Nusse, 2012).

Conditional knockout strategies in the mouse have been central to investigating the effect of *APC* loss, alone and in combination with other mutations, on the intestinal epithelium. More

recently, intestinal organoids have been used to model colorectal cancer and examine the requirements for different mutations in growth and invasion (Matano *et al*., 2015). Despite this, many of the interactions between Wnt components in the pathological context of colorectal cancer are yet to be fully understood. Numerous mutations have been found enriched in colorectal cancer patients, and in many cases it is unclear whether these are key 'drivers' of tumourigenesis, or merely bystanders to the process. For example, both amplification and loss-of-function mutations of UBR5 and Naked (the subject of chapters 2 and 3 of this thesis, respectively) have been found in colorectal tumours. Non-canonical Wnt signalling pathways may also contribute to the development of pathology (see, for example Zhan *et al*., 2017). A fuller understanding of these interactions is required if therapeutic targeting of the Wnt pathway is to be achieved.

1.4. Therapeutic targeting of the Wnt pathway

The undisputed role of Wnt signalling in numerous human diseases implies that it has strong potential as a target for therapeutic intervention. Indeed, whilst adenomas with Wnt-activating *APC* mutations often reach severe dysplasia, those with only K-RAS mutations usually fail to progress to large tumours (Jen *et al*., 1994). Despite this, there are no Wnt-targeting therapeutic agents currently in use in the clinic. An overarching aim of the Bienz lab, and thus of this thesis, is to identify and understand Wnt pathway components, so as to determine their potential as targets for therapeutic intervention.

Extensive efforts from multiple groups, using a number of different approaches, have been made to identify or design small molecules that interfere with Wnt signal transduction. Some compounds that reduce signalling have been successfully identified; for example, the stability of Axin, which is controlled by tankyrase-mediated ADP-ribosylation, is one aspect of the pathway that appears to be targetable. Treatment of non-cancerous cells with tankyrase inhibitors, such as XAV939, leads to increased Axin, and concomitantly lowered β-catenin levels, inhibiting signalling (Huang *et al*., 2009; Kulak *et al*., 2015). However, tankyrase inhibitors are ineffective under conditions of chronic Wnt signalling in colorectal cancer cell lines (de la Roche *et al*., 2014). Specific inhibitors of Porcupine, the acyltransferase that catalyzes palmitoylation of Wnt, have also been identified. These molecules, which include IWP2 and LGK974, lead to a complete block in Wnt secretion and receptor binding, and may have efficacy in treatment of metastatic lesions that appear to require the presence of Wnt itself (Lu *et al*., 2009; Madan *et al*., 2016). Wnt-receptor interactions have also been probed as potential targets, with antibodies directed at Fzs and R-spondins (a family of Wnt agonists) both showing promise in certain model systems (Steinhart *et al*., 2017; Storm *et al*., 2016). Perhaps most successfully, a monoclonal antibody targeting SOST (known as Romosozumab) has proven useful in treating Wnt-related osteoporosis in clinical trials (Cosman *et al*., 2016).

Despite these successes, therapeutic agents that would be expected to function in the majority of colorectal tumours (which carry mutations of APC or β-catenin) have yet to be identified. One obvious target is the complex formed between TCF and β-catenin, which is absolutely required for signalling, and acts at a node in the pathway that is downstream of almost all activating mutations (Clevers & Nusse, 2012). Like many protein-protein interactions, however, targeting this complex has proven fraught with difficulty. The large, shallow groove of the β-catenin armadillo repeat domain, which binds to numerous positive and negative regulators of signalling, seems to be difficult to target selectively (Huber *et al*., 1997; Daniels *et al*., 2001). A unique difficulty with targeting the Wnt pathway seems to be that much of the signal transduction process relies on changes in the oligomeric state and interactions of protein components, rather than the post-translational modifications that are pervasive in other pathways, and which necessitate modifying enzymes that constitute potential targets for therapeutic intervention. Despite this, post-translational modification does occur on numerous Wnt pathway components, and enzymatic positive regulators of the pathway are sought after as potential targets (a theme explored in more detail in **Chapter 2** of this thesis).

As well as blocking signalling, there is also potential clinical value in *stimulating* the Wnt pathway for tissue regrowth and regeneration. Wnt itself is unsuitable for use as a drug, due to its hydrophobicity, which complicates delivery (and also because producing significant quantities is currently challenging). Recently, however, soluble protein agonists of Wnt have been shown to activate signalling *in vivo*, whilst several small molecule inhibitors of GSK3 have been identified that induce Wnt target gene expression (Janda *et al*., 2017; Licht-Murava *et al*., 2016). A more detailed understanding of physiological and pathological Wnt signalling pathways, both canonical and non-canonical, is required for us to be able to identify the most likely points for therapeutic intervention, and to predict the efficacy and side-effects of the Wnt inhibitors and activators that target these components.

1.5. Outstanding questions in the Wnt signalling field

Through the efforts of a large number of different labs over almost three decades, the core components of the Wnt pathway have now been identified, and many of their individual interactions defined. The next goal of the Bienz lab, and thus of this thesis, is to understand the Wnt-induced molecular changes that trigger the assembly and disassembly of the three multiprotein complexes that govern Wnt signal transduction (the degradasome, signalosome and enhanceosome), and their switching between inactive and active states. This represents a significant challenge, given that these transitions involve numerous and often subtle changes in the activities, conformations and/or oligomeric states of the constituent proteins of these complexes.

This thesis covers progress towards answering two key questions, each of which relate to the switching of one of these complexes from one state to another:

In **Chapter 2**, I examine the mechanisms underlying the switching of the Wnt enhanceosome from a poised to an active state upon docking of β-catenin. Crucially, this transition requires inactivation of Gro/TLE, a key co-repressor of Wnt target genes. I outline our progress towards understanding this inactivation, and the essential role that ubiquitylation of Gro/TLE by a HECT E3 ubiquitin ligase, termed UBR5, plays in this process.

In **Chapter 3**, I investigate the mechanisms by which signalosomes are switched off in a timely fashion to effect the cessation of canonical Wnt signalling. I focus in particular on the role of a key cytoplasmic negative regulator of the pathway, Naked, which acts at the level of Dishevelled, but whose mechanism of action is largely unknown.

2. Control of the Wnt transcriptional switch by ubiquitylation

2.1 Introduction

A key step in Wnt signal transduction is the conversion of the nuclear enhanceosome complex from a poised, silent state into an active one that is permissive for transcription. Operating this transcriptional switch involves binding of the central effector, β-catenin, to TCF, and the concomitant release of transcriptional repression imposed on the Wnt target genes by TCF-associated Gro/TLE. Despite the central importance of this step, which occurs downstream of almost all Wnt pathway-activating mutations, it remains poorly understood. In this chapter we identify a new mechanism within this transcriptional switch, whereby a HECT ubiquitin ligase, UBR5, ubiquitylates and subsequently inactivates Gro/TLE during Wnt signalling.

2.1.1 The ubiquitin system

The ubiquitin system is responsible for the post-translational, covalent addition of a highly conserved protein termed ubiquitin (Ub) onto intracellular substrates. This system, which is involved in controlling almost all processes in eukaryotic cells, provides an essential mechanism for communication between cellular pathways (Yau & Rape, 2016). It can target damaged, misfolded or otherwise abnormal proteins in a constitutive fashion, but it can also regulate protein stability or activity in a switch-like manner (Varshavsky *et al.*, 2012).

Ubiquitin is a highly stable protein of 76 amino acids, consisting of a single β-grasp fold (Vijay-Kumar *et al.*, 1987). The sequence of ubiquitin is almost invariant from yeast to man, suggesting a strong evolutionary pressure to conserve the structure, and implying that much of its surface is involved in recognition by ubiquitin-binding domains (UBDs; Dikic *et al.*, 2009). Substrate modification with ubiquitin is known as 'ubiquitylation'. In the simplest version of the process, monoubiquitylation, a single ubiquitin moiety is covalently conjugated via its flexible C-terminal tail to the ε-amino group of a target lysine residue, yielding a 'branched' protein conjugate with multiple exposed N-termini (the initial observation that led to the discovery of ubiquitin; Goldknopf & Busch, 1977). Multi-monoubiquitylation, where a single ubiquitin is conjugated to multiple lysine residues on a substrate, can also occur (**Fig. 2.1A**).

Furthermore, ubiquitin itself contains eight primary amines (seven lysine residues and an N-terminus) that constitute sites for additional of further ubiquitin, permitting the formation of polyubiquitin 'chains' (**Fig. 2.1A**; Hershko & Heller, 1985). In most of these polyubiquitin (polyUb) conjugates, each ubiquitin moiety is linked to the next via the same lysine (or methionine) residue, creating chains that adopt distinct, dynamic conformations that can be

specifically recognised by specialised UBDs (Ye *et al*., 2012). The idea that different types of chain, such as K48-, K63- and Met1-linked polyubiquitin, can serve as distinct signals has lead to the proposal of a 'ubiquitin code', whereby ubiquitin chains encode information that is deciphered by UBDs to effect specific biological outcomes (**Fig. 2.1B**; Komander & Rape, 2012; Yau & Rape, 2016).

All of the different possible chain types have been identified in cells, although their proportions vary drastically (Meierhofer *et al*., 2009). K48-linked chains constitute the majority of polyubiquitin found in cells, and have been known for a long time to promote 26S-proteasome-mediated degradation of modified substrates (Chau *et al*., 1989). Accordingly, these chain types are known to be the product of several E3 ligases associated with degradation, such as the cell-cycle associated E3 ligase SCF (Skp, Cullin, F-box containing), and their levels increase upon proteasome inhibition (Petroski & Deshaies, 2005; Xu *et al*., 2009). In some cases, proteins destined for degradation can be escorted to the proteasome by chaperones, such as VCP/p97 (valosin-containing protein/protein of 97 kDa), that specifically recognize K48-linked polyubiquitin (van den Boom & Meyer, 2017; see also **Section 2.1.4**). The ubiquitin system is also able to act independently of this 'ubiquitin-proteasome system' (UPS), by recruiting proteins to participate in signalling, controlling substrate localisation via trafficking factors, or by directly controlling substrate activity (Hoege *et al*., 2002; Terrell *et al*., 1998; Rahighi *et al*., 2009). These functions often depend upon monoubiquitylation or Met1- and Lys63-linked polyubiquitin modifications (Chen & Sun, 2009). Work to identify the physiological roles of other 'atypical' ubiquitin chain types, including K27-, K29- and K33-linked polyubiquitin, is ongoing (Kulathu & Komander, 2012).

In some cases, multiple linkage types are present on a single substrate, either as separate chains, or in the form of mixed or branched heterotypic chains (**Fig. 2.1A**). Binding of IL-1 to its cognate receptor triggers the assembly of both K63- and Met1-linked polyubiquitin on IRAK1, much of which is in the form of hybrid chains (Emmerich *et al*., 2013). The extent to which the context of a single ubiquitin linkage produces a specific response remains unclear, although it is thought that some ubiquitin branch points can be specifically recognised by certain UBDs (Ohtake *et al*., 2016). In some cases, polyubiquitin can be released from substrates and the unanchored chains act as second messengers (Xia *et al*., 2009). Further expanding the complexity of the code, ubiquitin itself has recently been found to be subject to (non-ubiquitin) post-translational modifications, including phosphorylation and acetylation (Koyano *et al*., 2014; Ohtake *et al*., 2015). The ubiquitin kinase PINK1 generates Ser-65-modified phosphoubiquitin, a potent signalling molecule that promotes mitophagy through allosteric activation of the E3 ligase Parkin (Wauer *et al*., 2015). Furthermore, there are multiple ubiquitin-like proteins (Ubls, such as small ubiquitin-like modifier (SUMO)) that

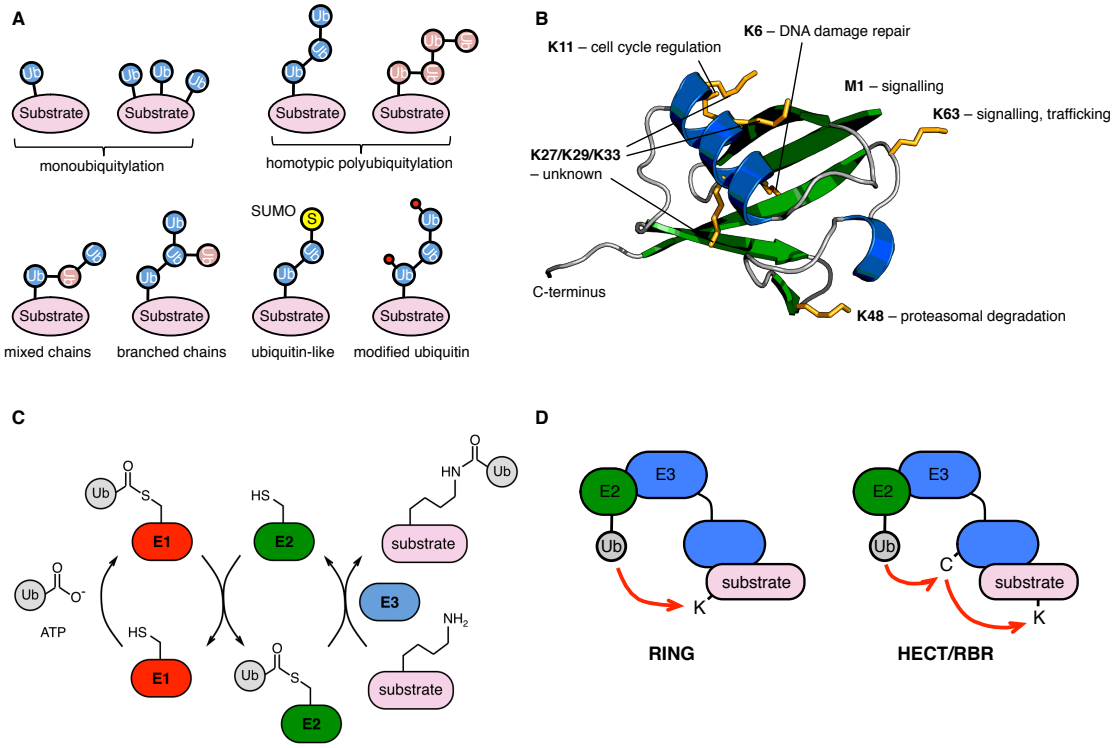

Figure 2.1 Summary of the ubiquitin system.

(A) Diversity of potential ubiquitin modifications. Blue and pink moieties represent ubiquitin linked via different lysine residues. Red dots indicate phosphorylated ubiquitin.

(B) Structure of ubiquitin, highlighting (in bold) the 8 potential sites for further ubiquitin modification, and the known cellular roles of some of these polyubiquitin chains.

(C) The ubiquitylation cascade. Ubiquitin is activated by an E1 ubiquitin-activating enzyme in an ATP-dependent fashion, and transferred to a catalytic cysteine residue of an E2 ubiquitin-conjugation enzyme. This in turn transfers ubiquitin directly or indirectly onto the substrate with the aid of an E3 ligase.

(D) Mechanisms of E3 ubiquitin ligases. RING ligases (left) catalyse the direct transfer of ubiquitin from E2 to substrate. In contrast, HECT/RBR ligases (right) operate via a two-step mechanism, involving transfer of ubiquitin onto a catalytic cysteine residue of the E3, prior to substrate transfer.

operate in parallel with ubiquitin, often but not exclusively employing components of the ubiquitin system for their own conjugation (van der Veen & Ploegh, 2012). In some cases, these different modification systems can act on substrates in simultaneous and even coordinated fashion (Prudden et al., 2007).

Ubiquitylation is executed via a three-step cascade involving ATP-dependent activation of ubiquitin by an E1 ubiquitin activating enzyme, conjugation of ubiquitin to an E2 ubiquitin conjugating enzyme, and the transfer of ubiquitin to substrate mediated by the E3 ubiquitin ligases that have already been touched upon (**Fig. 2.1C**). There are two E1s, approximately 40 E2s, and over 600 E3 ligases in humans, demonstrating the scale of the ubiquitin system

(Schulman & Harper, 2009). This cascade allows the system to be tightly regulated at several stages of ubiquitin transfer, and can also be reversed through the activity of deubiquitylating enzymes (DUBs). E3 ligases and DUBs are focal points of study within ubiquitin research, since they impart the majority of the substrate and linkage-type specificity.

Three classes of E3 ubiquitin ligases have been identified to date: RING (really interesting new gene), HECT (homologous to E6-AP C-terminus) and RBR (RING-Between-RING; Zheng & Shabek, 2017). The HECT and RBR families have different characteristic catalytic folds but share a common mechanism, in which ubiquitin is accepted from the E2 enzyme onto a catalytic cysteine before transfer onto the substrate (**Fig. 2.1D**, see also **Section 2.1.3**). In contrast the RING family, which contains the vast majority of known E3 ligases, do not contain a catalytic cysteine, and ubiquitin is transferred directly from E2 to substrate in a fashion facilitated by the RING domain. Within each family of E3 ligases there are numerous subfamilies; the HECT family is subdivided into the NEDD4, HERC and 'other HECT' subfamilies, for example (Rotin & Kumar, 2009). Similarly, there are several families of deubiquitylases, with a remarkable variety of different catalytic folds and mechanisms, displaying numerous determinants of substrate and ubiquitin linkage specificity (Komander *et al*., 2009; Mevissen *et al*., 2013). Based on the current rate of advance, further classes of both E3 ligase and DUB are likely to be identified in the future (see for example Pau *et al*., 2018). As enzymes that modulate a myriad of signalling pathways through regulation of protein ubiquitylation, these proteins represent attractive targets for therapeutic intervention (Huang & Dixit, 2016).

2.1.2 Ubiquitylation in the Wnt pathway

As in many intracellular pathways, ubiquitin-dependent mechanisms operate at multiple steps of Wnt signalling, targeting both positive and negative components of the pathway, and providing addition layers of control through the regulation of protein stability, activity and localisation (Tauriello & Maurice, 2010a).

Wnt signalling hinges on the crucial step of ubiquitin-mediated degradation of the key transcriptional regulator β-catenin. In the off state, the RING E3 ligase β-TrCP targets phosphorylated β-catenin for degradation through the assembly of K48-linked polyubiquitin chains on N-terminal lysine residues (Wu *et al*., 2003). Interestingly, other E3 ligases have been implicated in ubiquitylation and degradation of β-catenin, including Jade-1 and HUWE1 (HECT, UBA and WWE domain-containing protein 1; Chitalia *et al*., 2008; Dominguez-Brauer *et al*., 2017), whilst one report proposed that assembly of atypical ubiquitin chains by the HECT E3 ligase UBR5 could stabilise β-catenin and thereby promote Wnt signalling (Hay-Koren *et al*., 2011).

Whilst components of the degradasome function to earmark β-catenin for degradation, they are themselves subject to ubiquitin-dependent regulation. Recall that Axin is constitutively targeted for degradation by the poly-ADP-ribose activated RING E3 ligase RNF146, keeping its concentration low (Zhang *et al*., 2011; **Section 1.1.1**). Moreover, Wnt-treatment of cells leads to a further reduction in Axin levels, which was recently shown to be mediated by an E3 ligase termed SIAH (Ji *et al*., 2017). The SIAH binding site on Axin overlaps with that of GSK3, meaning that SIAH-dependent Axin degradation only occurs upon Wnt-induced degradasome disassembly. Knockout of SIAH-1 attenuates β-catenin stabilisation and Wnt signalling, seemingly at odds with previous reports implicating it in ubiquitylation of β-catenin (Liu *et al*., 2001; Dimitrova *et al*., 2010). On the other hand, K63-linked polyubiquitylation of APC by HECTD1 is reported to negatively regulate signalling through promotion of the APC-Axin interaction, although the role of the ubiquitin chains in this process is unclear (Tran *et al*., 2013). Confusingly, UBR5 has also been identified as an APC-associated E3 that decreases levels of active β-catenin (Ohshima *et al*., 2007), although this mechanism is reportedly independent of E3 ligase activity and contradicts the report mentioned above (Hay-Koren *et al*., 2011).

Positive regulators of the Wnt pathway are also subject to regulation via ubiquitylation. The transmembrane RING E3 ligases RNF43 and ZNRF3 inhibit Wnt signalling by promoting the ubiquitylation and subsequent lysosomal degradation of Frizzled and LRP6 in a fashion dependent upon the Dvl DEP domain (Mukai *et al*., 2010; Koo *et al*., 2012; Jiang *et al*., 2015b). This cycle is in turn inhibited by R-spondins, which bind to LGR4/5 receptors and promote the internalization of RNF43 and ZNRF3, thereby acting as potent Wnt agonists (de Lau *et al*., 2011; Hao *et al*., 2012). Dvl itself is also heavily ubiquitylated by a number of E3 ligases, including several from the NEDD4 (Neuronal precursor cell-expressed developmentally downregulated 4) subfamily of HECT E3s, although the function of these modifications has not been fully elucidated. ITCH and NEDD4L each negatively regulate Dvl levels in a manner dependent on a conserved PPxY motif in Dvl (Wei *et al*., 2012; Ding *et al*., 2013). HUWE1 can also modify Dvl, reportedly with K63-linked non-proteolytic polyubiquitin (de Groot *et al*., 2014). These modifications, which can be removed by the deubiquitylase CYLD, may function by modulating the ability of Dvl to polymerize through the DIX domain (Tauriello *et al*., 2010b; Madrzak *et al*., 2015, see also **Chapter 3**).

Despite this plethora of reported modifications, relatively few roles for ubiquitylation have been identified at downstream steps of Wnt signal transduction. The DUB Uch37 binds TCF/LEF and promotes Wnt signalling, but this is seemingly independent of catalytic activity (Han *et al*., 2017). Monoubiquitylation of the N-terminal Q domain of Gro/TLE by XIAP (X-linked inhibitor of apoptosis protein) has been reported to activate Wnt signalling, by

promoting the dissociation of Gro/TLE from TCF, but this ubiquitylation is not Wnt-dependent (Hanson *et al*., 2012). Intriguingly, the scaffolding protein BCL9 contains a PPxY motif, similar to that of Dvl, which could recruit E3 ligases to the enhanceosome, although none have been conclusively demonstrated as physiologically relevant ligands at this stage.

It is clear that ubiquitin is a key regulatory protein in the Wnt pathway, controlling the stability of crucial components through proteasomal degradation, as well as protein localisation, trafficking and activity through non-proteolytic mechanisms (Tauriello & Maurice, 2010a). Although a few of these ubiquitin-dependent mechanisms have been outlined in some detail, in many cases the literature is unclear, largely due to the relatively subtle effects that many modifications have, and the fact that conclusive identification of E3 ligase-substrate pairs is technically very challenging (Iconomou & Saunders, 2016). For example, whilst UBE3C has been implicated in Wnt pathway activation in cancer, no mechanistic details or substrates have so far been identified (Wen *et al*., 2015). The case of UBR5 further highlights this, with two completely different substrates, chain types and corresponding effects on the pathway reported (Ohshima *et al*., 2007; Hay-Koren *et al*., 2011).

2.1.3 UBR5 is an unusual HECT E3 ubiquitin ligase

UBR5 was first identified in *Drosophila* as the gene *hyperplastic discs* (*hyd*), mutation of which causes massive overgrowth of somatic tissue in larval wing discs. Cloning of the *hyd* gene identified a large protein, subsequently shown to be homologous to a mammalian protein termed UBR5 (Mansfield *et al*., 1994; Callaghan *et al*., 1999).

UBR5, also known as EDD1 (E3 identified by differential display 1), is a 309 kDa HECT E3 ubiquitin ligase (of the 'other HECT' subfamily) found exclusively in metazoa. HECT ligases have a well-characterised mechanism for ubiquitin transfer, involving formation of a thioester linkage between ubiquitin and a conserved catalytic cysteine within the HECT domain (Komander & Rape, 2012). The HECT domain is located at the extreme C-terminus of UBR5 and consists of archetypal N- and C-lobes, separated by a flexible linker, but displays several unique features. The HECT domain itself does not appear to contain a binding site for ubiquitin (usually located within the C-lobe), instead relying on a distant UBA domain (Kozlov *et al*., 2007). UBR5 also contains a UBR zinc finger required for recognition of substrates with destabilising N-terminal residues (N-end-rule substrates; Tasaki *et al*., 2005; Sriram *et al*., 2011), and a MLLE domain (containing a characteristic MLLE motif), separated by large regions presumed to be natively unstructured (**Fig. 2.2A**). Intriguingly, sequence comparisons reveal homology between the region immediately upstream of the MLLE domain and N-terminal portions of certain extended HECT domains, such as that of HUWE1, implying that the MLLE domain is present as an insert *within* the HECT domain (**Fig. 2.2B**). Accordingly, a minimal UBR5 HECT construct lacking this N-terminal region is not capable of polyubiquitin

synthesis *in vitro* (Kristariyanto *et al.*, 2015). The MLLE domain is thought to be principally involved in recruitment of substrates (such as PAIP2; Kozlov *et al.*, 2004), but may also regulate ubiquitin transfer catalyzed by the adjacent HECT (Munoz-Escobar *et al.*, 2015). The full architecture of the MLLE-HECT region is not known, although a crystal structure of the HECT C-lobe alone has been solved (Matta-Camacho *et al.*, 2012).

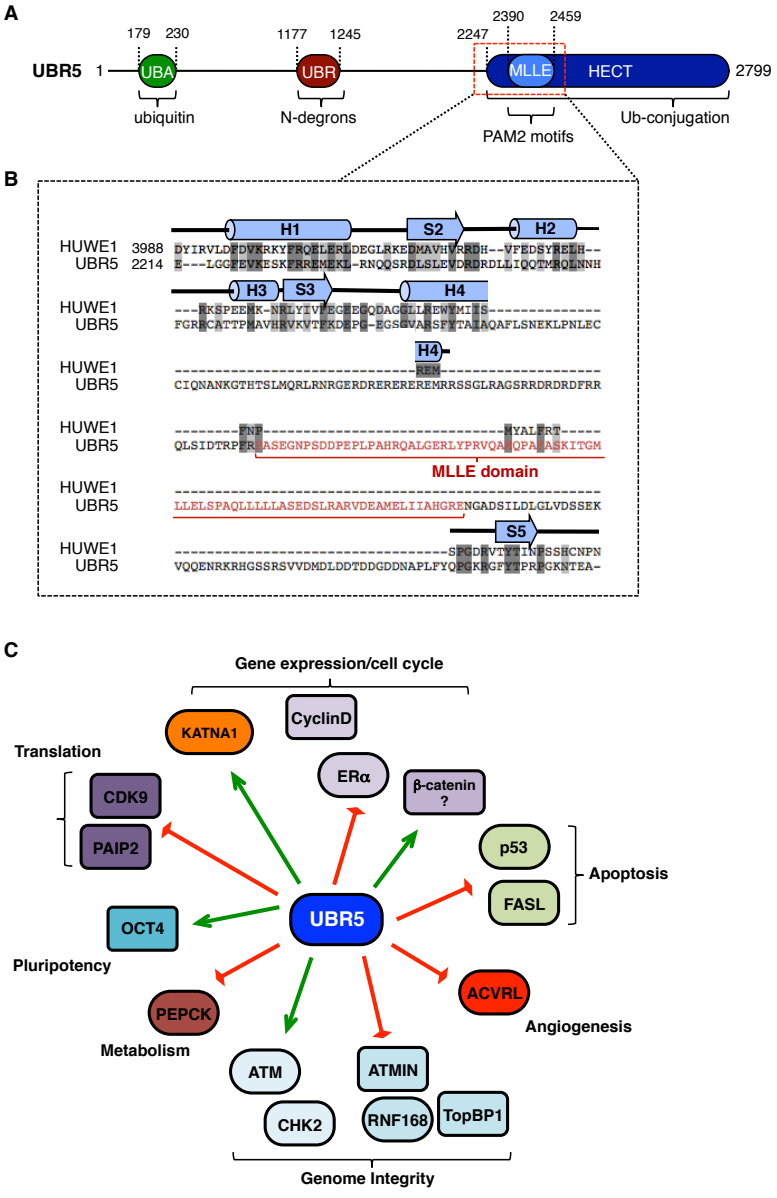

Figure 2.2 UBR5 domain architecture and cellular functions.

(A) Domain architecture and key interactions of UBR5.

(B) Sequence alignment of HUWE1 and UBR5 HECT domains. Note the region of HECT domain homology N-terminal of the UBR5 MLLE domain (shown in crimson). Alpha helices (H) are shown as cylinders, β-strands (S) as arrows. See text for more details.

(C) Reported substrates and cellular roles of UBR5. Red arrows indicate proteins that are destabilised or inactivated by UBR5 activity, green indicates stabilisation or activation. Adapted from Shearer *et al.*, 2015.

UBR5 is predominantly localised to the nucleus, as a result of two nuclear localisation sequences (Henderson *et al*., 2002), and has been implicated it in a wide variety of cellular processes including DNA damage repair, translation and cell cycle regulation, as well as Wnt signalling (Munoz *et al*., 2007; Yoshida *et al*., 2006). As mentioned, identification of substrates of E3 ligases is technically challenging, and many interacting partners appear to be independent of UBR5 catalytic activity, suggesting that UBR5-mediated ubiquitylation is context dependent and tightly regulated. Reported substrates of UBR5 include DNA damage repair factors TopBP1, RNF168 and ATMIN (Honda *et al*., 2002; Zhang *et al*., 2014), translational machinery proteins CDK9 and PAIP2 (Cojocaru *et al*., 2011), and the KATNA1 subunit of the cell cycle-related protein KATANIN (Maddika *et al*., 2009; see **Fig. 2.2C** for more details). In some cases, these substrates are destabilised by UBR5-dependent ubiquitylation, but this certainly does not seem to be an exclusive mechanism by which UBR5 acts, and the polyubiquitin chain type(s) assembled by UBR5 remains a point of contention (Hay-Koren *et al*., 2011). In several cases, UBR5 cooperates with other E3 ligases, including TRIP12, and its activity may also be counteracted by associated deubiquitylases acting as part of ubiquitin chain-editing complexes (Gudjonsson *et al*., 2012; Rutz *et al*., 2015).

Numerous studies have implicated UBR5 in various facets of cancer biology, and many of the reported molecular functions of UBR5 are consistent with a role in cancer (Shearer *et al*., 2015). *hyd* was originally labelled as a tumour suppressor gene in *Drosophila*, but the most common genetic changes in UBR5 associated with cancers are amplifications, often in the form of allelic imbalances that result in increased levels of *UBR5* mRNA, implying an oncogenic nature (Mansfield *et al*., 1994; Clancy *et al*., 2003). Indeed, *UBR5* amplification correlates with negative outcomes in breast cancer, was identified in a mutagenesis screen for cooperative mutations in pancreatic adenocarcinomas, and has been shown to mediate therapeutic resistance in ovarian cancers (Mann *et al*., 2012; O'Brien *et al*., 2008). Clearly, the specific mechanisms by which UBR5 contributes to carcinogenesis remain poorly understood. This controversy also applies in the Wnt field, with conflicting reports labelling UBR5 as both a tumour suppressor (Ohshima *et al*., 2007) and an oncogene (Hay-Koren *et al*., 2011) with respect to colorectal cancer. Despite a plethora of research, there thus remains a lack of understanding of UBR5 activity in various physiological and pathological states, and any potential development of this E3 ligase as a therapeutic target is dependent on the identification of *bona fide* substrates in the context of carcinogenesis. The findings presented in this chapter are the results of a study initiated to clarify the literature with respect to UBR5 function in Wnt signalling and cancer.

2.1.4 VCP/p97 is a cellular unfoldase/segregase

As briefly mentioned, an important feature of the ubiquitin-proteasome system (UPS) is the capacity to specifically recruit chaperones to polyubiquitylated proteins in order to execute particular functions related to protein folding and/or unfolding. One example, highly relevant for this thesis, is the abundant hexameric ATPase known as VCP/p97 (van den Boom & Meyer, 2017).

VCP/p97 was originally discovered in yeast genetic screens as Cdc48 (Moir *et al*., 1982), and the mammalian homolog was later identified as a 97 kDa precursor of the small peptide valosin, hence termed valosin-containing protein (VCP) or p97 (although it subsequently emerged that valosin is actually unrelated to p97; Koller & Brownstein, 1987). VCP/p97 belongs to the AAA+ family of ATPases, members of which function in all three domains of life, and is now understood in intricate structural detail (Zhang *et al*., 2000). VCP/p97 is a symmetrical hexamer, with each subunit consisting of a regulatory N-terminal domain and tandem ATP-binding domains, D1 and D2 (**Fig 2.3A**). ATP hydrolysis by the D2 domain allows VCP/p97 to impose conformational changes on substrate proteins, underlying VCP/p97's diverse ability to unfold proteins for proteasomal degradation, or to segregate them from binding partners, membranes or protein complexes (Xia *et al*., 2016). VCP/p97 is assisted in these functions by over 25 cofactor proteins, which are recruited via dedicated domains that bind either the N domain or the C-terminal tail of VCP/p97. These cofactors often act as substrate or ubiquitin adapters, but in some cases confer additional enzymatic activities such as deubiquitylation (Meyer *et al*., 2002; Buchberger *et al*., 2015).

VCP/p97 is localised throughout the cell, including large nuclear and organelle fractions, and has many reported functions that cover all aspects of cellular physiology (**Fig 2.3B**; Song *et al*., 2015; Ye *et al*., 2017). VCP/p97 clearly plays a critical role in the UPS, binding to a large number of polyubiquitylated proteins in various cellular locations and facilitating their proteasomal degradation, and also appears to be essential for autophagy-mediated degradation in lysosomes (Meyer *et al*., 2012; Papadopoulos *et al*., 2017). However, in some cases, VCP-associated deubiquitylases appear to act immediately upon segregation, potentially preventing degradation of the substrate (Rumpf & Jentsch, 2006; Bodnar & Rapoport, 2017). VCP/p97 has crucial regulatory roles in various signalling pathways, including NF-κB (Li *et al*., 2014), either through the proteasomal degradation of key regulators, or through the release of proteins from macromolecular complexes or membranes. Furthermore, VCP/p97-mediated segregation of ubiquitylated proteins from chromatin is now known to be essential for diverse DNA-related processes including replication, repair and transcription (Maric *et al*., 2014; van den Boom *et al*., 2016). Most of these processes involve recognition of K48-linked polyubiquitin, although other chain types, including K6- and K11-

linked, have also been reported to recruit VCP/p97 (van den Boom & Meyer, 2017; Locke *et al.*, 2014; Heidelberger *et al.*, 2018).

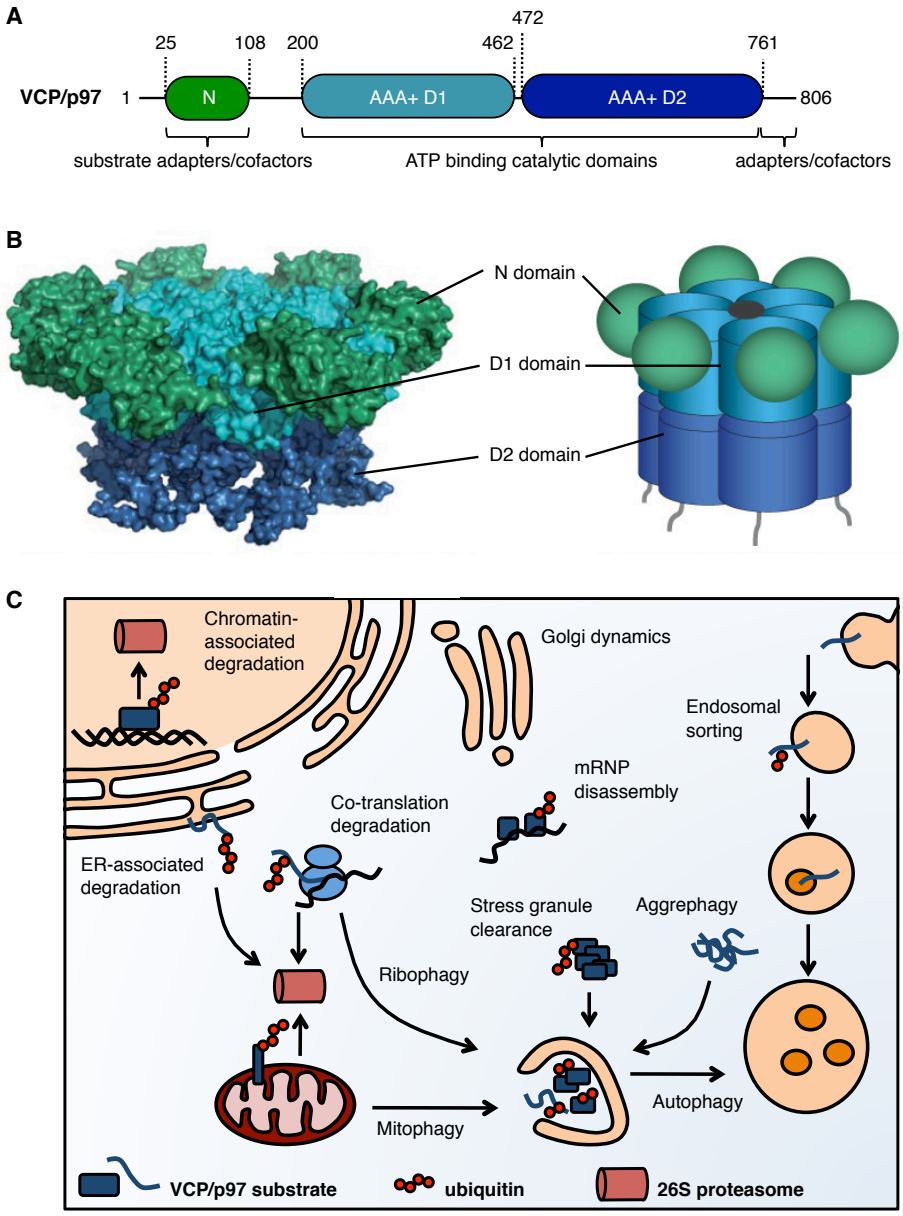

Figure 2.3 Structure and function of VCP/p97.
(A) Domain architecture and key interactions/functions of VCP/p97.
(B) Structure of a VCP/p97 hexamer, with key domains colour as in (A). Adapted from Meyer *et al.*, 2012.
(C) Cellular roles of VCP/p97. See text for more details. Adapted from Meyer & Weihl, 2014.

Unsurprisingly, given its manifold cellular functions, mutation of VCP/p97 is associated with various diseases. Though homozygous knockout in mice is lethal, dominant mutations in regulatory regions cause a late-onset multisystem proteinopathy (MSP-1), also known as IBMPFD (Inclusion Body Myopathy with Paget's Disease and Frontotemporal Dementia; Johnson *et al*., 2010). On the other hand, VCP/p97 is upregulated in certain cancers, apparently in response to increased proteotoxic stress (Deshaies, 2014). Small-molecule inhibitors of VCP/p97 are now are now available as research tools, and several are also in clinical trials (Chapman *et al*., 2015; Anderson *et al*., 2015). However, a detailed understanding of many aspects of VCP/p97 function is still lacking. In particular, the features of ubiquitylated proteins that define them as substrates of VCP/p97 and/or the proteasome are unclear, although particularly stable, folded proteins often seem to require VCP/p97. Specific features of the ubiquitin chain, including branching, may also be relevant (Blythe *et al*., 2017). Understanding of these basic biochemical questions will be required for the success of therapeutic strategies designed to target VCP/p97. In this chapter we identify the co-repressor Gro/TLE as a client of VCP/p97, and hence outline a key role for VCP/p97 in Wnt pathway regulation.

2.1.5 Gro/TLE maintains transcriptional repression at Wnt enhanceosomes

As discussed, the Wnt enhanceosome is a protein complex poised for transcriptional activation upon docking of β-catenin, but maintained in an inactive state by the co-repressor Groucho (Gro) in *Drosophila*, or its ortholog TLE in mammals (see **Section 1.1.3**). For the purposes of this thesis it is pertinent to give a more detailed introduction to the mechanisms by which Gro/TLE exerts transcriptional repression upon Wnt target genes, and to discuss some of the mechanisms proposed as means by which this repression is removed upon signalling, although both of these remain very much open questions.

Gro/TLE proteins are broadly expressed and highly pleiotropic. Alongside Wnt, they regulate other developmental signalling pathways, including Notch, playing crucial roles in body segmentation, neurogenesis and sex determination (Paroush *et al*., 1994; Nagel *et al*., 2005). The primary structure of Gro/TLE includes five regions, of which the N-terminal Q domain and C-terminal WD-repeat (WD40) domain are most highly conserved (**Fig 2.4A, B**). The Q domain contains two coiled-coil motifs that facilitate oligomerisation, whilst the WD40 domain folds to form a β-propeller that mediates numerous protein-protein interactions (Jennings & Ish-Horowicz, 2008). These structured domains are linked by a flexible region containing the GP, CcN and SP motifs (**Fig 2.4A**).

The repressive function of Gro/TLE is dependent on a combination of histone modifications and local changes to chromatin structure (**Fig 2.4C)**. Gro/TLE does not interact with DNA

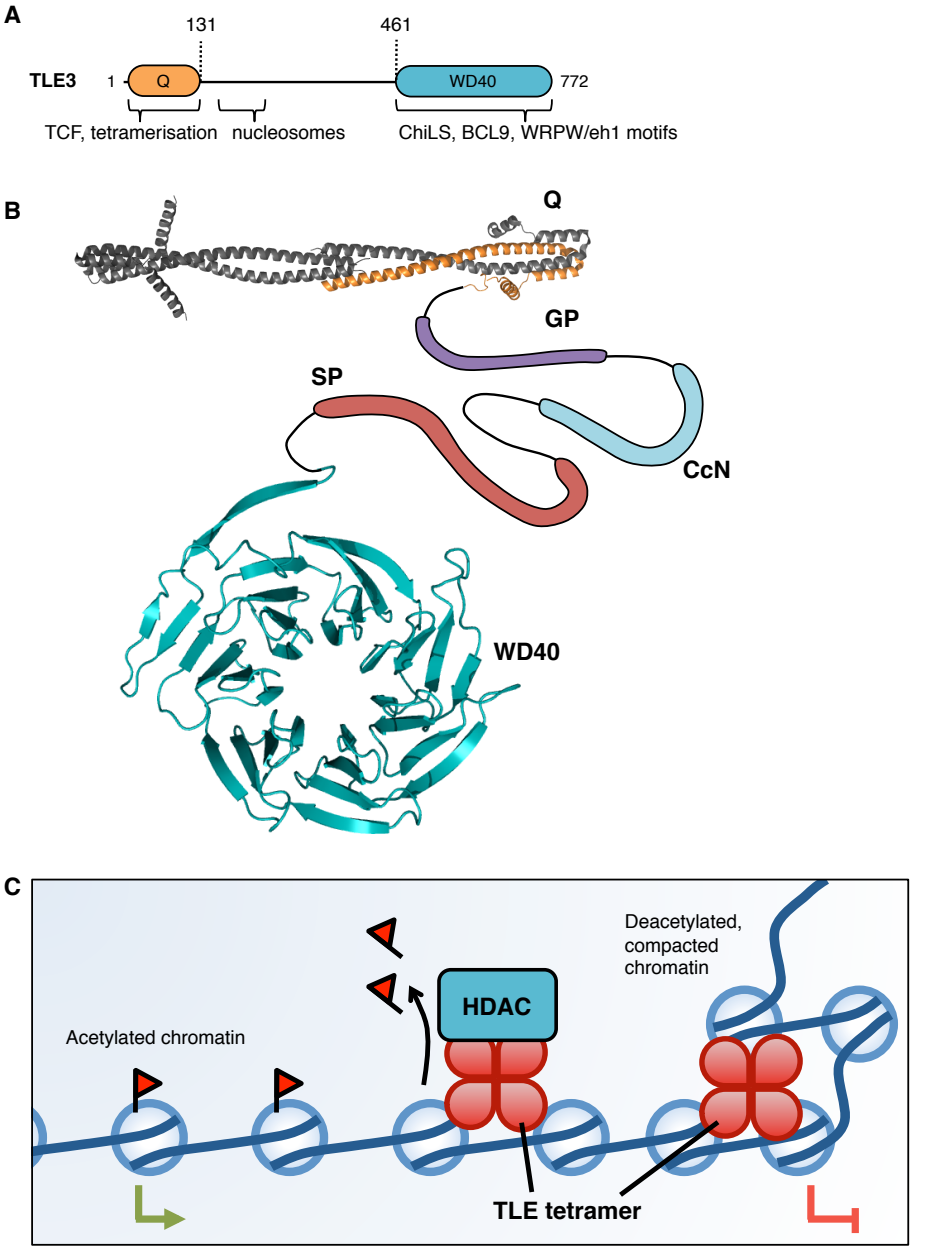

Figure 2.4 Structure and function of Gro/TLE.

(A) Domain architecture and key interactions of TLE3.

(B) Structure of TLE, incorporating crystal structures of the tetrameric N-terminal Q domain (monomer shown in orange; Chodaparambil *et al.*, 2014) and C-terminal WD40 (Pickles *et al.*, 2002). No structures have been solved for the largely unstructured linker between the Q and WD40 domains, although it contains several regions of interest. Adapted from Buscarlet & Stifani, 2007. PDB: 4OM3, 1GXR.

(C) Model of Gro/TLE-dependent transcriptional repression. Gro/TLE recruits HDAC complexes which remove activatory modifications to histone tails, whilst also contributing to the generation of a repressive chromatin state through physical interaction of Gro/TLE tetramers with multiple nucleosomes. See text for more details.

directly, and instead is localised to Wnt-responsive enhancers via the interaction of its Q domain with TCF/LEF (Cavallo *et al.*, 1998; Chodaparambil *et al.*, 2014). Histone deacetylase (HDAC) complexes are then recruited via the GP region to mediate transcriptional repression

(Chen *et al.*, 1999; Arce *et al.*, 2009). However, Gro/TLE is also able to directly bind to histones, potentially leading to nucleosome clustering (due to the oligomeric nature of Gro/TLE). The determinants of this interaction remain controversial, with conflicting reports both implicating and dismissing a role for the Q domain in histone binding (Flores-Saaib & Courey, 2000; Sekiya & Zaret, 2007). Whatever the mechanism, it is clear that Q domain tetramerization is absolutely required for transcriptional repression, even though dimerisation appears to be sufficient for interaction with TCF/LEF (Chen *et al.*, 1998; Song *et al.*, 2004). The WD40 domain, meanwhile, assists in anchoring Gro/TLE to the Wnt enhanceosome through multivalent interactions with the ChiLS complex, as well as BCL9/B9L (Fiedler *et al.*, 2015; van Tienen *et al.*, 2017). This domain also interacts with transcription factors containing characteristic WRPW or eh1 motifs (such as Engrailed and Goosecoid) via the central pore region of the propeller, integrating Gro/TLE-dependent repression with other positional inputs and providing a means for cross-talk between pathways (Jimenez *et al.*, 1999; Jennings *et al.*, 2006). Interestingly, a large number of WD40 domains are able to bind ubiquitin (Pashkova *et al.*, 2010), although this has not been demonstrated for Gro/TLE.

The Wnt transcriptional switch is thus controlled by the opposing effects of β-catenin and Gro/TLE. Transcriptional activation by β-catenin requires the inactivation of Gro/TLE, but how this takes place is largely unknown. Early models, based on *in vitro* data, suggested that β-catenin might simply outcompete Gro/TLE for binding to TCF (Daniels & Weis, 2005), but this is inconsistent with the lack of overlap between the β-catenin and Gro/TLE binding sites on TCF/LEF (van de Wetering *et al.*, 1997; Brantjes *et al.*, 2001). Indeed, a subsequent study from the same group demonstrated that β-catenin and a Gro/TLE Q domain construct can bind LEF1 simultaneously (Chodaparambil *et al.*, 2014). Moreover, very recent evidence from the Bienz lab, employing proximity labelling methods throughout the course of Wnt induction, suggests that Gro/TLE is not removed from the enhanceosome at any stage of signalling (van Tienen *et al.*, 2017).

One potential mechanism proposed for Gro/TLE inactivation involves the RING E3 ligase XIAP (X-linked inhibitor of apoptosis), which was reported to monoubiquitylate the Gro/TLE Q domain, promoting its dissociation from TCF (Hanson *et al.*, 2012). However, this ubiquitylation was found to be independent of Wnt signalling. The authors proposed a model in which XIAP limits the amount of 'free' (non-ubiquitylated) Gro/TLE available to repress TCF, thereby maintaining a β-catenin-inducible switch. Other factors have also been implicated, including Lbx2, which activates Wnt transcriptional readouts in zebrafish, reportedly by directly binding Gro/TLE and blocking its ability to associate with TCF (Lu *et al.*, 2014). However, the mechanism by which the Wnt transcriptional switch is activated is very much an open question, and one on which this chapter is focused.

2.2 Results

2.2.1 A screen for HECT E3 ligases modulating Wnt signalling

Given the somewhat confusing state of the literature regarding the roles of HECT E3 ubiquitin ligases in control of Wnt signal transduction, I decided to clarify the roles of several candidate proteins from the enigmatic 'other HECT' subfamily (**Fig. 2.5A**) that have previously been implicated in Wnt regulation, using a small-scale deletion screen.

Employing the CRISPR/Cas9 genome editing system, I designed single-guide RNAs (sgRNAs) to induce double-strand breaks in early exons of the genes coding for these E3 ligases (Ran *et al.*, 2013). Using Western blot analysis and DNA sequencing, I confirmed that these ligases were deleted from clonal HEK293T (human embryonic kidney 293 T-antigen) cell lines (**Fig. 2.5B**; **Appendix 1**). I then sought to test Wnt responses in these edited cell lines, using a luciferase-based TCF-dependent reporter assay (SuperTOP; Veeman *et al.*, 2003) to monitor Wnt transcriptional activity in the KO cell lines after stimulation of the pathway with either Wnt3a or LiCl (which stabilises β-catenin via inhibition of GSK3; Klein & Melton, 1996).

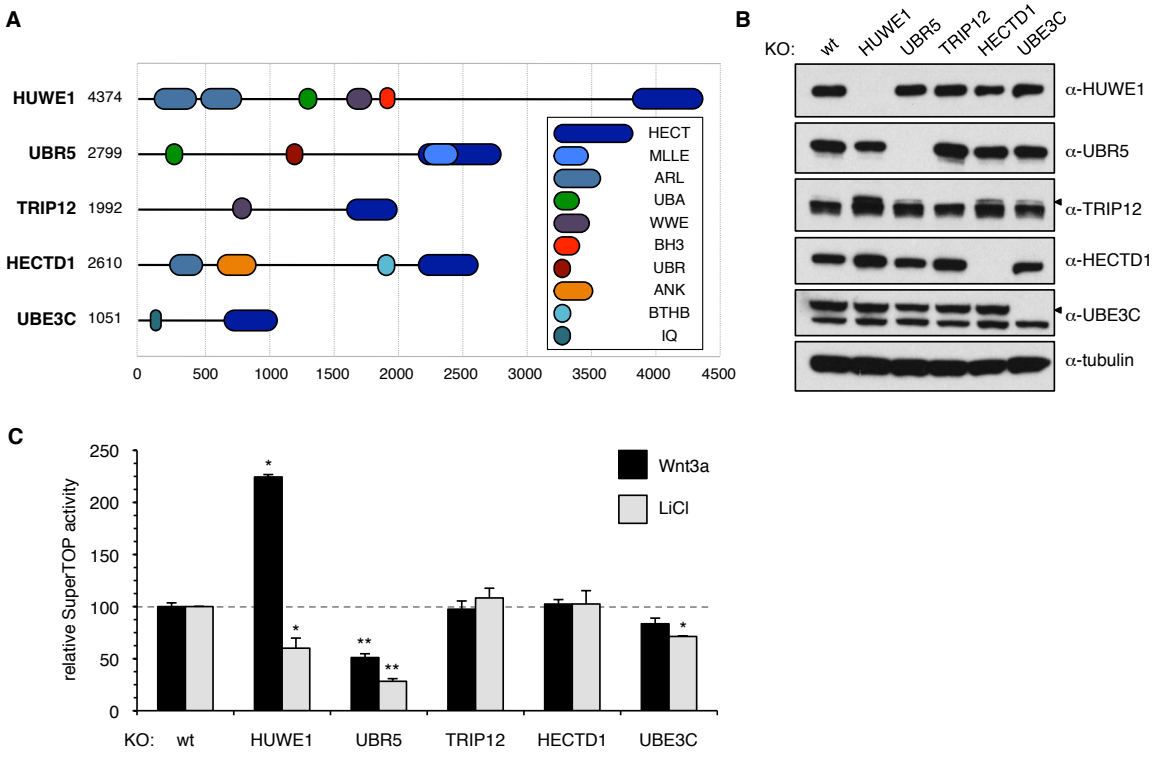

Figure 2.5 CRISPR/Cas9 screen for HECT E3 ubiquitin ligases modulating Wnt signal transduction.

(A) Domain architectures of candidate E3 ligases selected for CRISPR/Cas9 knockout.

(B) Western blots of cell lysates from KO lines (see also **Appendix 1**), probed with antibodies as indicated, to confirm absence of protein expression.

(C) SuperTOP assays to measure Wnt signalling activity in KO cell lines stimulated with Wnt3a-conditioned media or LiCl. Values are presented as mean ± SEM (n=3), relative to wt cells (set to 100).

HEK293T cell lines in which one HECT E3 ligase, UBR5, was deleted, showed significantly reduced transcriptional responses upon both Wnt3a and LiCl stimulation (**Fig. 2.5C**). Contrastingly, deletion of the other ligases (HUWE1, TRIP12, HECTD1 and UBE3C) did not reduce the response, although HUWE1 deletion caused hypersensitivity to Wnt3a, perhaps expectedly since HUWE1 has been reported to negatively regulate the upstream signalosome component Dvl (de Groot *et al.*, 2014). UBR5, uniquely among the ligases studied, is thus a candidate positive regulator of Wnt-induced transcription in human cells.

2.2.2 UBR5 is a positive regulator of Wnt signal transduction

Given my results, and the contradictory previous literature linking UBR5 to Wnt signalling (Ohshima *et al.*, 2007; Hay-Koren *et al.*, 2011), I sought to confirm the suggestion from the CRISPR/Cas9 deletion screen that UBR5 acts as a positive regulator of Wnt signal transduction.

Repeating the SuperTOP assays used for the initial screen, I found that the Wnt transcriptional output was again significantly reduced in UBR5 KO cells treated with Wnt3a or LiCl, compared to wt cells. This transcriptional response can, however, be rescued toward normal by re-expression of a GFP (green fluorescent protein)-tagged UBR5 (**Fig. 2.6A**), but not a catalytically dead UBR5 (UBR5-CS, bearing a cysteine-to-serine substitution, C2768S, in its catalytic site). Additionally, overexpression of a stabilised β-catenin construct (Δ45-β-catenin, carrying a Δ45 deletion of a key phosphodegron residue that was identified in colorectal cancer cell lines; Morin *et al.*, 1997) induces hyperactive signalling in wt cells, but this activity is significantly reduced in the UBR5 KO cells (**Fig. 2.6B**), suggesting that UBR5 functions downstream of β-catenin in human cells. Furthermore, using RT-qPCR I found that endogenous mRNA levels of the Wnt target genes *NKD1*, *AXIN2*, and *SP5* (Hanson *et al.*, 2012; Lustig *et al.*, 2002; see also **Appendix 2**) are less inducible in LiCl-stimulated UBR5 KO cells compared to wt controls (**Fig. 2.6C**).

In order to minimise potential off-target effects of the CRISPR/Cas9 editing process (which involves the growth of clones from single cells), I further confirmed that an independently isolated UBR5 KO line behaves the same way in SuperTOP assays (**Fig. 2.6D**). Taken together, these results confirm that UBR5 does indeed function as a positive regulator of Wnt signalling, at a downstream step of signal transduction, and that this function is dependent upon its catalytic activity as a ubiquitin ligase.

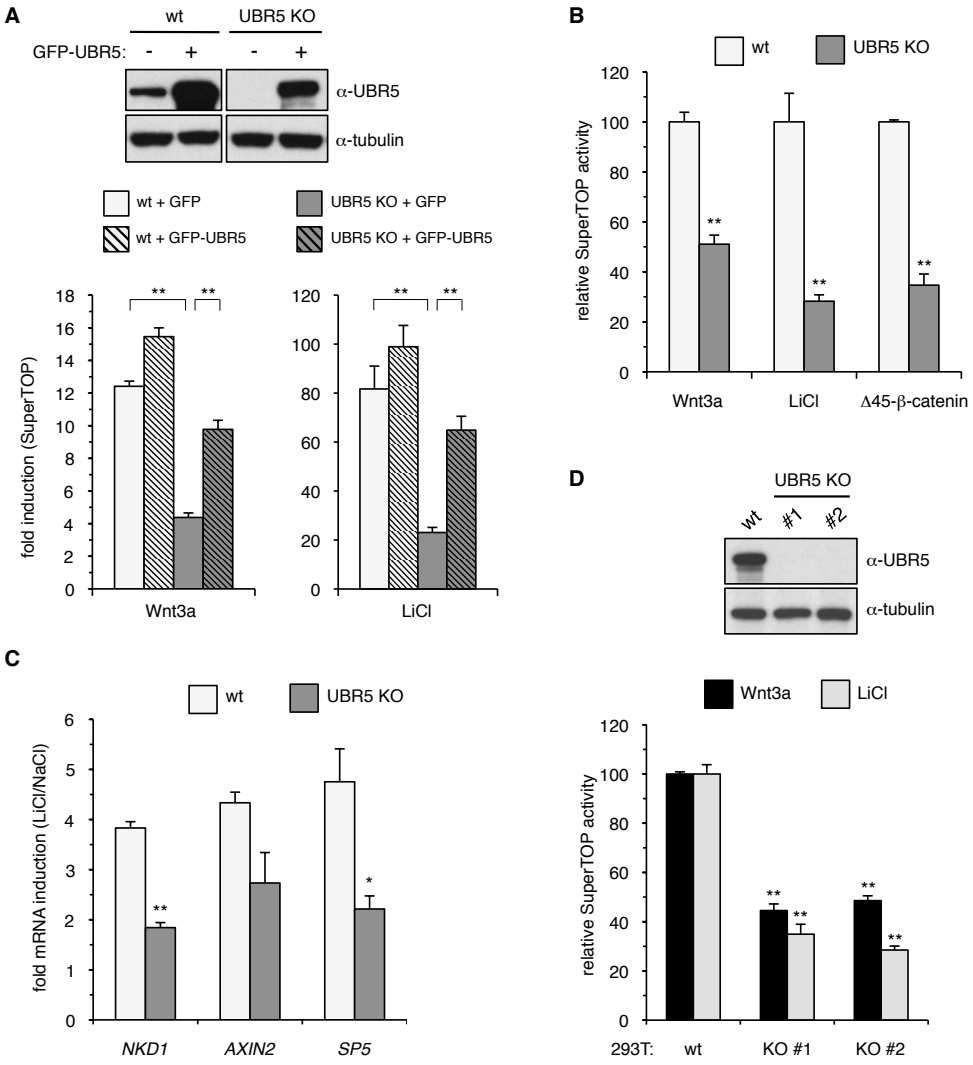

Figure 2.6 UBR5 is a positive regulator of Wnt signal transduction.

(A) Overexpression of UBR5 rescues the signalling defect in UBR5 KO cells. Top: Western blots of lysates from wt and KO cells, expressing proteins as indicated above, and probed with antibodies as indicated on the right. Bottom: SuperTOP assays to measure signalling activity in these conditions upon (left) Wnt3a or (right) LiCl stimulation. Values are presented as mean ± SEM (n=3), relative to unstimulated cells (set to 1).

(B) SuperTOP assays measuring signalling responses to Wnt3a, LiCl and overexpressed Δ45-β-catenin in wt and UBR5 KO cells. Values are presented as mean ± SEM (n=3), with wt cells set to 100 in each case.

(C) RT-qPCR assays to quantify mRNA levels of Wnt target genes in wt and UBR5 KO cells treated with LiCl. Values were normalised to *PMM1* levels and presented as mean ± SEM (n=3), relative to NaCl treated cells (set to 1).

(D) Top: Western blots of lysates from wt and two different UBR5 KO cell lines. Bottom: SuperTOP assays, as above, in these cell lines. Values are presented as mean ± SEM (n=3) relative to wt cells (set to 100).

2.2.3 UBR5 function is conserved in *Drosophila melanogaster*

Given my results implying a role for UBR5 in Wnt signalling in cells, we looked to confirm these findings in an animal model by studying the role of the UBR5 homolog, Hyd in Wnt pathway regulation in *Drosophila melanogaster*. All fly genetics, crosses, and analyses were carried out by Juliusz Mieszczanek.

We examined the consequences of loss of Hyd on Wnt (termed Wingless (Wg) in the fly) responses by generating *hyd* mutant clones in wing imaginal discs (see **Section 4.3** for details of fly genetic analyses). *hyd* is essential for viability and germline development (Mansfield *et al*., 1994), precluding analysis of Wg responses in embryonic stages. Imaginal discs bearing *hyd* mutant clones produce wings with significant margin defects and ectopic bristles, similar to the phenotype observed with *pygopus* (*pygo*) mutant clones (**Fig. 2.7A**).

In order to further assess the role of Hyd in Wg target gene expression, we stained clone-bearing wing discs for Senseless (Sens) and Wg. Wg is normally expressed in a stripe along the prospective wing margin, where it activates Sens expression in neighbouring cells, whilst inhibiting its own expression through a negative feedback loop (**Fig. 2.7B**; Rulifson *et al*., 1996). Sens expression is lost in *hyd* mutant clones near the wing margin, while Wg is derepressed within these clones, similar to the pattern seen in *pygo* mutant clones (**Fig. 2.7C, D**; Parker et al., 2002). We also stained for Vestigial (Vg), encoded by a Wg target gene expressed in a broad region straddling the margin (Schweizer *et al*., 2003), which is downregulated in *pygo* mutant clones in the prospective wing blade (Fiedler *et al*., 2015), and likewise in *hyd* mutant clones (**Fig. 2.7E**). In other words, *hyd* mutant clones phenocopy *pygo* mutant clones, causing a loss of Wg responses in the wing disc.

Finally, given the similarities in the *hyd* and *pygo* mutant phenotypes, we asked whether *hyd* blocks the activity of a stabilised Armadillo construct similar to Δ45-β-catenin (called Arm^{S10}; Pai *et al*., 1997), as *pygo* has been shown to (Thompson *et al*., 2002). Indeed, *hyd* mutant clones expressing Arm^{S10} lack Sens expression and show ectopic Wg (**Fig. 2.7F**). Taken together, these *Drosophila* analyses demonstrate that *hyd* is a positive regulator of Wg signalling in the fly, which, like *pygo*, acts downstream of stabilised Armadillo.

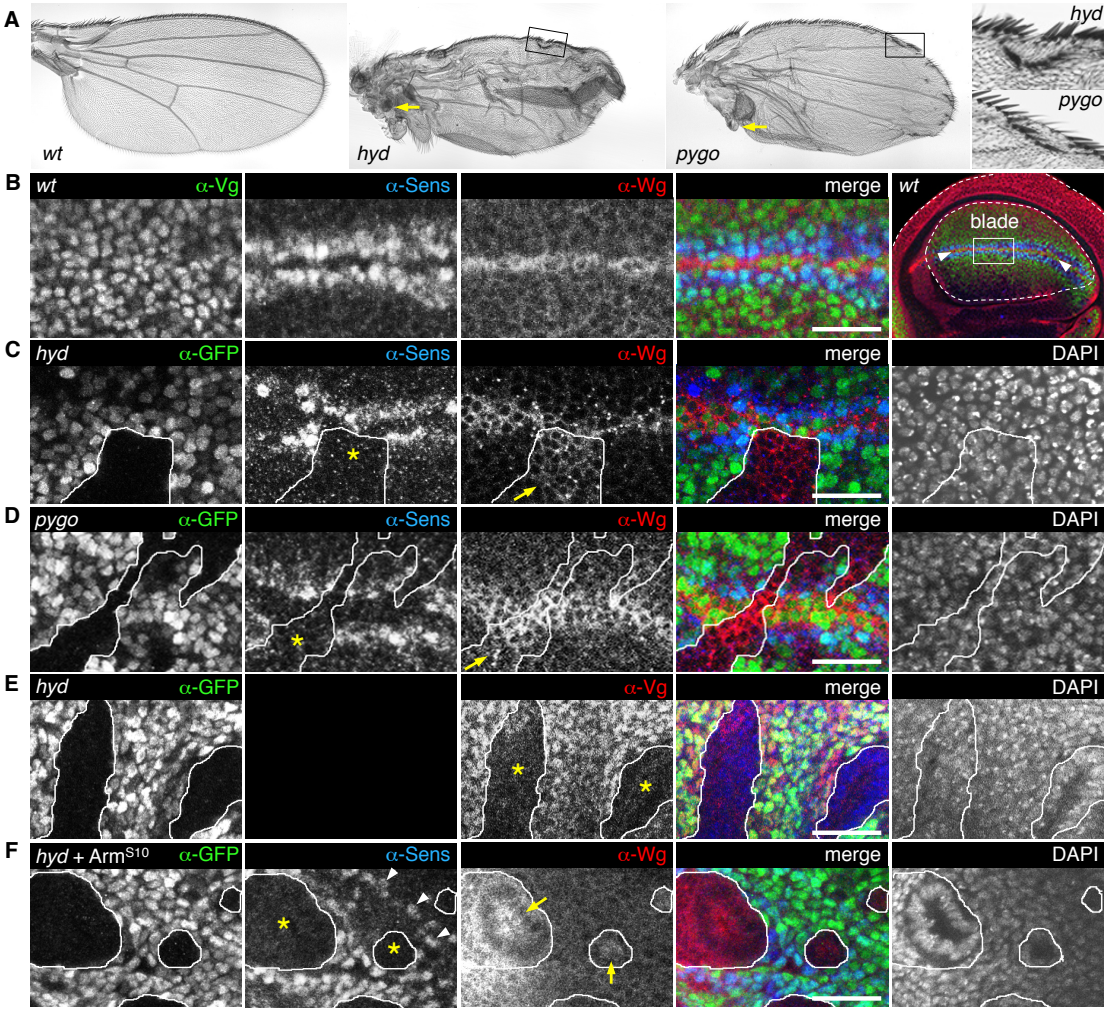

Figure 2.7 UBR5 homolog Hyd is required for Wingless signalling in *Drosophila*.

(A) Wings with mutant clones (as labelled), showing margin defects (boxed; higher magnification on the right) and overgrowths in the hinge (arrows). A wt wing is shown on the left for comparison.

(B–F) Sections of wing discs from late third-instar larvae, fixed and co-stained with DAPI (blue) and antibodies as indicated above panels: (B) wt disc (as boxed in low-magnification view on the right); discs bearing (C, E, F) $hyd^{K7\text{-}19}$ mutant clones (marked by absence of GFP, green), or (D) $pygo^{S123}$ mutant clones. (F) also expressing Arm^{S10}. Note the lack of Vg and Sens within clones near the margin (asterisks), which also show derepressed *wg* (arrows), leading to ectopic Sens in adjacent wt cells (arrowheads). Size bars, 10 μm.

2.2.4 TLE is a substrate of UBR5 upon Wnt signalling

Having confirmed that UBR5 is a positive regulator of Wnt signalling, and that its catalytic activity is required for this function, we next wanted to identify its relevant physiological substrate(s). Identification of E3 ligase substrates has traditionally been challenging, due to the weak and transient nature of ligase-substrate interactions (Iconomou & Saunders, 2016). However, we reasoned that a proteomics approach, combined with our epistasis analysis of UBR5/Hyd function and prior knowledge of Wnt enhanceosome components, could yield candidate substrates for further study. The mass spectrometry and subsequent experiments detailed in this section were carried out in collaboration with Nikola Novčić.

Our proteomics approach was based on co-immunoprecipitation (coIP) of proteins associated with UBR5, using a Flag-tagged catalytically dead version (Flag-UBR5-CS) as bait with the aim of stabilising ligase/substrate interactions and thus maximizing substrate capture (**Fig. 2.8A**, see **Section 4.11** for further details). Mass spectrometry analysis of factors co-eluted with this bait revealed a number of proteins consistently associated with UBR5, but not with the empty vector control (**Fig. 2.8B**). UBR5-specific hits identified in two independent experiments included known UBR5 substrates, including BUB1 and RANGAP1 (Jiang *et al.*, 2015a), proteins containing PAM2 motifs (known to interact with MLLE domains; Kozlov *et al.*, 2010) such as ATXN2L, as well as several proteins previously unlinked to UBR5. The only known Wnt enhanceosome component identified was TLE3, albeit with low counts. This potential association was intriguing given the essential role TLE plays as a co-repressor of Wnt-dependent transcription. Although there are four isoforms of TLE in humans (known as TLE1-4) with different expression patterns (see for example Cloonan *et al.*, 2008), these proteins are very closely related in sequence and significant differences in their molecular function would not be expected (Gasperowicz & Otto, 2005). I thus focused on TLE3 for the majority of the subsequent experiments.

Immunofluorescence experiments to study the subcellular localisation of UBR5 confirmed that both endogenous and overexpressed GFP-UBR5 are confined to the nucleus (**Fig. 2.8C**), as expected (Henderson *et al.*, 2002), suggesting that most physiological substrates of UBR5 ought to be nuclear proteins. In order to confirm the association indicated by our proteomics analysis, I performed coIP assays in UBR5 KO HEK293T cells expressing GFP-tagged UBR5-CS and HA-tagged TLE3 (**Fig. 2.8D**). A weak, but seemingly robust interaction was detected between GFP-UBR5-CS and HA-TLE3, but not with GFP alone. Intriguingly, this interaction was significantly stabilised upon Wnt pathway stimulation with LiCl.

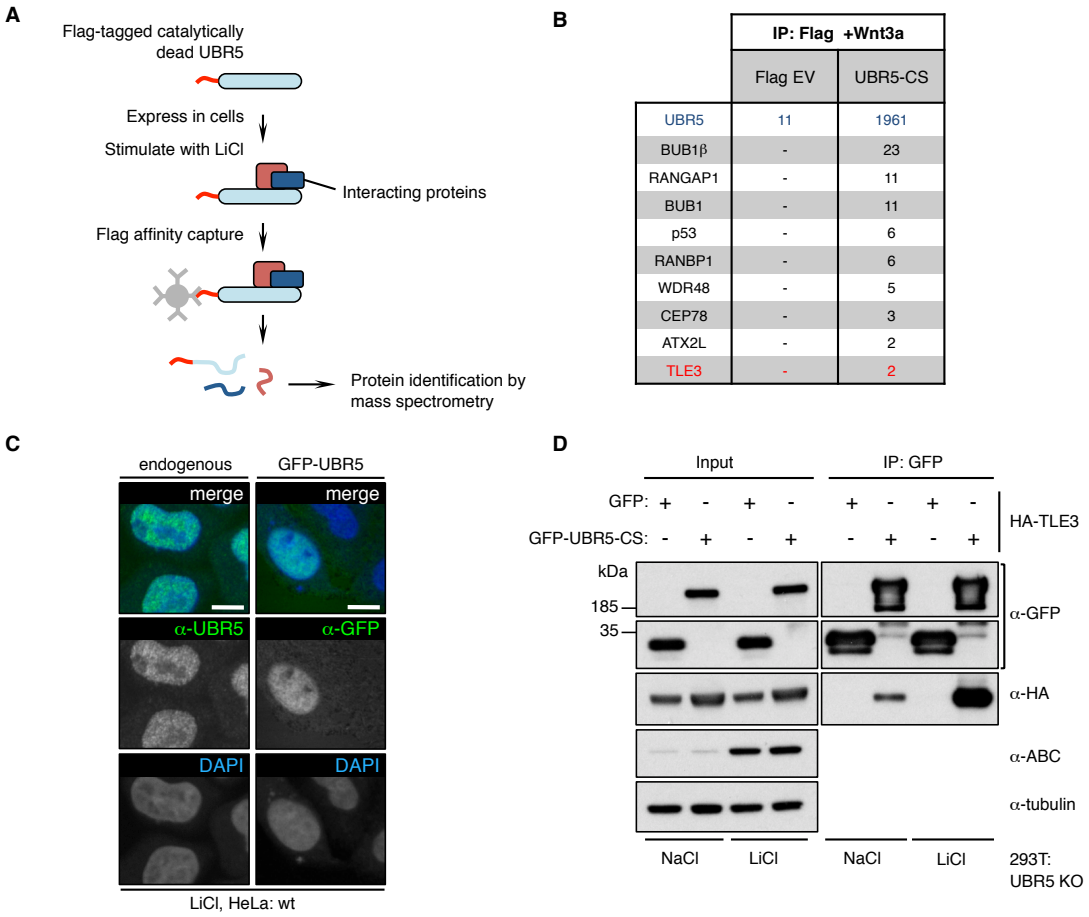

Figure 2.8 Proteomics identifies TLE3 as a UBR5-interacting protein.

(A) Outline of the Flag-affinity purification strategy used to identify candidate interacting proteins/substrates of UBR5.

(B) Table of selected proteins identified by mass spectrometry. Values represent total unweighted spectral counts (>95% probability).

(C) Confocal sections through HeLa cells, with or without co-expression of GFP-UBR5, co-stained with DAPI (blue) and antibodies as labelled. Size bars, 10 μm.

(D) CoIP assays examining binding of UBR5 to TLE3; shown are Western blots of UBR5 KO cell lysates after co-expression of proteins, treatments, and immunoprecipitation (IP) as indicated above and below panels, probed with antibodies as indicated on the right. ABC, active β-catenin.

Given these results, we next wanted to test whether TLE is a substrate of UBR5-dependent ubiquitylation during Wnt signalling. To this end, I conducted *in vivo* ubiquitylation assays in UBR5 KO cells, expressing Myc-tagged TLE3, GFP-UBR5 (or GFP-UBR5-CS as a control) and His-tagged Ub, and following TLE3 ubiquitylation after affinity purification of ubiquitylated proteins (see **Section 4.8** for details). GFP-UBR5, but not GFP-UBR5-CS, generated a high molecular weight smear of TLE3, indicating conjugation with multiple ubiquitin moieties (Ub-TLE3). Notably, this activity was very significantly enhanced upon LiCl treatment, whilst chemical inhibition of the proteasome with MG132 had only a small effect (**Fig. 2.9A**).

Interestingly, I also detected substantial levels of LiCl-dependent Ub-TLE3 in wt HEK293T cells, but not UBR5 KO cells, in the absence of UBR5 overexpression, suggesting that endogenous UBR5 is also able to modify TLE3 with ubiquitin. Indeed, re-expression of GFP-UBR5 to near-endogenous levels restores the LiCl-induced Ub-TLE3 in these KO lines (**Fig. 2.9B**). Furthermore, endogenous TLE can also be ubiquitylated in LiCl-treated cells in a UBR5-dependent fashion, although this is technically challenging to detect (**Fig. 2.9C**). Finally, although LiCl is a potent activator of the Wnt pathway, and extremely useful from an

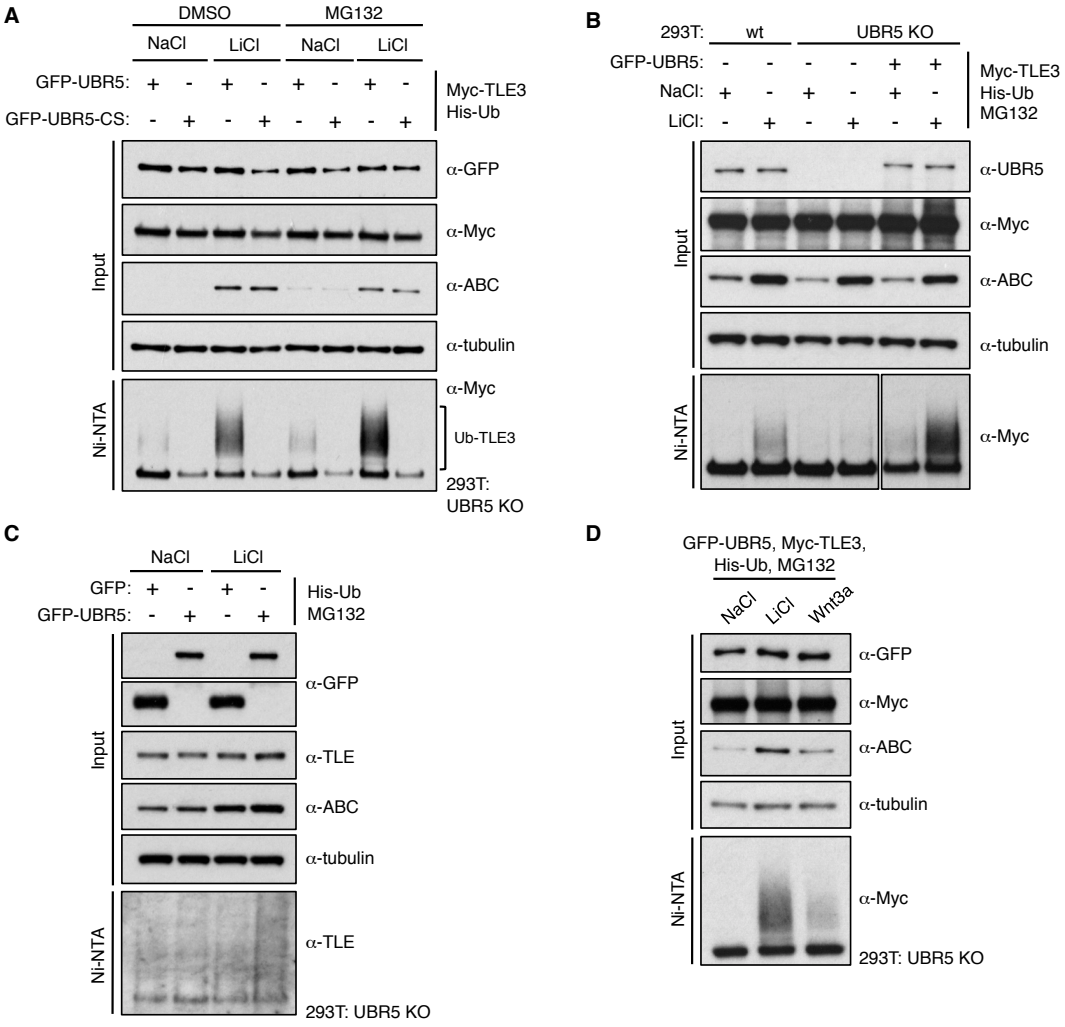

Figure 2.9 UBR5 binds and ubiquitylates TLE3 upon Wnt signalling.

(A) Assays for Ub-TLE3; shown are Western blots of UBR5 KO cell lysates, after co-expression of proteins and treatments as indicated above, and affinity purification of His-tagged ubiquitin with Ni-NTA, probed with antibodies as indicated on the right, to reveal Ub-TLE3 (highlighted with a bracket).

(B) As (A), but assaying for Ub-TLE3 by endogenous UBR5 by comparison of wt and UBR5 KO cell lines.

(C) As (A), but assaying for ubiquitylation of endogenous TLE.

(D) As (A), but after stimulation of the Wnt pathway with LiCl or Wnt3a-conditioned media.

experimental point of view, I also wanted to confirm that a physiologically relevant ligand also has the same effect on TLE3 ubiquitylation. Indeed, treatment of cells with Wnt3a does induce Ub-TLE3, although the level of ubiquitylation is less pronounced, potentially reflecting the reduced levels of active-β-catenin in Wnt3a-stimulated compared to LiCl-stimulated cells (**Fig. 2.9D**).

One potential corollary of these findings is that TLE (and presumably its *Drosophila* homolog, Groucho) is inactivated during Wnt signalling by Hyd/UBR5-dependent ubiquitylation. If so, one would expect that genetic inactivation of Gro/TLE should restore Wnt responses in cells lacking Hyd/UBR5. Due to time constraints, I did not attempt to generate human cell lines in which all four TLE isoforms were deleted. However, we were able to test this in *Drosophila*, in collaboration with Juliusz Mieszczanek, by studying wing disc clones double mutant for Hyd and Gro. Indeed, we observed partial restoration of Sens expression in *hyd gro* double mutant clones (**Fig. 2.10**). Furthermore, the clones with restored Sens expression do not exhibit ectopic Wg, in contrast to *hyd* mutant clones. Hyd therefore seems to be dispensable to a significant extent for Wg responses in the absence of Gro, suggesting that Gro is indeed a functionally relevant substrate of Hyd in Wg-stimulated cells. Taken together, the striking Wnt-induced E3 ubiquitin ligase activity of Hyd/UBR5 towards Gro/TLE indicates that Gro/TLE is a physiological substrate of UBR5 in cells upon Wnt signalling.

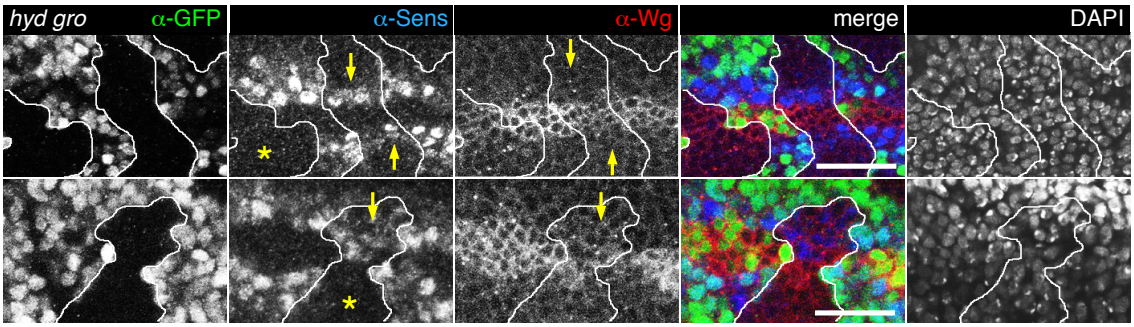

Figure 2.10 UBR5 and Groucho act antagonistically in *Drosophila*.
hyd$^{K7\text{-}19}$ *gro*^{MB36} double mutant clones, with Sens expression and Wg repression (arrows) restored within clones by Groucho loss (compare to *hyd*$^{K7\text{-}19}$ single mutant clones, **Fig. 2.7**). Asterisks mark examples of clones without restored Sens. Size bars, 10 μm.

2.2.5 β-catenin apposes UBR5 and TLE

Having established that Gro/TLE is a substrate of UBR5, I next wished to investigate the mechanism underlying the remarkable Wnt-dependency of TLE ubiquitylation. Our epistasis analyses in human cells and *Drosophila* indicated that UBR5 acts below β-catenin in the Wnt pathway (**Fig. 2.6B, 2.7F**). I therefore asked whether β-catenin alone could induce UBR5-dependent Ub-TLE3, by overexpressing Δ45-β-catenin in UBR5 KO cells, with or without GFP-UBR5, and monitoring Ub-TLE3. TLE3 ubiquitylation was indeed induced by expression of Δ45-β-catenin to a similar level as by LiCl treatment (**Fig. 2.11B**).

I initially considered two models that could explain these data. The first, 'activation' model, supposes that UBR5 is somehow autoinhibited, and that its activation directly or indirectly requires β-catenin. However, UBR5 is perfectly able to modify other substrates, such as PAIP2, in the absence of Wnt signalling (Shearer *et al.*, 2015, Yoshida *et al.*, 2006). I confirmed that Flag-UBR5 can efficiently ubiquitylate HA-PAIP2 in the presence or absence of LiCl stimulation (**Fig. 2.11C**), suggesting that UBR5 is intrinsically catalytically active and does not require disinhibition by β-catenin.

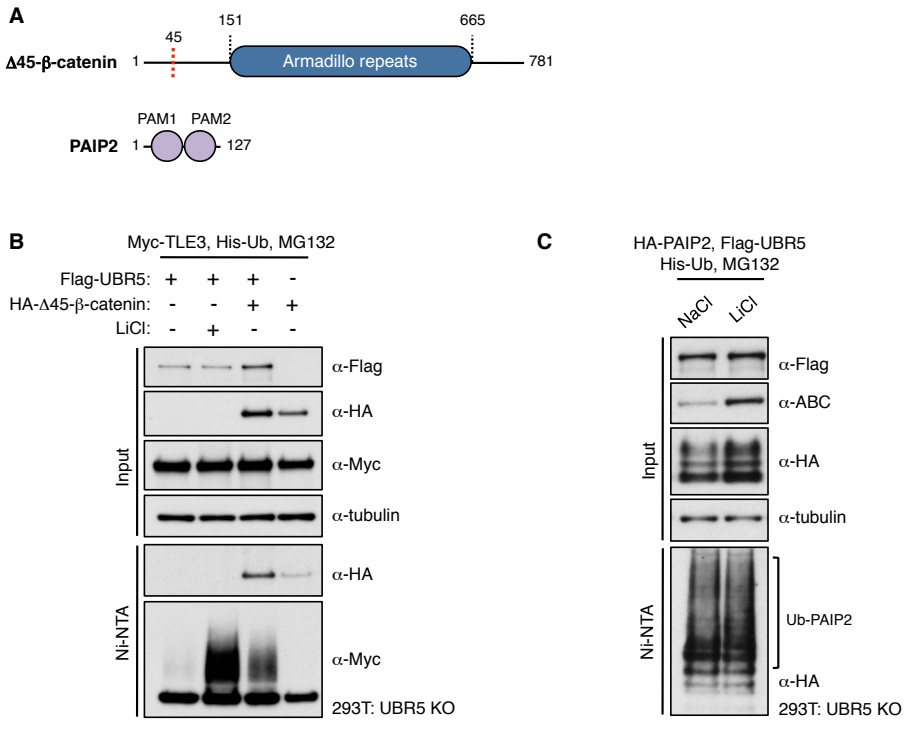

Figure 2.11 β-catenin activates UBR5 towards TLE.
(A) Domain architectures and mutagenesis of proteins expressed in these experiments.
(B) Assays for Ub-TLE3 as previously; shown are Western blots of UBR5 KO cell lysates, after co-expression of proteins and treatments as indicated above, and affinity purification of His-tagged ubiquitin with Ni-NTA, probed with antibodies as indicated on the right.
(C) As (B), but assaying for Ub-PAIP2.

In contrast, the 'recruitment' model supposes that stabilised β-catenin binds to UBR5 and apposes it to TLE3, thereby directing its E3 ubiquitin ligase activity toward its substrate. If this was the case, one would expect that the interaction of UBR5 with TLE3 should be enhanced upon Wnt signalling, as previously observed (**Fig. 2.8D**). In support of this model, endogenous β-catenin coIPs with GFP-UBR5-CS, but transient depletion of β-catenin by CRISPR/Cas9 completely blocks this interaction, and also abrogates binding of UBR5 to TLE3 (**Fig. 2.12A**). Furthermore, this 'recruitment' would appear to occur within the context of the Wnt enhanceosome: Flag-UBR5-CS coIPs with GFP-tagged enhanceosome components TCF4 and PYGO1, regardless of LiCl stimulation (**Fig. 2.12B, C**).

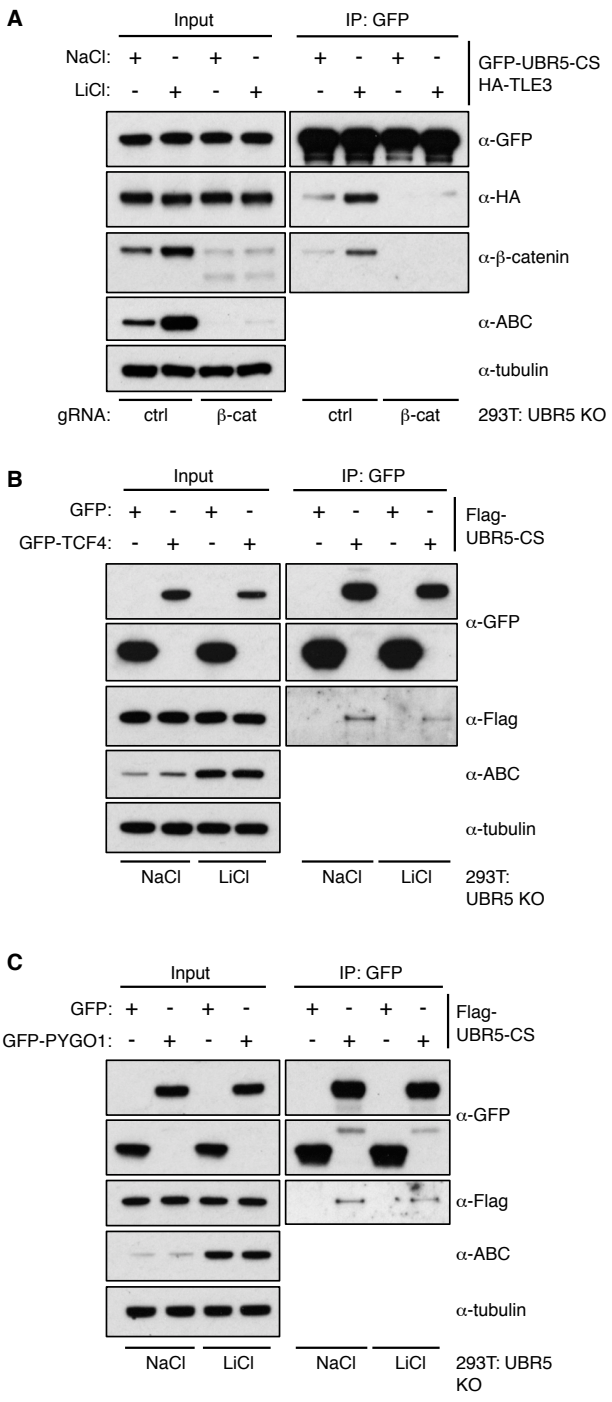

Figure 2.12 β-catenin binds UBR5 and apposes it to TLE.

(A) CoIP assays examining binding of UBR5 to β-catenin; shown are Western blots of UBR5 KO cell lysates, after transient knockdown of β-catenin by CRISPR/Cas9 (or control treatment), co-expression of proteins, treatments, and IP as indicated above and below panels, probed with antibodies as indicated on the right.

(B-C) CoIP assays as previously, examining (B) binding of TCF4 or (C) PYGO1 to UBR5.

2.2.6 UBR5 decorates the TLE WD40 domain with K48-linked polyubiquitin

Having established how Wnt signalling triggers the ubiquitylation of TLE by UBR5, I sought to understand how this modification might lead to inactivation of TLE, a key requirement for activation of Wnt target genes. I thus looked to characterise the ubiquitylation of TLE by UBR5, hoping that this might provide insight into such a mechanism.

I first mapped the domain of TLE3 that is the substrate of UBR5-dependent ubiquitylation by expressing different TLE3 truncations (**Fig. 2.13A**) and testing them for UBR5-dependent ubiquitylation in LiCl-stimulated cells. These experiments revealed that the C-terminal WD40 domain is both necessary and sufficient for ubiquitylation (**Fig. 2.13B**). Furthermore, HA-tagged WD40 domain coIPs with GFP-UBR5-CS at a similar level to wt TLE3, in contrast to a ΔWD40 construct, and this interaction is enhanced by LiCl (**Fig. 2.13C**). TLE3 thus appears to interact with UBR5 via the WD40 domain, which becomes ubiquitylated as a result.

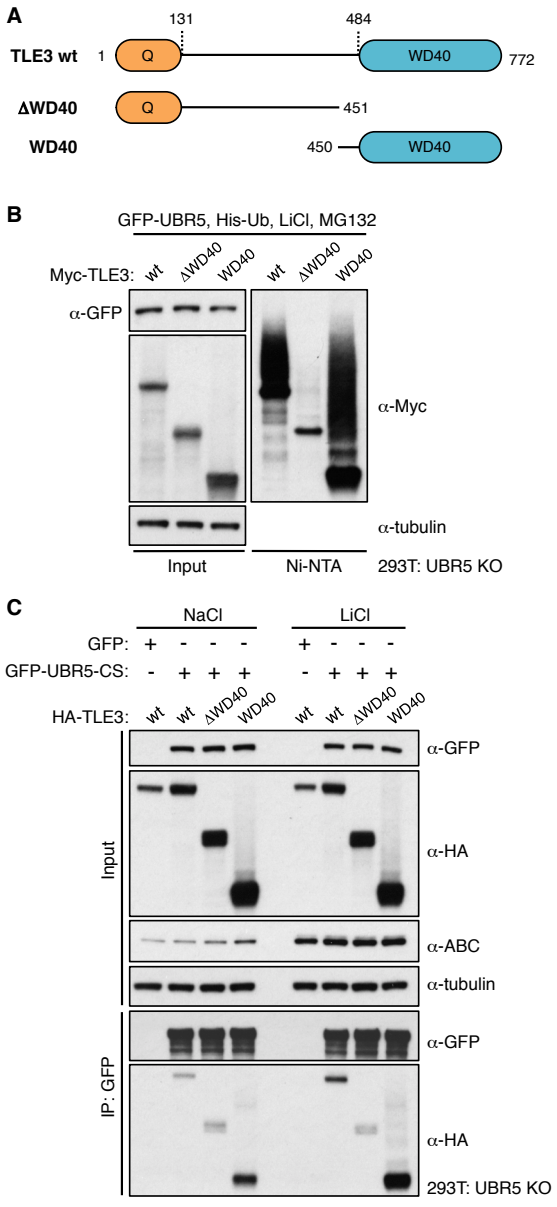

I next wondered what polyubiquitin linkage types were assembled on the WD40 domain by UBR5, given that previous analysis of UBR5 linkage specificity was not definitive (Hay-Koren *et al.*, 2011; **Section 2.1.3**). In collaboration with Nikola Novčić, I carried out *in vitro* autoubiquitylation assays (see **Section 4.15** for details) with bacterially expressed UBR5 HECT domain ($UBR5_{2217-2799}$, either wt, or bearing a C to S catalytic site mutation; **Fig. 2.14A**) and K-only Ub mutants (bearing arginine-to-lysine substitutions of all but one lysine). Catalytically active

Figure 2.13 UBR5 ubiquitylates the WD40 domain of TLE3.
(A) Domain architecture of TLE3 wt and mutant constructs used in these experiments.
(B) Assays for Ub-TLE3 as previously, using the TLE3 constructs illustrated in (A).
(C) CoIP assays as previously, again using the TLE3 constructs illustrated in (A).

UBR5 HECT domain autoubiquitylated with wt or K48-only Ub, but not with any of the other K-only Ub mutants (**Fig. 2.14B**). Consistent with this, pilot analysis of affinity-purified Flag-TLE3 by mass spectrometry revealed di-Ub peptides derived exclusively from K48-linked Ub in addition to unlinked Ub peptides (data not shown). Finally, I used 'UbiCRest' deubiquitylation assays (Hospenthal *et al.*, 2015), to interrogate the polyubiquitin chain types assembled by UBR5 on TLE3 itself. Attempts to cleave Ub-TLE3 with K11-, K29-, K33-, K48-, and K63-linkage specific deubiquitylases (DUBs) revealed that only the K48-specific DUB OTUB1 is significantly active toward Ub-TLE3 (**Fig. 2.14C**). Taken together, these data demonstrate that UBR5 assembles K48-linked polyUb conjugates on the TLE3 WD40 domain.

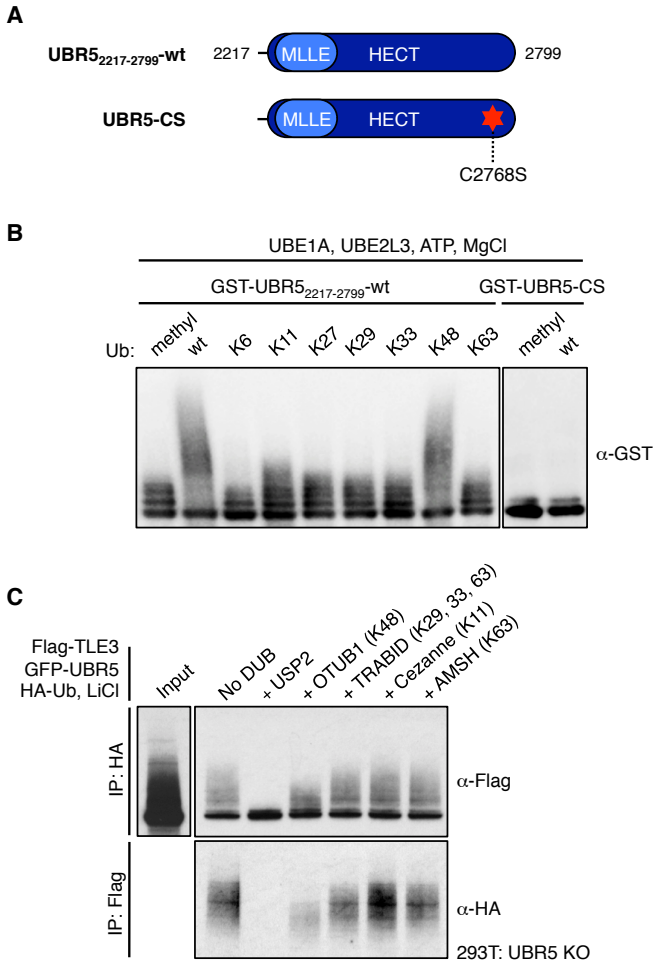

Figure 2.14 UBR5 decorates the TLE WD40 domain with K48-linked polyubiquitin.

(A) Catalytic domain constructs of UBR5 expressed in bacteria for use in these experiments.
(B) *In vitro* ubiquitylation assay with bacterially expressed GST-UBR5$_{2217-2799}$ or catalytically-inactive GST-UBR5-$_{2217-2799}$-CS, incubated for 2 hrs with wt or methylated Ub, or with K-only Ub mutants (as indicated above), and supplemented with E1 and E2 (UBE2L3) enzymes. Shown is a Western blot probed with α-GST to recognise Ub-GST-HECT.
(C) UbiCREST assays of Ub-TLE3; shown are Western blots of UBR5 KO lysates after co-expression of proteins, treatment and IP as indicated, followed by *in vitro* treatment of IPs with linkage-specific DUBs (specificity in brackets), or USP2 (non-linkage specific control) for 45 min.

2.2.7 TLE is not destabilised by UBR5-dependent ubiquitylation

A likely implication of the K48-linkage specificity of UBR5 is that TLE is earmarked for degradation by this ubiquitylation. I thus sought to ask whether TLE levels change during Wnt signalling, and, if so, whether the presence or absence of UBR5 affects these changes. However, experiments using cycloheximide to block protein synthesis during Wnt stimulation did not reveal any differences in the steady-state levels of endogenous TLE upon LiCl stimulation, in either wt or UBR5 KO cells (**Fig. 2.15A**). The same was also true upon overexpression of GFP-tagged UBR5 (or a catalytically dead mutant as control, **Fig. 2.15B**).

These steady-state experiments corroborate with the data presented earlier, showing that the levels of Ub-TLE3 are only mildly elevated after proteasome inhibition (**Fig. 2.9A**), and the observation that Gro levels (as estimated by antibody staining) are unaltered within *hyd* mutant clones (Juliusz Mieszczanek, data not shown). While these data would suggest that proteasomal degradation is not the primary mechanism by which UBR5 inactivates Gro/TLE, it is possible that these assays are not sensitive enough to detect UBR5-dependent destabilisation of the TCF-associated Gro/TLE (which represents only a small proportion of total cellular Gro/TLE).

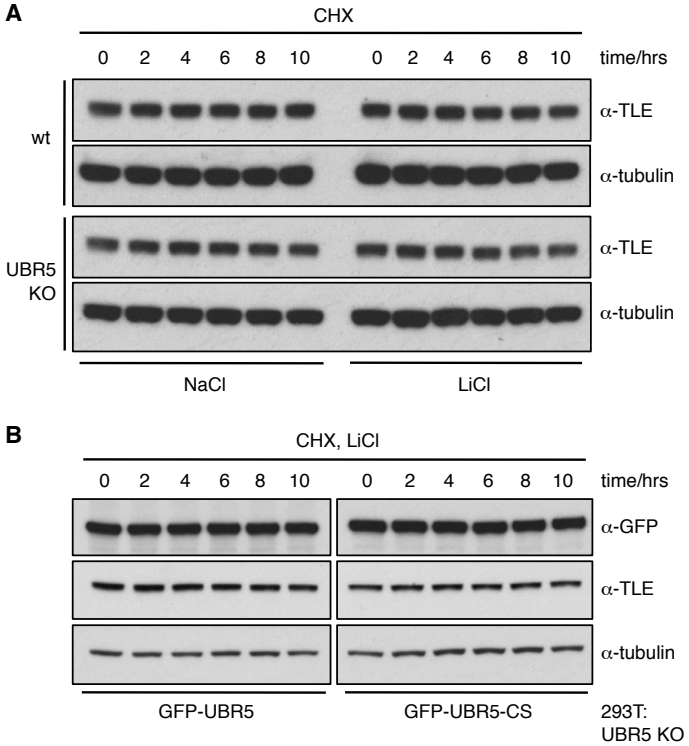

Figure 2.15 TLE is not destabilised by UBR5-dependent ubiquitylation. Cycloheximide (CHX) chase experiments to examine the stability of endogenous TLE under different conditions; shown are Western blots of lysates from (A) UBR5 KO cells or parental controls, or (B) UBR5 KO cells overexpressing GFP-UBR5-wt or CS, lysed 0-10 hrs after treatment with 50 μg ml^{-1} cycloheximide and 20 mM LiCl (or NaCl as control), probed with antibodies as indicated.

2.2.8 Ubiquitylation does not interfere with WD40-ligand interactions

Given that TLE does not seem to be targeted for degradation by UBR5, I attempted to test other possible mechanisms by which TLE ubiquitylation could lead to its inactivation. The WD40 domain is primarily a protein-protein interaction domain, employed to both anchor TLE at the enhanceosome and recruit ligands that exert a repressive function on the associated genes. I thus sought to determine which residues within the WD40 domain are modified with Ub, and test whether these individual modifications might have an effect on the capacity of the WD40 domain to bind to its cognate ligands. The TLE3 WD40 domain contains 16 lysine residues, most of which are highly conserved between TLE orthologs (**Fig. 2.16A**).

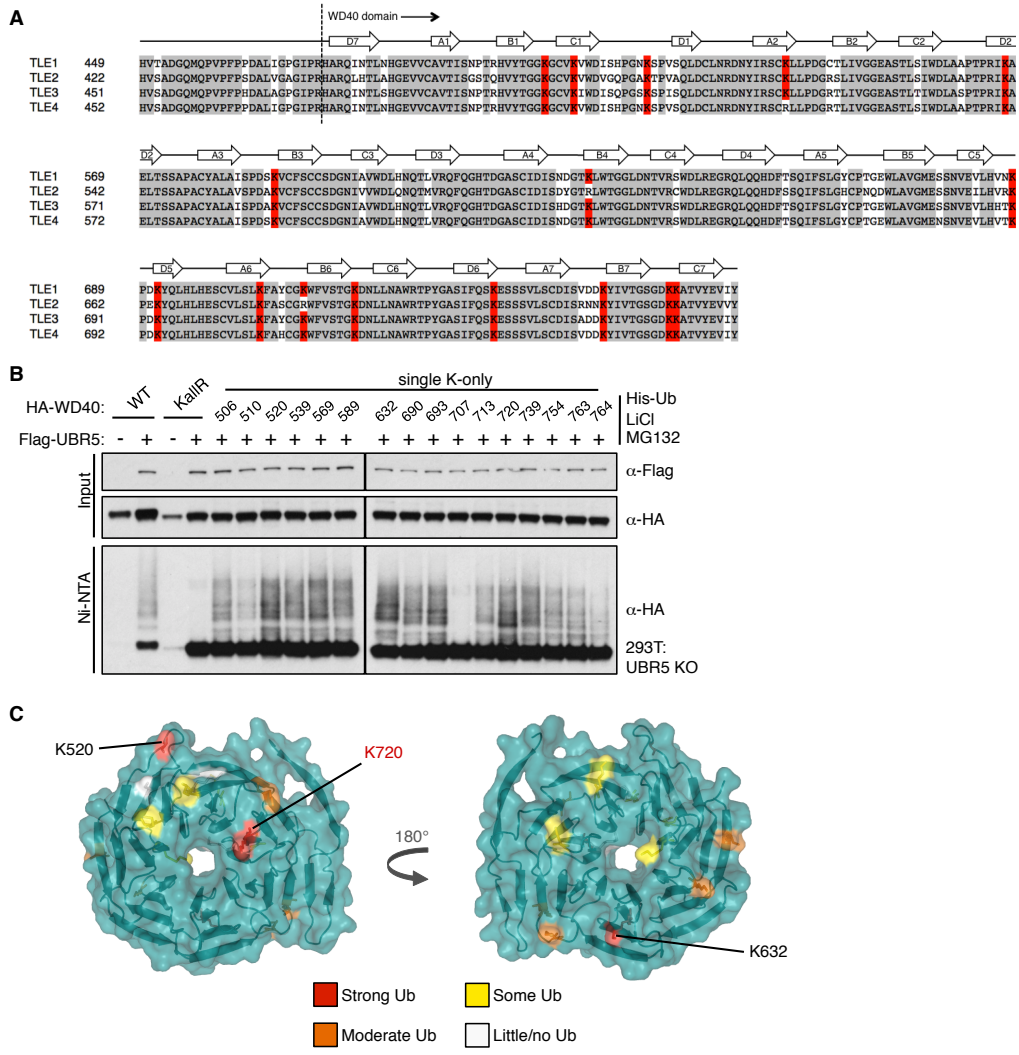

Figure 2.16 UBR5 ubiquitylates multiple WD40 residues.

(A) Sequences of WD40 domains from human TLE1-4, with conserved K residues highlighted in red.

(B) *In vivo* Ub assay in LiCl-treated UBR5 KO cells co-expressing wt or K-only HA-WD40 mutants with His-Ub, ± Flag-UBR5 as indicated; note the varying levels of ubiquitylation of the K-only mutants. KallR indicates a mutant in which all 16 K residues were substituted with R.

(C) Heat-maps of the WD40 domain (Jennings *et al.*, 2006; left, ligand-binding surface; right, reverse side), indicating Ub levels of K-only mutants shown in (B). Selected highly modified lysine residues are indicated on the structure. PDB: 2CE9.

I attempted to identify sites of Ub modification within the WD40 domain using a proteomics approach but was largely unsuccessful, likely due to my inability to obtain significant quantities of ubiquitylated material from an *in vitro* WD40 ubiquitylation assay. I therefore examined the ubiquitylation of single K-only WD40 mutants (bearing arginine-to-lysine substitutions of all but one lysine) by UBR5 *in vivo*, which showed that most of the lysine residues within the WD40 domain can be efficiently ubiquitylated, with K520, K632 and K720 proving the strongest ubiquitin acceptors (**Fig. 2.16B, C**). Notably, K720 is located close to the pore region of the WD40 propeller, and is critical for binding to short C-terminal motifs in HES and RUNX proteins (Jennings *et al*., 2006). I thus asked whether WD40 modified at these residues is still able to associate with known WD40 binding partners, HES1 and the ChiLS complex (Jiménez *et al*., 1997; Fiedler *et al*., 2015). However, WD40 domain ubiquitylated *in vivo* at K520, K632 or K720 coIPs efficiently with GFP-HES1 and GFP-ChiLS (**Fig. 2.17A, B** respectively). Thus, ubiquitylation of the WD40 does not seem to interfere with the ability of this domain to bind to cognate ligands.

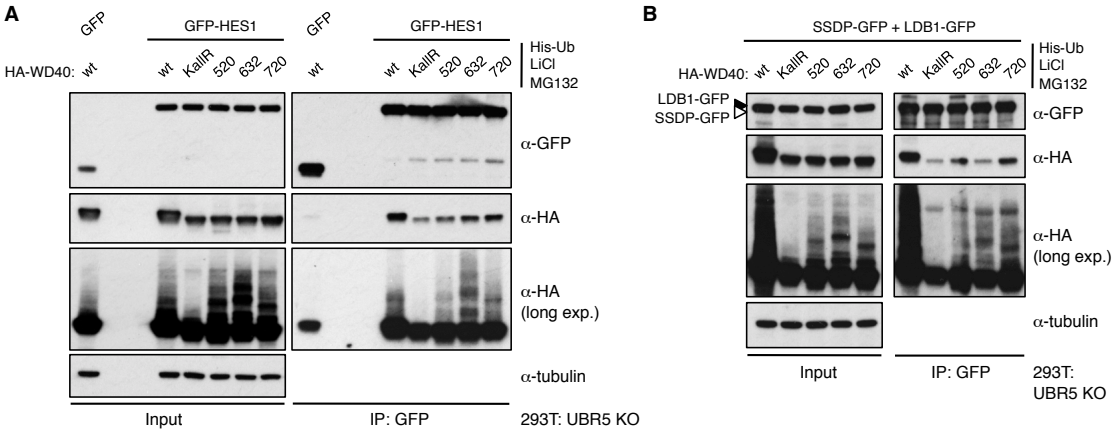

Figure 2.17 WD40 ubiquitylation does not seem to interfere with its interaction with binding partners.
CoIP assays, as previously, after co-expression of K-only HA-WD40 mutants with His-Ub and GFP-tagged (A) HES1, or (B) LDB1 and SSDP, showing comparable associations of these ligands with HA-WD40, regardless of their ubiquitylation status.

2.2.9 Ubiquitylated TLE is a substrate of VCP/p97

During my unsuccessful proteomics attempt to identify ubiquitylated residues within the C-terminus of TLE (using a Flag-tagged WD40 domain as bait), I identified peptides corresponding to VCP/p97 associated with the ubiquitylated WD40 (**Fig. 2.18B**). VCP/p97 is an AAA+ family ATPase implicated in the extraction of ubiquitylated proteins from chromatin during various nuclear processes (Dantuma *et al.*, 2014; Xia *et al.*, 2016, **Section 2.1.4**). I therefore wondered whether VCP/p97 might contribute to TLE inactivation by UBR5.

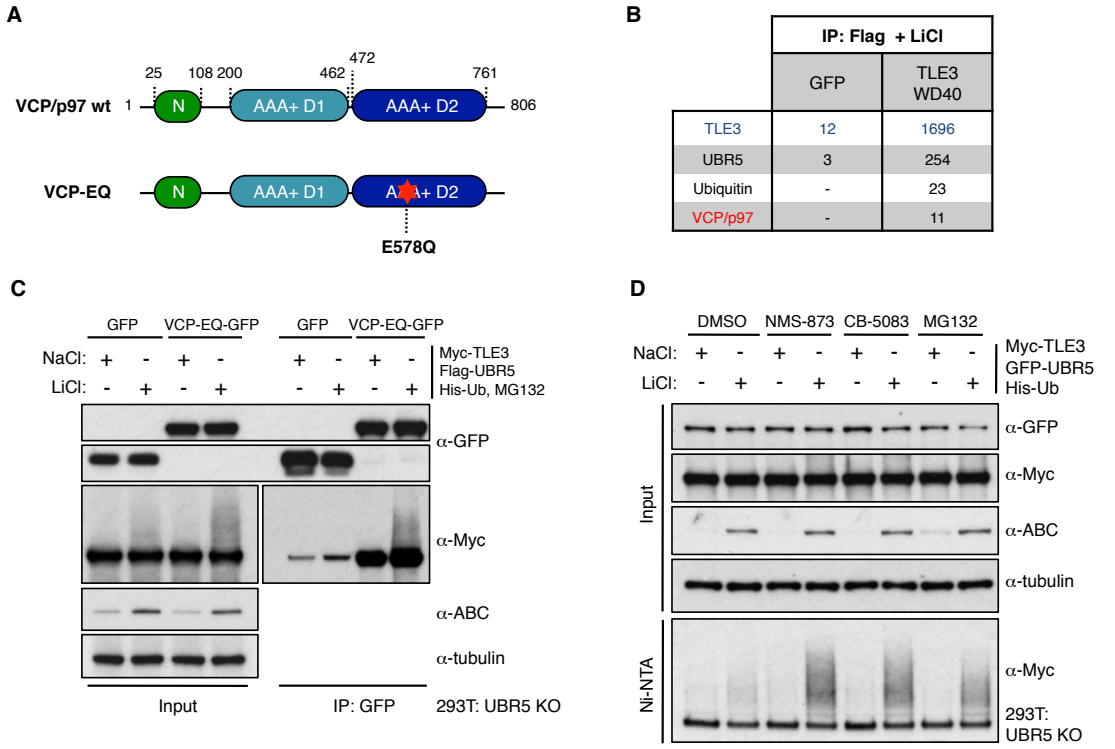

Figure 2.18 Ubiquitylated TLE3 is a substrate of VCP/p97.

(A) Domain architecture and mutagenesis of VCP/p97 constructs used in these experiments.

(B) Table of selected proteins identified by mass spectrometry after Flag-affinity purification of TLE3 WD40 domain. Values represent total unweighted spectral counts (>95% probability).

(C) CoIP assays examining binding of VCP/p97 and TLE3, using the VCP-EQ construct illustrated in (A).

(D), (E) Assays for Ub-TLE3 as previously, after (D) treatment with small molecule inhibitors of VCP/p97, NMS-873 and CB-5083 (DMSO as a negative control, MG132 for comparison), or (E) expression of dominant negative VCP-EQ.

In order to confirm the association indicated by our proteomics analysis, I performed coIP assays between a GFP-tagged catalytically dead VCP/p97 (with a point mutation, E578Q, in its D2 ATPase domain; VCP-EQ-GFP) and Myc-TLE3 (**Fig. 2.18C**). TLE3 did indeed coIP with VCP/p97, although unexpectedly this did not seem to fully depend on TLE3 being ubiquitylated. I thus asked whether VCP/p97 catalytic function is required for the removal of Ub-TLE, using two small molecule inhibitors, NMS-873 and CB-5083, with differing mechanisms of VCP/p97 inhibition (allosteric and competitive, respectively). Treatment of cells with these inhibitors indeed lead to an increase in levels of Ub-TLE3, more so than proteasome inhibition with MG132 (**Fig. 2.18D**). Inhibiting VCP/p97 function in a different way, through overexpression of VCP-EQ (which has a dominant-negative effect), was even more effective in stabilising Ub-TLE3, whilst overexpression of wt VCP/p97 had no effect (**Fig. 2.18E**). These data thus suggest that TLE becomes a substrate of VCP/p97 upon ubiquitylation.

2.2.10 VCP/p97 activity is required for Wnt signal transduction

I next asked whether the association identified between VCP/p97 activity and TLE ubiquitylation is functionally relevant for Wnt signalling. I therefore measured Wnt transcriptional output, using SuperTOP assays, in wt and UBR5 KO cells, with or without treatment with VCP/p97 inhibitors. LiCl-induced SuperTOP activity is indeed strongly reduced in wt cells upon treatment with either NMS-873 or CB-5083, but only slightly in UBR5 KO cells (**Fig. 2.19A**), as would be expected if VCP/p97 acted downstream of UBR5. SuperTOP activity is also sensitive to VCP/p97 inhibition by NMS-873 when induced by overexpression of Δ45-β-catenin (**Fig. 2.19B**), further implying that VCP/p97 activity is required for a downstream step of signal transduction. Finally, NMS-873 treatment also blocks the expression of the endogenous Wnt target genes *NKD1*, *AXIN2* and *SP5* upon LiCl treatment in wt cells, but has a reduced effect upon UBR5 KO cells (**Fig. 2.19C**). These results, and those from **Section 2.2.9** therefore implicate VCP/p97 in the inactivation of TLE by UBR5, and suggest that the ATPase activity of this chaperone is essential for Wnt signal transduction.

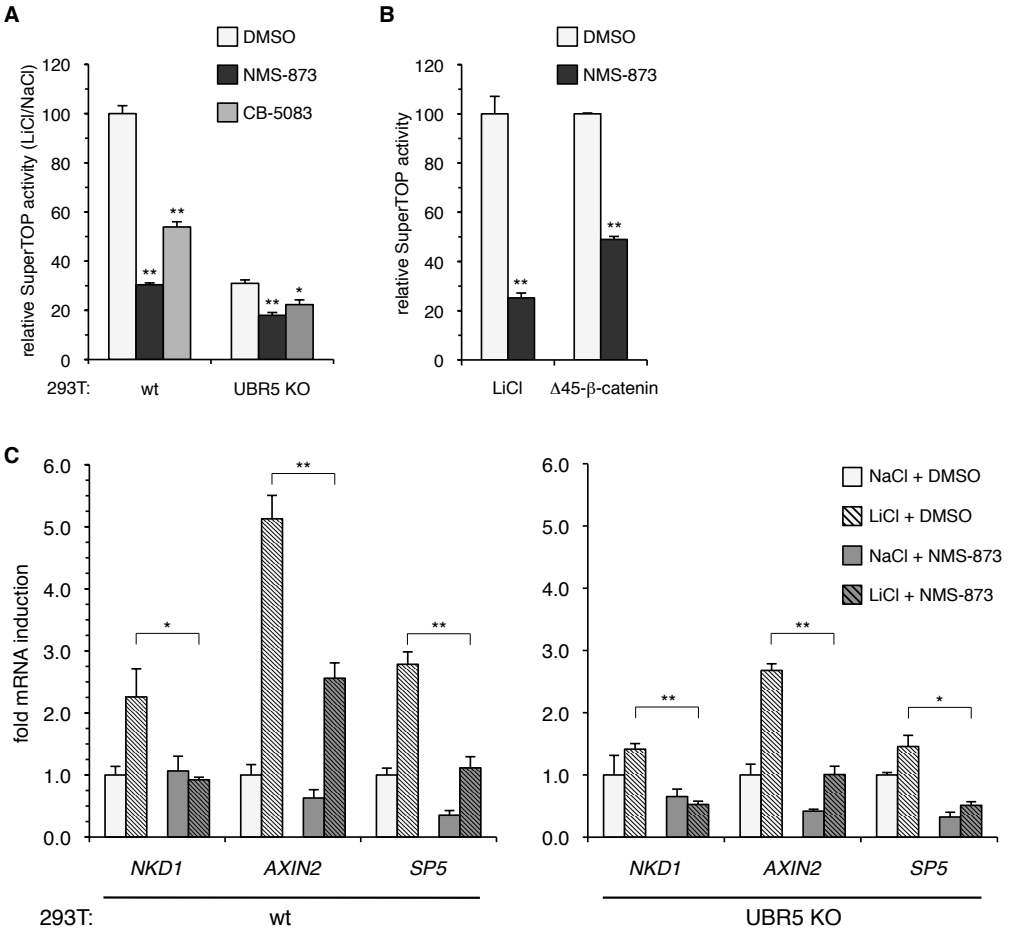

Figure 2.19 VCP/p97 activity is required for Wnt signal transduction.

(A), (B) SuperTOP assays, as previously, measuring (A) Wnt signalling activity in wt and KO cell lines stimulated with LiCl and treated with small molecule inhibitors of VCP/p97, NMS-873 and CB-5083, or (B) wt cells stimulated with LiCl or Δ45-β-catenin and treated with NMS873. Values are presented as mean ± SEM (n=3) relative to wt cells treated with DMSO (set to 100).

(C) RT-qPCR assays to quantify mRNA levels of Wnt target genes in wt and UBR5 KO cells stimulated with LiCl and treated with NMS-873 (or DMSO control). Values were normalised to *PMM1* levels and presented as mean ± SEM (n=3), relative to cells treated with NaCl and DMSO (set to 1).

2.2.11 Ubiquitylation of TLE3 by UBR5 is XIAP-independent

Previous reports have implicated the RING E3 ligase XIAP in TLE ubiquitylation and Wnt signal transduction (Hanson *et al.*, 2012, see also **Section 2.1.5**). Given this similarity with our data, I sought to ask whether XIAP and UBR5 might act on TLE in a cooperative fashion, by generating cell lines in which XIAP was deleted by CRISPR/Cas9 (as employed previously; **Section 2.2.1**). However, I found that UBR5-dependent polyUb of TLE3 is normal in XIAP KO cells, suggesting that the two ligases act independently (**Fig. 2.20A**). These data corroborated siRNA knockdown experiments previously conducted in the Bienz lab (Nikola Novčić, unpublished data). Furthermore, I noted that the reduction of Wnt-dependent transcription in

XIAP KO cells, as measured by SuperTOP assays, is significantly reduced in comparison to that observed in UBR5 KO cells (**Fig. 2.20B**). These data would suggest that XIAP plays a less significant role than UBR5 in promoting Wnt responses, although compensation (perhaps in terms of upregulation of another E3 ligase) during the process of establishing the XIAP KO cells cannot be ruled out.

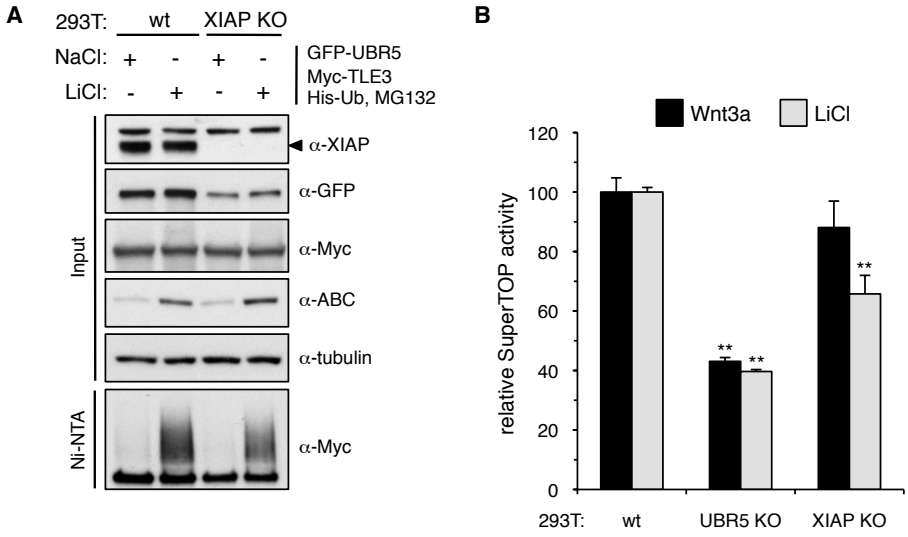

Figure 2.20 UBR5-dependent ubiquitylation of TLE3 is independent of XIAP.

(A) Ub-TLE3 assays, as previously, in wt and XIAP KO cells, showing that the UBR5-dependent ubiquitylation of TLE3 is independent of XIAP.

(B) SuperTOP assays, as previously, showing that UBR5 KO reduces the Wnt- and LiCl-inducibility of HEK293T more severely than XIAP KO. Values are presented as mean ± SEM (n=3), relative to wt cells (set to 100).

2.2.12 UBR5 is a potential therapeutic target in Wnt-driven cancers

Given our data suggesting that UBR5 is a crucial component of the Wnt transcriptional switch in HEK293T cells, which have an inducible Wnt signalling pathway, I wondered whether UBR5-dependent ubiquitylation of TLE3 also occurs in colorectal cancer cell lines that carry constitutively activating mutations of Wnt pathway components. I therefore used the CRISPR/Cas9 system to delete UBR5 in the HCT116 colorectal cancer cell line, whose Wnt pathway activity is elevated due to a Δ45 mutation of an allele of β-catenin (Morin *et al.*, 1997). Indeed, ubiquitylated TLE3 is detectable in wt HCT116 cells in the absence of any additional Wnt stimulation, but not in the UBR5 KO derivatives (**Fig. 2.21A**). Furthermore, β-catenin-dependent transcription is significantly reduced in the UBR5 KO cells, as measured by SuperTOP assays (**Fig. 2.21B**). These data suggest that, in this cell line at least, UBR5 activity is required for full Wnt signal transduction.

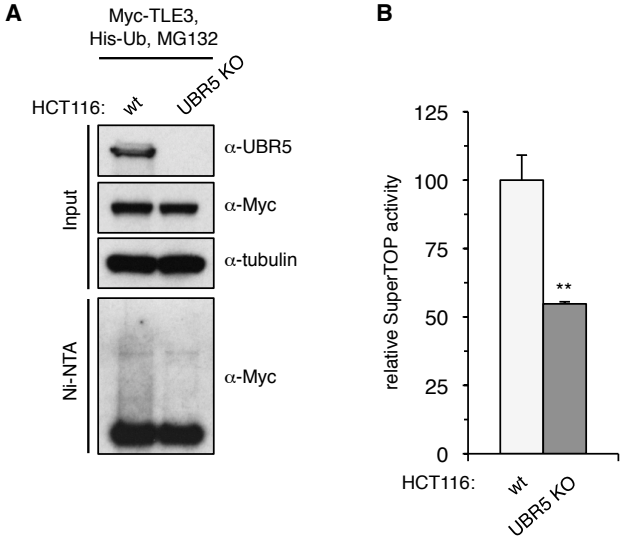

Figure 2.21 UBR5 is a potential therapeutic target in Wnt-driven cancers.
wt or UBR5 KO HCT116 cells, assayed for (A) Ub-TLE3 (as previously) or (B) SuperTOP activity. Values are presented as mean ± SEM (n=3), relative to wt cells (set to 100).

2.3 Discussion

A crucial downstream step of Wnt signal transduction is the inactivation of the transcriptional co-repressor Gro/TLE. In this chapter, I have presented evidence demonstrating a requirement for the HECT E3 ubiquitin ligase UBR5 in this process. Our data suggest that β-catenin binds to UBR5 upon Wnt signalling and directs the activity of this E3 ligase toward Gro/TLE. We further suggest that the ATPase VCP/p97 is involved in this UBR5-dependent Gro/TLE inactivation. Nevertheless, several aspects of the mechanism outlined are somewhat speculative, and numerous of features of Wnt enhanceosome regulation require further study. Alongside the discussion, suggestions for further experiments to expand on the data presented are outlined below.

2.3.1 UBR5 is a conserved positive regulator of Wnt signalling

I initially set out to identify HECT E3 ubiquitin ligases of the 'other HECT' subfamily that regulate the Wnt signalling pathway, with a particular interest in those that act at downstream steps of the pathway, using a CRISPR/Cas9 deletion screen. The rationale behind this decision was twofold. Firstly, numerous HECT ligases from this subfamily have been reported to modulate Wnt signalling, and the use of cutting-edge genome editing techniques offers an opportunity to clarify the literature regarding these large and (often) enigmatic proteins. Secondly, as enzymatic regulators of a key cancer pathway, such ligases might constitute attractive targets for therapeutic intervention in human diseases. I selected five candidate E3 ligases for deletion in HEK293T cells, based on previous reports implicating them in Wnt pathway regulation (de Groot *et al*., 2014; Hay-Koren *et al*., 2011, Tran *et al*., 2013; Wen *et al*., 2015).

My deletion screen immediately highlighted one E3 ligase, UBR5, as an interesting candidate for further study (**Fig. 2.5**). When this protein was deleted, cells showed significantly reduced responses to both Wnt3a and LiCl stimulation, thus resolving the previous inconsistency regarding the effects of UBR5 depletion on Wnt/β-catenin responses in human cell lines (Ohshima *et al*., 2007; Hay-Koren *et al*., 2011). UBR5 KO cells showed no changes in β-catenin levels, but consistently reduced Wnt transcriptional responses. These data parallel our results from *hyd* mutant clones in flies, which display a lack of expression of the Wnt target genes *sens* and *vestigial* (reminiscent of the phenotype observed in *pygo* clones; Parker *et al*., 2002), and providing unequivocal evidence for UBR5 as a positive regulator of Wnt signalling in human and fly cells. A previous report suggesting that UBR5 might negatively regulate Wnt signalling was based largely on the observation that overexpression of UBR5 leads to increased levels of co-expressed APC (Ohshima *et al*., 2007). However, we noted that upregulation of proteins co-expressed with UBR5 was a general phenomena, not specific to APC or any other factor (Joshua Flack & Nikola Novčić, data not shown). We

hypothesise that this expression artefact could be due to titration of the general translation inhibitor PAIP2 by the UBR5 MLLE domain, although this requires confirmation.

Interesting, we also found that deletion of HUWE1 caused hypersensitivity to Wnt3a, but not LiCl, in agreement with published findings that HUWE1 negatively regulates the upstream component Dvl (de Groot *et al*., 2014). HUWE1 KO HEK293T cell lines show somewhat abnormal growth phenotypes (notably a slower rate of division), potentially complicating analyses, as we and other studies have noted (Choe *et al*., 2016). However, HUWE1 clearly represents an interesting candidate for further study in the context of Wnt signalling, particularly in light of its reported role in stem cell niche maintenance and tumour suppression (Dominguez-Brauer *et al*., 2016; Dominguez-Brauer *et al*., 2017). In contrast, despite previous reports implicating HECTD1 and UBE3C in regulation of Wnt signalling, we did not find any evidence in our deletion screen for a significant role of either of these ligases. There are several potential reasons for these inconsistencies. The report implicating HECTD1 was largely based upon siRNA knockdown experiments (Tran *et al*., 2013), which can be complicated by off-target effects (Echeverri *et al*., 2006). Indeed, in the Bienz lab, siRNA knockdown of UBR5 itself proved highly unreliable (Nikola Novčić, data not shown). However, the CRISPR/Cas9 editing process itself is not risk-free, with its own problems of off-target effects, as well as the possibility of adaptation during the expansion process (which takes several weeks). Differences in the behaviour of different cell lines is also a distinct possibility, particularly in the case of UBE3C, where the previous study was conducted only in cancer cells (Wen *et al*., 2015).

2.3.2 Groucho/TLE is a substrate of UBR5

Having identified UBR5 as a positive regulator of Wnt signal transduction, we next wanted to identify the relevant physiological substrate(s) of the E3 ubiquitin ligase activity of UBR5. Using a Flag-IP-based proteomics approach, we isolated candidate interactors of UBR5, including several previously reported substrates, although the only Wnt component identified was TLE3, a homolog of the *Drosophila* co-repressor Groucho (**Fig. 2.8B**). The mechanism by which Gro/TLE is inactivated, though crucial for Wnt signalling, is unknown, and we were intrigued by a previous report that Gro/TLE ubiquitylation regulates Wnt responses (Hanson *et al*., 2012). We thus proceeded to study Gro/TLE, and found that it was robustly ubiquitylated by UBR5 upon Wnt stimulation (**Fig. 2.9A**).

Several corroborating lines of evidence suggest that Gro/TLE is indeed the physiologically relevant substrate of UBR5 during Wnt signalling. Firstly, epistasis experiments in *Drosophila* demonstrate that Hyd/UBR5 acts below Armadillo/β-catenin in the pathway (**Fig. 2.7**), implying that substrates are likely nuclear proteins (and consistent with the nuclear localisation of UBR5 itself, **Fig. 2.9C**). In *Drosophila* wing discs, Hyd is largely dispensable in

the absence of Gro (as shown by *hyd gro* double mutant clones; **Fig. 2.10**), suggesting that Hyd acts by antagonizing Gro. Finally, and crucially, the enzymatic activity of UBR5 towards Gro/TLE in human cells is highly specific, in that it only occurs upon Wnt stimulation of cells (with either Wnt3a or LiCl; **Fig. 2.9**). Our data are the first to propose Gro/TLE as a substrate of UBR5. One report previously suggested that β-catenin itself may be a substrate of UBR5 (Hay-Koren *et al.*, 2011). However, whilst we did find robust binding of UBR5 to β-catenin (either endogenous or overexpressed), we observed no UBR5-dependent ubiquitylation of β-catenin in any of our assays. It is possible that the use of a HECT domain construct tagged at the C-terminus (which is known to inactivate HECT catalytic function; Salvat *et al.*, 2004) may have affected the conclusions made by these authors. Nevertheless, we do not discount the possibility that there are other substrates of UBR5 that might contribute to its role in Wnt regulation. Indeed, Sens expression is not fully rescued in all *hyd gro* double mutant clones, implying that there might be further repressive factors that are targeted by UBR5.

2.3.3 β-catenin triggers Wnt enhanceosome rearrangements that promote UBR5-dependent modification of TLE

The β-catenin-dependency of Gro/TLE ubiquitylation by UBR5 was immediately intriguing to us, given that such mechanisms are unusual in the pathway, and indicate functional relevance. We initially considered two possible mechanisms by which β-catenin might activate UBR5 toward Gro/TLE during Wnt signalling (**Fig. 2.22A, B**). The 'activation' model supposes that UBR5 can access TLE at all times, but is normally autoinhibited, and β-catenin somehow activates the catalytic activity of UBR5. Such a mechanism would be reminiscent of the NEDD4 subfamily of HECT ligases, which are relieved from autoinhibitory interactions by the binding of NDFIP proteins (Wiesner *et al.*, 2007; Mund & Pelham, 2009; Mari *et al.*, 2014). However, the strong activity of UBR5 toward other substrates, such as PAIP2, in the absence of Wnt signalling argues against this mechanism (**Fig. 2.11C**).

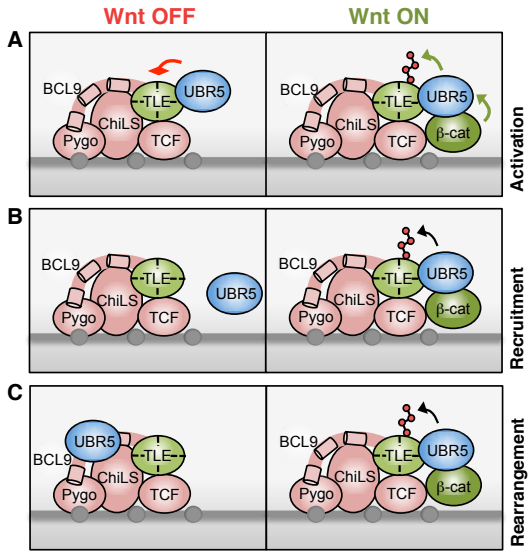

Figure 2.22 Models for Wnt-dependent ubiquitylation of Gro/TLE.
(A) 'Activation' model, in which β-catenin activates or derepresses the catalytic activity of UBR5, permitting ubiquitylation of TLE.
(B) 'Recruitment' model, in which β-catenin binds UBR5 and recruits it to the Wnt enhanceosome.
(C) 'Rearrangement' model, whereby β-catenin triggers conformational changes in the Wnt enhanceosome that leads to apposition of UBR5 and TLE. See text for more details.

In contrast, the 'recruitment' model proposes that β-catenin is required to appose an initially separate enzyme and substrate, bringing together UBR5 and Gro/TLE upon Wnt signalling. CoIP assays show that β-catenin promotes the association of UBR5 with TLE, as would be predicted by the recruitment model (**Fig. 2.11**). Unexpectedly, however, I also found that UBR5 is associated with Wnt enhanceosome components, including TCF4 and PYGO1, in a constitutive fashion. These data are in agreement with those of a recent study from the Bienz lab, which employed proximity-dependent biotin labelling methodology (BioID) to investigate the composition and structure of the enhanceosome, and which also identified UBR5 as associated with this complex in the absence of signalling (van Tienen *et al.*, 2017). Taken together, these data thus imply that UBR5 is constitutively associated with the enhanceosome, and suggest that a variation of the recruitment model, termed here the 'rearrangement' model, in fact most accurately reflects the biological mechanism. This model supposes that the recruitment and docking of β-catenin triggers conformational rearrangements within the Wnt enhanceosome that results in proximity between UBR5 and Gro/TLE (**Fig. 2.22C**). Indeed, numerous other conformational changes are also likely to occur, and further experiments are needed to understand the mechanisms by which β-catenin alters the transcriptional complexes regulating Wnt target genes.

2.3.4 VCP/p97 contributes to remodeling of the Wnt enhanceosome

Prior to this study, the mechanisms underlying the inactivation of Gro/TLE were largely unknown, in part because the methods that Gro/TLE employs in order to repress transcription are themselves unclear (Ramakrishnan *et al.*, 2017). The identification of UBR5 as a Gro/TLE-targeted E3 ligase offers a significant insight into this process, and how UBR5-dependent ubiquitylation of Gro/TLE leads to inactivation of its transcriptional co-repressor function is thus a question of critical importance.

A previous study employing single point-mutants of ubiquitin had suggested UBR5 generates atypical ubiquitin chains, linked via K11 or K27 (Hay-Koren *et al.*, 2011). However, our rigorous *in vitro* and *in vivo* ubiquitylation assays both show that UBR5 assembles predominantly K48-linked polyubiquitin (**Fig. 2.14**). The most obvious mechanism for UBR5-dependent inactivation therefore involves degradation of ubiquitylated TLE (**Fig. 2.23A**), given that these chain types constitute the archetypal signal for proteasomal targeting (Chau *et al.*, 1989). Levels of UBR5-dependent Ub-TLE3 are somewhat elevated after treatment with the proteasome inhibitor MG132, but no destabilisation of endogenous TLE was observed in cycloheximide chase experiments (**Fig. 2.15)**, arguing against rapid proteasomal degradation being the primary mechanism underlying Gro/TLE inactivation. Furthermore, the proximity labelling experiments discussed earlier found that the association of TLE with the

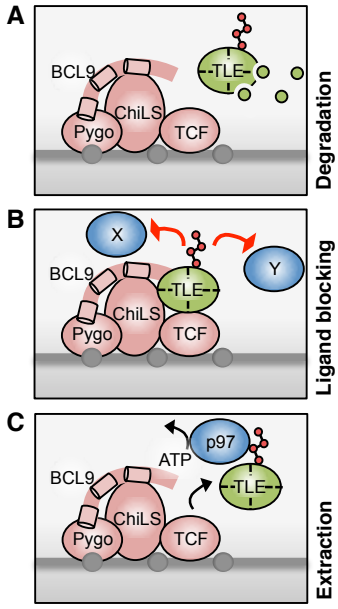

Figure 2.23 Models for inactivation of Gro/TLE by ubiquitylation.
(A) Ubiquitylation of TLE by UBR5 promotes its proteasomal degradation.
(B) Ubiquitylation of the WD40 domain prevents the interaction of this domain with binding partners, such as Wnt enhanceosome components or transcriptional co-repressors.
(C) Ubiquitylation serves to recruit an ATPase such as VCP/p97, which 'extracts' TLE from the enhanceosome or disrupts its tetrameric structure. See text for more details.

enhanceosome is not altered upon Wnt signalling (van Tienen *et al.*, 2017), although it is unclear whether this methodology is sufficient time-resolved to fully answer this question, given that certain proteins, including β-catenin, are reported to 'cycle' on and off the enhanceosome on relatively rapid timescales (Sierra *et al.*, 2006).

I was thus forced to consider alternative mechanisms by which Gro/TLE may be inactivated by ubiquitylation. Mapping experiments demonstrated that the C-terminal ligand-binding WD40 domain of Gro/TLE is the target for ubiquitylation (**Fig. 2.13**). I therefore envisaged that modification of the WD40 domain might interfere with its binding to protein partners, such as the Chip/LDB1-SSDP (ChiLS) complex, weakening the association of Gro/TLE with the Wnt enhanceosome, or with other transcriptional co-repressors (**Fig. 2.23B**). However, Ub-TLE3 appears to bind to its ligands just as efficiently as the unmodified protein. I reasoned that our samples of ubiquitylated WD40 would contain domains ubiquitylated at many different lysines, which could complicate the interpretation. Nevertheless, a single-lysine WD40 mutant that can only be ubiquitylated at K720 (a pore residue crucial for binding to WRPW/eh1 motifs; Jennings *et al.*, 2006) still binds to ChiLS and HES1, suggesting that the ubiquitin C-terminus is flexible enough to accommodate ligand binding (**Fig. 2.17**). I have thus far been unable to test whether ubiquitylation of TLE directly affects its ability to promote chromatin compaction (Sekiya & Zaret, 2007), although it seems plausible that the attachment of multiple ubiquitin chains to the WD40 domain could directly or indirectly 'loosen' the binding of Gro/TLE to nucleosomes, attenuating its ability to compact chromatin into repressive structures.

During a proteomics experiment designed to identify ubiquitylation sites within the WD40 domain, I identified peptides corresponding to VCP/p97 associated with the ubiquitylated

WD40, which was confirmed by coIP (**Fig. 2.18**). VCP/p97 is a hexameric AAA+ family ATPase known to regulate numerous ubiquitylated proteins (including components of DNA repair and chromatin complexes) by promoting their unfolding and segregation from large cellular structures (van den Boom & Meyer, 2017). I found that VCP/p97 inhibition dramatically stabilised Ub-TLE, suggesting that VCP/p97 might contribute to Gro/TLE inactivation by UBR5 (**Fig. 2.18D, E**). A recent proteomic screen for VCP/p97-associated proteins identified TLE1 and TLE3, along with several adaptor proteins and other known substrates, consistent with our proposal of Gro/TLE as a novel substrate of this ATPase (Xue *et al*., 2016). VCP/p97 activity on individual monomers is likely to trigger the destabilisation of Gro/TLE oligomers, in the similar fashion to the mechanism by which VCP/p97 promotes disassembly of a hexameric CMG helicase complex during DNA replication (Maric *et al*., 2015). Since Q domain-mediated tetramerization is absolutely required for transcriptional repression (Song *et al*., 2004; Chodaparambil *et al*., 2014), this would lead to Gro/TLE inactivation. This proposed 'extraction' mechanism (**Fig. 2.23C**) is also consistent with a recent proposal that the relief of Gro-dependent repression is based on kinetic destabilisation (Chambers *et al*., 2017), which could be facilitated by unfolding of ubiquitylated Gro/TLE by VCP/p97. Notably, this mechanism would predict that only a subset of all enhanceosome-associated Gro/TLE molecules would need to be modified by UBR5 in order that all Gro/TLE repressive function is inactivated, allowing for rapid transcriptional switching.

It is important to note that the different mechanisms discussed here are certainly not mutually exclusive, and could well be acting in a co-operative fashion. For example, VCP/p97 dependent extraction could occur rapidly upon ubiquitylation, whereas degradation might occur on a slower timescale. Furthermore, it is possible that UBR5 is not the only E3 ligase that regulates Gro/TLE. Overexpression of BCL9/B9L triggers Gro/TLE ubiquitylation in a fashion that is independent of UBR5 (Moore van Tienen, unpublished data), whilst the role of XIAP is uncertain, given that XIAP KO has little effect on Wnt responses in HEK293T cells (**Fig. 2.20**). Whatever the mechanism, we propose that disassembly of the Gro/TLE tetramer is likely to be a crucial step required for inactivation. Further experiments, designed to characterise the oligomeric state of Gro/TLE during different stages of Wnt signalling, will be required to confirm this hypothesis.

2.3.5 A model for Wnt transcriptional switching

In light of the data presented in this chapter, along with recent advances from our lab and others, we would like to present an updated model for Wnt transcriptional switching (Flack *et al*., 2017; van Tienen *et al*., 2017; **Fig. 2.24**).

In the off state, Gro/TLE tetramers are stably anchored to the Wnt enhanceosome through multivalent interactions with TCF (via the Q domain), ChiLS and BCL9/B9L (via the WD40

domain), and maintain a compact chromatin state that is non-permissive for transcription. The enhanceosome is primed for Wnt responsiveness, however, by BCL9/B9L, which is able to capture β-catenin via its free HD2 domain. Several crucial cofactors, including UBR5, as well as chromatin modifying and remodeling complexes, are located at or near the enhanceosome and are poised for activity. Upon Wnt signalling, the captured β-catenin triggers conformational rearrangements that appose UBR5 with the C-terminal WD40 domain of Gro/TLE, allowing ubiquitylation to proceed. This ubiquitylation leads to disruption of Gro/TLE tetramerization via the activity of VCP/p97, which is recruited to the K48-linked polyubiquitin. At the same time, chromatin remodeling complexes present at the enhanceosome such as SWI/SNF are activated to alleviate the repressive chromatin structure imposed by Gro/TLE, working in concert with chromatin modifying enzymes (such as the histone acetyltransferase complex, CBP/p300).

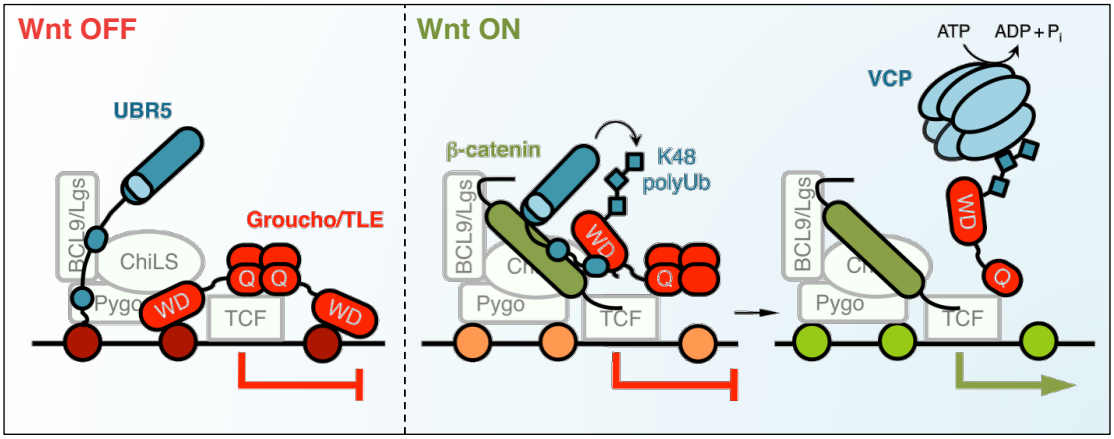

Figure 2.24 Updated model of the Wnt transcriptional switch.
In the absence of Wnt signalling, Gro/TLE tetramers represses transcription of TCF-bound Wnt target genes (nucleosomes in crimson). Upon Wnt signalling, stabilised β-catenin docks the Wnt enhanceosome and induces a conformational change (van Tienen *et al.*, 2017) resulting in the apposition of UBR5 to TCF-bound Gro/TLE, enabling it to modify this substrate with K48-linked polyUb. This renders it a substrate for VCP/p97-dependent unfolding, destabilising the Gro/TLE tetramer and relieving chromatin compaction (nucleosomes in light green), allowing transcriptional activation. See text for more details. Adapted from Flack *et al.*, 2017.

Despite advances in our understanding of this process, several aspects of this model remain unclear. **Fig. 2.24** depicts Gro/TLE molecules as remaining at the enhanceosome, as suggested by proximity-labelling experiments (van Tienen *et al.*, 2017), but in an inactive (perhaps monomeric or dimeric) state. Further experiments to determine the oligomeric state of endogenous Gro/TLE (or that expressed at near-endogenous levels) at different stages of the Wnt transcriptional cycle will be required to shed light on this issue. In similar fashion, the mechanisms that anchor UBR5 at Wnt enhancers also require further study. Interestingly,

although UBR5 is named for its characteristic UBR domain, our studies did not identify a specific role for this domain in Wnt regulation. It seems likely that regions within the UBR5 N-terminus, whether folded or not, are responsible for recruiting UBR5 to the enhanceosome, but the details of such interactions are yet to be confirmed. It would also be useful to develop new techniques to determine the constitution of the enhanceosome at a single point in time, given the low resolution that the BioID methodology has in this respect. The development of chromatin immunoprecipitation (ChIP)-quality antibodies for key enhanceosome factors will assist in this respect.

Furthermore, many questions currently remain as to how transcriptional repression is reestablished upon the cessation of Wnt signalling, and what role Gro/TLE might play in this process. In *Drosophila*, one potentially important factor might be the transcriptional repressor Brinker, which has been shown to bind the WD40 domain of Groucho through an FKPY motif and imposes silencing on Wnt-responsive elements in cooperation with another factor, Teashirt (Hasson *et al*., 2001; Saller *et al*., 2002). This could fit with a model in which Gro/TLE remains at the enhanceosome throughout the period of active Wnt signalling, and is then switched back on in order to effect transcriptional repression. How Gro/TLE might be 'reactivated' is unclear, but could involve removal of UBR5-dependent ubiquitylation by an as-yet unidentified deubiquitylase, or the 'replacement' of the ubiquitylated subset of Gro/TLE with freshly translated, unmodified molecules. Although several deubiquitylases are associated with VCP/p97, none have so far been implicated in regulation of Wnt signalling (Liu & Ye, 2012).

2.3.6 Implications for cancer therapeutics

From the data in this chapter, and our revised model for Wnt transcriptional switching, we propose that UBR5 and VCP/p97 represent candidates for further study in terms of therapeutic intervention in the Wnt pathway. As introduced (**Section 2.1.3**), UBR5 has been heavily implicated in cancer, although it is somewhat unclear whether it promotes or prevents tumour progression, and its effect may be context-dependent (Shearer *et al*., 2015). However, amplification is the predominant genetic alteration of *UBR5* identified in many types of cancers (far more so than loss-of-function mutations; Clancy *et al*., 2003), implying a tumour-promoting role that is consistent with the new role we propose it plays in relieving Gro/TLE-dependent transcriptional repression of Wnt target genes. Given our results, it will be therefore be important to test whether loss-of-function or inhibition of UBR5 inhibits Wnt-dependent tumourigenesis, as might be expected given our results in colorectal cancer cells. Proliferation of wt HCT116 cells is slowed by VCP/p97 inhibition (Magnaghi *et al*., 2013), whilst cells in which UBR5 is knocked out show attenuated Wnt-dependent transcription (**Fig. 2.21B**). It will be interesting to test whether this applies generally to other cancer cell lines that are dependent upon hyperactive Wnt signalling, colon or otherwise.

There is certainly a precedent for designing drugs that could target either UBR5 or VCP/p97. A small molecule has been identified that acts as a general inhibitor of HECT E3 ligases through oxidation of the catalytic cysteine (Mund *et al*., 2014). The unusual architecture of the UBR5 HECT domain could allow for development of a more specific therapeutic. On the other hand, CB-5083 is an orally bioavailable VCP/p97 inhibitor that is already in clinical trials (Zhou *et al*., 2015). The current rationale behind CB-5083 use is that cancer cells are under increased proteotoxic stress, and are thus highly sensitive to VCP/p97 inhibition, although how this effect would synergise with a reduction in Wnt-dependent transcription is unknown. Whether targeting these enzymes could actually have therapeutic benefits, without significant side-effects, is another matter. Organoid cultures, in which the *UBR5* or *VCP* genes could be easily manipulated using genome-editing techniques, and genetically engineered mouse models are potential tools that could be used to understand the effect of UBR5 or VCP/p97 inhibition in carcinogenesis. Indeed, one recent study hints that knockdown of UBR5 reduces the growth of colorectal tumours in a xenograft assay (Xie *et al*., 2017). Further studies using applicable models such as these will be required to validate UBR5 and VCP/p97 as new enzymatic targets for therapeutic intervention in colorectal and other β-catenin-dependent cancers.

3. Wnt signalosome switching by Naked

3.1 Introduction

The ability to rapidly terminate Wnt/β-catenin signal transduction is an absolute requirement for accurate, timely signalling to occur. Several negative regulators which work to inactivate Wnt receptors, including Dickkopf and RNF43 (Niehrs, 2006; Koo *et al*., 2012), or function at the level of Wnt itself, such as WIF-1 (Wnt inhibitory factor 1) and Notum (Malinauskas *et al*., 2011; Kakugawa *et al*., 2015), are now understood in structural detail. However, this transition from active to inactive signalling also requires the disassembly, or switching, of Wnt signalosome complexes, such that key components of the degradasome, including Axin, are released and can resume their function in marking β-catenin for degradation. Surprisingly, although it has been a significant focus of research in the Wnt field, how this key event occurs is not well understood. In this chapter, we investigate the mechanism of action of a cytoplasmic negative regulator of Wnt signalling, Naked, which acts at the level of the Wnt signalosome. Despite extremely clear genetic experiments implicating Nkd as part of a crucial negative feedback loop in the canonical Wnt signalling pathway (Zeng *et al*., 2000), no convincing mechanistic basis for its function has thus far been identified.

3.1.1 Dishevelled is the central cytoplasmic Wnt signal transducer

In order to understand signalosome function, it is essential to understand Dishevelled (Dvl), the lynchpin of cytoplasmic Wnt signalling which assembles signalosomes, and provides the crucial link between the receptor complexes and components of the degradasome (Mlodzik *et al*., 2016). Dvl was first identified as a segment polarity gene in *Drosophila*, a mutant of which showed a characteristic 'dishevelled' phenotype as a result of loss of body and wing hair orientation (Fahmy & Fahmy, 1959). Cloning of the fly *dishevelled* (*dsh*) gene identified a novel protein, which acts as an essential positive component of the Wnt signalling pathway (Klingensmith *et al*., 1994). Subsequently, three mammalian homologs were identified (termed Dvl1-3; Sussman *et al*., 1994; Sokol *et al*., 1995), all of which share a characteristic conserved domain architecture (**Fig. 3.1**). Dvl contains an N-terminal DIX (Dishevelled and Axin) domain, shared uniquely with Axin, a central PDZ (Postsynaptic density 95, Discs Large, Zona-occludens-1) domain which binds to numerous signalling partners, and a C-terminal DEP (Dvl, Egl-10, Pleckstrin) domain whose role has previously been controversial (Boutros & Mlodzik, 1999).

Through a large number of comprehensive studies, we now have a detailed molecular understanding of the mechanism by which Dvl enables Wnt signal transduction. An interesting and highly unusual property of the DIX domain is its ability to homopolymerize in a concentration-dependent manner, both *in vitro* and *in vivo* (Schwarz-Romond *et al*., 2005).

Overexpression of Dvl is sufficient to drive this polymerization and activate Wnt signalling, but mutations in the DIX domain that abolish polymerization completely block this effect (Schwarz-Romond *et al.*, 2007a). As well as forming homopolymers, Dvl can heteropolymerize with Axin to recruit the central degradasome component via its own DIX domain, the key step that initiates degradasome inhibition and thus stabilisation of β-catenin (Fiedler *et al.*, 2011; see also **Section 1.1.2**). The specific triggering of DIX polymerization upon Wnt binding to its receptors is thus crucial, and involves the generation of a high local concentration of Dvl molecules. This depends on recruitment of Dvl to Wnt receptor complexes through interaction of the Dvl DEP domain with the cytoplasmic face of Fz (Tauriello *et al.*, 2012). Once concentrated, Dvl subsequently undergoes dimerization via the DEP domain which occurs, unusually, through domain-swapping of a single α-helix from one DEP moiety to another, a process that is energetically unfavourable to reverse and could thus impose unidirectionality on signalosome assembly (Rousseau *et al.*, 2003; Gammons *et al.*, 2016a). In the absence of signalling the DEP domain also plays a key role, binding to and facilitating the ubiquitylation of Fz by the E3 ligases RNF43/ZNRF3, leading to its clathrin-mediated endocytosis and subsequent lysosomal degradation (Jiang *et al.*, 2015b).

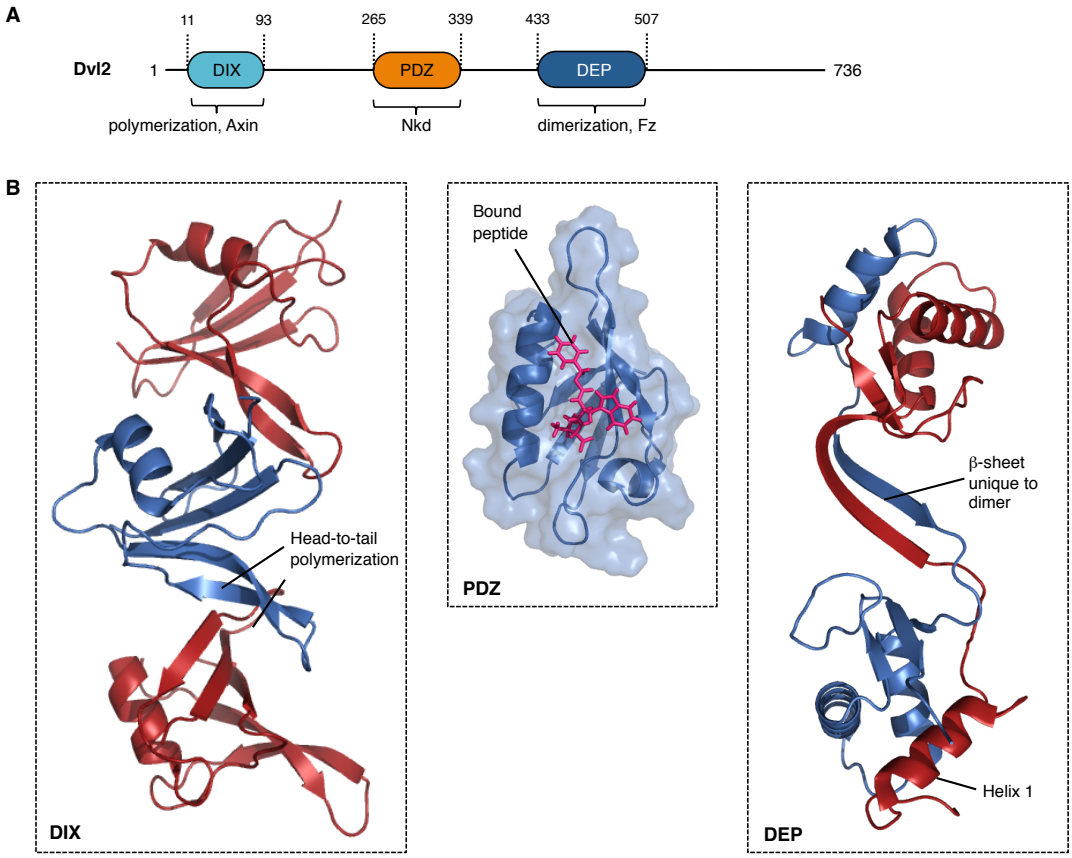

Figure 3.1 Structure and mechanisms of Dvl.
(A) Domain architecture and key interactions of Dvl.
(B) Structure of folded domains of Dvl, including polymerized DIX domain (Madrzak *et al.*, 2015), PDZ domain with bound peptide (Zhang *et al.*, 2009) and domain-swapped DEP dimer (Gammons *et al.*, 2016a). PDB: 4WIP, 3CBZ, 5SUY.

Whilst the DIX and DEP domains are thus clearly required for canonical Wnt signal transduction, the PDZ domain is more enigmatic. Although originally thought to play a key role, more recent data demonstrated that the PDZ domain is completely dispensable for canonical signalling (Gammons *et al*., 2016b). This domain is, however, known to bind numerous proteins, including Dvl inhibitors Dapper and Frodo (Wong *et al*., 2003), often through C-terminal motifs, although it can also bind internal motifs, or even folded domains, such as that of Naked (Rousset *et al*., 2001; see also **Section 3.1.2**). The PDZ domain also binds to the C-terminus of Dvl itself, promoting a 'closed' conformation of Dvl that may be autoinhibitory (Lee *et al*., 2015; Qi *et al*., 2017), in a similar fashion to that proposed for Axin (Kim *et al*., 2013). It therefore seems likely that the PDZ domain represents a primary region for regulation of Dvl function. Furthermore, the multitude of ligands for the PDZ suggests that it may be able to dictate the choice of downstream signalling effectors activated, and hence control the transition from canonical to non-canonical Wnt outputs (Axelrod *et al*., 1998). Indeed, planar cell polarity (PCP) signalling in *Drosophila* has been shown to involve the formation of signalosome-like structures by Dsh, triggered by complexes of Fz and the non-canonical co-receptor Flamingo (Strutt *et al*., 2016).

As well as polymerization, a further notable feature of Dvl is the extent to which it is post-translationally modified. Numerous modifications, including phoshorylation and ubiquitylation, occur extensively in the unstructured linker regions between domains (as well as occasionally within the domains themselves). Dvl becomes heavily phosphorylated upon Wnt signalling by a number of kinases, including CK1ε and γ isoforms, although the timing of these events (relative to polymerization) and their functions are somewhat unclear (González-Sancho *et al*., 2004; Mlodzik, 2016). A number of E3 ubiquitin ligases have been shown to regulate the stability of Dvl, including KLHL12 (Angers *et al*., 2006), through the promotion of proteasomal degradation. However, Dvl behaviour may also be regulated more subtly, through conjugation of non-degradative K63-linked ubiquitin chains (Tauriello *et al*., 2010b; de Groot *et al*., 2014; see also **Section 2.1.2**). Polymerized Dvl itself is able to activate a number of NEDD4 family E3 ligases, including WWP2, potentially providing a mechanism whereby ubiquitylation of substrates can be specifically triggered at active Wnt signalosomes (Mund *et al*., 2015; Mund *et al*., 2018).

Much remains to be discovered regarding Dvl function. As mentioned, the monomeric and domain-swapped dimeric conformations of the DEP domain are separated by a large energetic barrier, suggesting that once triggered, signalosome formation is not easily reversed. The mechanism by which Dvl signalosomes are thus inactivated upon the cessation of Wnt signalling is unknown, but it is likely that negative regulators of the Wnt pathway which target Dvl, such as Naked, might play a key role.

3.1.2 Naked proteins are negative regulators of Dvl

Alongside the components described so far that are essential for core signalosome function, there are numerous accessory factors that can impart regulation upon the process of signalosome assembly and, presumably, disassembly. One of these factors is Naked (Nkd), a segment polarity gene first described over 30 years ago (Jürgens *et al*., 1984; Martinez Arias *et al*., 1988; McEwen & Peifer, 2001). Whilst wt embryos display bands of hair-like denticles, *nkd* mutants instead display a characteristic 'naked' cuticle, a phenotype representing a potent activation of Wnt signalling. Consistent with Nkd functioning as a negative regulator of Wnt signalling, misexpression of *Drosophila* Nkd phenocopies loss-of-function of Wingless, whilst injection of *nkd* RNA from flies into *Xenopus* embryos disrupts anterior-posterior axis specification and blocks induction of secondary axes, events that are exquisitely dependent on canonical Wnt signalling (Zeng *et al*., 2000). Two mammalian homologs of Nkd (Nkd1 and Nkd2) were soon identified (Wharton *et al*., 2001), and Nkd transcripts are upregulated by Wnt signalling in both flies and mammals, implying that Nkd acts as part of a negative feedback loop to attenuate Wnt signals (Zeng *et al*., 2000; Yan *et al*., 2001). Recall that there are, in fact, several well described negative feedback regulators of Wnt signalling, including Dickkopf and Notum (Niida *et al*., 2004; Gerlitz & Basler, 2002), but Nkd and Axin2 are the only known examples that act cytosolically, and hence could directly affect the signalosome. Both Nkd1 and 2 are recurrently mutated in several cancers, including colorectal, underscoring the importance of these Wnt pathway brakes as key tumour suppressors, and Nkd mRNA expression has been used as a prognostic marker for tumours displaying aberrant Wnt signalling (Guo *et al*., 2009; Stancikova *et al*., 2015).

Drosophila Nkd and mammalian Nkd1/2 share a broadly similar domain architecture, including a single EF-hand motif and a highly unusual C-terminal histidine-rich region (henceforth referred to as the histidine-rich domain; HRD), although the poorly conserved linker between these regions is significantly larger in the fly protein (**Fig. 3.2**). The EF-hand is a Ca^{2+}-binding domain found in many calcium regulated proteins, although they are more usually found in tandem, making Nkd somewhat unusual (Lewit-Bentley & Réty, 2000). Furthermore, despite containing a near-optimal consensus motif (of four acidic residues) for Ca^{2+} binding, it is unclear whether the Nkd EF-hand actually binds Ca^{2+}, with one report suggesting that the domain instead recruits a Zn^{2+} ion for binding to Dvl (Rousset *et al*., 2002). No detailed study has been made of the HRD, nor a role proposed for it, although similarly histidine-rich regions can be found in other proteins. The regions between these domains are not highly conserved, although there are several sequences that resemble Ca^{2+} binding motifs, suggesting that Nkd may once have contained tandem EF-hands. Interestingly, mammalian Nkd1 and 2 are myristoylated on at their second residue (a glycine),

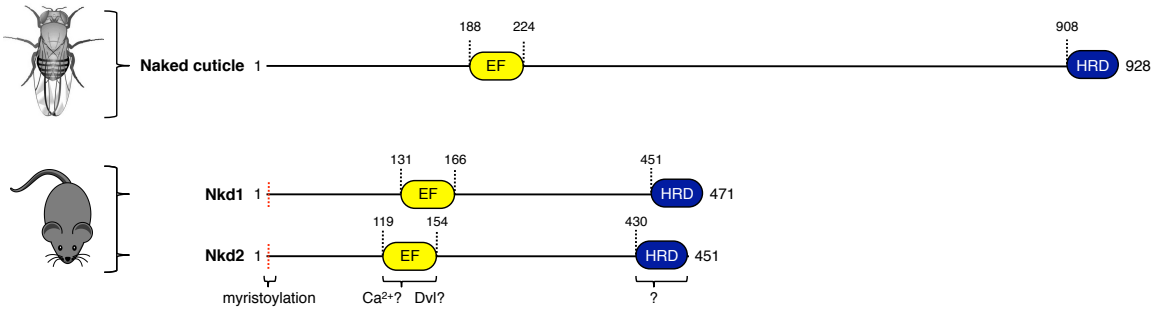

Figure 3.2 Domain structure of Naked proteins.
Comparison of domain architectures of *Drosophila* Naked with mammalian Nkd1 and Nkd2. Note the extended C-terminus in the fly protein, and the lack of an N-terminal myristoylation sequence. Putative ligands of the EF-hand are also shown. See text for more details.

as a result of N-terminal signal sequences, which serves to localise Nkd to the plasma membrane, whilst fly Nkd is also membrane-localised, despite lacking a consensus myristoylation sequence (Li *et al.*, 2004; Chan *et al.*, 2007).

Early genetic experiments in *Drosophila* defined the epistatic relationships between Nkd and other components of the canonical Wnt signalling pathway. Nkd functions cell autonomously, and overexpression can suppress the effect of overexpressing Wingless or Dishevelled, although not of constitutively active Armadillo. Furthermore, they showed that Nkd antagonises Wnt signalling upstream of Zw3 (the *Drosophila* homolog of GSK3), implying that Nkd functions above the level of the degradasome (Rousset *et al.*, 2001). Epistasis experiments in mammalian cells similarly placed murine Nkd1 upstream of β-catenin (Wharton *et al.*, 2001). Through yeast two-hybrid and *in vitro* coIP experiments, Dvl was identified as an interacting partner of Nkd, and a series of Dvl fragments used to demonstrate that Nkd, like many Dvl regulators, binds to the PDZ domain (Rousset *et al.*, 2001).

However, despite nearly two decades of study, the mechanism(s) by which Nkd functions to reduce Wnt signalling remains mysterious. Several reports have suggested that Nkd promotes the proteasomal degradation of Dvl, a plausible model, although no E3 ubiquitin ligases have been reported, nor a clear mechanistic basis outlined (Hu *et al.*, 2010; Schneider *et al.*, 2010). Others have suggested that Nkd engages nuclear import receptors, inhibiting a downstream step of signal transduction, such as β-catenin import (Chan *et al.*, 2008). These models for Nkd function suppose that the Nkd/Dvl interaction serves to somehow activate Nkd, which then acts on a step of the pathway distinct from the signalosome, although this would not seem to be consistent with myristoylation locating Nkd to the plasma membrane in mammalian cells. More recently, interactions of Nkd with several other Wnt components,

including β-catenin (Larraguibel *et al*., 2015) and Axin (Gao *et al*., 2016), have been mooted. There is also evidence that Nkd might function to redirect Wnt signal transduction towards non-canonical outputs (Yan *et al*., 2001; Marsden *et al*., 2018), although loss of Nkd function in the *Drosophila* wing fails to disrupt planar cell polarity, suggesting Nkd is not essential for non-canonical signalling in this particular instance (Zeng *et al*., 2000). A role for Nkd in Wnt/Ca^{2+} signalling could also be plausible, if it was determined conclusively that the Nkd EF-hand binds to Ca^{2+} ions. Clearly, the mechanism of Nkd function has clearly not been conclusively identified, and our work towards understanding this enigmatic protein is the topic of this chapter.

3.1.3 The autophagy system

For reasons that will become clear in this chapter, it is relevant to give an introduction to a cellular degradation pathway, alternative to the proteasome, known as autophagy. Autophagy is a conserved cellular recycling pathway that engulfs intracellular material, including protein complexes, aggregates and entire organelles, within a double membrane and targets it for lysosomal degradation (Mizushima *et al*., 2011). Autophagy thus constitutes a highly versatile process that has multiple roles in the cell, including the provision of nutrients during starvation, maintenance of homeostasis, protein quality control and pathogen defence (Kaur & Debnath, 2015). Autophagy initiates with the formation of a phagophore (also known as isolation membrane), which subsequently elongates and seals to generate a mature autophagosome capable of fusion with endosomes and lysosomes, which contain hydrolytic enzymes. Various cellular organelles, including the endoplasmic reticulum, Golgi apparatus and plasma membrane can supply membrane to the growing autophagic structure. Deregulation of autophagy is known to play a role in numerous diseases, including cancer and various degenerative conditions, although the mechanisms remain controversial (Mizushima *et al*., 2008). Beclin1 (the mammalian homolog of ATG6) is deleted in over half of breast, ovarian and prostate cancers, implying a tumour suppressive role (Aita *et al*., 1999), but in some cases autophagy seems to favour cancer cell survival. Autophagy is also known to be deployed against certain bacterial infections (Randow, 2011), and can protect against pathogenic protein aggregates such as those formed by tau (Falcon *et al*., 2017).

Autophagy is a complex and tightly regulated process that is executed by a large number of autophagy-related genes (ATGs; **Fig. 3.3A**). Originally identified in yeast genetic screens, most of these have conserved orthologs in mammals (Tsukada & Ohsumi, 1993; Ohsumi, 2014). These factors form several complexes that control sequential steps of autophagosome formation (**Fig. 3.3B**). Biogenesis begins at the phagophore assembly site, where proteins of the UNC51-like kinase (ULK) complex assemble to initiate formation of the isolation membrane (Jung *et al*., 2009). In the nucleation stage, the activated ULK complex targets a class III PI3K (phosphoinositide 3-kinase) complex to promote production of a phagophore-

specific pool of phosphatidylinositol 3-phosphate (PI3P; Obara *et al*., 2006). This phospholipid assists in recruitment of the ATG12–ATG5–ATG16 complex to the isolation membrane, where it directs lipidation of MAP1LC3 (also known simply as LC3) family proteins with phosphatidylethanolamine, a process that is absolutely required for LC3-directed autophagosome expansion (Dooley *et al*., 2014; Nakatogawa *et al*., 2007). The isolation membrane continues to expand until a mature autophagosome is formed upon closure of the double membrane, a process that is not fully understood (Fujita *et al*., 2008).

Autophagosome formation is thus the key step that regulates autophagy. Formerly considered to be a largely non-selective degradation pathway, more recent studies have revealed a high degree of selectivity in autophagy, conferred by specialised autophagy receptors that specify cellular material and physically link it with the autophagy machinery through simultaneous interactions with the cargo and LC3 proteins on autophagosomes (Stolz *et al*., 2014). Many of these autophagy receptors, including p62 and NBR1, contain ubiquitin-binding domains (often with a preference for K63-linked polyubiquitin; Seibenhener *et al*, 2004) indicating a

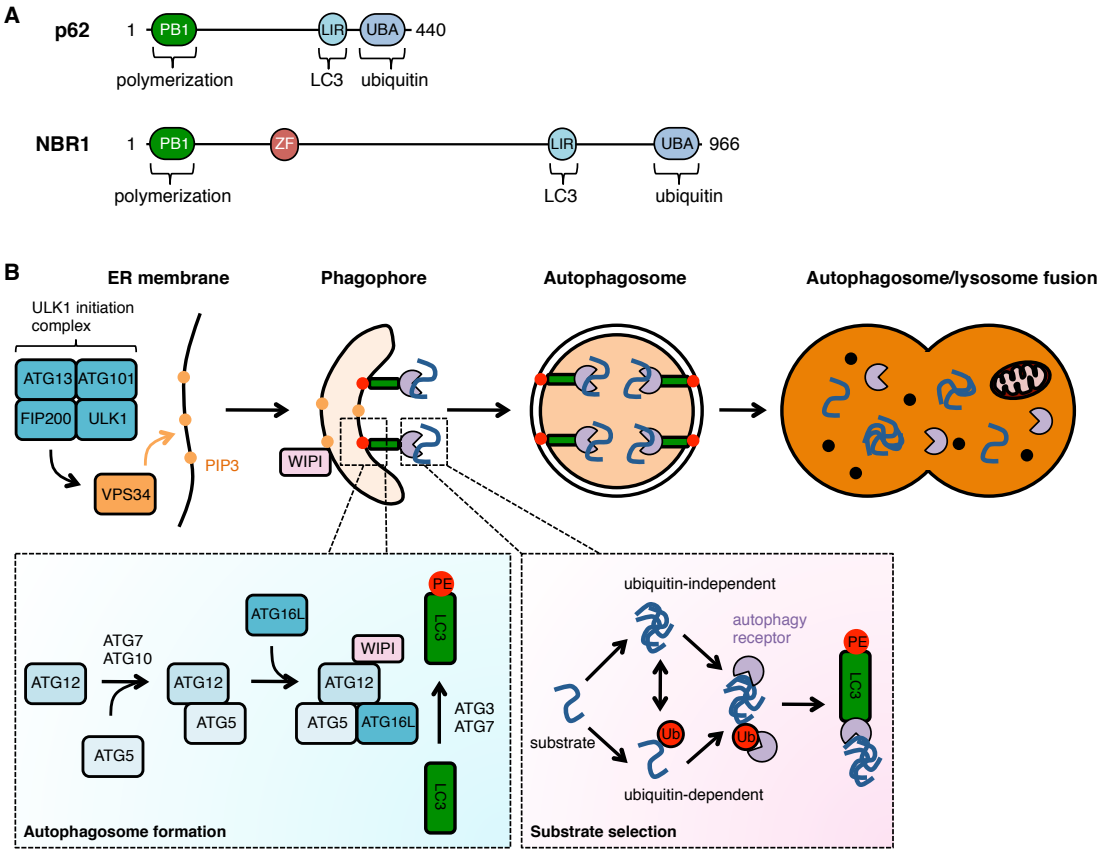

Figure 3.3 Summary of the autophagy pathway.
(A) Domain architecture and interactions of the key autophagy receptors p62 and NBR1.
(B) Overview of the canonical autophagy pathway: initiation takes place at the ER membrane, with recruitment of the ULK1 initiation complex. Subsequent recruitment of the VPS34 PI3K complex generates PIP3 required for recruitment of downstream effectors that promote autophagosome formation (lower left) and are responsible for the selection of cargo (lower right). See text for more details.

fundamental role for ubiquitin in marking substrates for selective autophagy (Pankiv *et al*., 2007; Kirkin *et al*., 2009; Rogov *et al*., 2014). This may be related to the ability of long ubiquitin chains to induce aggregation of substrates (Morimoto *et al*., 2015). In some cases, the AAA+ ATPase VCP/p97 (discussed in detail in **Chapter 2**) appears to be required for the autophagic degradation of ubiquitylated proteins (Ju & Weihl, 2010; Papadopoulos *et al*., 2017). However, in other circumstances autophagy can be initiated in a ubiquitin-independent fashion, particularly if substrates are already aggregation-prone (Khaminets *et al*., 2016). One prominent autophagy adaptor is ALFY (autophagy-linked FYVE protein), which can interact with PI3P-containing membranes to facilitate degradation of model aggregation-prone proteins (Filimonenko *et al*., 2010). In some cases autophagy receptors that contain UBDs, including p62, have been implicated in ubiquitin-independent autophagy (Watanabe & Tanaka, 2011).

Autophagy has previously been reported to regulate the Wnt pathway. One report found that autophagy negatively regulates signalling through the promotion of Dvl degradation (Gao *et al*., 2010). These authors proposed that ubiquitylation of Dvl by the Von Hippel-Lindau (VHL) E3 ligase promotes the binding of Dvl2 to p62, which in turn facilitates aggregation and LC3-mediated autophagosome recruitment under conditions of starvation. Interestingly, p62 contains an N-terminal PB1 domain (**Fig. 3.3A**), the closest structural relative to the DIX domain, and is able to mediate self-association in a similar fashion, but cannot bind directly to Dvl in the absence of modification (Bienz *et al*., 2014; Ciara Metcalfe, PhD thesis). Autophagy-dependent Dvl degradation may be promoted by other factors, including the negative regulator Dapper (Zhang *et al*., 2006), and a negative correlation was observed between autophagy and Dvl expression in late stages of colon cancer, suggesting that autophagy may contribute to the aberrant activation of Wnt signalling during carcinogenesis (Gao *et al*., 2010). Autophagy is a complex set of processes, integrating multiple membrane trafficking pathways, regulatory factors and mechanisms. Whilst this pathway seems to play a role in Wnt regulation, this has not been fully explored, and many of the mechanisms underlying specificity within the autophagy system are yet to be understood.

3.2 Results

3.2.1 Nkd inhibits signal transduction at the level of Dvl

In order to determine the mechanism(s) by which Nkd acts to inhibit Wnt signalling, I first set about confirming previous data and establishing our own assays of Nkd function in the lab. Mammalian Nkd1 has been well characterised as a Wnt target gene (Zeng *et al*., 2000), and I confirmed by Western blot analysis and RT-qPCR that Nkd1 protein and mRNA levels, respectively, are significantly increased when transcription of Wnt target genes is stimulated with LiCl in HEK293T cells (**Fig. 3.4**). Interestingly, this analysis showed that Nkd1 protein levels do not increase until around six hrs after initial stimulation, and continue to increase post-12 hrs of treatment, in contrast to active β-catenin levels, which rapidly increase within two hrs, but peak around 12 hrs after stimulation. This timeframe would certainly fit the purported role of Nkd1 as a negative feedback regulator, through reducing β-catenin activity and hence dampening canonical Wnt transcriptional responses.

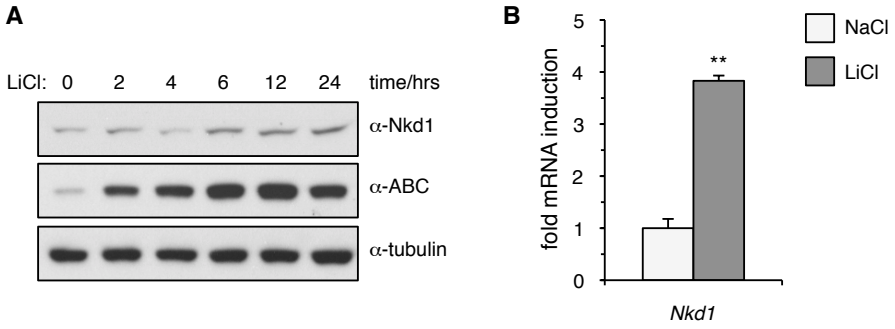

Figure 3.4 Nkd1 is a Wnt target gene.
(A) Western blots of wt HEK293T cell lysates, after indicated treatments, probed with the indicated antibodies.
(B) RT-qPCR assays to quantify *Nkd1* mRNA levels in HEK293T cells treated with NaCl or LiCl. Values were normalised to *PMM1* levels, and presented as mean ± SEM (n=3).

I therefore asked whether expression of Nkd1 leads to a reduction of Wnt transcriptional responses in these cells. Using SuperTOP assays, I found that the Wnt transcriptional output was significantly reduced in cells treated with Wnt3a upon overexpression of HA-tagged Nkd1, in comparison to HA-GFP (**Fig. 3.5**). The same result was obtained when stimulating the Wnt pathway by overexpression of the key signalosome component Dvl2 (recall that this is sufficient to activate Wnt signalling in the absence of stimulation), but not by LiCl treatment or expression of stabilised β-catenin (Δ45-β-catenin, as employed in **Chapter 2**), both of which act epistatically to Dvl (**Fig. 3.5B**). These data confirm that Nkd1 functions as a negative regulator of canonical Wnt signal transduction, at the level of the signalosome.

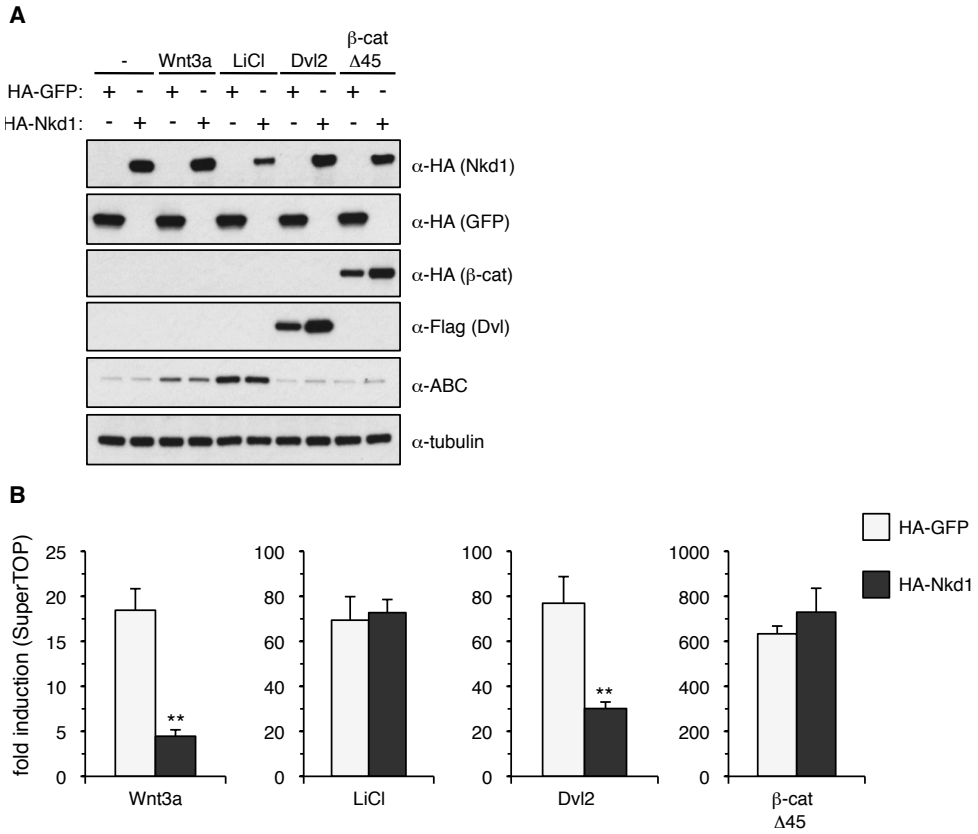

Figure 3.5 Nkd1 inhibits Wnt signalling at the level of Dvl2.

(A) Western blots of HEK293T cell lysates, after the expression of proteins and treatments indicated above, probed with the indicated antibodies. Note that, for reasons which are unclear, expression of Dvl2 does not lead to a significant stabilisation of active β-catenin.

(B) SuperTOP assays to measure Wnt signalling activity in cells treated as in (A). Values are presented as mean ± SEM (n=3), relative to untreated cells.

3.2.2 Nkd1 EF-hand and histidine-rich domains are required for Wnt inhibition

Given the lack of insight into the mechanism by which Nkd1 functions, I sought to undertake a detailed structural and functional study of Nkd1. Analysis of the domain architecture, and conservation between Nkd orthologs, highlighted several potential regions of interest, namely the central EF-hand fold and C-terminal HRD (**Fig. 3.6A**; see also **Section 3.1.2**). I therefore decided to examine whether these domains play an important role, using our established SuperTOP assays of Nkd1 function. Point mutation of four essential ion-coordinating residues within the EF-hand to alanine ('4A'; predicted to disrupt the fold of the EF-hand), and deletion of the HRD ('ΔHRD'; through introduction of a premature stop codon after Ala-449) both significantly reduced the ability of Nkd1 to attenuate canonical Wnt transcriptional responses induced by either Wnt3a treatment, or expression of Dvl2, indicating that both of these regions are required for full Nkd1 function (**Fig. 3.6B**). Interestingly, whilst the 4A mutant seemed to express at levels similar to the wt protein, the ΔHRD mutant was expressed at much higher levels than wt Nkd1 if the same amount of DNA was transfected (**Fig. 3.6C**).

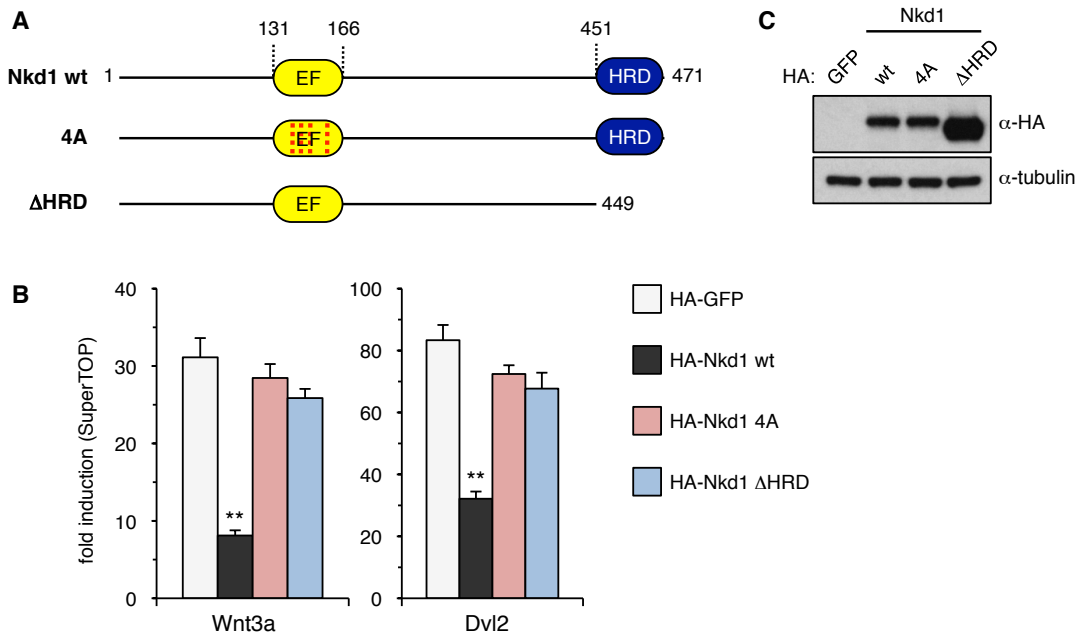

Figure 3.6 Nkd1 EF-hand and histidine-rich domain are required for inhibition of Wnt signalling.

(A) Nkd1 wt and mutant constructs used in these experiments.

(B) SuperTOP assays to measure Wnt signalling activity in cells after co-expression of proteins and treatments indicated. Values are presented as mean ± SEM (n=3), relative to untreated cells.

(C) Western blots of HEK293T cell lysates, after expression of Nkd1 constructs as in (A), probed with the indicated antibodies.

3.2.3 Nkd1 EF-hand interacts with the Dvl PDZ domain

I next sought to determine the mechanistic basis for the requirement of the EF-hand and HRD in the ability of Nkd1 to inhibit Wnt signalling. Previous work suggested Nkd1 binds directly to Dvl, and that the EF-hand may be key to this interaction, although a role for other regions close downstream of the EF-hand was also mooted (Rousset *et al.*, 2002). Indeed, Nkd1 colocalises with Dvl puncta when both proteins are overexpressed and visualised by immunofluorescence in COS-7 cells (**Fig. 3.7A**). Using 'BioIP' proximity labelling assays (see **Section 4.12**), I found that stably expressed wt and ΔHRD Nkd1 both associate efficiently with endogenous Dvl2, whilst 4A Nkd1 associates only weakly (**Fig. 3.7B**). These data were in contrast to coIP assays between overexpressed proteins, which showed no clear difference between binding of wt and 4A Nkd1 to Dvl2 (data not shown). Previous studies have mapped the Nkd-interacting region to Dvl to the PDZ domain (Rousset *et al.*, 2001). Using coIP assays, I found that wt, but not ΔPDZ, Dvl interacted robustly with Nkd1, indeed suggesting the PDZ domain constitutes the sole binding site for Nkd1 (**Fig. 3.7C**). Furthermore, the ability of Nkd1 to reduce canonical Wnt transcriptional output was reduced when SuperTOP activity

was stimulated by expression of ΔPDZ Dvl, as would be expected if Nkd1 could no longer bind (**Fig. 3.7D**). Note that the ΔPDZ Dvl construct is not as active as wt Dvl in SuperTOP activation, although we believe this to be an artefact of overexpression, since ΔPDZ Dvl signals to the same level as the wt protein when expressed at endogenous levels in Dvl KO cells (Gammons *et al.*, 2016b).

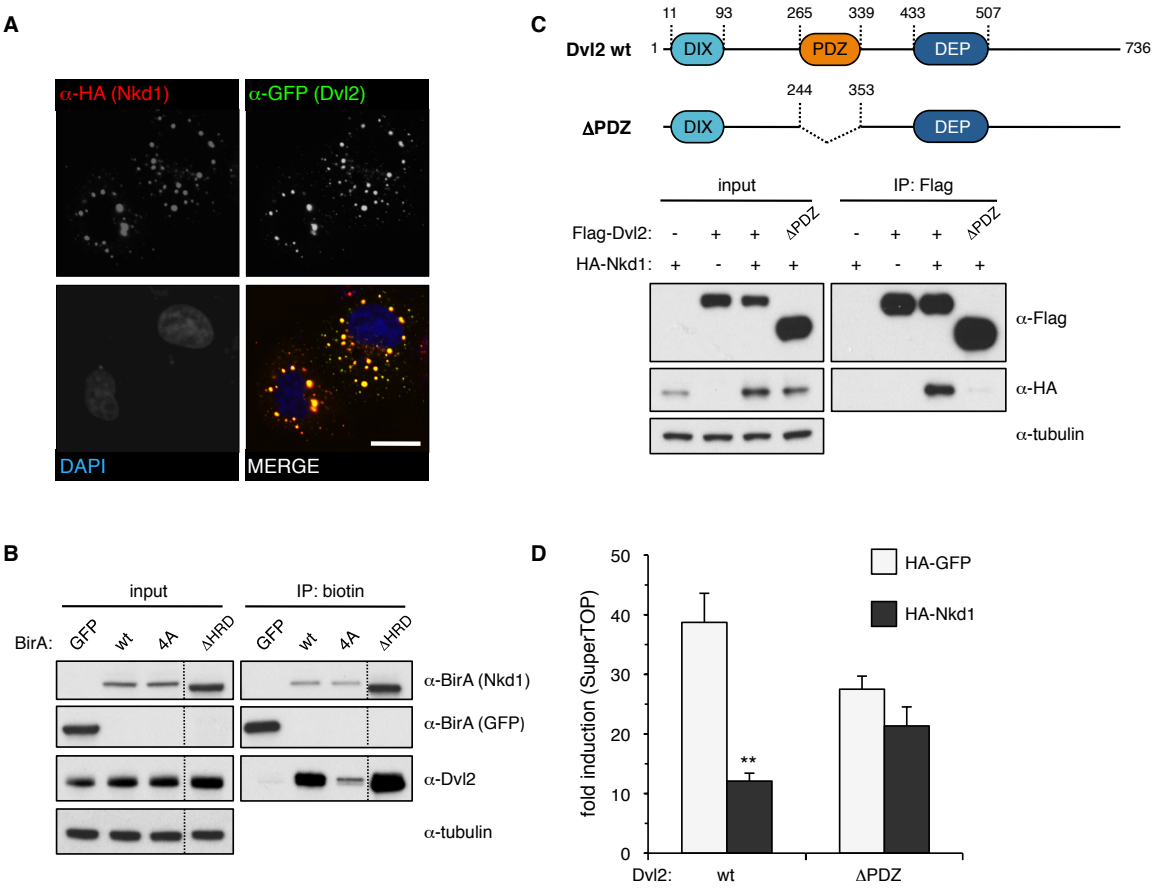

Figure 3.7 Nkd1 EF-hand interacts with the Dvl PDZ domain.

(A) Confocal sections through COS-7 cells after co-expression of indicated proteins, co-stained with DAPI (blue) and antibodies as labelled. Size bars, 10 μm.

(B) Proximity biotinylation ('BioIP') assays investigating binding between Nkd1 and Dvl2; shown are Western blots of HEK293T cell lysates stably expressing BirA*-tagged Nkd1 bait proteins, after treatment with biotin and immunoprecipitation (IP) as indicated above panels, probed with antibodies as indicated on the right.

(C) Top: wt and mutant Dvl2 constructs used in these experiments. Bottom: coIP assays investigating binding between Nkd1 and Dvl2; shown are Western blots of HEK293T cell lysates, after co-expression of proteins and IP as indicated above panels, probed with antibodies as indicated on the right.

(D) SuperTOP assays to measure Wnt signalling activity in cells after co-expression of constructs (shown in (C)) indicated. Values are presented as mean ± SEM (n=3), relative to untransfected cells.

Having demonstrated an interaction between the EF-hand and PDZ domain *in vivo*, I next sought to further characterise this interaction *in vitro* using purified proteins, in collaboration with Miha Renko. Expression of a number of different EF-hand constructs (with variable N- and C-terminal boundaries) was trialled (data not shown), with a construct containing approximately 20 residues downstream of the predicted EF-hand fold yielding significant quantities of folded, soluble protein (**Fig. 3.8A**, see **Section 4.13** for details). Using the same boundaries, expression of a '4A' mutant EF-hand did not yield soluble protein, likely due to this mutation disrupting protein folding. Dvl2 PDZ domain was expressed using the same constructs and purification schemes as previously established in the Bienz lab (Gammons *et*

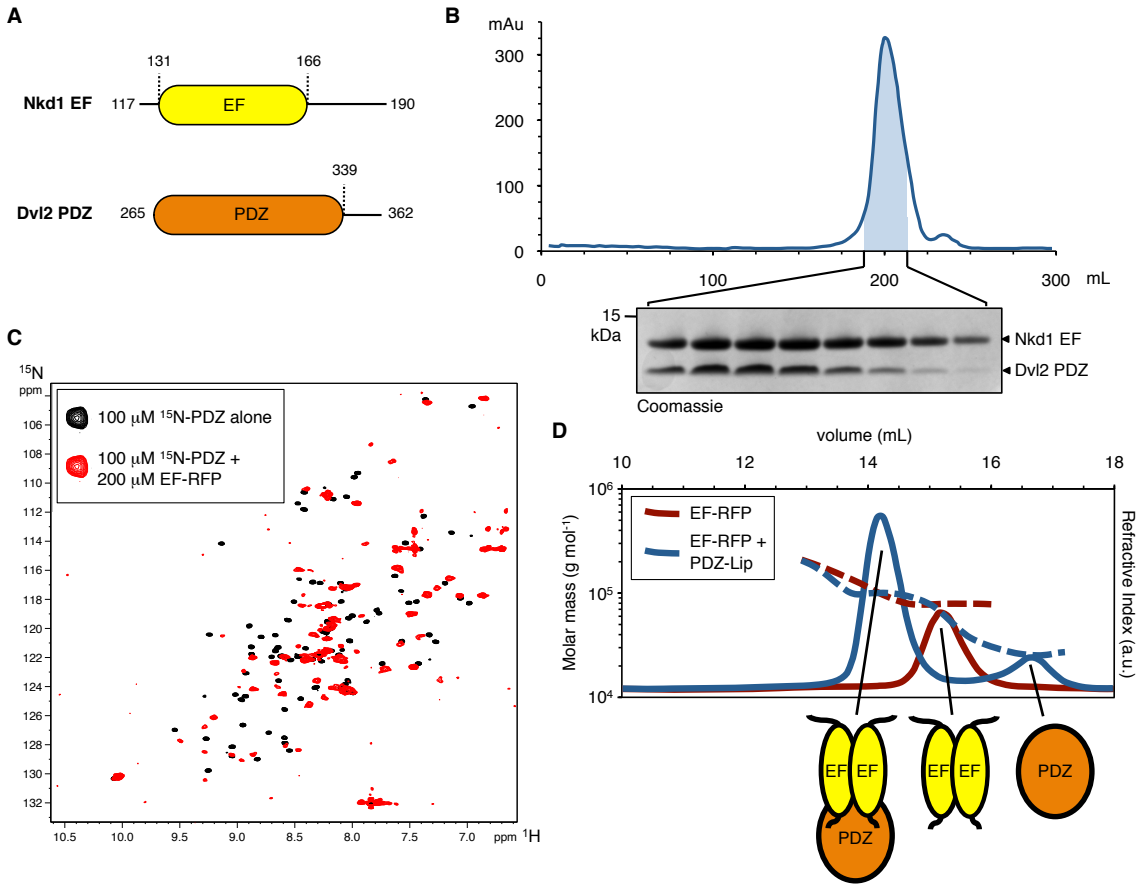

Figure 3.8 Nkd1 EF-hand interacts with the Dvl PDZ *in vitro*.

(A) Minimal Nkd1 EF-hand and Dvl2 PDZ constructs expressed for use in these experiments.

(B) Top: gel filtration profile of untagged EF-hand-PDZ complex after mixing. Bottom: fractions from the indicated peak are resolved on SDS-PAGE.

(C) NMR experiments demonstrating direct binding between purified EF-hand and PDZ domains. Shown are overlays of HSQC spectra of 100 μM ^{15}N-labelled PDZ domain when alone (black), or when probed with 200 μM RFP-tagged EF-hand (red).

(D) SEC-MALS of RFP-tagged EF-hand (red), or EF-hand-PDZ complex (blue). Solid lines indicate the elution profile as detected by the Refractive Index detector; dashed lines indicate the measured molecular mass; cartoons below indicate stoichiometries consistent with these masses.

al., 2016b). Gel filtration analysis, after mixing of wt EF-hand and PDZ domain, yielded a single, symmetrical peak containing both proteins, although the stoichiometry was not clear (**Fig. 3.8B**).

We next asked whether a binding site (or sites) for the EF-hand on the PDZ domain could be identified using an NMR approach (for which a full assignment of the Dvl PDZ has previously been obtained; Gammons *et al*., 2016b). In collaboration with Trevor Rutherford, we recorded heteronuclear single-quantum correlation (HSQC) spectra of ^{15}N-PDZ before and after incubation with purified RFP (red fluorescent protein)-tagged EF-hand (**Fig. 3.8C**). Significant line broadening and chemical shift of a majority of peaks were observed upon addition of EF-RFP, suggesting that the EF-hand interacts with a large surface of the PDZ domain, and/or causes significant changes in the PDZ structure upon binding.

Finally, we wanted to determine the stoichiometry of the complexes formed by the EF-hand alone, and when bound to the PDZ domain. Size exclusion chromatography coupled to multi-angle light scattering (SEC-MALS, carried out in collaboration with Chris Johnson) revealed an apparent molecular mass of approximately 75 kDa for EF-RFP alone, corresponding to a dimer (**Fig. 3.8D**), as has previously been observed for EF-hand folds (Huang *et al*., 2009b). When mixed in an equimolar ratio with Lip (lipoyl)-tagged PDZ domain, the complex formed is approximately 100 kDa, suggesting the EF-hand dimer binds a single PDZ domain, and a smaller peak corresponding to the excess monomeric PDZ (approximately 25 kDa) can also be observed. These data would seem to fit with the stoichiometry observed upon SDS-PAGE analysis of the untagged complex (**Fig. 3.8B**). Taken together, these data show that the Nkd1 EF-hand is able to stably interact with the Dvl PDZ domain, with a stoichiometry of 2:1. Mutations of the EF-hand that abrogate binding to Dvl also abolish the ability of Nkd1 to inhibit Wnt signalling, explaining the requirement for the EF-hand in SuperTOP assays.

3.2.4 The Nkd1 HRD forms stable clusters *in vivo* and *in vitro*

Having characterised the mechanism underlying the requirement for the Nkd1 EF-hand in Wnt inhibition, I next focused on the histidine-rich domain (HRD). When re-analysing samples from cells expressing Nkd1 by Western blot analysis, I observed protein bands corresponding to high molecular weight (HMW; greater than 250 kDa) species of wt, but never ΔHRD, Nkd1 (**Fig. 3.9A**). This observation accounts for the apparent lower expression of wt and 4A Nkd noted earlier (**Fig. 3.6C**). The slow migration of these species was not due to polyUb of Nkd1, as no signal was observed with an α-ubiquitin antibody (data not shown). I reasoned that these HMW species might instead correspond to insoluble clusters or aggregates of Nkd1, the formation of which is dependent upon the presence of the HRD. I thus asked whether

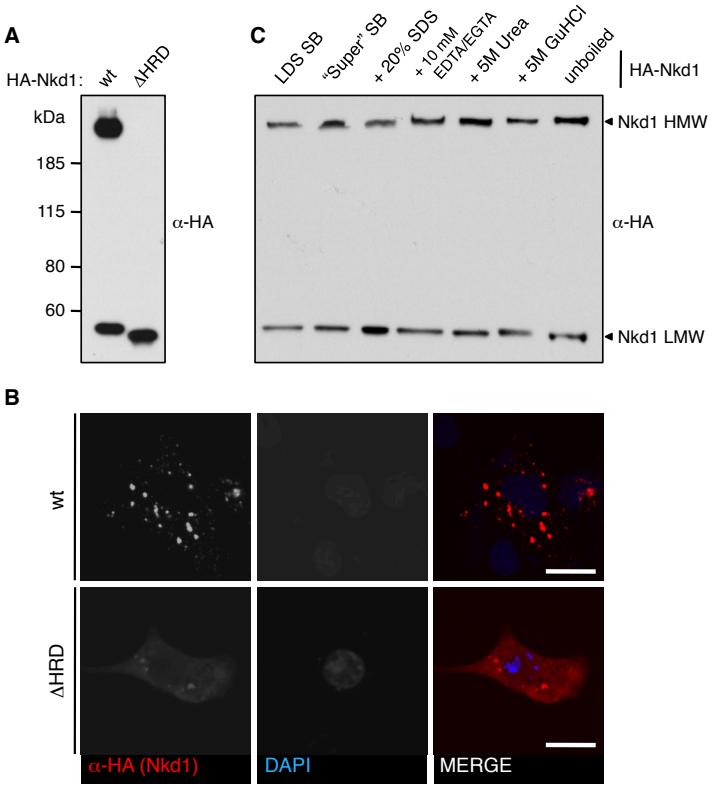

Figure 3.9 Nkd1 HRD promotes the formation of high molecular weight species.

(A) Western blots of HEK293T cell lysates, after the expression of proteins indicated, probed with α-HA antibody.

(B) Confocal sections through COS-7 cells after co-expression of indicated proteins, co-stained with DAPI (blue) and a-HA antibody as labelled. Size bars, 10 μm.

(C) Western blots as in (A), after treatment of cell lysate samples with the indicated sample buffers or additives.

HRD-dependent clustering of Nkd1 is observable in cells. Indeed, wt Nkd1 forms distinct puncta (not dissimilarly to Dvl, though the puncta are usually larger and fewer) when visualised by immunofluorescence in COS-7 cells, whilst ΔHRD Nkd1 is diffuse (**Fig. 3.9B**).

My observation of HMW species by Western blot implies that these species are resistant to solubilisation by boiling in 1% LDS (lithium dodecyl sulphate), as this was present in the sample buffer. Unexpectedly, treatment of Nkd1 lysates with other sample buffers, or addition of various harsh denaturants including SDS, Urea or GuHCl, did not reduce the proportion of Nkd1 found in the HMW bands (**Fig. 3.9C**), suggesting the presence of unusually strong intermolecular interactions between HRDs.

Given this unusual tendency of the Nkd1 HRD to form HMW species, I sought to further investigate this behaviour *in vitro* using bacterially-expressed HRD constructs, in collaboration with Miha Renko. A Lip-tagged minimal HRD also formed HMW species, indicating that the HRD alone is fully sufficient for this clustering process to occur (**Fig. 3.10A, B**). Analysis of several HRD mutants revealed that maximal formation of HMW species is dependent upon the presence of numerous histidine residues, including those in the N-terminal part of the HRD (compare mutants 1 and 2), and two residues either side of a highly conserved tyrosine (mutant 5). Mutation of specific hydrophobic (in a conserved YHHF motif, mutant 6) or glutamate (mutant 7) residues had a reduced, though still observable effect on formation of HMW aggregates.

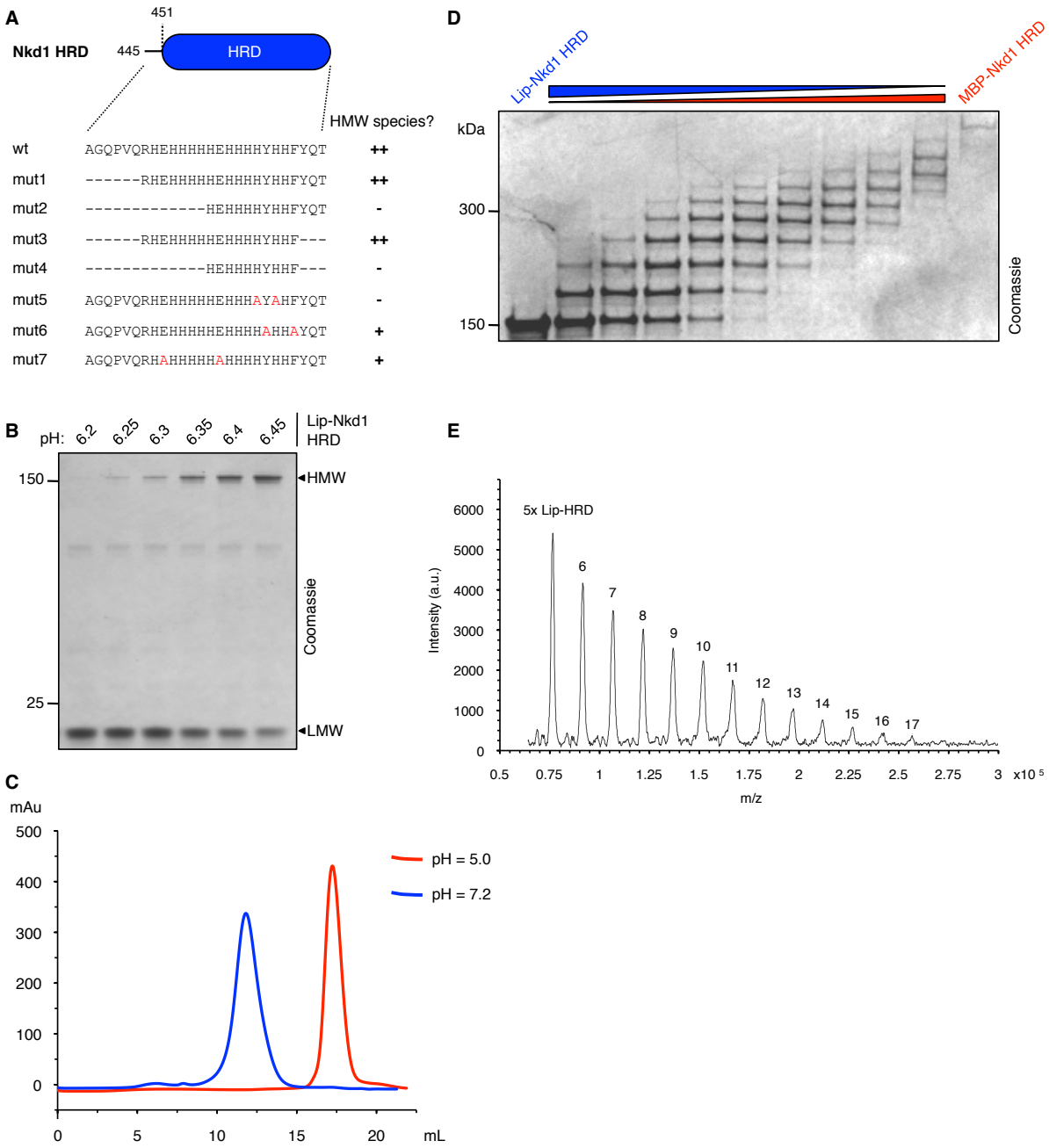

Figure 3.10 Nkd1 HRD forms distinct HMW species *in vitro*.

(A) Top: minimal Nkd1 HRD construct expressed for use in these experiments. Bottom: amino acid sequence of HRD domain of wt and seven mutant constructs, tested for their ability to form HMW species at neutral pH (indicated on right).

(B) pH dependency of the formation of HMW species. Shown is SDS-PAGE analysis of Nkd1 HRD samples treated in buffer at the indicated pH.

(C) Gel filtration profiles of Lip-Nkd1 HRD run at acidic (red) and neutral (blue) pH. At neutral pH, the protein elutes as a single peak of approximately 250 kDa; At acidic pH, a single peak corresponding to approximately 20 kDa (Lip-Nkd1 HRD = 17 kDa).

(D) Estimating the stoichiometry of HMW species. Shown is SDS-PAGE analysis of samples in which (small) Lip-tagged Nkd1 HRD is mixed with (large) MBP-tagged Nkd1 HRD in differing ratios. 'Steps' upwards from the lower band indicate complexes containing incrementally more MBP-Nkd1-HRD.

(E) Mass spectrometry analysis of purified Lip-tagged Nkd1 HRD. Shown is a portion of a MALDI-TOF spectrum with peaks indicating stable complexes formed from the indicated number of Lip-HRD moieties.

Given that the formation of HMW species presumably involves close proximity between histidine residues of different HRDs, and considering that the pK_a for histidine protonation is in a physiologically relevant range (approximately 6.5 in most proteins; Edgcomb & Murphy, 2002), we wondered whether this behaviour of the HRD might vary in a pH-dependent fashion. SDS-PAGE analysis of Lip-Nkd1 HRD boiled in sample buffer of varying pH revealed that whilst most protein resides in the HMW band at pH 6.4, this band is almost entirely absent at pH 6.2 (**Fig. 3.10B**). The same trend was also observed by gel-filtration; Lip-HRD forms a broad peak (representing a range of high molecular weight stoichiometries) at pH 7.2, but collapses to a sharp peak of monomer at pH 5.0 (**Fig. 3.10C**). This pH dependency of HRD clustering could have implications for Nkd function (see **Section 3.3.3**).

Finally, we wished to more accurately assess the stoichiometry of Nkd1 HMW complexes formed under various conditions. Gel filtration analysis at pH 7.2 suggested an approximate molecular weight of 250 kDa for the centre of the peak, indicating a mean stoichiometry of around 14-16 HRD moieties (**Fig. 3.10C**). In contrast, resolution of HMW species formed after boiling, by mixing 'small' Lip-HRD with 'large' MBP (maltose-binding protein)-tagged HRD suggested a maximum stoichiometry of only 10 monomers (**Fig. 3.10D**), although MALDI-TOF mass spectrometry analysis was able to detect species corresponding to a 17-mer of Nkd1 (**Fig. 3.10E**). Unfortunately, pilot experiments aiming to investigate the structure of the HMW species by electron microscopy were complicated by a large degree of sample heterogeneity. Overall, these data show that the Nkd1 HRD is a unique domain displaying some highly unusual properties, and the propensity of this region to aggregate, forming stable HMW species of defined stoichiometry, may be required for Nkd1 function.

3.2.5 Axin interacts with Nkd1 through mutual HRD binding

Intrigued by the observed behaviour of the Nkd1 HRD, we wondered whether the formation of high molecular weight species might be a more general property of proteins containing histidine-rich sequences. Employing a bioinformatic analysis (conducted by Miha Renko) to identify such proteins, we found approximately 60 proteins with HRD motifs (containing at least eight histidine residues within a span of 14) in the human genome, a selection of which are shown (**Fig. 3.11A,** see **Appendix 3** for complete list). Interestingly, this list contained human Axin1 (the central component of the β-catenin destruction complex and thus a major Wnt component; see **Section 1.1.1**) as a protein containing a histidine-rich domain. The Axin1 HRD is slightly smaller than that of Nkd1, consisting of 9 histidine residues (within a span of 12), and is located centrally within the protein (**Fig. 3.11A, B**). No functions have been clearly assigned to the Axin1 HRD, although this region of the protein has previously been implicated in an autoinhibitory interaction with the Axin DIX domain (Kim *et al.*, 2013). We thus wondered whether Axin1 would display any of the same tendencies as Nkd1, in

A

	HRD sequence	Formation of HMW species	Association with Nkd1 HMW species
Nkd1	HEHHHHHEHHHHYHH	+++	N/A
Axin1	HHHRHVHHHVHH	-	+++
Prickle3	HHHHNHHHHHNRH	-	-
USP34	HHHHHHHHHHHHDGH	-	+/-
Cbl	HHHHHHHLSPH	-	-
DLGAP3	HTSHHHHHHHHHHHHQSRH	-	-
FoxF2	HAHPHHHHHHHVPH	-	-

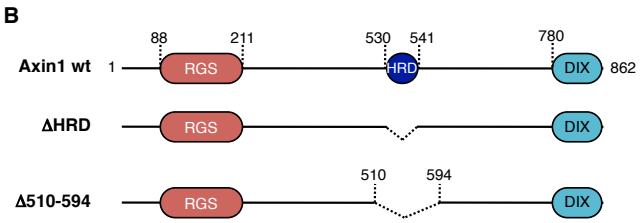

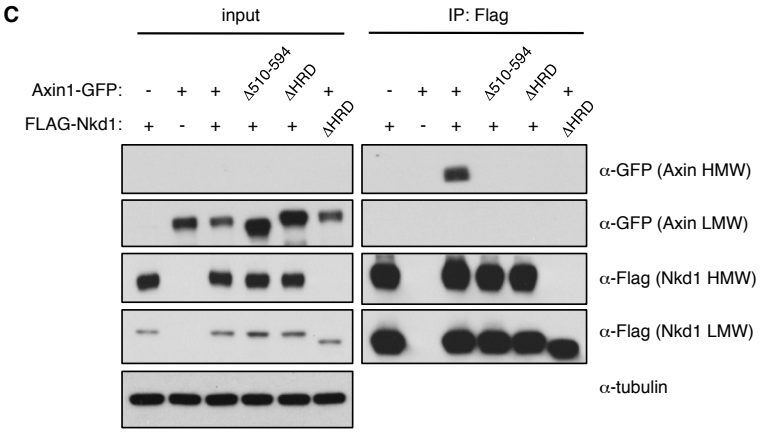

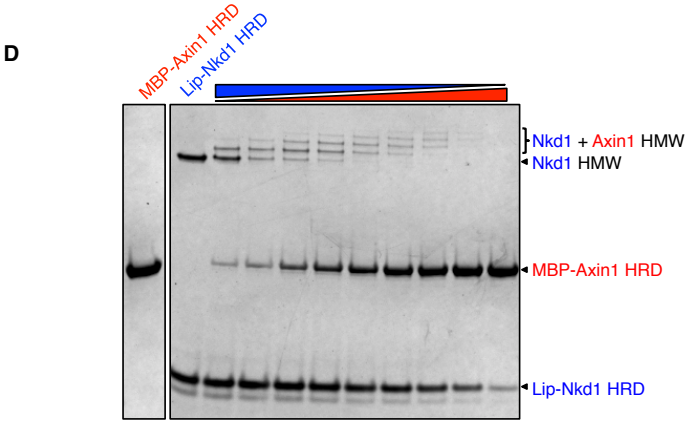

Figure 3.11 Nkd1 HRD interacts with the Axin HRD.

(A) Summary of selected HRD-containing proteins (see also **Appendix 3**).

(B) Domain architecture of Axin1 wt and mutant constructs used in these experiments.

(C) CoIP assays, as previously, investigating binding between Nkd1 and Axin1. Two slices are shown for α-GFP and α-HA blots, to show high and low molecular weight species.

(D) Formation of Nkd1-Axin1 HMW species *in vitro*. Shown is SDS-PAGE analysis of samples in which Lip-tagged Nkd1 HRD is mixed with MBP-tagged Axin1 HRD in differing ratios. The banding pattern at high molecular weight indicates species containing both Nkd1 and Axin1 HRD moieties.

terms of formation of HMW species. GFP-tagged Axin1 did not yield any HMW bands upon overexpression and analysis by SDS-PAGE (as can be seen in **Fig. 3.11C**). However, coIP assays between Nkd1 and Axin1 revealed that wt, but not ΔHRD Axin1 (carrying either a larger, Δ510-594, or more minimal, Δ530-541, deletion) was able to associate with Nkd1 HMW species *in vivo* (**Fig. 3.11C**). As expected, no association was observed with Nkd1 ΔHRD. The equivalent result was also obtained between minimal Nkd1 and Axin1 HRDs *in vitro*, where MBP-Axin1 HRD is incorporated into HMW species with Nkd1 HRD, but cannot form them by itself (**Fig. 3.11D**).

One simple model for how Nkd could function to reduce Wnt signalling, given its ability to bind both Dvl (through its EF-hand) and Axin1 (through their respective HRDs), is that it could somehow block the interaction between Dvl and Axin, thereby releasing Axin to reform the β-catenin destruction complex. We thus wondered whether expression of Nkd1 would interfere with the binding of Dvl to Axin1. However, coIP assays showed that the interaction between Dvl2 and Axin1 is actually enhanced, not reduced, upon expression of Nkd1, and the robust presence of Nkd1 in these immunoprecipitates indicates that the three proteins are apparently able to form a ternary complex (**Fig. 3.12A**). Corroborating this, Nkd1 and Axin1 both colocalise in the same Dvl2 puncta when visualised by immunofluoresence (**Fig. 3.12B**). These data suggest that, whilst Nkd1 is able to associate with Axin1, via mutual interaction of their HRDs, this interaction does not immediately explain the mechanism of Nkd function (for example by competing with the Dvl/Axin interaction), and could serve simply as a second means of targeting Nkd1 to active Wnt signalosomes.

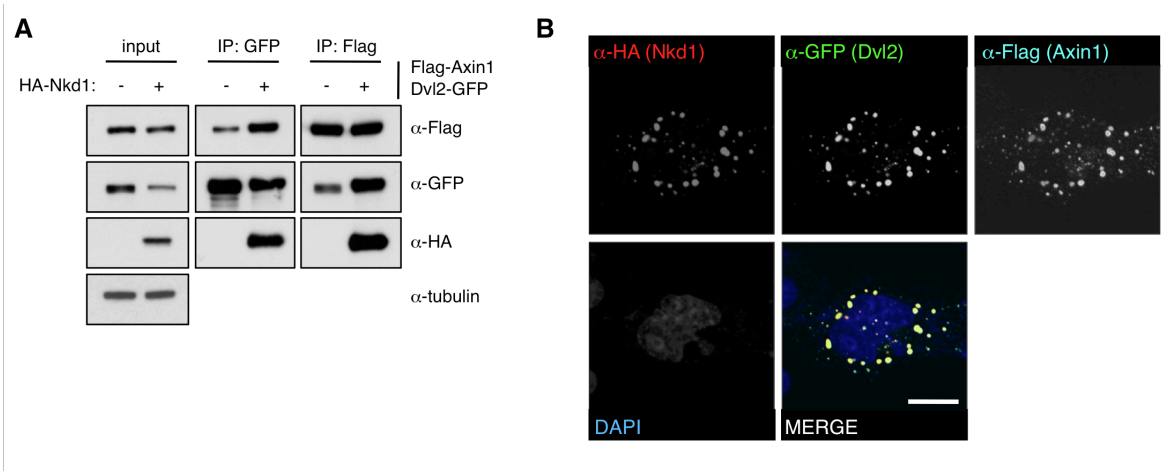

Figure 3.12 Nkd1 forms a ternary complex with Dvl2 and Axin1.
(A) CoIP assays, as previously, investigating binding between Nkd1, Dvl2 and Axin1. For clarity, only low molecular weight species are shown.
(B) Confocal sections through COS-7 cells after co-expression of indicated proteins, co-stained with DAPI (blue) and antibodies as labelled. Size bars, 10 μm.

3.2.6 BioID-MS reveals candidate interactors of the Nkd1 HRD

Although we identified Axin1 as an interactor of the HRD, I wondered whether further hitherto unidentified binding partners of the Nkd1 HRD might explain the absolute requirement of this domain for the ability of Nkd to inhibit cytoplasmic β-catenin dependent signal transduction. I thus set out to use a proximity-dependent biotin labelling technique (termed BioID; Roux *et al.*, 2012) to identify novel ligands of the HRD, and other domains, of Nkd1. This method relies on the generation of a 'cloud' of reactive biotin moieties by a promiscuous biotin ligase (*E. coli* BirA, carrying an R118G mutation, termed BirA*) that is fused to the protein of interest, leading to biotinylation of proximal endogenous proteins and allowing their selective isolation by biotin-affinity capture (**Fig. 3.13A**). One important consideration when using this method is the design of the BirA*-bait fusion protein, in order to mimic the interactions of the endogenous protein as closely as possible, seeing as the BirA* module is rather large (~30

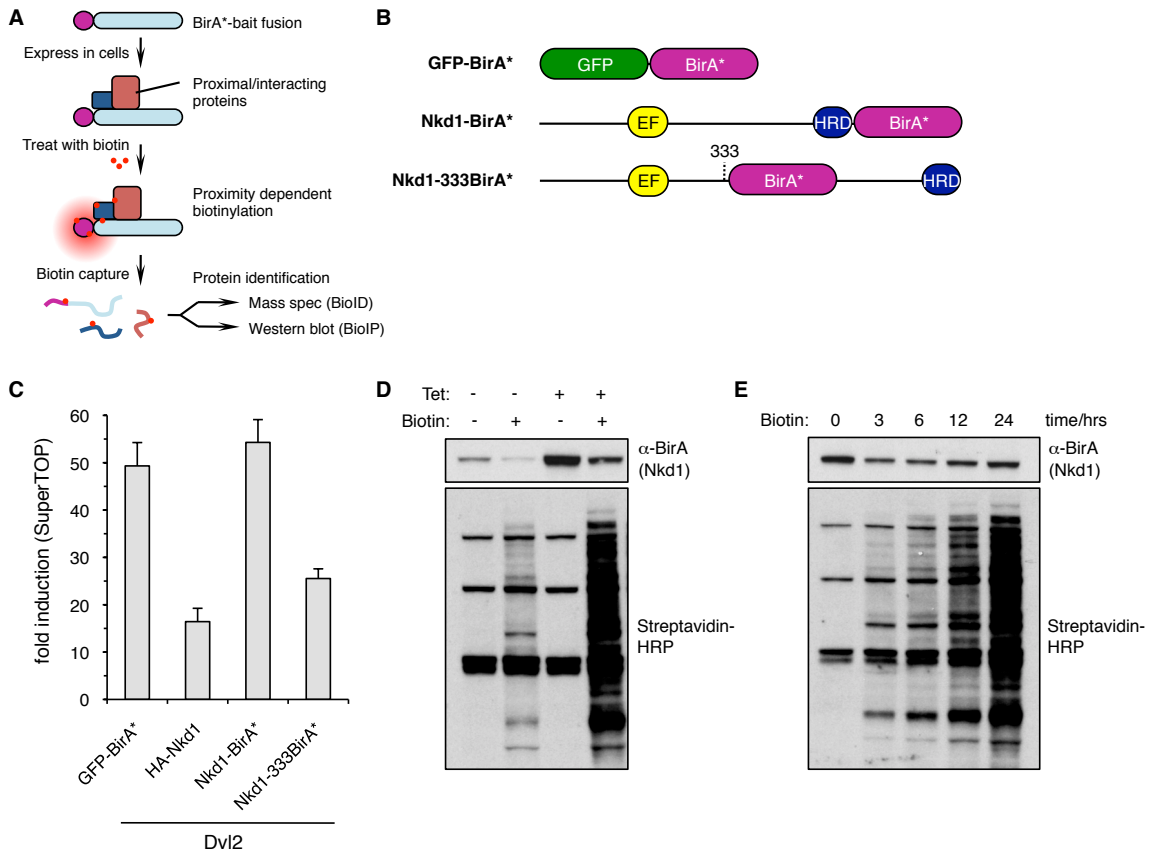

Figure 3.13 BioID methodology and construct design.

(A) Outline of BioID proximity labelling methodology (Roux *et al.*, 2012).

(B) Nkd1-BirA* fusion constructs used in these experiments.

(C) SuperTOP assays to measure Wnt signalling activity in cells after co-expression of proteins indicated. The pathway was stimulated by overexpression of Dvl2. Values are presented as mean ± SEM (n=3), relative to cells in which Dvl2 was not expressed.

(D) Validation of Flp-in HEK293 cell lines inducibly expressing Nkd1-BirA* fusions. Shown are Western blots of cell lysates indicating the extent of biotin labelling after the treatments indicated above, probed with the antibody or reagent shown on the right.

(E) Time course of biotinylation. Shown are Western blots, as in (D), indicating the extent of biotin labelling from 0 to 24 hrs.

kDa). I therefore designed several Nkd1-BirA* fusions and tested their ability to reduce Wnt transcriptional output using SuperTOP assays (**Fig. 3.13B**). An N-terminal BirA* would be unsuitable, as it would interfere with membrane localisation of Nkd1, whilst a C-terminal fusion of BirA* rendered Nkd1 inactive in reducing SuperTOP (**Fig. 3.13C**), potentially because the BirA* somehow interferes with a function of the HRD. In contrast, with an internally fused BirA* (located after Gln-333, referred to as Nkd1-333BirA*), Nkd1 remained able to reduce Wnt signalling output. This location of the tag was selected as it is proximal to the site of a large insertion in the *Drosophila* Nkd protein relative to human Nkd1 (see **Section 3.1.2**).

HEK293 cell lines stably expressing this Nkd1-333BirA* bait were generated using the Flp-In system (O'Gorman *et al*., 1991; see **Section 4.12**). These cells contain a recombinase site allowing for a single integration of the fusion construct at a defined genomic locus, such that the expression levels are controllable by a tetracycline-inducible promoter. I confirmed that the bait was expressed in tetracycline-inducible fashion by Western blotting with an α-BirA antibody, and that this bait triggered a smear of biotinylation of endogenous proteins (**Fig. 3.13D**). Conducting a time course, I established that significant biotinylation occurs within 12 hrs of biotin treatment (**Fig. 3.13E**). This time point, although shorter than the recommended 24 hrs of labelling (Roux *et al*., 2013), fits more closely with the physiological duration of Wnt signalling events, and so was used during the proteomics screen. Having confirmed the labelling methodology was working, I proceeded to generate stable cell lines for three Nkd1 mutants (constructs shown in **Fig. 3.14A**). In addition to the 4A and ΔHRD mutations previously identified, I included a glycine-to-alanine substitution of the second amino acid of Nkd1 (G2A). Mutation of this glycine residue blocks N-terminal myristoylation and hence prevents targeting of Nkd1 to the plasma membrane (Li *et al*., 2004). An N-terminally GFP-tagged BirA* was used to generate a background proteomics profile for comparison.

The BioID cells lines were treated with Wnt3a-conditioned media and biotin for 12 hrs, after which biotinylated proteins were affinity purified and resolved by SDS-PAGE (**Fig. 3.14B**, see Section **4.12**). Mass spectrometry analysis of purified proteins revealed a number of interesting candidate interacting proteins of Nkd1 (which were enriched 5-fold or greater, relative to GFP; **Fig. 3.14C**). I was pleased to note that all three orthologs of Dvl were identified at high spectral counts with wt Nkd1, but were reduced with the 4A mutation. Other cytoplasmic Wnt signalling components identified included APC, Axin1 (notably with fewer counts with the ΔHRD bait), CK1ε and β-catenin, as well as the transmembrane co-receptor LRP6. As expected, almost all of the plasma membrane proteins identified were significantly reduced in their association with the G2A mutant. Of particular interest were a number of Nkd-associated proteins, several of which were previously unlinked to Wnt signalling, which were

significantly reduced with the ΔHRD mutant. These included two related to K63-linked polyUb signalling (N4BP1 and CYLD), as well as several related to the autophagy pathway (including NBR1, KEAP1 and p62). The BioID labelling approach was thus successful in identifying previously reported ligands, as well as novel candidate interacting proteins of Nkd1.

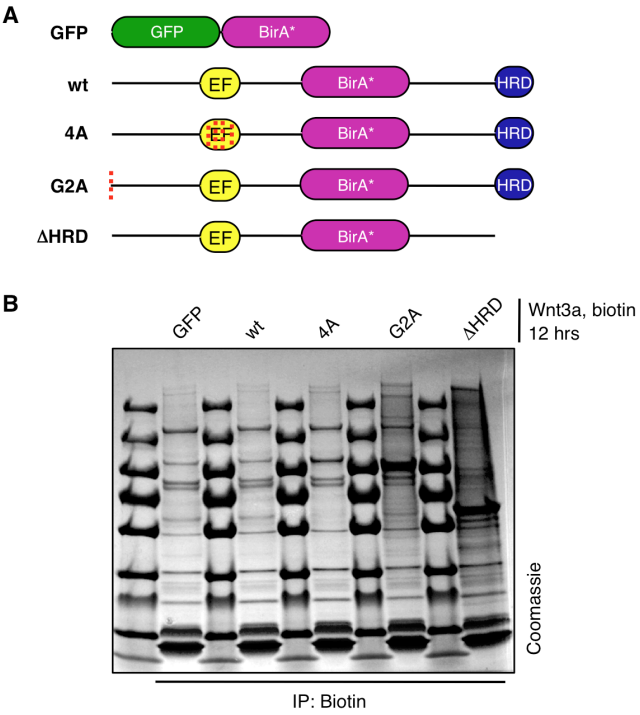

C

	BioID +Wnt3a				
	GFP	WT	4A	G2A	Δ HRD
Nkd1	-	84	91	130	230
Dvl2	29	178	105	303	157
Dvl3	24	160	91	240	146
Dvl1	8	93	46	127	69
APC	1	157	54	20	125
N4BP1	9	102	102	22	11
CYLD	4	70	63	27	3
NBR1	-	56	58	24	0
KEAP1	5	52	43	53	6
p62	2	47	67	23	-
VANGL1	2	41	36	7	46
VANGL2	2	35	27	3	34
ROR2	1	29	26	2	37
LRP6	-	23	13	-	-
NOTCH2	-	22	14	1	66
Axin1	-	9	4	-	2
Amer1	-	6	5	-	-
CK1ε	-	5	2	8	5
β-catenin	1	5	2	-	11
LRP5	-	4	5	-	-
NOTCH1	-	4	2	-	3

Figure 3.14 BioID screen for interactors of Nkd1.

(A) GFP- and Nkd1-BirA* fusion constructs used in this screen.

(B) SDS-PAGE gel, prior to cutting into slices, showing biotin pulldowns from Flp-In HEK293 cell lines expressing the indicated BioID baits.

(C) Table of selected proteins identified by mass spectrometry. Values represent total unweighted spectral counts (>95% probability).

3.2.7 Autophagy adapters interact with Nkd1

One group of proteins that particularly stood out from the BioID analysis were those involved in the autophagy pathway, including p62, NBR1 and KEAP1, all of which seemed to be fully dependent on the HRD of Nkd1 for association (**Fig. 3.15A, B**). Autophagy has previously been implicated in Wnt signalling (Gao *et al.*, 2010), and although a conclusive demonstration of a role is lacking, the HMW aggregates formed by the Nkd1 HRD could constitute a substrate for selective autophagy (see **Section 3.1.3**). I thus sought to validate the findings of the BioID experiment, focusing on p62 and NBR1, both key adapter proteins involved in the selection of cargo for autophagy-mediated degradation.

Using BioIP proximity labelling assays, I confirmed that endogenous p62 and NBR1 are both efficiently biotinylated by wt Nkd1-BirA*, but are completely untouched by ΔHRD Nkd1 (**Fig. 3.15C**). I further wanted to confirm the results of these proximity-labelling experiments using an alternative methodology: 'Lumier' assays allow direct quantification of binding by comparing the enrichment of luciferase-tagged preys in immunoprecipitates of control and protein-of-interest baits (**Fig. 3.15D**; Blasche & Koegl, 2013). Using this assay, I found that p62 binds to Nkd1 at levels significantly above background (**Fig. 3.15E**). However, whilst both

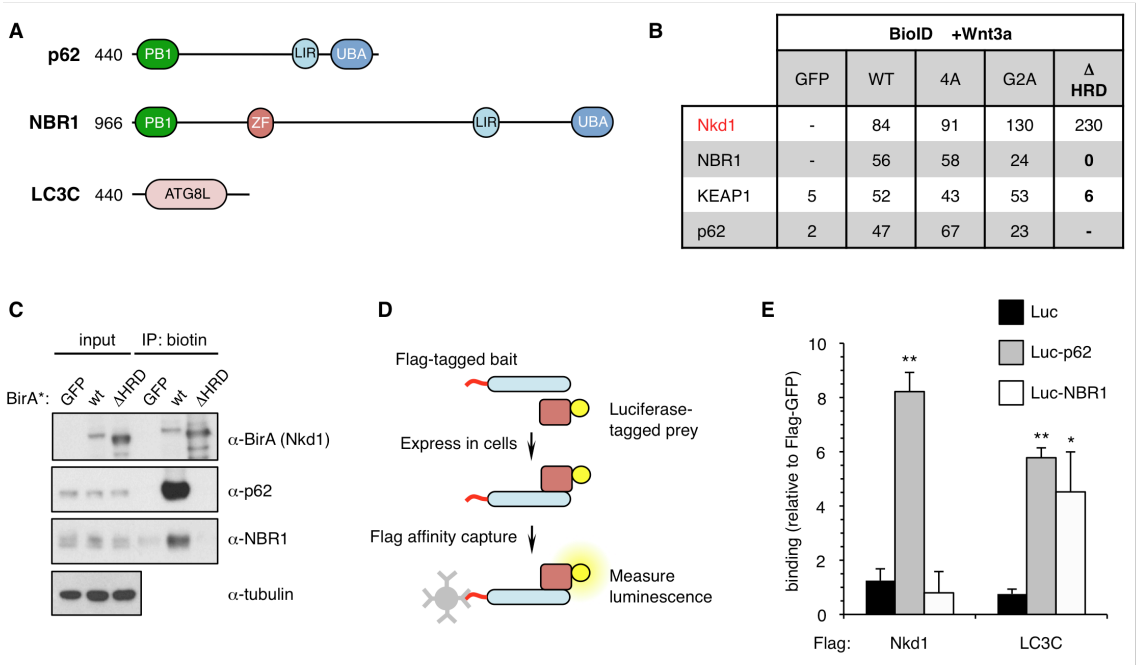

Figure 3.15 Autophagy adapter proteins identified by BioID interact with Nkd1.
(A) Domain architectures of autophagy related proteins used in these experiments.
(B) Table of selected proteins from **Fig. 3.14C**. Values represent total unweighted spectral counts (>95% probability).
(C) Proximity biotinylation assays, as previously, investigating binding between Nkd1 and autophagy proteins.
(D) Outline of Lumier assay methodology (Blasche & Koegl, 2013).
(E) Binding of Nkd1 and LC3C baits to autophagy adapter proteins. Shown are Lumier assay data indicating the binding of luciferase-tagged preys to Flag-Nkd1 and Flag-LC3C, relative to Flag-GFP (set to 1). Values are presented as mean ± SEM (n=3).

p62 and NBR1 associated with a known binding partner, LC3C, NBR1 did not bind Nkd1 at above-background levels, suggesting that NBR1 does not bind Nkd1 directly, but comes into close proximity later, perhaps after delivery to autophagosomes is initiated by p62.

3.2.8 Autophagy is not required for the function of overexpressed Nkd1

Having established that autophagy adapter proteins bind to Nkd1, either directly or indirectly, it was crucial to establish whether activity of any of these proteins, or indeed the autophagy pathway in general, is required for Nkd1 to inhibit cytoplasmic Wnt signal transduction. I therefore chose to test the effect of Nkd1 in cell lines in which p62 and NBR1 had been deleted. Given that these proteins are somewhat redundant with each other, and other autophagy adapters, I also wanted to generate a cell line in which autophagy is completely blocked, by deleting the essential component ATG5 (Tsukada & Ohsumi, 1993). Furthermore, given previous reports that Dvl ubiquitylation might be a crucial moderator of Wnt signal transduction, and a reported role for DUBs in this process (Tauriello *et al*., 2010b), I also elected to delete N4BP1 and CYLD, both identified as HRD-associated proteins, in the same screen.

I thus employed the CRISPR/Cas9 system, designing sgRNAs to induce double-strand breaks in 5'-proximal exons of the genes coding for these proteins, and confirmed their deletion from clonal HEK293T cell lines using Western blot analysis and DNA sequencing (**Fig. 3.16A, B**). ATG5 KO cells showed a marked increase in levels of p62 and NBR1, as would be expected when autophagy is completely abrogated (Bjørkøy *et al*., 2005). However, using SuperTOP assays I found no significant reduction in the ability of Nkd1 to inhibit Wnt3a-induced transcriptional responses in any of these cell lines (**Fig. 3.16C**). In all cell lines, as in wt cells, Nkd1 ΔHRD showed a greatly reduced ability to inhibit signalling. Similar results were observed when signalling was induced by overexpression of Dvl2 in the same cell lines (**Fig. 3.16D**). These data would suggest that none of these autophagy- or K63 polyUb-related proteins are cofactors essential for Nkd1 to function. However, it is important to note that Nkd1 is overexpressed in these assays, a major caveat in interpreting these results (see **Section 3.3.3** for discussion). Further work is clearly required to elucidate the mechanism(s) that Nkd employs to inhibit canonical Wnt signal transduction.

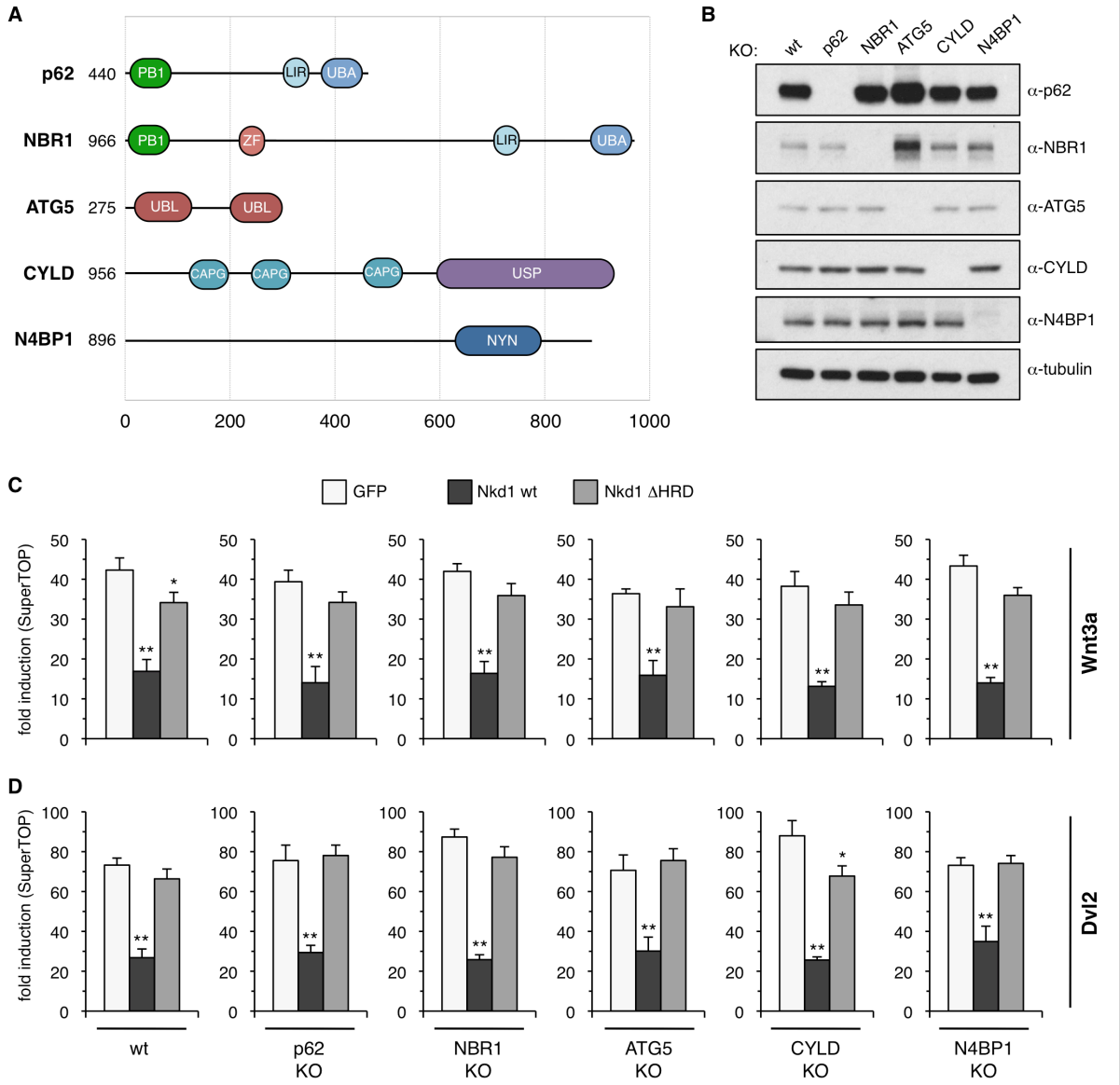

Figure 3.16 Knockout of candidate Nkd1 interactors does not interfere with Nkd1 function.

(A) Domain architectures of candidate interactors from BioID screen selected for further study by CRISPR/Cas9 knockout.

(B) Western blots of lysates from KO lines, probed with antibodies as indicated, to demonstrate absence of protein expression (see also **Appendix 1**).

(C) SuperTOP assays to measure Wnt signalling activity in KO cell lines (as indicated below) expressing the indicated proteins, and stimulated with Wnt3a. Values are presented as mean ± SEM (n=3), relative to control-treated cells.

(D) As (C), but Wnt pathway was stimulated by overexpression of Dvl2.

3.3 Discussion

The timely cessation of β-catenin dependent Wnt signal transduction is essential for normal development and physiology, and for the prevention of pathologies including cancer. However, how this key event occurs remains poorly understood. In this chapter, I set out to perform a detailed structural and functional analysis of Nkd, a conserved cytoplasmic negative regulator of canonical Wnt signal transduction, aiming to understand the mechanism by which it inhibits signalling. This study is still ongoing and, as such, all our conclusions remain tentative at this stage. Alongside the discussion, suggestions for further experiments that would help to consolidate and expand on our preliminary data are also outlined.

3.3.1 Conserved domains within Nkd are required for function

Wanting to begin the study with no preconceived ideas of how Nkd might function biochemically to reduce Wnt signalling, I sought to confirm previous genetic evidence suggesting that Nkd acts at the level of Dvl (Rousset *et al.*, 2001; Rousset *et al.*, 2002), using Wnt signalling assays in human cell lines. Overexpression of Nkd1 reduced Wnt transcriptional output in cells stimulated with either Wnt3a or Dvl2 overexpression, but not with LiCl or β-catenin expression (**Fig. 3.5**), confirming that Nkd acts at the level of Dvl.

Analysis of the primary sequence of Nkd, and alignments from several species including humans and *Drosophila* (**Fig. 3.2**) highlighted two conserved regions that seemed attractive candidates for further study, namely the central EF-hand fold and C-terminal HRD. Mutations that cause misfolding or deletion (respectively) of either of these regions completely abrogate the ability of Nkd to reduce Wnt signalling (**Fig. 3.6**). Previous evidence had suggested that the EF-hand might constitute a binding site for Dvl on Nkd (Rousset *et al.*, 2002). Indeed, our endogenous proximity labelling assays, as well as protein expression *in vitro*, confirm that this is the case, and mutations of the EF-hand which abrogate binding to Dvl also block the ability of Nkd to inhibit Wnt signalling *in vivo* (**Fig. 3.7, 3.8**). Interestingly, coIP assays between overexpressed proteins showed no clear difference between wt and 4A Nkd in binding to Dvl (data not shown). This could be because a weak secondary binding site (such as that reported immediately C-terminal to the EF-hand; Rousset *et al.*, 2002) is sufficient for interaction at the high protein concentrations achieved during overexpression.

Our data furthermore show that the central PDZ domain of Dvl constitutes the interaction site for Nkd, corroborating previous data (Rousset *et al.*, 2001). NMR data show that Nkd binding causes chemical shifts in numerous PDZ domain residues, implying binding to a region much more extensive than the peptide binding cleft through which ligands usually interact with the PDZ (**Fig. 3.8C**; Gammons *et al.*, 2016b). It is unclear whether this unusual mode of Nkd binding would be compatible or competitive with the binding of a peptide from another ligand

into the cleft, which could conceivably contribute to Nkd function, though this could easily be tested. Further biophysical characterization of this unusual interaction would be very interesting, not only from the point of view of understanding Nkd, but also to further appreciate the diverse range of interactions in which the Dvl PDZ domain appears able to participate. For example, using intermediate concentrations of EF-hand could allow peaks to be followed more closely and potentially identify key individual interacting residues within the PDZ, whilst an assignment of the Nkd EF-hand would be required to map the interacting region on the EF-hand. Miha Renko has purified a soluble, untagged EF-hand-PDZ complex, but no crystals have thus far been obtained from preliminary attempts at solving the structure.

Intriguingly, SEC-MALS analysis of bacterially expressed Nkd1 EF-hand strongly suggests that it is dimeric (**Fig. 3.8D**). Since Nkd has only a single EF-hand, this suggests that it forms intermolecular dimers, as opposed to the *intra*molecular dimers formed by most EF-hands, which occur in tandem (Babu *et al*., 1988). Although this is unusual, it is not unprecedented: an isolated EF-hand in STIM1 forms a calcium-sensing dimer, whilst calpain contains no fewer than five EF-hand folds, and dimerises via mutual interaction of the fifth EF-hand (Huang *et al*., 2009b; Blanchard *et al*., 1997). Furthermore, each EF-hand dimer interacts with a single PDZ domain, implying that the stoichiometry of the Nkd:Dvl interaction is 2:1. This stoichiometry would permit a high concentration of Nkd to be established at Wnt signalosomes, which could be crucial to its function.

Although the EF-hand has previously been suggested to bind several different cations, including Ca^{2+} (as is typical for EF-hand folds) and Zn^{2+} (Rousset *et al*., 2002), we found no evidence for this in our *in vitro* studies of Nkd. Treatment of Nkd1 EF-hand with high concentrations of EDTA or EGTA has no effect on folding *in vitro*, as observed during gel filtration, and does not disrupt the interaction of the EF-hand with the Dvl PDZ domain (Miha Renko, data not shown). However, these are preliminary experiments, and further studies using specialised mass spectrometry techniques might be required to answer the question of which, if any, metal cations are bound by Nkd.

Overall, our data suggest that the EF-hand represents a targeting domain, which serves to recruit plasma membrane-localised Nkd to Wnt signalosomes via a direct interaction with Dvl. This interaction occurs with the Dvl PDZ domain, which is not required for signalosome assembly (Gammons *et al*., 2016b), suggesting that this interaction alone cannot serve to catalyse signalosome disassembly.

3.3.2 The Nkd HRD is a unique domain that forms unusual structures

Having established a key role for the EF-hand in Nkd function, the second domain that we focused on was the highly unusual C-terminal HRD (histidine rich domain). Recall that the HRD is required for full inhibition of Wnt signalling by Nkd (**Fig. 3.6**). Given that Nkd can be recruited to Wnt signalosomes via its EF-hand, we were intrigued by the possibility that the HRD might serve to recruit an effector protein (or proteins) that could facilitate signalosome disassembly or otherwise inhibit canonical Wnt signalling.

Surprisingly, I observed bands on Western blots corresponding to extremely high molecular weight (HMW) species of overexpressed wt Nkd, but never ΔHRD Nkd. This serendipitous observation suggested that the HRD might somehow promote the clustering or aggregation of Nkd molecules, which can indeed be observed using fluorescence microscopy (**Fig. 3.9B**). Positioning and/or cutting of the PDVF membrane used for blotting means that these bands had initially escaped notice. Although we were skeptical that these HMW species might be artefacts of gel running, they are clearly also present in solution and are highly stable, proving resistant to harsh treatments up to (and including) boiling in 20% SDS (**Fig. 3.9C**). Although unusual, the formation of stable HMW species is not unprecedented, having previously been observed for proteins that are modified by addition of C-terminal alanine/threonine (CAT) tails (Shen *et al.*, 2015, Yonashiro *et al.*, 2016), or those containing expanded polyglutamine (polyQ) tracts (Kim *et al.*, 2002). As expected, mutation of histidine residues within the HRD abrogates the ability to form these species, and it will be essential to test such mutations in our *in vivo* assays of Nkd function.

Data from our *in vitro* experiments give some clues as to the nature of these HMW species. Gel filtration analysis estimates the stoichiometry of these species to be variable, with a mean of around 16 Nkd moieties per cluster, a figure was corroborated by MALDI-TOF mass spectrometry. Boiling appears to reduce the clusters to a stable ‘core’ of 10 molecules. Although our preliminary attempts at structure solution have so far yielded no crystals or promising electron microscopy data, we speculate that this stable ‘core’ might be ring-shaped, as occurs in several other well-described aggregates (see for example Tran *et al.*, 2016), and that further HRDs are then able to associate with this core. Although histidine residues are known to coordinate metal cations in many instances, addition of EDTA has no effect on HRD clustering either *in vivo* or *in vitro*, implying that such cations are not required for this process.

Given that our data was collected with overexpressed Nkd, a crucial question is whether this ‘histidine clustering’ effect occurs when Nkd is present at endogenous levels, seeing as it is expected to be concentration-dependent. We did not observe HMW species in gels when BirA*-tagged Nkd1 constructs were stably expressed in mammalian cells. However, in the context of the signalosome, where high local concentrations of Nkd are achieved as a result

of binding to polymerized Dvl, would seem to provide ideal conditions for the association of multiple Nkd HRDs to form clusters. Further experiments, perhaps employing super-resolution microscopy techniques, will be required to fully elucidate the structures formed by Nkd, and how they interact with the signalosome. Studies are also needed to determine the dynamicity of these clusters. Fluorescence recovery after photobleaching (FRAP) experiments have revealed that the puncta formed upon Dvl overexpression are highly dynamic (recovering within ~10 s), with Axin puncta being marginally less so (Schwarz-Romond *et al*., 2005; Schwarz-Romond *et al*., 2007b). On the basis of their stability *in vitro*, we might predict Nkd clusters to be much more long-lived if studied by the same method. This could have the effect of stabilising the entire signalosome, preventing the exchange of Dvl molecules, although it is difficult to predict what this might mean in terms of Wnt signal transduction. Alternatively, it could allow the stable recruitment of further factors to the signalosome.

Intriguingly, the formation of HMW clusters by the Nkd HRD is pH dependent, being strongly disfavoured at pH values lower than around 6.3 (very close to mean pK_a values for histidine residues within proteins; Edgcomb & Murphy, 2002). Protonation of histidine residues likely blocks the interaction of one positively charged HRD with another, suggesting that highly stable Nkd clusters could nonetheless be rapidly disassembled in a low pH environment, such as that found within the lysosome. Although speculative, this could have implications for Nkd function in signalosome disassembly.

A final interesting question is whether this property of histidine-dependent clustering is a more general phenomenon. Relatively few proteins contain histidine rich regions, and these are rarely as pronounced at that of mammalian Nkd1. Multiple histidine residues are clearly required for formation of these species, but mutation of non-histidine residues also has a negative effect on clustering of Nkd1. Indeed, preliminary testing of a selection of 11 HRDs from other proteins, including Axin1 (carried out by Miha Renko; **Fig. 3.11A**) suggests that they will not cluster alone in the same fashion as Nkd, although it is notable that the Axin1 HRD is able to associate with the Nkd HRD, forming clusters containing both proteins. This interaction does not, however, seem to compete with Axin's interaction with Dvl or directly promote signalosome disassembly (**Fig. 3.12**). It will be interesting to test whether *Drosophila* Nkd is able to cluster in a similar fashion, as although it does contains a histidine-rich region, this is more extended, with a lower density of histidine residues. Further analysis is clearly required to identify the exact determinants of the Nkd1 HRD that make it so prone to clustering.

3.3.3 Models for Naked-dependent switching of cytoplasmic Wnt signalling

Given the requirement of the HRD for the ability of Nkd to inhibit canonical Wnt signalling, the unusual properties of this domain, and the lack of any obvious enzymatic (or other) activity within Nkd, I decided to search for interacting partners of Nkd using a proteomics approach, hypothesizing that hitherto unknown factors might be required in order for Nkd to promote signalosome disassembly or switching. Standard coIP-based methodologies failed to yield useful results (data not shown), but a screen using BioID proximity labelling successfully identified a number of interesting candidate interacting partners of the Nkd HRD (**Fig. 3.14C**), including multiple proteins involved in the autophagy pathway, and several implicated in the regulation of K63-linked polyUb chains, which were subsequently confirmed by other methods. Given the preliminary data presented in this chapter, I would thus like to present three models for mechanisms by which Nkd could catalyse signalosome switching, and hence to promote the cessation of canonical Wnt signalling (**Fig. 3.17**). Although these models remain highly speculative, they constitute a starting point for further studies to confirm or discount.

Three proteins identified in the BioID screen that I focused on were the key autophagy receptors p62 and NBR1, and the associated adapter protein KEAP1. A mechanism whereby Nkd might promote the autophagic degradation of Dvl, through recruitment of these adapters, would be elegant and simple, particularly in light of the aggregation-prone nature of the HRD (**Fig. 3.17A**). Several reports have previously implicated p62 and autophagy in regulation of Dvl (Zhang *et al*., 2006; Gao *et al*., 2010). Although p62 contains a DIX-like PB1 domain, it cannot bind directly to Dvl (Ciara Metcalfe, PhD thesis). Instead, various proteins including Dapper1 and receptor for activated C kinase 1 (RACK1) have been proposed to provide the link between these components (Ma *et al*., 2015; Cheng *et al*., 2016). However, evidence from genetics would suggest that Nkd plays a far more widespread role in negative regulation of the Wnt pathway than either of these factors, and could represent the primary mechanism through which autophagy regulates Dvl.

In many cases, including those already proposed to regulate Dvl, autophagy is directed by the assembly of ubiquitin on substrates, which serves to recruit autophagy receptors including p62 and NBR1 (Pankiv *et al*., 2007; Kirkin *et al*., 2009). However, our data suggest that Nkd is not heavily ubiquitylated *in vivo*, and indeed may not require this modification, given that protein aggregates appear to constitute prime targets for autophagic degradation (Khaminets *et al*., 2016). If this model turned out to be correct, it will be crucial to test which signalosome components are degraded, and whether there is any selectivity for Dvl in this process. Given that Nkd also interacts with Axin, one might expect that the entire signalosome complex would

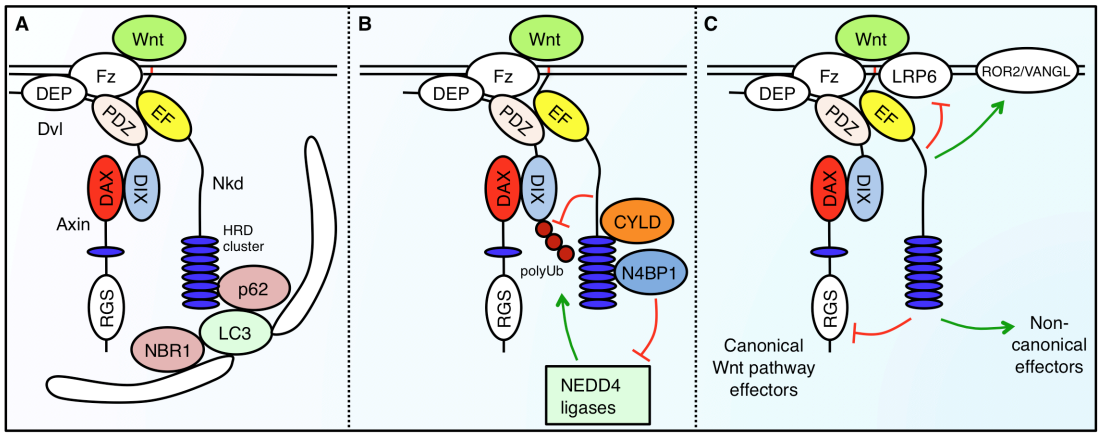

Figure 3.17 Models for Naked function.

(A) Nkd is localised to Wnt signalosomes via the interaction of the EF-hand with the Dvl PDZ domain. The 2:1 stoichiometry of this interaction, along with the polymerized nature of Dvl, creates a high local concentration of Nkd, permitting HRD-dependent clustering to occur. These clusters, which may also recruit Axin, are recognised by autophagy receptors such as p62 and earmarked for autophagy-mediated degradation.

(B) Nkd is localised to signalosomes as in (A), but the HRD serves to recruit components of the ubiquitin system, including CYLD and N4BP1, which inhibit ubiquitylation of the DIX domain and could serve to thus block DIX-dependent polymerization (Tauriello *et al.*, 2010b).

(C) Nkd is localised to canonical Wnt signalosomes, where it promotes the exchange of canonical Wnt signalling factors and receptors (including the key canonical co-receptor, LRP5/6) for those involved in non-canonical signalling. Details of how this switch might occur are yet to be elucidated.

be sequestered within the autophagic membrane. It would then be interesting to test whether the acidic conditions found in the lysosome allow for disassembly of these clusters, as might be predicted by the pH-dependency of Nkd HRD aggregation (**Fig. 3.10B**).

An alternative model for the role of Nkd is that it regulates the ubiquitylation status of Dvl (**Fig. 3.17B**), through the concomitant recruitment of the deubiquitylase CYLD and N4BP1, an inhibitor of NEDD4-family E3 ubiquitin ligases such as ITCH (Oberst *et al.*, 2007). Dvl is modified with non-degradative K63-linkages by a number of ligases (including ITCH; Wei *et al.*, 2012), and CYLD has previously been implicated in Dvl regulation, having been shown to cleave these chain types from the Dvl1 DIX domain, promoting signalosome disassembly by abrogating DIX-dependent polymerization (Tauriello *et al.*, 2010b). Importantly, this study could not demonstrate direct binding between Dvl and CYLD *in vitro*, suggesting that another factor, such as Nkd, may be required to in order to promote this interaction and permit deubiquitylation to occur. However, the effect of DIX ubiquitylation is residue-dependent, given that modification of Lysine-54 abrogates polymerization, whilst ubiquitylation of Lysine-58 has no effect (Madrzak *et al.*, 2015). It is important to note that these models for Nkd function are not mutually exclusive; indeed, given that K63-linked ubiquitin chains are a

primary signal for autophagy (Seibenhener *et al.*, 2004), they may well be working in concert. Such a mechanism would require some complexity, however, given that the predicted effect of CYLD and N4BP1 recruitment to Dvl would be to remove ubiquitin, rather than add it.

However, despite the simplicity and attractiveness of these two models, it is important to recognize that they are not immediately consistent with our data. Most principally, deletion of p62, NBR1, or the key autophagy mediator ATG5 using CRISPR/Cas9 does not appear to block the ability of Nkd to reduce Wnt signalling responses. Similarly, Nkd seems to function in the absence of CYLD or N4BP1 (**Fig. 3.16**). Whilst concerning, these experiments do not necessarily imply that these models are incorrect. For example, there may be redundancy between different components and pathways, particularly if Nkd is acting via multiple mechanisms. An overriding concern with all of these data is that overexpression of Nkd might mask a more subtle effects that the protein would have at endogenous levels, and it may be important to establish assays of Nkd function that do not rely on this in order to establish the true mechanism of Nkd function. One way to achieve this might be to generate cell lines in which Nkd1 and Nkd2 are deleted using CRISPR/Cas9. Wt or mutant Nkd constructs could then be stably reexpressed at near-endogenous level, as has been achieved for Dvl in our lab (Gammons *et al.*, 2016b).

It is certainly also possible that the models proposed are incorrect, and that we have not yet identified a key cofactor of Nkd. Another potential avenue for further study, which we have not touched upon in this chapter, is a potential role for Nkd in the endocytosis of Wnt receptors or other signalosome components. The Nkd HRD contains a C-terminal YHHF motif that constitutes a classical YXXΦ signal sequence for clathrin-mediated endocytosis (Olsen & Grose, 1998). The endocytic pathway can selectively deliver contents to lysosomes, and shares much of the machinery for degradation with the autophagy pathway (Lamb *et al.*, 2013), potentially providing an alternative route by which Nkd could promote the degradation of signalosome components. On the other hand, our BioID data also hints at a potential role for Nkd in controlling the switch between canonical and non-canonical Wnt outputs, as has previously been suggested (Yan *et al.*, 2001; **Fig. 3.17C**). Although Nkd does not seem to direct PCP signalling in the context of the *Drosophila* wing (Zeng *et al.*, 2000), this could be due to redundancy with another factor, such as Diego (Schwarz-Romond *et al.*, 2002). Interestingly, the only other protein that appears to employ a folded domain to interact with the Dvl PDZ domain, in a similar fashion to Nkd, is diversin (the mammalian homolog of Diego), which acts to redirect Dvl such that canonical Wnt signalling is inhibited and the PCP pathway promoted (Jenny *et al.*, 2005). Nkd could promote a similar 'switching' of Wnt signalosomes. Multiple Fz co-receptors implicated in non-canonical Wnt signalling were identified in the BioID screen, including VANGL1/2 and ROR2 (Murdoch *et al.*, 2001; Takeuchi *et al.*, 2000). Intriguingly, VANGL2 has also been identified as an interacting partner

of p62 (Puvirajesinghe *et al*., 2016). Further work will be required to validate these interactions, and improved biochemical tools to assay non-canonical signalling outputs needed to study a potential role for Nkd in redirecting the output of Wnt signalling towards these pathways.

In conclusion, in this chapter I have presented initial results towards the understanding of the mechanistic basis of Nkd function. We have determined the biochemical properties of two key domains of Nkd, and identified a number of candidate proteins that could constitute key interactors of the Nkd HRD. Further work is now required to fully understand the role(s) of this enigmatic protein in terminating canonical Wnt signalling.

4. Materials & Methods

Some passages in this chapter have been quoted verbatim, or adapted from, the Materials & Methods section of Flack *et al*., 2017.

4.1 Key Resources Table

This following key resources and reagents were used during the course of this study:

Reagent	Source
Antibodies	
α-UBR5	Abcam
α-GFP (rabbit)	Sigma
α-GFP (mouse)	Sigma
α-Flag (mouse)	Sigma
α-Flag (rabbit)	Sigma
α-HA (rat)	Sigma
α-HA (rabbit)	Abcam
α-Myc	Santa Cruz Biotechnology
α-active β-catenin (ABC)	Cell Signaling Technologies
α-β-catenin	BD Transduction Laboratories
α-XIAP	BD Transduction Laboratories
α-HUWE1	Abcam
α-TRIP12	Abcam
α-HECTD1	Abcam
α-UBE3C	Abcam
α-β-tubulin	Sigma
α-TLE1-4	Santa Cruz Biotechnology
α-GST	Abcam
α-Nkd1	Abcam
α-BirA	Abcam
α-Ub (FK2)	Sigma
α-Dvl2	Cell Signalling Technologies
α-p62	Abnova
α-NBR1	Abnova
α-ATG5	Sigma
α-CYLD	Cell Signaling Technologies
α-N4BP1	Abcam
HRP conjugated Goat α-Mouse	Santa Cruz Biotechnology
HRP conjugated Goat α-Rabbit	Santa Cruz Biotechnology
HRP conjugated Goat α-Rat	Santa Cruz Biotechnology
HRP conjugated Goat α-Chicken	Santa Cruz Biotechnology
HRP conjugated Donkey α-Goat	R&D Systems
Alexa Fluor 488 conjugated Goat α-Rabbit	Life Technologies
Alexa Fluor 488 conjugated Goat α-Mouse	Life Technologies
Alexa Fluor 546 conjugated Goat α-Mouse	Life Technologies
Alexa Fluor 546 conjugated Goat α-Rat	Life Technologies
Alexa Fluor 647 conjugated Goat α-Mouse	Life Technologies
Alexa Fluor 647 conjugated Goat α-Guinea pig	Invitrogen

α-Senseless	Prof. Hugo J. Bellen
α-Vestigial	Prof. Sean B. Carroll
α-Wingless	DSHB
α-Armadillo	DSHB
Chemicals, peptides and recombinant proteins	
Ni-NTA Agarose	Qiagen
α-FLAG M2 Affinity Gel	Sigma
EZview Red α-HA Affinity Gel	Sigma
GFP-trap_A	Chromotek
Glutathione Sepharose 4b	GE Healthcare
Dynabeads MyOne Streptavidin C1	Invitrogen
Lipofectamine2000	Invitrogen
Polyethylenimine, linear, MW25000	Polysciences
EDTA-free Protease Inhibitor Cocktail	Roche
MG132	Sigma
NMS-873	Cayman Chemical Co.
CB-5083	Cayman Chemical Co.
Cycloheximide	Sigma
Puromycin dihydrochloride	Sigma
Hygromycin B	Sigma
Tetracycline	Sigma
3xFLAG-Peptide	Sigma
L-Glutathione reduced	Sigma
VectaShield with DAPI	Vector Laboratories
Ubiquitin-activating enzyme E1 (UBE1A)	Boston Biochem
Ubiquitin-conjugating enzyme E2 (UBE2L3)	Boston Biochem
Ubiquitin	Boston Biochem
Methyl-ubiquitin	Boston Biochem
K6-only ubiquitin	Boston Biochem
K11-only ubiquitin	Boston Biochem
K27-only ubiquitin	Boston Biochem
K29-only ubiquitin	Boston Biochem
K33-only ubiquitin	Boston Biochem
K48-only ubiquitin	Boston Biochem
K63-only ubiquitin	Boston Biochem
Histone H2A (1-22) - GK(Biotin)	AnaSpec Inc.
Histone H3 (1-21) Biotinylated	AnaSpec Inc.
Histone H4 (1-23) - GGK(Biotin)	AnaSpec Inc.
Commercial assays/kits	
Dual-Luciferase Reporter Assay System	Promega
UbiCRest Deubiquitinase Enzyme Kit	Boston Biochem
RNeasy Mini Kit (RNA Purification)	Qiagen
iScript cDNA synthesis kit	Biorad
SYBR Select Master Mix	Applied Biosystems

4.2 Cloning

The following key parental plasmids were used during the course of these studies:

Plasmid	Source
Flag-UBR5	Prof. Rina Rosin-Arbesfeld (Hay-Koren *et al*., 2011)
GFP-UBR5	subcloned from Flag-UBR5
GST-UBR5 HECT	Bienz Lab, MRC-LMB
GFP (empty vector)	Bienz Lab, MRC-LMB
Flag-GFP	subcloned from GFP (empty vector)
HA-GFP	subcloned from GFP (empty vector)
HA-β-catenin-Δ45	Bienz Lab, MRC-LMB (Morin *et al*., 1997)
Myc-TLE3	Prof. Ethan Lee (Hanson *et al*., 2012)
HA-TLE3	subcloned from Myc-TLE3
Flag-TLE3	subcloned from Myc-TLE3
VCP-GFP	Prof. Nico Dantuma (Tresse *et al*., 2010)
HA-PAIP2	Bienz Lab, MRC-LMB
His-Ub	Dr. Thomas Mund
GST-HES1	Prof. Stefano Stifani
SSDP-GFP	Bienz Lab, MRC-LMB (Fiedler *et al*., 2015)
LDB1-GFP	Bienz Lab, MRC-LMB (Fiedler *et al*., 2015)
GFP-TCF4	Bienz Lab, MRC-LMB
GFP-Pygo1	Bienz Lab, MRC-LMB
HA-Nkd1	Bienz Lab, MRC-LMB
Flag-Nkd1	Bienz Lab, MRC-LMB
Flag-Dvl2	Bienz Lab, MRC-LMB
Lip-Dvl2 PDZ	Bienz Lab, MRC-LMB
Axin-GFP	Bienz Lab, MRC-LMB
GFP-p62	Randow Lab, MRC-LMB
Flag-LC3C	Randow Lab, MRC-LMB
Luciferase-p62	Randow Lab, MRC-LMB
Luciferase-NBR1	Randow Lab, MRC-LMB
pcDNA5/FRT/TO	van Breugel Lab, MRC-LMB
pOG44	van Breugel Lab, MRC-LMB
PX458	(Ran *et al*., 2013)
PX459	(Ran *et al*., 2013)
Super 8x TopFLASH (SuperTOP)	(Veeman *et el*., 2003)
CMV-Renilla	Promega (Cat #E2261)

Cloning and mutagenesis of parental plasmid DNA to generate other constructs was carried out using standard PCR-based methods, using either KOD DNA polymerase (Merck Millipore) or Phusion DNA polymerase (NEB), and verified by sequencing.

4.3 *Drosophila* strains and analysis

All Drosophila analysis was performed by Juliusz Mieszczanek. The following strains of *Drosophila melanogaster* were used during the course of this study:

Strain	Source	Identifier
$hyd^{K7\text{-}19}$	Prof. Jessica E. Treisman	FlyBase: FBal0144234
gro^{MB36}	Prof. David Ish-Horowicz	FlyBase: FBal0230454
$axin^{p}$	Prof. Tetsu Akiyama	FlyBase: FBal0097414
UAS.SoxF	Dr. Fernando Casares	FlyBase: FBtp0051564
$pygo^{S123}$	Bloomington Drosophila Stock Centre	FlyBase: FBal0146872
$UAS.Arm^{S10}$	Bloomington Drosophila Stock Centre	FlyBase: FBtp0001723
UAS.MamDN	Prof. Sarah Bray	FlyBase: FBtp0014588
Vg-Gal4, UAS-flp; FRT82b GFP	Bienz Laboratory, MRC-LMB	(Miller *et al.*, 2013)

Double mutant *Drosophila* strains were generated from parental strains with standard techniques, and checked by complementation.

Fly wings were dissected and mounted in 6:5 mixture of lactic acid:ethanol, and imaged with a Nikon Eclipse TE2000-E microscope.

Wing disc clones were generated with *vg.GAL4, UAS.flp; FRT82b GFP* (also used for overexpression of UAS transgenes), as previously described (Miller *et al.*, 2013). Wing discs were dissected from late third-instar larvae, fixed in phosphate-buffered saline (PBS) containing 4% formaldehyde, 0.1% Triton X-100 for 30 min and permeabilised in 0.1% Triton X-100 in PBS for 5x 5 min. Discs were blocked in blocking buffer (PBS supplemented with 0.5% bovine serum albumin, 0.1% Tween-20) for 1 hr and incubated with primary antibodies in blocking buffer at 4 °C. Discs were washed in blocking buffer and incubated with secondary antibodies. Discs were embedded in VectaShield with DAPI mounting media, and single confocal images acquired at identical settings on a Zeiss LSM510 or LSM710 confocal microscope.

4.4 Mammalian cell culture

HEK293T, HEK293, HCT116, HeLa and COS-7 cells were cultured in DMEM (ThermoFisher Scientific), supplemented with 10% FBS (fetal bovine serum) at 37 °C in a humidified atmosphere with 5% CO_2. No antibiotics were included in the media, and cell lines were regularly screened for *Mycoplasma* infection.

For transfections, cells were plated 10-12 hrs prior to transfection in plates pre-treated with poly-L-lysine (Sigma). Cells were transfected with polyethylenimine (PEI) or Lipofectamine 2000 according to the manufacturer's instructions.

Wnt inductions were for 6 hrs, either with Wnt3a-conditioned media or 20 mM LiCl. L-cell conditioned media or 20 mM NaCl, respectively, were used as controls. Where noted, 10 μM MG132, 5 μM NMS-873, 2.5 μM CB-5083 or 50 μg mL^{-1} cycloheximide was added for the same time.

4.5 CRISPR/Cas9 genome editing

HEK293T or HCT116 KO cell lines were generated essentially as described (Ran *et al.*, 2013). The Optimized CRISPR Design tool (*crispr.mit.edu*) was used to design sgRNA-encoding plasmid derivatives of pSpCas9(BB)-2A-GFP (PX458) for each gene to be targeted (see **Appendix 1**). Cells were selected for high expression of GFP by FACS 48 hrs post-transfection, and individual clones expanded in 96-well plates. Clones were screened by Western blot analysis and subsequently by DNA sequencing (**Appendix 1**) to confirm the presence of frameshifting indels. To ensure consistency, multiple lines were isolated and sequenced for each gene being knocked out. MicroLYSIS-Plus (Microzone) was used as per the manufacturer's instructions for sequencing of genomic DNA.

For transient knockdowns, sgRNAs were cloned into pSpCas9(BB)-2A-Puro (PX459). Selection with puromycin was initiated 48 hrs post-transfection and carried out for 96 hr. Cells were left to recover for 72 hrs prior to seeding for experiments.

4.6 Cell-based signalling assays

For luciferase reporter (SuperTOP) assays, cells were lysed 20 hrs post-transfection with SuperTOP and CMV-Renilla (control) plasmids, and analysed with the Dual-Glo Luciferase Reporter Assay kit (Promega) according to the manufacturer's protocol. Values were normalised to Renilla, and are shown as mean ± SEM relative to unstimulated controls (set to 1) or to stimulated wt cells (set to 100%) for at least three independent experiments.

4.7 Co-immunoprecipitation assays

For coIP assays, cells were lysed 24-36 hrs post-transfection in lysis buffer (20 mM Tris-HCl pH 7.4, 200 mM NaCl, 10% glycerol, 5 mM NaF, 2 mM Na_3VO_4, 0.2% Triton X-100, protease inhibitor cocktail). Lysates were clarified by centrifugation (16,100x *g*, 10 min), and supernatants incubated with (Flag- or HA-) affinity gel or GFP-trap for 90 min at 4 °C. Subsequently, immunoprecipitates were washed 4x in lysis buffer and eluted by boiling in LDS (lithium dodecyl sulphate) sample buffer for 10 min.

CoIP assays using biotinylated histone tail peptides were conducted in similar fashion, except that lysates were incubated with 1.5 μM biotinylated peptide for 45 min, prior to the addition of streptavidin dynabeads.

4.8 *In vivo* ubiquitylation assays

Ni-NTA pull-down experiments to enrich proteins modified with His-ubiquitin were conducted in the same fashion as coIP assays, except that cells were lysed in urea buffer (8 M urea, 50 mM Na_2HPO_4 pH 8.0, 300 mM NaCl, 2 mM N-ethylmaleimide (NEM), 5 mM chloroacetamide, 0.5% NP40, 25 mM imidazole, protease inhibitor cocktail) and sonicated for 2x 10 sec with a Soniprep 150 plus sonicator (MSE) prior to addition of Ni-NTA agarose. Beads were washed 6x in urea buffer and ubiquitylated proteins eluted by boiling in LDS sample buffer.

4.9 "UbiCRest" deubiquitylation assays

For UbiCRest assays (Hospenthal *et al*., 2015), the UbiCRest DUB Enzyme kit was used, following the manufacturer's protocol. Briefly, immunoprecipitates of Flag-TLE3 or HA-Ub (generated as above) were washed twice and resuspended in '1X DUB reaction buffer'. DUBs were added and reactions incubated for 45 min at 37 °C (while rotating), and subsequently quenched by addition of LDS sample buffer. An aliquot of each reaction was resolved via SDS-PAGE and analysed by Western blotting.

4.10 Immunofluorescence

HeLa or COS-7 cells were fixed on coverslips for 10 min with 4% formaldehyde, and permeabilised for 5 min in 0.2% Triton X-100 in PBS. Cells were then blocked in 5% bovine serum albumin (BSA) in PBS, and incubated with primary antibodies. Cells were washed (in 0.1% Triton X-100 in PBS) and incubated with secondary antibodies. Coverslips were washed and embedded with VectaShield with DAPI mounting media. Images were acquired at identical settings on a Zeiss LSM510 or LSM710 Confocal Microscope.

4.11 Mass spectrometry

For affinity purification of UBR5-associated proteins, 20x 175 cm^2 flasks of HEK293T cells transfected with UBR5 or control baits were used for each experiment. Cells were lysed in 40 mL lysis buffer (20 mM Tris-HCl pH 7.4, 10% glycerol, 100 mM NaCl, 5 mM NaF, 2 mM Na_3PO_4, 0.2% Triton X-100, protease inhibitor cocktail), and sonicated 10x 10 sec at 40% intensity with a Branson 250 Sonifier. Cell lysates were clarified by centrifugation (21,000x *g*, 30 min, 4 °C) and incubated (while rotating) for 2 hrs with Flag affinity gel at 4 °C. Immunoprecipitates were washed 5x with lysis buffer, and subsequently eluted with lysis buffer supplemented with 250 mg mL^{-1} 3xFlag-Peptide. Eluates were boiled in LDS sample buffer and resolved on 4-12% Bis-Tris SDS-polyacrylamide gels. These were stained with Imperial Protein Stain, and gel lanes cut into 1-2 mm slices.

WD40 domain-associated proteins and post-translational modifications were affinity purified in the above fashion, except that 8x 175 cm^2 flasks were used for transfection.

All mass spectrometry analysis was performed by the LMB Mass Spectrometry Facility. Briefly, peptides from *in situ* trypsin digestion were extracted in 2% formic acid/2% acetonitrile mix. Digests were analysed by nano-scale capillary LC-MS/MS using an Ultimate U3000 HPLC and C18 Acclaim PepMap100 nanoViper (Thermo Scientific Dionex). LC-MS/MS data were searched against a protein database (UniProt KB) with the Mascot search engine program (Matrix Science). MS/MS data were validated using the Scaffold program (Proteome Software).

4.12 BioID methodology

BirA*(R118G) and Nkd1 coding sequences were subcloned into pcDNA5/FRT/TO to generate vectors for expression of BioID bait proteins. Stably transfected HEK293 cell lines inducibly expressing BioID baits were generated using the Flp-In system (ThermoFisher Scientific) according to the manufacturer's protocol. Briefly, Flp-in HEK293 cells were transfected with a 4:1 ratio of pOG44 recombinase:pcDNA5 bait plasmid, left to recover for 36 hrs and then selected with 250 μg/ml hygromycin B for at least 7 days.

For large scale BioID experiments, cells were induced with 1 μg/ml tetracyline for 24 hr, and treated with 50 μM biotin for 12 hrs prior to lysis. BioID pulldowns were carried out using Streptavidin MyOne dynabeads (ThermoFisher) essentially as described (Roux *et al.,* 2013), and biotinylated proteins eluted by boiling in LDS sample buffer. SDS-PAGE (for 'BioIP' experiments) and mass spectrometry analysis were carried out as above.

4.13 Protein expression and purification

All recombinant proteins were purified from BL21 (DE3) pRIL *E. coli* bacterial strains. Bacteria were grown in LB media supplemented with appropriate antibiotic to an OD600 of approximately 0.7 and induced by addition of 0.4 mM isopropyl-β-D-1-thiogalactopyranoside (IPTG). Proteins were expressed for 6 hrs at 37 °C or for 12 hrs at 22 °C. Cells were resuspended in lysis buffer (25 mM Tris-HCl pH 8.0, 200 mM NaCl, 10% glycerol, 5 mM β-mercaptoethanol, 10 mg mL^{-1} DNase, protease inhibitor cocktail) and lysed by high-pressure homogenization with an Emulsiflex C-3. Lysates were clarified by ultracentrifugation (140,000x *g*, 30 min, 4 °C). His-tagged proteins were purified on Ni-NTA agarose beads (Qiagen) and washed 4x with lysis buffer (containing 20 mM imidazole) prior to elution (in lysis buffer contain 250 mM imidazole).

For purification of GST-tagged proteins, lysates were mixed with glutathione Sepharose 4B. Beads were washed 7x with lysis buffer, including a high salt (500 mM NaCl) fourth wash, and GST-tagged protein eluted with 20 mM L-glutathione (reduced).

All proteins were purified by a final size exclusion chromatography step, and purity was assessed by SDS-PAGE prior to use in experiments.

4.14 SEC-MALS

SEC-MALS analysis was performed in collaboration with Chris Johnson and Miha Renko. 100 μl Nkd EF-hand and/or Dvl2 PDZ samples were resolved on a Superdex S-200 analytical gel filtration column (GE Healthcare) in gel filtration buffer (150 mM NaCl, 25 mM Na_2HPO_4, pH 6.7) before light scattering and concentration determination using refractive index (RI) or UV absorbance in a standard SEC-MALS configuration (containing a Wyatt Heleos II 18 angle light scattering instrument coupled to a Wyatt Optilab rEX online RI detector).

4.15 *In vitro* ubiquitylation assays

In vitro ubiquitylation assays were carried out essentially as previously reported (Mund & Pelham, 2009). Assays were conducted in 20 μL format in buffer consisting of 25 mM Tris-HCl pH 7.4, 10 mM $MgCl_2$, 1 mM ATP, 200 ng UBE1A, 750 ng UBE2L3, 800 ng GST-$HECT_{2217-2799}$-wt or GST-$HECT_{2217-2799}$-CS (each produced as above, **Section 4.13**), and 500 ng ubiquitin (wt, methyl- or K-only mutant). Reactions were incubated for 2 hrs at 30 °C and quenched by the addition of LDS sample buffer. An aliquot of each reaction was resolved via SDS-PAGE and analysed by Western blotting.

4.16 Protein NMR

All NMR spectroscopy was performed in collaboration with Trevor Rutherford and Miha Renko. Nkd1 EF-hand and Dvl2 PDZ samples were prepared in NMR buffer (150 mM NaCl, 25 mM Na_2HPO_4, pH 7.4). Spectra were acquired on a Bruker Avance-3 spectrometer operating at 600 MHz and 25 °C.

4.17 RT-qPCR

RNA was extracted with the RNeasy mini kit and converted to cDNA using the iScript cDNA synthesis kit, as described in the manufacturer's protocols. RT-qPCR reactions were run in 20 μL, 96-well format on a Vii7 Real-Time PCR System (Applied Biosystems) using SYBR Select Mix with the primer pairs listed (**Appendix 2**). Values were normalised to *PMM1* (Hanson *et al*., 2012), and are shown as mean ± SEM relative to unstimulated controls (set to 1) for at least three independent experiments.

4.18 Quantitation and statistical analysis

All error bars represent mean ± SEM for at least three independent experiments. Statistical significance was calculated using the Student's t-test and denoted as follows in all cases: * = $p < 0.01$, ** = $p < 0.001$.

References

Aberle H, Bauer A, Stappert J, Kispert A, Kemler R (1997) Beta-catenin is a target for the ubiquitin-proteasome pathway. *EMBO J.* **16**: 3797-804

Acebron SP, Karaulanov E, Berger BS, Huang Y-L, Niehrs C (2014) Mitotic Wnt signaling promotes protein stabilization and regulates cell size. *Mol. Cell* **54**: 663-74

Aita VM, Liang XH, Murty VV, Pincus DL, Yu W, Cayanis E *et al.* (1999) Cloning and genomic organization of beclin 1, a candidate tumor suppressor gene on chromosome 17q21. *Genomics* **59**: 59-65

Albuquerque C, Breukel C, van der Luijt R, Fidalgo P, Lage P, Slors FJ *et al.* (2002) The 'just-right' signaling model: APC somatic mutations are selected based on a specific level of activation of the beta-catenin signaling cascade. *Hum. Mol. Genet.* **11**: 1549-60

Alexandre C, Baena-Lopez A, Vincent J-P (2014) Patterning and growth control by membrane-tethered Wingless. *Nature* **505**: 180-5

Amit S, Hatzubai A, Birman Y, Andersen JS, Ben-Shushan E, Mann M *et al.* (2002) Axin-mediated CK1 phosphorylation of β-catenin at Ser 45: a molecular switch for the Wnt pathway. *Genes Dev.* **16**: 1066-76

Anderson DJ, Le Moigne R, Djakovic S, Kumar B, Rice J, Wong S, Wang J, Yao B, Valle E, Kiss von Soly S *et al.* (2015) Targeting the AAA ATPase p97 as an approach to treat cancer through disruption of protein homeostasis. *Cancer Cell* **28**: 653-65

Angers S, Thorpe CJ, Biechele TL, Goldenberg SJ, Zheng N, MacCoss MJ, Moon RT (2006) The KLHL12-Cullin-3 ubiquitin ligase negatively regulates the Wnt-beta-catenin pathway by targeting Dishevelled for degradation. *Nat. Cell Biol.* **8**: 348-57

Anvarian Z, Nojima H, van Kappel EC, Madl T *et al.* (2016) Axin cancer mutants form nanoaggregates to rewire the Wnt signaling network. *Nat. Struct. Mol. Biol.* **23**: 324-32

Arce L, Pate KT, Waterman ML (2009) Groucho binds two conserved regions of LEF-1 for HDAC-dependent repression. *BMC Cancer* **9**: 159

Assié G, Letouzé E, Fassnacht M, Jouinot A, Luscap W, Barreau O, Omeiri H, Rodriguez S, Perlemoine K, René-Corail F *et al.* (2014) Integrated genomic characterization of adrenocortical carcinoma. *Nat. Genet.* **46**: 607-12

Axelrod JD, Miller JR, Shulman JM, Moon RT, Perrimon N (1998) Differential recruitment of Dishevelled provides signaling specificity in the planar cell polarity and Wingless signaling pathways. *Genes Dev.* **12**: 2610-22

Babu YS, Bugg CE, Cook WJ (1988) Structure of calmodulin refined at 2.2 A resolution. *J. Mol. Biol.* **204**: 191-204

Barker N, Hurlstone A, Musisi H, Miles A, Bienz M, Clevers H (2001) The chromatin remodelling factor Brg-1 interacts with beta-catenin to promote target gene activation. *EMBO J.* **20**: 4935-43

Barker N, van Es JH, Kuipers J, Kujala P, van den Born M, Cozijnsen M, Haegebarth A *et al.* (2007) Identification of stem cells in small intestine and colon by marker gene Lgr5. *Nature* **449**: 1003-7

Baron R, Kneissel M (2013) WNT signaling in bone homeostasis and disease: from human mutations to treatments. *Nat. Med.* **19**: 179-92

Bartscherer K, Pelte N, Ingelfinger D, Boutros M (2006) Secretion of Wnt ligands requires Evi, a conserved transmembrane protein. *Cell* **125**: 523-33

Bhanot P, Brink M, Samos CH, Hsieh JC, Wang Y, Macke JP, Andrew D, Nathans J, Nusse R (1996) A new member of the frizzled family from *Drosophila* functions as a Wingless receptor. *Nature* **382**: 225-30

Bienz M, Clevers H (2000) Linking Colorectal Cancer to Wnt Signaling. *Cell* **103**: 311-20

Bienz M, Hamada F (2004) Adenomatous polyposis coli proteins and cell adhesion. *Curr. Opin. Cell Biol.* **16**: 528-35

Bienz M (2014) Signalosome assembly by domains undergoing dynamic head-to-tail polymerization. *TIBS* **39**: 487-95

Bilic J, Huang YL, Davidson G, Zimmermann T, Cruciat CM, Bienz M, Niehrs C (2007) Wnt induces LRP6 signalosomes and promotes Dishevelled-dependent LRP6 phosphorylation. *Science* **316**: 1619-22

Bjørkøy G, Lamark T, Brech A, Outzen H, Perander M, Overvatn A, Stenmark H, Johansen T (2005) p62/SQSTM1 forms protein aggregates degraded by autophagy and has a protective effect on huntingtin-induced cell death. *J. Cell Biol.* **171**: 603-14

Blanchard H, Grochulski P, Li Y, Arthur JS, Davies PL, Elce JS, Cygler M (1997) Structure of a calpain Ca(2+)-binding domain reveals a novel EF-hand and Ca(2+)-induced conformational changes. *Nat. Struct. Biol.* **4**: 532-8

Blasche S, Koegl M (2013) Analysis of protein-protein interactions using LUMIER assays. *Methods Mol. Biol.* **1064**: 17-27

Blythe EE, Olson KC, Chau V, Deshaies RJ (2017) Ubiquitin- and ATP-dependent unfoldase activity of P97/VCP•NPLOC4•UFD1L is enhanced by a mutation that causes multisystem proteinopathy. *PNAS* **30**: 4380-8

Bodnar NO, Rapoport TA (2017) Molecular mechanism of substrate processing by the Cdc48 ATPase complex. *Cell* **169**: 722-35

Boutros M, Mlodzik M (1999) Dishevelled: at the crossroads of divergent intracellular signaling pathways. *Mech. Dev.* **83**: 27-37

Brantjes H, Roose J, van de Wetering M, Clevers H (2001) All Tcf HMG box transcription factors interact with Groucho-related co-repressors. *Nucleic Acids Research* **29**: 1410-9

Brembeck FH, Schwarz-Romond T, Bakkers J, Wilhelm S, Hammerschmidt M, Birchmeier W (2004) Essential role of BCL9-2 in the switch between β-catenin's adhesive and transcriptional functions. *Genes Dev.* **18**: 2225-30

Bronstein R, Segal D (2011) Modularity of Chip/LDB transcription complexes regulates cell differentiation. *Fly* **5**: 200-5

Buchberger A, Schindelin H, Hänzelmann P (2015) Control of p97 function by cofactor binding. *FEBS Lett.* **589**: 2578-89

Buscarlet M, Stifani S (2007) The 'Marx' of Groucho on development and disease. *Trends Cell Biol.* **17**: 353-61

Cadigan KM, Waterman ML (2012) TCF/LEFs and Wnt Signaling in the Nucleus. *Cold Spring Harb. Perspect. Biol.* **4**: a007906

Callaghan MJ, Russell AJ, Woollatt E, Sutherland GR, Sutherland RL, Watts CK (1999) Identification of a human HECT family protein with homology to the *Drosophila* tumor suppressor gene hyperplastic discs. *Oncogene* **17**: 3479-91

Cavallo RA, Cox RT, Moline MM, Roose J, Polevoy GA, Clevers H, Peifer M, Bejsovec A (1998) *Drosophila* Tcf and Groucho interact to repress Wingless signalling activity. *Nature* **395**: 604-8

Chambers M, Turki-Judeh W, Kim MW, Chen K, Gallaher SD, Courey AJ (2017) Mechanisms of Groucho-mediated repression revealed by genome-wide analysis of Groucho binding and activity. *BMC Genomics* **18**: 215

Chan CC, Zhang S, Cagatay T, Wharton KA (2007) Cell-autonomous, myristyl-independent activity of the *Drosophila* Wnt/Wingless antagonist Naked cuticle (Nkd). *Dev. Biol.* **311**: 538-53

Chan CC, Zhang S, Rousset R, Wharton KA (2008) *Drosophila* Naked cuticle (Nkd) engages the nuclear import adaptor Importin-alpha3 to antagonize Wnt/beta-catenin signaling. *Dev. Biol.* **318**: 17-28

Chapman E, Maksim N, de la Cruz F, La Clair JJ (2015) Inhibitors of the AAA+ chaperone p97. *Molecules* **20**: 3027-49

Chau V, Tobias JW, Bachmair A, Marriott D, Ecker DJ, Gonda DK, Varshavsky A (1989) A multiubiquitin chain is confined to specific lysine in a targeted short-lived protein. *Science* **243**: 1576-83

Chen G, Nguyen PH, Courey AJ (1998) A role for Groucho tetramerization in transcriptional repression. *Mol. Cell. Biol.* **18**: 7259-68

Chen G, Fernandez J, Mische S, Courey AJ (1999) A functional interaction between the histone deacetylase Rpd3 and the corepressor Groucho in *Drosophila* development. *Genes Dev.* **13**: 2218-30

Chen G, Courey AJ (2000) Groucho/TLE family proteins and transcriptional repression. *Gene* **249**: 1-16

Chen ZJ, Sun LJ (2009) Nonproteolytic functions of ubiquitin in cell signaling. *Mol. Cell* **33**: 275-86

Cheng M, Xue H, Cao W, Li W, Chen H, Liu B, Ma B *et al.* (2016) Receptor for Activated C Kinase 1 (RACK1) promotes Dishevelled protein degradation via autophagy and antagonizes Wnt signaling. *JBC* **291**: 12871-9

Chitalia VC, Foy RL, Bachschmid MM, Zeng L, Panchenko MV, Zhou MI, Bharti A, Seldin DC, Lecker SH, Dominguez I, Cohen HT (2008) Jade-1 inhibits Wnt signalling by ubiquitylating beta-catenin and mediates Wnt pathway inhibition by pVHL. *Nat. Cell Biol.* **10**: 1208-16

Chodaparambil JV, Pate KT, Hepler MR, Tsai BP, Muthurajan UM, Luger K, Waterman ML, Weis WI (2014) Molecular functions of the TLE tetramerization domain in Wnt target gene repression. *EMBO J.* **33**: 719-31

Choe KN, Nicolae CM, Constantin D, Imamura Kawasawa Y, Delgado-Diaz MR, De S *et al.* (2016) HUWE1 interacts with PCNA to alleviate replication stress. *EMBO Rep.* **17**: 874-86

Clancy JL, Henderson MJ, Russell AJ, Anderson DW, Bova RJ, Campbell IG *et al.* (2003) EDD, the human orthologue of the hyperplastic discs tumour suppressor gene, is amplified and overexpressed in cancer. *Oncogene* **22**: 5070-81

Clevers H, Nusse R (2012) Wnt/β-catenin Signaling and Disease. *Cell* **149**: 1192-1205

Cloonan N, Forrest AR, Kolle G, Gardiner BB, Faulkner GJ, Brown MK *et al.* (2008) Stem cell transcriptome profiling via massive-scale mRNA sequencing. *Nat. Methods.* **5**: 613-9

Cojocaru M, Bouchard A, Cloutier P, Cooper JJ, Varzavand K, Price DH *et al.* (2011) Transcription factor IIS cooperates with the E3 ligase UBR5 to ubiquitinate the CDK9 subunit of the positive transcription elongation factor B. *JBC* **286**: 5012-22

Cosman F, Crittenden DB, Adachi JD, Binkley N, Czerwinski E, Ferrari S, Hofbauer LC, Lau E, Lewiecki EM, Miyauchi A *et al.* (2016) Romosozumab treatment in postmenopausal women with osteoporosis. *N. Eng. J. Med.* **375**: 1532-43

Daniels DL, Spink KE, Weis WI (2001) Beta-catenin: molecular plasticity and drug design. *TIBS* **26**: 672-8

Daniels DL, Weis WI (2002) ICAT inhibits β-catenin binding to Tcf/Lef-family transcription factors and the general coactivator p300 using independent structural modules. *Mol. Cell* **10**: 573-84

Daniels DL, Weis WI (2005) β-catenin directly displaces Groucho/TLE repressors from Tcf/Lef in Wnt-mediated transcription activation. *Nat. Struct. Mol. Biol.* **12**: 364-71

Dann CE, Hsieh JC, Rattner A, Sharma D, Nathans J, Leahy DJ (2001) Insights into Wnt binding and signalling from the structures of two Frizzled cysteine-rich domains. *Nature* **412**: 86-90

Dantuma NP, Acs K, Luijsterburg MS (2014) Should I stay or should I go: VCP/p97-mediated chromatin extraction in the DNA damage response. *Exp. Cell Res.* **329**: 9-17

DaRosa PA, Wang Z, Jiang X, Pruneda JN, Cong F, Klevit RE, Xu W (2015) Allosteric activation of the RNF146 ubiquitin ligase by a poly(ADP-ribosyl)ation signal. *Nature* **517**: 223-6

DasGupta R, Fuchs E (1999) Multiple roles for activated LEF/TCF transcription complexes during hair follicle development and differentiation. *Development* **126**: 4557-68

Davidson G, Wu W, Shen J, Bilic J, Fenger U, Stannek P *et al.* (2005) Casein kinase 1γ couples Wnt receptor activation to cytoplasmic signal transduction. *Nature* **438**: 867-72

de Groot RE, Ganji RS, Bernatik O, Lloyd-Lewis B, Seipel K *et al.* (2014) Huwe1-mediated ubiquitylation of dishevelled defines a negative feedback loop in the Wnt signaling pathway. *Science Signaling* **7**: ra26

de la Roche M, Bienz M (2007) Wingless-independent association of Pygopus with dTCF target genes. *Curr. Biol.* **17**: 556-61

de la Roche M, Ibrahim AE, Mieszczanek J, Bienz M (2014) LEF1 and B9L shield β-catenin from inactivation by Axin, desensitizing colorectal cancer cells to tankyrase inhibitors. *Cancer Research* **74**: 1495-1505

de Lau W, Barker N, Low TY, Koo BK, Li VS, Teunissen H, Kujala P, Haegebarth A, Peters

PJ, van de Wetering M *et al.* (2011) Lgr5 homologues associate with Wnt receptors and mediate R-spondin signalling. *Nature* **476**: 293-7

DeBruine ZJ, Ke J, Harikumar KG, Gu X, Borowsky P, Williams BO, Xu W, Miller LJ, Xu HE, Melcher K (2017) Wnt5a promotes Frizzled-4 signalosome assembly by stabilizing cysteine-rich domain dimerization. *Genes Dev.* **31**: 916-26

Deshaies RJ (2014) Proteotoxic crisis, the ubiquitin-proteasome system, and cancer therapy. *BMC Biol.* **12**: 94

Dijksterhuis JP, Baljinnyam B, Stanger K, Sercan HO, Ji Y, Andres O, Rubin JS, Hannoush RN, Schulte G (2015) Systematic Mapping of WNT-Frizzled Interactions Reveals Functional Selectivity by Distinct WNT-Frizzled Pairs. *JBC* **290**: 6789-98

Dikic I, Wakatsuki S, Walters KJ (2009) Ubiquitin-binding domains - from structures to functions. *Nat. Rev. Mol. Cell Biol.* **10**: 659-71

Dimitrova YN, Li J, Lee YT, Rios-Esteves J, Friedman DB, Choi HJ, Weis WI, Wang CY, Chazin WJ (2010) Direct ubiquitination of beta-catenin by Siah-1 and regulation by the exchange factor TBL1. *JBC* **30**: 13507-16

Ding Y, Zhang Y, Xu C, Tao Q-H, Chen Y-G (2013) HECT domain-containing E3 Ubiquitin Ligase NEDD4L negatively regulates Wnt signaling by targeting Dishevelled for proteasomal degradation. *JBC* **288**: 8289-98

Dominguez-Brauer C, Hao Z, Elia AJ, Fortin JM, Nechanitzky R, Brauer PM *et al.* (2016) Mule regulates the intestinal stem cell niche via the Wnt pathway and targets EphB3 for proteasomal and lysosomal degradation. *Cell Stem Cell* **4**: 205-16

Dominguez-Brauer C, Khatun R, Elia AJ, Thu KL, Ramachandran P, Baniasadi SP, Hao Z, Jones LD, Haight J, Sheng Y, Mak TW (2017) E3 ubiquitin ligase Mule targets β-catenin under conditions of hyperactive Wnt signaling. *PNAS* **14**: 1148-57

Dooley HC, Razi M, Polson HE, Girardin SE, Wilson MI, Tooze SA (2014) WIPI2 links LC3 conjugation with PI3P, autophagosome formation, and pathogen clearance by recruiting Atg12-5-16L1. *Mol. Cell.* **55**: 238-52

Dosemeci A, Thein S, Yang Y, Reese TS, Tao-Cheng J-H (2013) CYLD, a deubiquitinase specific for lysine63-linked polyubiquitins, accumulates at the postsynaptic density in an activity-dependent manner. *Biochem. Biophys. Res. Commun.* **430**: 245-49

Echeverri CJ, Beachy PA, Baum B, Boutros M, Buchholz F, Chanda SK *et al.* (2006) Minimizing the risk of reporting false positives in large-scale RNAi screens. *Nat. Methods* **3**: 777-9

Edgcomb SP, Murphy KP (2002) Variability in the pKa of histidine side-chains correlates with burial within proteins. *Proteins* **49**: 1-6

Emmerich CH, Ordureau A, Strickson S, Arthur JS, Pedrioli PG, Komander D, Cohen P (2013) Activation of the canonical IKK complex by K63/M1-linked hybrid ubiquitin chains. *PNAS* **110**: 15247-52

Fagotto F, Glück U, Gumbiner BM (1998) Nuclear localization signal-independent and importin/karyopherin-independent nuclear import of β-catenin. *Curr. Biol.* **8**: 181-90

Fahmy OG, Fahmy MJ (1959) Differential gene response to mutagens in *Drosophila melanogaster*. *Genetics* **44**: 1149-71

Falcon B, Noad J, McMahon H, Randow F, Goedert M (2017) Galectin-8-mediated selective autophagy protects against seeded tau aggregation. *JBC* **293**: 2438-51

Faux MC, Coates JL, Catimel B, Cody S, Clayton AHA, Layton MJ, Burgess AW (2008) Recruitment of adenomatous polyposis coli and β-catenin to axin-puncta. *Oncogene* **27**: 5808-20

Fiedler M, Sánchez-Barrena MJ, Nekrasov M, Mieszczanek J, Rybin V, Müller J *et al.* (2008) Decoding of methylated histone H3 tail by the Pygo-BCL9 Wnt signaling complex. *Mol. Cell* **30**: 507-18

Fiedler M, Mendoza-Topaz C, Rutherford TJ, Mieszczanek J, Bienz M (2011) Dishevelled interacts with the DIX domain polymerization interface of Axin to interfere with its function in down-regulating β-catenin. *PNAS* **108**: 1937-42

Fiedler M, Graeb M, Mieszczanek J, Rutherford TJ, Johnson CM, Bienz M (2015) An ancient Pygo-dependent Wnt enhanceosome integrated by Chip/LDB-SSDP. *eLife* **4**: e09073

Filimonenko M, Isakson P, Finley KD, Anderson M, Jeong H, Melia TJ, Bartlett BJ *et al.* (2010) The selective macroautophagic degradation of aggregated proteins requires the PI3P-binding protein Alfy. *Mol. Cell* **38**: 265-79

Flack JE, Mieszczanek J, Novcic, Bienz M (2017) Wnt-Dependent inactivation of the Groucho/TLE co-repressor by the HECT E3 ubiquitin ligase Hyd/UBR5. *Mol. Cell* **67**: 181-93

Flores-Saaib RD, Courey AJ (2000) Analysis of Groucho–histone interactions suggests mechanistic similarities between Groucho- and Tup1-mediated repression. *Nucleic Acids Research* **28**: 4189-96

Franz A, Shlyueva D, Brunner E, Stark A, Basler K (2017) Probing the canonicity of the Wnt/Wingless signaling pathway. *PLoS Genet.* **13**: e1006700

Fujita N, Hayashi-Nishino M, Fukumoto H, Omori H, Yamamoto A, Noda T, Yoshimori T (2008) An Atg4B mutant hampers the lipidation of LC3 paralogues and causes defects in autophagosome closure. *Mol. Biol. Cell* **19**: 4651-9

Gammons MV, Renko M, Johnson CM, Rutherford TJ, Bienz M (2016a) Wnt signalosome assembly by DEP domain swapping of Dishevelled. *Mol. Cell* **64**: 92-104

Gammons MV, Rutherford TJ, Steinhart Z, Angers S, Bienz M (2016b) Essential role of the Dishevelled DEP domain in a Wnt-dependent human-cell-based complementation assay. *J. Cell Sci.* **129**: 3892-3902

Gammons MV, Bienz M (2017) Multiprotein complexes governing Wnt signal transduction. *Curr. Opin. Cell Biol.* **51**: 42-49

Gasperowicz M, Otto F (2005) Mammalian Groucho homologs: redundancy or specificity? *J. Cell. Biochem.* **95**: 670-87

Gao C, Cao W, Bao L, Zuo W, Xie G, Cai T, Fu W *et al.* (2010) Autophagy negatively regulates Wnt signalling by promoting Dishevelled degradation. *Nat. Cell Biol.* **12**: 781-90

Gao R, Ma LQ, Du X, Zhang TT, Zhao L, Liu L, Liu JC *et al.* (2016) Rnf25/AO7 positively regulates wnt signaling via disrupting Nkd1-Axin inhibitory complex independent of its ubiquitin ligase activity. *Oncotarget* **7**: 23850-9

Gerlitz O, Basler K (2002) Wingful, an extracellular feedback inhibitor of Wingless. *Genes Dev.* **16**: 1055-9

Giese K, Amsterdam A, Grosschedl R (1991) DNA-binding properties of the HMG domain of the lymphoid-specific transcriptional regulator LEF-1. *Genes Dev.* **5**: 2567-78

Goldknopf IL, Busch H (1977) Isopeptide linkage between nonhistone and histone 2A polypeptides of chromosomal conjugate-protein A24. *PNAS* **74**: 864-8

Goentoro L, Kirschner MW (2009). Evidence that fold-change, and not absolute level, of beta-catenin dictates Wnt signaling. *Mol. Cell* **36**: 872-84

Goldstein B, Takeshita H, Mizumoto K, Sawa H (2006) Wnt signals can function as positional cues in establishing cell polarity. *Dev. Cell* **10**: 391-6

González-Sancho JM, Brennan KR, Castelo-Soccio LA, Brown AM (2004) Wnt proteins induce dishevelled phosphorylation via an LRP5/6- independent mechanism, irrespective of their ability to stabilize beta-catenin. *Mol. Cell. Biol.* **24**: 4757-68

Grant SF, Thorleifsson G, Reynisdottir I, Benediktsson R, Manolescu A, Sainz J, Helgason A, Stefansson H, Emilsson V, Helgadottir A *et al.* (2006) Variant of transcription factor 7-like 2 (TCF7L2) gene confers risk of type 2 diabetes. *Nat. Genet.* **38**: 320-3

Groden J, Thliveris A, Samowitz W, Carlson M, Gelbert L, Albertsen H *et al.* (1991) Identification and characterization of the familial adenomatous polyposis coli gene. *Cell* **66**: 589-600

Gudjonsson T, Altmeyer M, Savic V, Toledo L, Dinant C, Grofte M *et al.* (2012) TRIP12 and UBR5 suppress spreading of chromatin ubiquitylation at damaged chromosomes. *Cell* **150**: 697-709

Guo J, Cagatay T, Zhou G, Chan CC, Blythe S, Suyama K, Zheng L *et al*. (2009) Mutations in the human naked cuticle homolog NKD1 found in colorectal cancer alter Wnt/Dvl/beta-catenin signaling. *PLoS One* **4**: e7982

Hagemann AI, Kurz J, Kauffeld S, Chen Q, Reeves PM, Weber S, Schindler S, Davidson G, Kirchhausen T, Scholpp S (2014) In vivo analysis of formation and endocytosis of the Wnt/β-catenin signaling complex in zebrafish embryos. *J. Cell Sci.* **127**: 3970-82

Han W, Lee H, Han J-K (2017) Ubiquitin C-terminal hydrolase37 regulates Tcf7 DNA binding for the activation of Wnt signalling. *Sci. Rep.* **7**: 42590

Hanlon CD, Andrew DJ (2015) Outside-in signaling – a brief review of GPCR signaling with a focus on the *Drosophila* GPCR family. *J. Cell. Sci.* **128**: 3533-42

Hanson AJ, Wallace HA, Freeman TJ, Beauchamp RD, Lee LA, Lee E (2012) XIAP monoubiquitylates Groucho/TLE to promote canonical Wnt signaling. *Mol. Cell* **45**: 619-28

Hao H-X, Xie Y, Zhang Y, Charlat O, Oster E, Avello M *et al.* (2012) ZNRF3 promotes Wnt receptor turnover in an R-spondin-sensitive manner. *Nature* **485**: 195-200

Hart MJ, de los Santos R, Albert IN, Rubinfeld B, Polakis P (1998) Downregulation of β-catenin by human Axin and its association with the APC tumor suppressor, β-catenin and GSK3β. *Current Biology* **8**: 573-81

Hasson P, Muller B, Basler K, Paroush Z (2001) Brinker requires two corepressors for maximal and versatile repression in Dpp signaling. *EMBO J.* **20**: 5725-36

Hay-Koren A, Caspi M, Zilberberg A, Rosin-Arbesfeld R (2011) The EDD E3 ubiquitin ligase ubiquitinates and up-regulates β-catenin. *Mol. Biol. Cell* **22**: 399-411

Hecht A, Vleminckx K, Stemmler MP, van Roy F, Kemler R (2000) The p300/CBP acetyltransferases function as transcriptional coactivators of β-catenin in vertebrates. *EMBO J.* **19**: 1839-50

Heidelberger JB, Voigt A, Borisova ME, Petrosino G, Ruf S, Wagner SA, Beli P (2018) Proteomic profiling of VCP substrates links VCP to K6-linked ubiquitylation and c-Myc function. *EMBO Rep.* e44754

Henderson MJ, Russell AJ, Hird S, Muñoz M, Clancy JL, Lehrbach GM *et al.* (2002) EDD, the human hyperplastic discs protein, has a role in progesterone receptor coactivation and potential involvement in DNA damage response. *JBC* **277**: 26468-78

Hershko A, Heller H (1985) Occurrence of a polyubiquitin structure in ubiquitin-protein conjugates. *Biochem. Biophys. Res. Comm.* **128**: 1079-86

Hoege C, Pfander B, Moldovan GL, Pyrowolakis G, Jentsch S (2002) RAD6-dependent DNA repair is linked to modification of PCNA by ubiquitin and SUMO. *Nature* **419**: 135-41

Hoffmans R, Basler K (2004) Identification and *in vivo* role of the Armadillo-Legless interaction. *Development* **131**: 4393-400

Honda Y, Tojo M, Matsuzaki K, Anan T, Matsumoto M, Ando M *et al.* (2002) Cooperation of HECT-domain ubiquitin ligase hHYD and DNA topoisomerase II-binding protein for DNA damage response. *JBC* **277**: 3599-605

Hospenthal MK, Mevissen TE, Komander D (2015) Deubiquitinase-based analysis of ubiquitin chain architecture using Ubiquitin Chain Restriction (UbiCRest). *Nat. Protoc*. **10**: 349-61

Hu T, Li C, Cao Z, Van Raay TJ, Smith JG, Willert K, Solnica-Krezel L, Coffey RJ (2010) Myristoylated Naked2 antagonizes Wnt-beta-catenin activity by degrading Dishevelled-1 at the plasma membrane. *JBC* **285**: 13561-8

Huang SM, Mishina, YM, Liu S, Cheung A, Stegmeier F, Michaud GA, Charlat O, Wiellette E, Zhang Y, Wiessner S *et al.* (2009a) Tankyrase inhibition stabilizes Axin and antagonizes Wnt signalling. *Nature* **461**: 614-20

Huang X, Dixit VM (2016) Drugging the undruggables: exploring the ubiquitin system for drug development. *Cell Research* **26**: 484-98

Huang Y, Zhou Y, Wong HC, Chen Y, Chen Y, Wang S *et al.* (2009b) A single EF-hand isolated from STIM1 forms dimer in the absence and presence of Ca^{2+}. *FEBS J.* **276**: 5589-97

Huber AH, Nelson WJ, Weis WI (1997) Three-dimensional structure of the armadillo repeat region of beta-catenin. *Cell* **90**: 871-82

Hwang W-L, Jiang J-K, Yang S-H, Huang T-S, Lan H-Y, Teng H-W *et al.* (2014) MicroRNA-146a directs the symmetric division of Snail-dominant colorectal cancer stem cells. *Nat. Cell Biol.* **16**: 268-80

Iconomou M, Saunders DN (2016) Systematic approaches to identify E3 ligase substrates. *Biochem. J.* **473**: 4083-101

Ingham PW, McMahon AP (2001) Hedgehog signaling in animal development: paradigms and principles. *Genes Dev.* **15**: 3059-87

Ireland H, Kemp R, Houghton C, Howard L, Clarke AR, Sansom OJ, Winton DJ (2004) Inducible Cre-mediated control of gene expression in the murine gastrointestinal tract: effect of loss of beta-catenin. *Gastroenterology* **126**: 1236-46

Jaks V, Barker N, Kasper M, van Es JH, Snippert HJ, Clevers H, Toftgård R (2008) Lgr5 marks cycling, yet long-lived, hair follicle stem cells. *Nat. Genet.* **40**: 1291-9

Janda CY, Waghray D, Levin AM, Thomas C, Garcia KC (2012) Structural basis of Wnt recognition by Frizzled. *Science* **337**: 59-64

Janda CY, Dang LT, You C, Chang J, de Lau W, Zhong ZA, Yan KS, Marecic O *et al*. (2017) Surrogate Wnt agonists that phenocopy canonical Wnt and β-catenin signalling. *Nature* **545**: 234-7

Jen J, Powell SM, Papadopoulos N, Smith KJ, Hamilton SR, Vogelstein B, Kinzler KW (1994) Molecular determinants of dysplasia in colorectal lesions. *Cancer Research* **54**: 5523-6

Jennings BH, Pickles LM, Wainwright SM, Roe SM, Pearl LH, Ish-Horowicz D (2006) Molecular recognition of transcriptional repressor motifs by the WD domain of the Groucho/TLE corepressor. *Mol. Cell* **22**: 645-55

Jennings BH, Ish-Horowicz D (2008) The Groucho/TLE/Grg family of transcriptional co-repressors. *Genome Biol*. **9**: 205

Jenny A, Reynolds-Kenneally J, Das G, Burnett M, Mlodzik M (2005) Diego and Prickle regulate Frizzled planar cell polarity signalling by competing for Dishevelled binding. *Nat. Cell Biol.* **7**: 691-7

Ji L, Jiang B, Jiang X, Charlat O, Chen A, Mickanin C, Bauer A, Xu W, Yan X, Cong F (2017) The SIAH E3 ubiquitin ligases promote Wnt/β-catenin signaling through mediating Wnt-induced Axin degradation. *Genes Dev.* **31**: 904-15

Jiang H, He X, Feng D, Zhu X, Zheng Y (2015a) RanGTP aids anaphase entry through Ubr5-mediated protein turnover. *J. Cell Biol.* **211**: 7-18

Jiang X, Charlat O, Zamponi R, Yang,Y, Cong F (2015b) Dishevelled promotes Wnt receptor degradation through recruitment of ZNRF3/RNF43 E3 ubiquitin ligases. *Mol. Cell* **58**: 522-33

Jiménez G, Paroush Z, Ish-Horowicz D (1997) Groucho acts as a corepressor for a subset of negative regulators, including Hairy and Engrailed. *Genes Dev.* **11**: 3072-82

Jiménez G, Verrijzer CP, Ish-Horowicz D (1999) A conserved motif in goosecoid mediates groucho-dependent repression in *Drosophila* embryos. *Mol. Cell. Biol.* **19**: 2080–7

Johnson JO, Mandrioli J, Benatar M, Abramzon Y, Van Deerlin VM, Trojanowski *et al.* (2010) Exome sequencing reveals VCP mutations as a cause of familial ALS. *Neuron* **68**: 857-64

Ju J-S, Weihl CC (2010) p97/VCP at the intersection of the autophagy and ubiquitin proteasome system. *Autophagy* **6**: 283-5

Jung CH, Jun CB, Ro SH, Kim YM, Otto NM, Cao J, Kundu M, Kim DH (2009) ULK-Atg13-FIP200 complexes mediate mTOR signaling to the autophagy machinery. *Mol. Biol. Cell* **20**: 1992-2003

Jürgens G, Wieschaus E, Nüsslein-Volhard C, Kluding H (1984) Mutations affecting the pattern of the larval cuticle in *Drosophila melanogaster*: II. Zygotic loci on the third chromosome. *Roux's Arch. Dev. Biol.* **193**: 283-95

Kakugawa S, Langton PF, Zebisch M, Howell S, Chang TH, Liu Y, Feizi T *et al*. (2015) Notum deacylates Wnt proteins to suppress signalling activity. *Nature* **519**: 187-92

Kaur J, Debnath J (2015) Autophagy at the crossroads of catabolism and anabolism. *Nat. Rev. Mol. Cell Biol.* **16**: 461-72

Khaminets A, Behl C, Dikic I (2016) Ubiquitin-dependent and independent signals in selective autophagy. *Trends Cell Biol.* **26**: 6-16

Kim S, Nollen EA, Kitagawa K, Bindokas VP, Morimoto RI (2002) Polyglutamine protein aggregates are dynamic. *Nat. Cell Biol.* **4**: 826-31

Kim SE, Huang H, Zhao M, Zhang X, Zhang A, Semonov MV, MacDonald BT *et al.* (2013) Wnt stabilization of beta-catenin reveals principles for morphogen receptor-scaffold assemblies. *Science* **340**: 867-70

Kinsella E, Dora N, Mellis D, Lettice L, Deveney P, Hill R, Ditzel M (2016) Use of a conditional Ubr5 mutant allele to investigate the role of an N-End rule ubiquitin-protein ligase in Hedgehog signalling and embryonic limb development. *PLoS ONE* **11**: e0157079

Kinzler KW, Nilbert MC, Su LK, Vogelstein B, Bryan TM, Levy DB, Smith KJ, Preisinger AC, Hedge P, McKechnie D *et al*. (1991) Identification of FAP locus genes from chromosome 5q21. *Science* **253**: 661-5

Kinzler KW, Vogelstein B (1996) Lessons from Hereditary Colorectal Cancer. *Cell* **87**: 159-70

Kitagawa M, Hatakeyama S, Shirane M, Matsumoto M, Ishida N, Hattori K *et al.* (1999) An F-box protein, FWD1, mediates ubiquitin-dependent proteolysis of beta-catenin. *EMBO J.* **18**: 2401-10

Kirkin V, Lamark T, Sou YS, Bjørkøy G, Nunn JL, Bruun JA, Shvets E, McEwan DG *et al.* (2009) A role for NBR1 in autophagosomal degradation of ubiquitinated substrates. *Mol. Cell* **33**: 505-16

Klein PS, Melton DA (1996) A molecular mechanism for the effect of lithium on development. *PNAS* **93**: 8455-9

Klingensmith J, Nusse R, Perrimon N (1994) The *Drosophila* segment polarity gene *dishevelled* encodes a novel protein required for response to the wingless signal. *Genes Dev.* **8**: 118-30

Knapp S, Zamai M, Volpi D, Nardese V, Avanzi N, Breton J, Plyte S, Flocco M, Marconi M, Isacchi A, Caiolfa VR (2001) Thermodynamics of the high-affinity interaction of TCF4 with beta-catenin. *J. Mol. Biol.* **306**: 1179-89

Kohler EM, Chandra SH, Behrens J, Schneikert J (2009) Beta-catenin degradation mediated by the CID domain of APC provides a model for the selection of APC mutations in colorectal, desmoid and duodenal tumours. *Hum. Mol. Genet.* **18**: 213-26

Kohn AD, Moon RT (2005) Wnt and calcium signalling: beta-catenin independent pathways. *Cell Calcium* **38**: 439-46

Koller KJ, Brownstein MJ (1987) Use of a cDNA clone to identify a supposed precursor protein containing valosin. *Nature* **325**: 542-5

Komachi K, Johnson AD (1997) Residues in the WD repeats of Tup1 required for interaction with α2. *Mol. Cell. Biol.* **17**: 6023-8

Komander D, Clague MJ, Urbé S (2009) Breaking the chains: structure and function of the deubiquitinases. *Nat. Rev. Mol. Cell Biol.* **10**: 550-63

Komander D, Rape M (2012) The ubiquitin code. *Annu. Rev. Biochem.* **81**: 203-29

Koo B-K, Spit M, Jordens I, Low TY, Stange DE, van de Wetering M *et al.* (2012) Tumour suppressor RNF43 is a stem-cell E3 ligase that induces endocytosis of Wnt receptors. *Nature*, **488**: 665-9

Korinek V, Barker N, Moerer P, van Donselaar E, Huls G, Peters PJ, Clevers H (1998) Depletion of epithelial stem-cell compartments in the small intestine of mice lacking Tcf-4. *Nat. Genet.* **19**: 379-83

Korswagen HC, Herman MA, Clevers HC (2000) Distinct beta-catenins mediate adhesion and signalling functions in *C. elegans*. *Nature* **406**: 527-32

Koyano F, Okatsu K, Kosako H, Tamura Y, Go E, Kimura M, Kimura Y, Tsuchiya H, Yoshihara H, Hirokawa T *et al*. (2014) Ubiquitin is phosphorylated by PINK1 to activate parkin. *Nature* **510**: 162-6

Kozlov G, De Crescenzo G, Lim NS, Siddiqui N, Fantus D, Kahvejian A *et al.* (2004) Structural basis of ligand recognition by PABC, a highly specific peptide-binding domain found in poly(A)-binding protein and a HECT ubiquitin ligase. *EMBO J.* **23**: 272-81

Kozlov G, Nguyen L, Lin T, De Crescenzo G, Park M, Gehring K (2007) Structural basis of ubiquitin recognition by the ubiquitin-associated (UBA) domain of the ubiquitin ligase EDD. *JBC* **282**: 35787-95

Kozlov G, Ménade M, Rosenauer A, Nguyen L, Gehring K (2010) Molecular determinants of PAM2 recognition by the MLLE domain of poly(A)-binding protein. *J. Mol. Biol*. **397**: 397-407

Kramps T, Peter O, Brunner E, Nellen D, Froesch B, Chatterjee S, Murone M, Züllig S, Basler K (2002) Wnt/wingless signaling requires BCL9/legless-mediated recruitment of pygopus to the nuclear β-catenin-TCF complex. *Cell* **109**: 47-60

Kristariyanto YA, Choi SY, Rehman SA, Ritorto MS, Campbell DG, Morrice NA, Toth R, Kulathu Y (2015) Assembly and structure of Lys33-linked polyubiquitin reveals distinct conformations. *Biochem. J*. **467**: 345-52

Kulak O, Chen H, Holohan B, Wu X, He H, Borek D, Otwinowski Z, Yamaguchi K, Garofalo LA, Ma Z *et al.* (2015) Disruption of Wnt/β-catenin signaling and telomeric shortening are inextricable consequences of tankyrase inhibition in human cells. *Mol. Cell. Biol.* **35**: 2425-35

Kulathu Y, Komander D (2012) Atypical ubiquitylation – the unexplored world of polyubiquitin beyond Lys48 and Lys63 linkages. *Nat. Rev. Mol. Cell Biol.* **13**: 508-23

Kunttas-Tatli E, Roberts DM, McCartney BM (2014) Self-association of the APC tumor suppressor is required for the assembly, stability, and activity of the Wnt signaling destruction complex. *Mol. Biol. Cell* **25**: 3424-36

Lamb CA, Dooley HC, Tooze SA (2013) Endocytosis and autophagy: Shared machinery for degradation. *Bioessays* **35**: 34-45

Larraguibel J, Weiss AR, Pasula DJ, Dhaliwal RS, Kondra R, Van Raay TJ (2015) Wnt ligand-dependent activation of the negative feedback regulator Nkd1. *Mol. Biol. Cell* **26**: 2375-84

Lee E, Salic A, Kruger R, Heinrich R, Kirschner MW (2003) The roles of APC and Axin derived from experimental and theoretical analysis of the Wnt pathway. *PLoS Biol*. **1**: E10

Lee HJ, Shi DL, Zheng JJ (2015) Conformational change of Dishevelled plays a key regulatory role in the Wnt signaling pathways. *eLife* **4**: e08142

Lee HY, Kleber M, Hari L, Brault V, Suter U, Taketo MM, Kemler R, Sommer L (2004) Instructive role of Wnt/beta-catenin in sensory fate specification in neural crest stem cells. *Science* **303**: 1020-3

Lee JD, Amanai K, Shearn A, Treisman JE (2002) The ubiquitin ligase Hyperplastic discs negatively regulates hedgehog and decapentaplegic expression by independent mechanisms. *Development* **129**: 5697-5706

Lee SJ, Imamoto N, Sakai H, Nakagawa A, Kose S, Koike M, Yamamoto M, Kumasaka T, Yoneda Y, Tsukihara T (2000) The adoption of a twisted structure of importin-beta is essential for the protein-protein interaction required for nuclear transport. *J. Mol. Biol.* **302**: 251-64

Lewit-Bentley A, Réty S (2000) EF-hand calcium-binding proteins. *Curr. Opin. Struct. Biol.* **10**: 637-43

Li C, Franklin JL, Graves-Deal R, Jerome WG, Cao Z, Coffey RJ (2004) Myristoylated Naked2 escorts transforming growth factor α to the basolateral plasma membrane of polarized epithelial cells. *PNAS* **101**: 5571-6

Li VS, Ng SS, Boersema PJ, Low TY, Karthaus WR, Gerlach JP, Mohammed S *et al.* (2012) Wnt signaling inhibits proteasomal β-catenin degradation within a compositionally intact Axin1 complex. *Cell* **149**: 1245-56

Li J-M, Wu H, Zhang W, Blackburn MR, Jin J (2014) The p97-UFD1L-NPL4 protein complex mediates cytokine-induced IκBα proteolysis. *Mol. Cell. Biol.* **34**: 335-47

Licht-Murava A, Paz R, Vaks L, Avrahami L, Plotkin B, Eisenstein M, Eldar-Finkelman H (2016) A unique type of GSK-3 inhibitor brings new opportunities to the clinic. *Sci. Signal.* **9**: 110

Liu C, Li Y, Semenov M, Han C, Baeg, GH, Tan Y, Zhang Z, Lin X, He X (2002) Control of beta-catenin phosphorylation/degradation by a dual-kinase mechanism. *Cell* **108**: 837-47

Liu J, Stevens J, Rote CA, Yost HJ, Hu Y, Neufeld KL, White RL, Matsunami N (2001) Siah-1 mediates a novel beta-catenin degradation pathway linking p53 to the adenomatous polyposis coli protein. *Mol. Cell* **7**: 927-36

Liu W, Dong X, Mai M, Seelan RS, Taniguchi K, Krishnadath KK *et al.* (2000) Mutations in AXIN2 cause colorectal cancer with defective mismatch repair by activating β-catenin/TCF signalling. *Nat. Genetics* **26**: 146-7

Liu Y, Ye Y (2012) Roles of p97-associated deubiquitinases in protein quality control at the endoplasmic reticulum. *Curr. Protein Pept. Sci.* **13**: 436-46

Locke M, Toth JI, Petroski MD (2014) K11- and K48-linked ubiquitin chains interact with p97 during endoplasmic reticulum-associated degradation. *Biochem. J.* **459**: 205-16

Loh KM, van Amerongen R, Nusse R (2016) Generating cellular diversity and spatial form: Wnt signaling and the evolution of multicellular animals. *Dev. Cell* **38**: 643-55

Losick VP, Morris LX, Fox DT, Spradling A (2011) *Drosophila* stem cell niches: a decade of discovery suggests a unified view of stem cell regulation. *Dev. Cell* **21**: 159-71

Lu F-I, Sun Y-H, Wei C-Y, Thisse C, Thisse B (2014) Tissue-specific derepression of TCF/LEF controls the activity of the Wnt/β-catenin pathway *Nat. Comm.* **5**: 5368

Lu J, Ma Z, Hsieh JC, Fan CW, Chen B, Longgood JC, Williams NS, Amatruda JF, Lum L, Chen C (2009) Structure-activity relationship studies of small-molecule inhibitors of Wnt response. *Bioorg. Med. Chem. Lett.* **19**: 3825-7

Lustig B, Jerchow B, Sachs M, Weiler S, Pietsch T, Karsten U, van de Wetering M *et al.* (2002) Negative feedback loop of Wnt signaling through upregulation of conductin/axin2 in colorectal and liver tumors. *Mol. Cell. Biol.* **22**: 1184-93

Ma B, Liu B, Cao W, Gao C, Qi Z, Ning Y, Chen YG (2015) The Wnt signaling antagonist Dapper1 accelerates Dishevelled2 degradation via promoting its ubiquitination and aggregate-induced autophagy. *JBC* **290**: 12346-54

MacDonald BT, Tamai K, He X (2009) Wnt/β-catenin signaling: components, mechanisms, and diseases. *Dev. Cell* **17**: 9-26

Madan B, Ke Z, Harmston N, Ho SY, Frois AO, Alam J, Jeyaraj DA, Pendharkar V, Ghosh K, Virshup IH *et al.* (2016) Wnt addiction of genetically defined cancers reversed by PORCN inhibition. *Oncogene* **35**: 2197-2207

Maddika S, Chen J (2009) Protein kinase DYRK2 is a scaffold that facilitates assembly of an E3 ligase. *Nat. Cell Biol.* **11**: 409-19

Madrzak J, Fiedler M, Johnson CM, Ewan R, Knebel A, Bienz M, Chin JW (2015) Ubiquitination of the Dishevelled DIX domain blocks its head-to-tail polymerization. *Nat. Comm.* **6**: 6718

Magnaghi P, D'Alessio R, Valsasina B, Avanzi N, Rizzi S, Asa D, Gasparri F, Cozzi L, Cucchi U, Orrenius C *et al.* (2013) Covalent and allosteric inhibitors of the ATPase VCP/p97 induce cancer cell death. *Nat. Chem. Biol.* **9**: 548-56

Malinauskas T, Aricescu AR, Lu W, Siebold C, Jones EY (2011) Modular mechanism of Wnt signaling inhibition by Wnt inhibitory factor 1. *Nat. Struct. Mol. Biol.* **18**: 886-93

Mann KM, Ward JM, Yew CC, Kovochich A, Dawson DW, Black MA *et al.* (2012) Sleeping Beauty mutagenesis reveals cooperating mutations and pathways in pancreatic adenocarcinoma. *PNAS* **109**: 5934-41

Mansfield E, Hersperger E, Biggs J, Shearn A (1994) Genetic and molecular analysis of hyperplastic discs, a gene whose product is required for regulation of cell proliferation in *Drosophila melanogaster* imaginal discs and germ cells. *Dev. Biol.* **165**: 507-26

Mari S, Ruetalo N, Maspero E, Stoffregen MC, Pasqualato S, Polo S, Wiesner S (2014) Structural and functional framework for the autoinhibition of Nedd4-family ubiquitin ligases. *Structure* **22**: 1639-49

Maric M, Maculins T, De Piccoli G, Labib K (2014) Cdc48 and a ubiquitin ligase drive disassembly of the CMG helicase at the end of DNA replication. *Science* **346**: 1253596

Marsden AN, Derry SW, Schneider I, Scott CA, Westfall TA, Brastrom LK, Shea MA *et al.* (2018) The Nkd EF-hand domain modulates divergent wnt signaling outputs in zebrafish. *Dev. Biol.* **434**: 63-73

Martinez Arias A, Baker NE, Ingham PW (1988) Role of segment polarity genes in the definition and maintenance of cell states in the *Drosophila* embryo. *Development* **103**: 157-70

Matano M, Date S, Shimokawa M, Takano A, Fujii M, Ohta Y, Watanabe T, Kanai T, Sato T (2015) Modeling colorectal cancer using CRISPR/Cas-9-mediated engineering of human intestinal organoids. *Nat. Med.* **21**: 256-62

Matta-Camacho E, Kozlov G, Menade M, Gehring K (2012) Structure of the HECT C-lobe of the UBR5 E3 ubiquitin ligase. *Acta Cryst. Sect. F Struct. Biol. Cryst. Commun.* **68**: 1158-63

McEwen DG, Peifer M (2001) Wnt signaling: The Naked truth? *Curr. Biol.* **11**: 524-6

McMahon AP, Moon RT (1989) Ectopic expression of the proto-oncogene int-1 in *Xenopus* embryos leads to duplication of the embryonic axis. *Cell* **58**: 1075-84

Meierhofer D, Wang X, Huang L, Kaiser P (2008) Quantitative analysis of global ubiquitination in HeLa cells by mass spectrometry. *J. Proteome Res.* **7**: 4566-76

Mendoza-Topaz C, Mieszczanek J, Bienz M (2011) The Adenomatous polyposis coli tumour suppressor is essential for Axin complex assembly and function and opposes Axin's interaction with Dishevelled. *Open Biol.* **1**: 110013

Metcalfe C, Mendoza-Topaz C, Mieszczanek J, Bienz M (2010) Stability elements in the LRP6 cytoplasmic tail confer efficient signalling upon DIX-dependent polymerization. *J. Cell Sci.* **123**: 1588-99

Metcalfe C, Bienz M (2011) Inhibition of GSK3 by Wnt signalling – two contrasting models. *J. Cell Sci.* **124**: 3537-44

Mevissen TE, Hospenthal MK, Geurink PP, Elliott PR, Akutsu M, Arnaudo N, Ekkebus R, Kulathu Y *et al.* (2013) OTU deubiquitinases reveal mechanisms of linkage specificity and enable ubiquitin chain restriction analysis. *Cell* **154**: 169-84

Meyer H, Wang Y, Warren G (2002) Direct binding of ubiquitin conjugates by the mammalian p97 adaptor complexes, p47 and Ufd1-Npl4. *EMBO J.* **21**: 5645-52

Meyer H, Bug M, Bremer S (2012) Emerging functions of the VCP/p97 AAA-ATPase in the ubiquitin system. *Nat. Cell Biol.* **14**: 117-23

Meyer H, Weihl CC (2014) The VCP/p97 system at a glance: connecting cellular function to disease pathogenesis. *J. Cell Sci.* **127**: 3877-83

Mieszczanek J, de la Roche M, Bienz M (2008). A role of Pygopus as an anti-repressor in facilitating Wnt-dependent transcription. *PNAS* **105**: 19324-9

Miller TC, Mieszczanek J, Sánchez-Barrena MJ, Rutherford TJ. Fiedler M, Bienz M (2013) Evolutionary adaptation of the fly Pygo PHD finger toward recognizing histone H3 tail methylated at arginine 2. *Structure* **21**: 2208-20

Mizushima N, Levine B, Cuervo AM, Klionsky DJ (2008) Autophagy fights disease through cellular self-digestion. *Nature* **451**: 1069-75

Mizushima N, Yoshimori T, Ohsumi Y (2011) The role of Atg proteins in autophagosome formation. *Annu. Rev. Cell Dev. Biol.* **27**: 107-32

Mlodzik M (2016) The Dishevelled protein family: still rather a mystery after over 20 years of molecular studies. *Curr. Top. Dev. Biol.* **117**: 75-91

Moir D, Stewart SE, Osmond BC, Botstein D (1982) Cold-sensitive cell-division-cycle mutants of yeast: isolation, properties, and pseudoreversion studies. *Genetics* **100**: 547-63

Morimoto D, Walinda E, Fukada H, Sou YS, Kageyama S, Hoshino M, Fujii T *et al.* (2015) The unexpected role of polyubiquitin chains in the formation of fibrillar aggregates. *Nat. Comm.* **6**: 6116

Morin PJ, Sparks AB, Korinek V, Barker N, Clevers H, Vogelstein B, Kinzler KW (1997) Activation of β-catenin-Tcf signaling in colon cancer by mutations in β-catenin or APC. *Science* **275**: 1787-90

Mosimann C, Hausmann G, Basler K (2009) β-catenin hits chromatin: regulation of Wnt target gene activation. *Nat. Rev. Mol. Cell Biol.* **10**: 276-86

Mukai A, Yamamoto-Hino M, Awano W, Watanabe W, Komada M, Goto S (2010) Balanced ubiquitylation and deubiquitylation of Frizzled regulate cellular responsiveness to Wg/Wnt. *EMBO J.* **29**: 2114-25

Mund T, Pelham HR (2009) Control of the activity of WW-HECT domain E3 ubiquitin ligases by NDFIP proteins. *EMBO Reports* **10**: 501-7

Mund T, Lewis MJ, Maslen S, Pelham HR (2014) Peptide and small molecule inhibitors of HECT-type ubiquitin ligases. *PNAS* **111**: 16736-41

Mund T, Graeb M, Mieszczanek J, Gammons M, Pelham HR, Bienz M (2015) Disinhibition of the HECT E3 ubiquitin ligase WWP2 by polymerized Dishevelled. *Open Biol.* **5**: 150185

Mund T, Pelham HR (2018) Substrate clustering potently regulates activity of WW-HECT domain-containing ubiquitin ligases. *JBC* **293**: 5200-9

Munoz MA, Saunders DN, Henderson MJ, Clancy JL, Russell AJ, Lehrbach G *et al.* (2007) The E3 ubiquitin ligase EDD regulates S-phase and G(2)/M DNA damage checkpoints. *Cell Cycle* **6**: 3070-7

Munoz-Escobar J, Matta-Camacho E, Kozlov G, Gehring K (2015) The MLLE domain of the ubiquitin ligase UBR5 binds to its catalytic domain to regulate substrate binding. *JBC* **290**: 22841-50

Murdoch JN, Doudney K, Paternotte C, Copp AJ, Stanier P (2001) Severe neural tube defects in the loop-tail mouse result from mutation of Lpp1, a novel gene involved in floor plate specification. *Hum. Mol. Genet.* **10**: 2593-601

Nagase H, Nakamura Y (1993) Mutations of the APC (adenomatous polyposis coli) gene. *Hum. Mutat.* **2**: 425-34

Nagel AC, Krejci A, Tenin G, Bravo-Patiño A, Bray S, Maier D, Preiss A (2005) Hairless-mediated repression of notch target genes requires the combined activity of Groucho and CtBP corepressors. *Mol. Cell. Biol.* **25**: 10433-41

Nakatogawa H, Ichimura Y, Ohsumi Y (2007) Atg8, a ubiquitin-like protein required for autophagosome formation, mediates membrane tethering and hemifusion. *Cell* **130**: 165-78

Nichols AS, Floyd DH, Bruinsma SP, Narzinski K, Baranski TJ (2013) Frizzled receptors signal through G proteins. *Cell Signal.* **25**: 1468-75

Niehrs C (2006) Function and biological roles of the Dickkopf family of Wnt modulators. *Oncogene* **25**: 7469-81

Niida A, Hiroko T, Kasai M, Furukawa Y, Nakamura Y, Suzuki Y, Sugano S, Akiyama T (2004) DKK1, a negative regulator of Wnt signaling, is a target of the beta-catenin/TCF pathway. *Oncogene* **23**: 8520-6

Nile AH, Mukund S, Stanger K, Wang W, Hannoush RN (2017) Unsaturated fatty acyl recognition by Frizzled receptors mediates dimerization upon Wnt ligand binding. *PNAS* **114**: 4147-52

Nishisho I, Nakamura Y, Miyoshi Y, Miki Y, Ando H, Horii A, Koyama K, Utsunomiya J, Baba S, Hedge P (1991) Mutations of chromosome 5q21 genes in FAP and colorectal cancer patients. *Science* **253**: 665-9

Nusse R, Clevers H (2017) Wnt/β-catenin signaling, disease, and emerging therapeutic modalities. *Cell* **169**: 985-99

Nusse R, Varmus HE (1982) Many tumors induced by the mouse mammary tumor virus contain a provirus integrated in the same region of the host genome. *Cell* **31**: 99-109

Nüsslein-Volhard C, Wieschaus E (1980) Mutations affecting segment number and polarity in *Drosophila*. *Nature* **287**: 795-801

Obara K, Sekito T, Ohsumi Y (2006) Assortment of phosphatidylinositol 3-kinase complexes - Atg14p directs association of complex I to the pre-autophagosomal structure in *Saccharomyces cerevisiae*. *Mol. Biol. Cell* **17**: 1527-39

Oberst A, Malatesta M, Aqeilan RI, Rossi M, Salomoni P, Murillas R (2007) The Nedd4-binding partner 1 (N4BP1) protein is an inhibitor of the E3 ligase Itch. *PNAS* **104**: 11280-5

O'Brien PM, Davies MJ, Scurry JP, Smith AN, Barton CA, Henderson MJ *et al.* (2008) The E3 ubiquitin ligase EDD is an adverse prognostic factor for serous epithelial ovarian cancer and modulates cisplatin resistance *in vitro*. *Br. J. Cancer* **98**: 1085-93

O'Gorman S, Fox DT, Wahl GM (1991) Recombinase-mediated gene activation and site-specific integration in mammalian cells. *Science* **251**: 1351-5

Ohshima R, Ohta T, Wu W, Koike A, Iwatani T, Henderson M, Watts CK, Otsubo T (2007) Putative tumor suppressor EDD interacts with and up-regulates APC. *Genes Cells* **12**: 1339-45

Ohsumi Y (2014) Historical landmarks of autophagy research. *Cell Res.* **24**: 9-23

Ohtake F, Saeki Y, Ishido S, Kanno J, Tanaka K (2016) The K48-K63 branched ubiquitin chain regulates NF-κB Signaling. *Mol Cell.* **20**: 251-66

Ohtake F, Saeki Y, Sakamoto K, Ohtake K, Nishikawa H, Tsuchiya H, Ohta T, Tanaka K, Kanno J (2015) Ubiquitin acetylation inhibits polyubiquitin chain elongation. *EMBO Rep*. **16**: 192-201

Olson JK, Grose C (1997) Endocytosis and recycling of varicella-zoster virus Fc receptor glycoprotein gE: internalization mediated by a YXXL motif in the cytoplasmic tail. *J. Virol.* **5**: 4042-54

Oshima H, Oshima M, Kobayashi M, Tsutsumi M, Taketo MM (1997) Morphological and molecular processes of polyp formation in Apc(delta716) knockout mice. *Cancer Res.* **57**: 1644-9

Pai LM, Orsulic S, Bejsovec A, Peifer M (1997) Negative regulation of Armadillo, a Wingless effector in *Drosophila*. *Development* **124**: 2255-66

Pankiv S, Clausen TH, Lamark T, Brech A, Bruun JA, Outzen H *et al.* (2007) p62/SQSTM1 binds directly to Atg8/LC3 to facilitate degradation of ubiquitinated protein aggregates by autophagy. *JBC* **282**: 24131-45

Pao KC, Wood NT, Knebel A, Rafie K, Stanley M, Mabbitt PD *et al.* (2018) Activity-based E3 ligase profiling uncovers an E3 ligase with esterification activity. *Nature* [Epub ahead of print]

Papadopoulos C, Kirchner P, Bug M, Grum D, Koerver L, Schulze N *et al.* (2017) VCP/p97 cooperates with YOD1, UBXD1 and PLAA to drive clearance of ruptured lysosomes by autophagy. *EMBO J.* **36**: 135-50

Parker DS, Jemison J, Cadigan KM (2002) Pygopus, a nuclear PHD-finger protein required for Wingless signaling in *Drosophila*. *Development* **129**: 2565-76

Paroush Z, Finley RL, Kidd T, Wainwright SM, Ingham PW, Brent R, Ish-Horowicz, D (1994) Groucho is required for *Drosophila* neurogenesis, segmentation, and sex determination and interacts directly with hairy-related bHLH proteins. *Cell* **79**: 805-15

Pashkova N, Gakhar L, Winistorfer SC, Yu L, Ramaswamy S, Piper RC (2010) WD40 repeat propellers define a ubiquitin-binding domain that regulates turnover of F box proteins. *Mol. Cell.* **40**: 433-43

Peifer M, McCrea PD, Green KJ, Wieschaus E, Gumbiner BM (1992) The vertebrate adhesive junction proteins beta-catenin and plakoglobin and the *Drosophila* segment polarity gene armadillo form a multigene family with similar properties. *J. Cell Biol.* **118**: 681-91

Peifer M, Sweeton D, Casey M, Wieschaus E (1994) wingless signal and Zeste-white 3 kinase trigger opposing changes in the intracellular distribution of Armadillo. *Development* **120**: 369-80

Peifer M (1995) Cell adhesion and signal transduction: the Armadillo connection. *Trends Cell Biol.* **5**: 224-9

Peng Y, Axelrod JD (2012) Asymmetric protein localization in planar cell polarity: mechanisms, puzzles, and challenges. *Curr. Top. Dev. Biol.* **101**: 33-53

Petersen J, Wright SC, Rodriguez D, Matricon P, Lahav N, Vromen A, Friedler A, Stromqvist J, Wennmalm S, Carlsson J, Schulte G (2017) Agonist-induced dimer dissociation as a macromolecular step in G protein-coupled receptor signaling. *Nat. Comm.* **8**: 226

Petroski MD, Deshaies RJ (2005) Mechanism of lysine 48-linked ubiquitin-chain synthesis by the cullin-RING ubiquitin-ligase complex SCF-Cdc34. *Cell* **123**: 1107-20

Pickles LM, Roe SM, Hemingway EJ, Stifani S, Pearl LH (2002) Crystal structure of the C-terminal WD40 repeat domain of the human Groucho/TLE1 transcriptional corepressor. *Structure* **10**: 751-61

Pinto D, Clevers H (2005) Wnt, stem cells and cancer in the intestine. *Biol. Cell* **97**: 185-96

Powell SM, Zilz N, Beazer-Barclay Y, Bryan TM, Hamilton SR, Thibodeau SN *et al.* (1992) APC mutations occur early during colorectal tumorigenesis. *Nature* **359**: 235-7

Pronobis MI, Rusan NM, Peifer M (2015) A novel GSK3-regulated APC:Axin interaction regulates Wnt signaling by driving a catalytic cycle of efficient β-catenin destruction. *eLife* **4**: e08022

Pronobis MI, Deuitch N, Posham V, Mimori-Kiyosue Y, Peifer M (2017) Reconstituting regulation of the canonical Wnt pathway by engineering a minimal β-catenin destruction machine. *Mol. Biol. Cell* **28**: 41-53

Prudden J, Pebernard S, Raffa G, Slavin DA, Perry JJ, Tainer JA, McGowan CH, Boddy MN (2007) SUMO-targeted ubiquitin ligases in genome stability. *EMBO J.* **26**: 4089-101

Puvirajesinghe TM, Bertucci F, Jain A, Scerbo P, Belotti E, Audebert S, Sebbagh M *et al.* (2016) Identification of p62/SQSTM1 as a component of non-canonical Wnt VANGL2-JNK signalling in breast cancer. *Nat. Commun.* **7**: 10318

Qi J, Lee HJ, Saquet A, Cheng XN, Shao M, Zheng JJ, Shi DL (2017) Autoinhibition of Dishevelled protein regulated by its extreme C terminus plays a distinct role in Wnt/β-catenin and Wnt/planar cell polarity (PCP) signaling pathways. *JBC* **292**: 5898-908

Rahighi S, Ikeda F, Kawasaki M, Akutsu M, Suzuki N *et al*. (2009) Specific recognition of linear ubiquitin chains by NEMO is important for NF-kappaB activation. *Cell* **136**: 1098-109

Ramakrishnan A-B, Sinha A, Fan VB, Cadigan KM (2017) The Wnt Transcriptional Switch: TLE Removal or Inactivation? *BioEssays* **1700162**

Ran FA, Hsu PD, Wright J, Agarwala V, Scott DA, Zhang F (2013) Genome engineering using the CRISPR-Cas9 system. *Nat. Protoc.* **8**: 2281-308

Randow F (2011) How cells deploy ubiquitin and autophagy to defend their cytosol from bacterial invasion. *Autophagy* **7**: 304-9

Reya T, Duncan AW, Ailles L, Domen J, Scherer DC, Willert K, Hintz L, Nusse R, Weissman IL (2003) A role for Wnt signalling in self-renewal of haematopoietic stem cells. *Nature* **423**: 409-14

Rijsewijk F, Schuermann M, Wagenaar E, Parren P, Weigel D, Nusse R (1987) The *Drosophila* homolog of the mouse mammary oncogene int-1 is identical to the segment polarity gene wingless. *Cell* **50**: 649-57

Ringrose JH, van den Toorn HW, Eitel M, Post H, Neerincx P, Schierwater B, Altelaar AF, Heck AJ (2013) Deep proteome profiling of *Trichoplax adhaerens* reveals remarkable features at the origin of metazoan multicellularity. *Nat. Comm.* **4**: 1408

Rios-Esteves J, Resh MD (2013) Stearoyl CoA desaturase is required to produce active, lipid-modified Wnt proteins. *Cell Rep.* **4**: 1072-81

Rogov V, Dötsch V, Johansen T, Kirkin V (2014) Interactions between autophagy receptors and ubiquitin-like proteins form the molecular basis for selective autophagy. *Mol. Cell* **53**: 167-78

Rong X, Zhou Y, Liu Y, Zhao B, Wang B, Wang C, Gong X *et al*. (2017) Glutathione peroxidase 4 inhibits Wnt/β-catenin signaling and regulates dorsal organizer formation in zebrafish embryos. *Development* **144**: 1687-97

Rosin-Arbesfeld R, Townsley F, Bienz M (2000) The APC tumour suppressor has a nuclear export function. *Nature* **406**: 1009-12

Rotin D, Kumar S (2009) Physiological functions of the HECT family of ubiquitin ligases. *Nat. Rev. Mol. Cell Biol.* **10**: 398-409

Rousseau F, Schymkowitz JW, Itzhaki LS (2003) The unfolding story of three-dimensional domain swapping. *Structure* **11**: 243-51

Rousset R, Mack JA, Wharton KA, Axelrod JD, Cadigan KM, Fish MP, Nusse R, Scott MP (2001) Naked cuticle targets dishevelled to antagonize Wnt signal transduction. *Genes Dev.* **15**: 658-71

Rousset R, Wharton KA Jr, Zimmermann G, Scott MP (2002) Zinc-dependent interaction between dishevelled and the *Drosophila* Wnt antagonist naked cuticle. *JBC* **277**: 49019-26

Roux KJ, Kim DI, Raida M, Burke B (2012) A promiscuous biotin ligase fusion protein identifies proximal and interacting proteins in mammalian cells. *J. Cell Biol.* **196**: 801-10

Roux KJ, Kim DI, Burke B (2013) BioID: a screen for protein-protein interactions. *Curr. Protoc. Protein Sci.* **74**: 1-19

Rubinfeld B, Souza B, Albert I, Müller O, Chamberlain SH, Masiarz FR, Munemitsu S, Polakis P (1993) Association of the APC gene product with beta-catenin. *Science* **262**: 1731-4

Rulifson EJ, Micchelli CA, Axelrod JD, Perrimon N, Blair SS (1996) Wingless refines its own expression domain on the *Drosophila* wing margin. *Nature* **384**: 72-4

Rumpf S, Jentsch S (2006) Functional division of substrate processing cofactors of the ubiquitin-selective Cdc48 chaperone. *Mol. Cell* **21**: 261-9

Rutz S, Kayagaki N, Phung QT, Eidenschenk C, Noubade R, Wang X, Lesch J *et al.* (2015) Deubiquitinase DUBA is a post-translational brake on interleukin-17 production in T cells. *Nature* **518**: 417-21

Saller E, Kelley A, Bienz M (2002) The transcriptional repressor Brinker antagonizes Wingless signaling. *Genes Dev.* **16**: 1828-38

Salvat C, Wang G, Dastur A, Lyon N, Huibregtse JM (2004) The -4 phenylalanine is required for substrate ubiquitination catalyzed by HECT ubiquitin ligases. *JBC* **279**: 18935-43

Sato T, Vries RG, Snippert HJ, van de Wetering M, Barker N, Stange DE, van Es JH, Abo A, Kujala P, Peters PJ, Clevers H (2009) Single Lgr5 stem cells build crypt-villus structures in vitro without a mesenchymal niche. *Nature* **459**: 262-5

Schmidtmann E, Anton T, Rombaut P, Herzog F, Leonhardt H (2016) Determination of local chromatin composition by CasID. *Nucleus* **7**: 476-84

Schneider I, Schneider PN, Derry SW, Lin S, Barton LJ, Westfall T, Slusarski DC (2010) Zebrafish Nkd1 promotes Dvl degradation and is required for left-right patterning. *Dev. Biol.* **348**: 22-33

Schuijers J, Mokry M, Hatzis P, Cuppen E, Clevers H (2014) Wnt-induced transcriptional activation is exclusively mediated by TCF/LEF. *EMBO J.* **33**: 146-56

Schulman BA, Harper JW (2009) Ubiquitin-like protein activation by E1 enzymes: the apex for downstream signalling pathways. *Nat. Rev. Mol. Cell Biol.* **10**: 319-31

Schwank G, Clevers H (2016) CRISPR/Cas-9-Mediated Genome Editing of Mouse Small Intestinal Organoids. *Methods Mol. Biol.* **1422**: 3-11

Schwarz-Romond T, Asbrand C, Bakkers J, Kühl M, Schaeffer HJ, Huelsken J *et al.* (2002) The ankyrin repeat protein Diversin recruits Casein kinase I epsilon to the beta-catenin

degradation complex and acts in both canonical Wnt and Wnt/JNK signaling. *Genes Dev.* **16**: 2073-84

Schwarz-Romond T, Merrifield C, Nichols BJ, Bienz M (2005) The Wnt signalling effector Dishevelled forms dynamic protein assemblies rather than stable associations with cytoplasmic vesicles. *J. Cell Sci.* **118**: 5269-77

Schwarz-Romond T, Fiedler M, Shibata N, Butler PJ, Kikuchi A, Higuchi Y, Bienz M (2007a) The DIX domain of Dishevelled confers Wnt signaling by dynamic polymerization. *Nat. Struct. Mol. Biol.* **14**: 484-92

Schwarz-Romond T, Metcalfe C, Bienz M (2007b) Dynamic recruitment of axin by Dishevelled protein assemblies. *J. Cell Sci.* **120**: 2402-12

Schweizer L, Nellen D, Basler K (2003) Requirement for Pangolin/dTCF in *Drosophila* Wingless signaling. *PNAS* **100**: 5846-51

Seibenhener ML, Babu JR, Geetha T, Wong HC, Krishna NR, Wooten MW (2004) Sequestosome 1/p62 is a polyubiquitin chain binding protein involved in ubiquitin proteasome degradation. *Mol. Cell. Biol.* **24**: 8055-68

Sekiya T, Zaret KS (2007) Repression by Groucho/TLE/Grg proteins: genomic site recruitment generates compacted chromatin *in vitro* and impairs activator binding *in vivo*. *Mol. Cell* **28**: 291-303

Semënov M, Tamai K, He X (2005) SOST is a ligand for LRP5/LRP6 and a Wnt signaling inhibitor. *JBC* **280**: 26770-5

Seshagiri S, Stawiski EW, Durinck S, Modrusan Z, Storm EE, Conboy CB, Chaudhuri S, Guan Y, Janakiraman V, Jaiswal BS *et al.* (2012) Recurrent R-spondin fusions in colon cancer. *Nature* **488**: 660-4

Sharma M, Jamieson C, Johnson M, Molloy MP, Henderson BR (2012) Specific armadillo repeat sequences facilitate β-Catenin nuclear transport in live cells via direct binding to nucleoporins Nup62, Nup153, and RanBP2/Nup358. *JBC* **287**: 819-31

Sharma RP (1973) wingless - a new mutant in *D. melanogaster*. *Drosophila Information Service* **50**: 134

Shearer RF, Iconomou M, Watts CK, Saunders DN (2015) Functional roles of the E3 ubiquitin ligase UBR5 in cancer. *Mol. Cancer Res.* **13**: 1523-32

Shen PS, Park J, Qin Y, Li X, Parsawar K, Larson MH, Cox J, Cheng Y *et al.* (2015) Rqc2p and 60S ribosomal subunits mediate mRNA-independent elongation of nascent chains. *Science* **347**: 75-8

Siegfried E, Chou TB, Perrimon N (1992) wingless signaling acts through zeste-white 3, the *Drosophila* homolog of glycogen synthase kinase-3, to regulate engrailed and establish cell fate. *Cell* **71**: 1167-79

Siegfried E, Wilder EL, Perrimon N (1994) Components of wingless signalling in *Drosophila*. *Nature* **367**: 76-80

Sierra J, Yoshida T, Joazeiro CA, Jones KA (2006). The APC tumor suppressor counteracts β-catenin activation and H3K4 methylation at Wnt target genes. *Genes Dev.* **20**: 586-600

Silva J, Barrandon O, Nichols J, Kawaguchi J, Theunissen TW, Smith A (2008) Promotion of reprogramming to ground state pluripotency by signal inhibition. *PLoS Biol.* **6**: e253

Sokol SY, Klingensmith J, Perrimon N, Itoh K (1995) Dorsalizing and neuralizing properties of Xdsh, a maternally expressed *Xenopus* homolog of *dishevelled*. *Development* **121**: 3487

Song C, Wang Q, Song C, Lockett SJ, Colburn NH, Li CC, Wang JM, Rogers TJ (2014) Nucleocytoplasmic shuttling of valosin-containing protein (VCP/p97) regulated by its N domain and C-terminal region. *Biochim. Biophys. Acta.* **1853**: 222-32

Song H, Hasson P, Paroush Z, Courey AJ (2004) Groucho oligomerization is required for repression *in vivo*. *Mol. Cell. Biol.* **24**: 4341-50

Spink KE, Polakis P, Weis WI (2000) Structural basis of the Axin-Adenomatous polyposis coli interaction. *EMBO J.* **19**: 2270-9

Spink KE, Fridman SG, Weis, WI (2001) Molecular mechanisms of β-catenin recognition by adenomatous polyposis coli revealed by the structure of an APC-β-catenin complex. *EMBO J.* **20**: 6203-12

Sriram SM, Kim BY, Kwon YT (2011) The N-end rule pathway: emerging functions and molecular principles of substrate recognition. *Nat. Rev. Mol. Cell Biol.* **12**: 735-47

Städeli R, Basler K (2005) Dissecting nuclear Wingless signalling: recruitment of the transcriptional co-activator Pygopus by a chain of adaptor proteins. *Mech. Dev.* **122**: 1171-82

Stamos JL, Weis WI (2013) The β-catenin destruction complex. *Cold Spring Harb. Perspect. Biol.* **5**: a007898

Stamos JL, Chu ML, Enos MD, Shah N, Weis WI (2014) Structural basis of GSK-3 inhibition by N-terminal phosphorylation and by the Wnt receptor LRP6. *eLife* **3**: e01998

Stancikova J, Krausova M, Kolar M, Fafilek B, Svec J, Sedlacek R *et al*. (2015) NKD1 marks intestinal and liver tumors linked to aberrant Wnt signaling. *Cell Signal.* **27**: 245-56

Stanganello E, Hagemann AIH, Mattes B, Sinner C, Meyen D, Weber S, Schug A, Raz E, Scholpp S (2015) Filopodia-based Wnt transport during vertebrate tissue patterning. *Nat. Comm.* **6**: 5846

Steinhart Z, Pavlovic Z, Chandrashekhar M, Hart T, Wang X, Zhang X, Robitaille M, Brown KR, Jaksani S, Overmeer R *et al.* (2017) Genome-wide CRISPR screens reveal a Wnt-FZD5 signaling circuit as a druggable vulnerability of RNF43-mutant pancreatic tumors. *Nat. Med.* **23**: 60-8

Stolz A, Ernst A, Dikic I (2014) Cargo recognition and trafficking in selective autophagy. *Nat. Cell Biol.* **16**: 495-501

Storm EE, Durinck S, de Sousa e Melo F, Tremayne J, Kljavin N, Tan C, Ye X, Chiu C, Pham T, Hongo JA *et al.* (2016) Targeting PTPRK-RSPO3 colon tumours promotes differentiation and loss of stem-cell function. *Nature* **529**: 97-100

Strutt D (2003) Frizzled signalling and cell polarisation in *Drosophila* and vertebrates. *Development* **130**: 4501-13

Strutt H, Gamage J, Strutt D (2016) Robust asymmetric localization of planar polarity proteins is associated with organization into signalosome-like domains of variable stoichiometry. *Cell Rep.* **17**: 2660-71

Su LK, Vogelstein B, Kinzler KW (1993) Association of the APC tumor suppressor protein with catenins. *Science* **262**: 1734-7

Sugioka K, Mizumoto K, Sawa H (2011) Wnt regulates spindle asymmetry to generate asymmetric nuclear beta-catenin in *C. elegans*. *Cell* **146**: 942-54

Sussman DJ, Klingensmith J, Salinas P, Adams PS, Nusse R, Perrimon N (1994) Isolation and characterization of a mouse homolog of the *Drosophila* segment polarity gene *dishevelled*. Dev. Biol. **166**: 73-86

Taelman VF, Dobrowolski R, Plouhinec J-L, Fuentealba LC, Vorwald PP, Gumper I *et al.* (2010) Wnt signaling requires sequestration of Glycogen Synthase Kinase 3 inside multivesicular endosomes. *Cell* **143**: 1136-48

Takeuchi S, Takeda K, Oishi I, Nomi M, Ikeya M, Itoh K, Tamura S, Ueda T *et al.* (2000) Mouse Ror2 receptor tyrosine kinase is required for the heart development and limb formation. *Genes to Cells* **5**: 71-8

Tamai K, Zeng X, Liu C, Zhang X, Harada Y, Chang Z, He X (2004) A mechanism for Wnt coreceptor activation. *Mol. Cell* **13**: 149-56

Tao L, Zhang J, Meraner P, Tovaglieri A, Wu X, Gerhard R, Zhang X, Stallcup WB, Miao J, He X *et al.* (2016) Frizzled proteins are colonic epithelial receptors for *C. difficile* toxin B. *Nature* **538**: 350-5

Tasaki T, Mulder LC, Iwamatsu A, Lee MJ, Davydov IV, Varshavsky A *et al.* (2005) A family of mammalian E3 ubiquitin ligases that contain the UBR box motif and recognize N-degrons. *Mol. Cell. Biol.* **25**: 7120-36

Takemaru KI, Moon RT (2000) The transcriptional coactivator CBP interacts with beta-catenin to activate gene expression. *J. Cell Biol.* **149**: 249-54

Tauriello DV, Maurice MM (2010a) The various roles of ubiquitin in Wnt pathway regulation. *Cell Cycle* **9**: 3724-33

Tauriello DV, Haegebarth A, Kuper I, Edelmann MJ, Henraat M, Canninga-van Dijk MR *et al.* (2010b). Loss of the tumor suppressor CYLD enhances Wnt/β-catenin signaling through K63-linked ubiquitination of Dvl. *Mol. Cell* **37**: 607-19

Tauriello DV, Jordens I, Kirchner K, Slootstra JW, Kruitwagen T, Bouwman BA *et al.* (2012) Wnt/β-catenin signaling requires interaction of the Dishevelled DEP domain and C terminus with a discontinuous motif in Frizzled. *PNAS* **109**: 812-20

Terrell J, Shih S, Dunn R, Hicke L (1998) A function for monoubiquitination in the internalization of a G protein–coupled receptor. *Mol. Cell* **1**: 193-202

Thompson B, Townsley F, Rosin-Arbesfeld R, Musisi H, Bienz M (2002) A new nuclear component of the Wnt signalling pathway. *Nat. Cell Biol.* **4**: 367-73

Thorvaldsen TE, Pedersen NM, Wenzel EM, Schultz SW, Brech A *et al.* (2015) Structure, dynamics, and functionality of Tankyrase inhibitor-induced degradasomes. *Mol. Cancer Res.* **13**: 1487-501

Tian H, Biehs B, Chiu C, Siebel CW, Wu Y, Costa M, de Sauvage FJ, Klein OD (2015) Opposing activities of Notch and Wnt signaling regulate intestinal stem cells and gut homeostasis. *Cell Rep.* **11**: 33-42

Tickenbrock L, Kossmeier K, Rehmann H, Herrmann C, Muller O (2003) Differences between the interaction of β-catenin with non-phosphorylated and single-mimicked phosphorylated 20-amino acid residue repeats of the APC protein. *J. Mol. Biol.* **327**: 359-67

Townsley FM, Cliffe A, Bienz M (2004) Pygopus and Legless target Armadillo/β-catenin to the nucleus to enable its transcriptional co-activator function. *Nat. Cell Biol.* **6**: 626-33

Tran H, Bustos D, Yeh R, Rubinfeld B, Lam C, Shriver S *et al.* (2013) HectD1 E3 ligase modifies Adenomatous Polyposis Coli (APC) with polyubiquitin to promote the APC-Axin interaction. *JBC* **288**: 3753-67

Tran L, Basdevant N, Prévost C, Ha-Duong T (2016) Structure of ring-shaped Aβ 42 oligomers determined by conformational selection. *Sci. Rep.* **6**: 21429

Tresse E, Salomons FA, Vesa J, Bott LC, Kimonis V, Yao TP, Dantuma NP, Taylor JP (2010) VCP/p97 is essential for maturation of ubiquitin-containing autophagosomes and this function is impaired by mutations that cause IBMPFD. *Autophagy* **6**: 217-27

Tsukada M, Ohsumi Y (1993) Isolation and characterization of autophagy-defective mutants of *Saccharomyces cerevisiae*. *FEBS Lett.* **333**: 169-74

Turki-Judeh W, Courey AJ (2012) Groucho: a corepressor with instructive roles in development. *Curr. Top. Dev. Biol.* **98**: 65-96

van Amerongen R, Nusse R (2009) Towards an integrated view of Wnt signaling in development. *Development* **136**: 3205-14

van de Wetering M, Castrop J, Korinek V, Clevers H (1996) Extensive alternative splicing and dual promoter usage generate Tcf-1 protein isoforms with differential transcription control properties. *Mol. Cell Biol.* **16**: 745-52

van de Wetering M, Cavallo R, Dooijes D, van Beest M, van Es J, Loureiro J *et al.* (1997) Armadillo coactivates transcription driven by the product of the *Drosophila* segment polarity gene dTCF. *Cell* **88**: 789-99

van de Wetering M, Sancho E, Verweij C, de Lau W, Oving I, Hurlstone A *et al.* (2002) The beta-catenin/TCF-4 complex imposes a crypt progenitor phenotype on colorectal cancer cells. *Cell* **111**: 241-50

van den Boom J, Wolf M, Weimann L, Schulze N, Li F, Kaschani F, Riemer A *et al.* (2016) VCP/p97 extracts sterically trapped Ku70/80 rings from DNA in Double-Strand Break repair. *Mol. Cell* **64**: 189-98

van den Boom J, Meyer H (2017) VCP/p97-Mediated unfolding as a principle in protein homeostasis and signaling. *Mol. Cell* **69**: 1-13

van der Flier LG, Clevers H (2009) Stem Cells, Self-Renewal, and Differentiation in the Intestinal Epithelium. *Ann. Rev. Phys.* **71**: 241-60

van der Veen AG, Ploegh HL (2012) Ubiquitin-like Proteins. *Ann. Rev. Biochem.* **81**: 323-57

Van Raay TJ, Coffey RJ, Solnica-Krezel L (2007) Zebrafish Naked1 and Naked2 antagonize both canonical and non-canonical Wnt signaling. *Dev. Biol.* **309**: 151-68

Van Raay TJ, Fortino NJ, Miller BW, Ma H, Lau G, Li C *et al.* (2011) Naked1 antagonizes Wnt signaling by preventing nuclear accumulation of β-catenin. *PLoS One* **6**: e18650

van Tienen LM, Mieszczanek J, Fiedler M, Rutherford TJ, Bienz M (2017) Constitutive scaffolding of multiple Wnt enhanceosome components by Legless/BCL9. *eLife* **6**: e20882

Varshavsky A (1996) The N-end rule: functions, mysteries, uses. *PNAS* **93**: 12142-9

Varshavsky A (2012) The Ubiquitin System, an Immense Realm. *Annu. Rev. Biochem.* **81**: 167-76

Veeman MT, Slusarski DC, Kaykas A, Louie SH, Moon RT (2003) Zebrafish prickle, a modulator of noncanonical Wnt/Fz signaling, regulates gastrulation movements. *Curr. Biol.* **13**: 680-5

Vijay-Kumar S, Bugg CE, Cook WJ (1987) Structure of ubiquitin refined at 1.8Å resolution. *J. Mol. Biol.* **194**: 531-44

Vleminckx K, Kemler R, Hecht A (1999) The C-terminal transactivation domain of β-catenin is necessary and sufficient for signaling by the LEF-1/β-catenin complex in *Xenopus laevis*. *Mech. Dev.* **81**: 65-74

Watanabe Y, Tanaka M (2011) p62/SQSTM1 in autophagic clearance of a non-ubiquitylated substrate. *J. Cell Sci.* **124**: 2692-701

Wauer T, Simicek M, Schubert A, Komander D (2015) Mechanism of phospho-ubiquitin-induced PARKIN activation. *Nature* **524**: 370-4

Wehrli M, Dougan ST, Caldwell K, O'Keefe L, Schwartz S, Vaizel-Ohayon D, Schejter E, Tomlinson A, DiNardo S (2000) arrow encodes an LDL-receptor-related protein essential for Wingless signalling. *Nature* **407**: 527-30

Wei W, Li M, Wang J, Nie F, Li L (2012) The E3 Ubiquitin Ligase ITCH negatively regulates canonical Wnt signaling by targeting Dishevelled protein. *Mol. Cellular Biol.* **32**: 3903-12

Wen JL, Wen XF, Li RB, Jin YC, Wang XL, Zhou L *et al.* (2015) UBE3C promotes growth and metastasis of renal cell carcinoma via activating Wnt/β-catenin pathway. *PLoS ONE* **10**: e0115622

Wenzel DM, Lissounov A, Brzovic PS, Klevit RE (2011) UBCH7 reactivity profile reveals parkin and HHARI to be RING/HECT hybrids. *Nature* **474**: 105-8

Wharton KA Jr, Zimmermann G, Rousset R, Scott MP (2001) Vertebrate proteins related to *Drosophila* Naked Cuticle bind Dishevelled and antagonize Wnt signaling. *Dev. Biol.* **234**: 93-106

Wiesner S, Ogunjimi AA, Wang HR, Rotin D, Sicheri F, Wrana JL, Forman-Kay JD (2007) Autoinhibition of the HECT-type ubiquitin ligase Smurf2 through its C2 domain. *Cell* **130**: 651-62

Willert K, Shibamoto S, Nusse R (1999) Wnt-induced dephosphorylation of Axin releases β-catenin from the Axin complex. *Genes Dev.* **13**: 1768-73

Willert K, Brown JD, Danenberg E, Duncan AW, Weissman IL, Reya T, Yates JR, Nusse R (2003) Wnt proteins are lipid-modified and can act as stem cell growth factors. *Nature* **423**: 448-52

Wodarz A, Nusse R (1998) Mechanisms of Wnt signaling in development. *Annu. Rev. Cell Dev. Biol.* **14**: 59-88

Wong H-C, Bourdelas A, Krauss A, Lee H-J, Shao Y, Wu D *et al.* (2003) Direct binding of the PDZ domain of Dishevelled to a conserved internal sequence in the C-terminal region of Frizzled. *Mol. Cell* **12**: 1251-60

Wu G, Xu G, Schulman BA, Jeffrey PD, Harper JW, Pavletich NP (2003) Structure of a β-TrCP1-Skp1-β-Catenin complex: destruction motif binding and lysine specificity of the SCFβ-TrCP1 ubiquitin ligase. *Mol. Cell* **11**: 1445-56

Wu J, Jiao Y, Dal Molin M, Maitra A, de Wilde RF, Wood LD, Eshleman JR, Goggins MG, Wolfgang CL, Canto MI *et al.* (2011) Whole-exome sequencing of neoplastic cysts of the pancreas reveals recurrent mutations in components of ubiquitin-dependent pathways. *PNAS* **108**: 21188-93

Wu J, Bowe DB, Sadlonova A, Whisenhunt TR, Hu Y, Rustgi AK, Nie Y, Paterson AJ, Yang X (2014) O-GlcNAc transferase is critical for transducin-like enhancer of split (TLE)-mediated repression of canonical Wnt signaling. *JBC* **289**: 12168-76

Wu Z-Q, Li X-Y, Hu CY, Ford M, Kleer CG, Weiss SJ (2012) Canonical Wnt signaling regulates Slug activity and links epithelial-mesenchymal transition with epigenetic Breast Cancer 1, Early Onset (BRCA1) repression. *PNAS* **109**: 16654-9

Xia D, Tang WK, Ye Y (2016) Structure and function of the AAA+ ATPase p97/Cdc48p. *Gene* **583**: 64-77

Xia ZP, Sun L, Chen X, Pineda G, Jiang X, Adhikari A, Zeng W, Chen ZJ (2009) Direct activation of protein kinases by unanchored polyubiquitin chains. *Nature* **461**: 114-9

Xie Z, Liang H, Wang J, Xu X, Zhu Y, Guo A, Shen X, Cao F, Chang W (2017) Significance of the E3 ubiquitin protein UBR5 as an oncogene and a prognostic biomarker in colorectal cancer. *Oncotarget* **8**: 108079-92

Xu P, Duong DM, Seyfried NT, Cheng D, Xie Y, Robert J, Rush J, Hochstrasser M, Finley D, Peng J (2009) Quantitative proteomics reveals the function of unconventional ubiquitin chains in proteasomal degradation. *Cell* **137**: 133-45

Xu Q, Wang Y, Dabdoub A, Smallwood PM, Williams J, Woods C, Kelley MW *et al.* (2004) Vascular development in the retina and inner ear: control by Norrin and Frizzled-4, a high-affinity ligand-receptor pair. *Cell* **116**: 883-95

Xue L, Blythe EE, Freiberger EC, Mamrosh JL, Hebert AS, Reitsma JM, Hess S, Coon JJ, Deshaies RJ (2016) Valosin-containing protein (VCP)-Adaptor interactions are exceptionally dynamic and subject to differential modulation by a VCP inhibitor. *Mol. Cell. Proteomics* 15: 2970-86

Yan D, Wallingford JB, Sun TQ, Nelson AM, Sakanaka C, Reinhard C, Harland RM, Fantl WJ, Williams LT (2001) Cell autonomous regulation of multiple Dishevelled-dependent pathways by mammalian Nkd. *PNAS* **98**: 3802-7

Yau R, Rape M (2016) The increasing complexity of the ubiquitin code. *Nat. Cell Biol.* **18**: 579-86

Ye Y, Blaser G, Horrocks MH, Ruedas-Rama MJ, Ibrahim S, Zhukov AA, Orte A *et al.* (2012) Ubiquitin chain conformation regulates recognition and activity of interacting proteins. *Nature* **13**: 266-70

Ye Y, Tang WK, Zhang T, Xia D (2017) A Mighty ‘‘Protein Extractor’’ of the Cell: Structure and Function of the p97/CDC48 ATPase. *Front. Mol. Biosci.* **4**: 39

Yokoya F, Imamoto N, Tachibana T, Yoneda Y (1999) β-Catenin can be transported into the nucleus in a Ran-unassisted manner. *Mol. Biol. Cell* **10**: 1119-31

Yonashiro R, Tahara EB, Bengtson MH, Khokhrina M, Lorenz H, Chen KC *et al.* (2016) The Rqc2/Tae2 subunit of the ribosome-associated quality control (RQC) complex marks ribosome-stalled nascent polypeptide chains for aggregation. *eLife* **5**: e11794

Yoshida M, Yoshida K, Kozlov G, Lim NS, De Crescenzo G, Pang Z, Berlanga JJ, Kahvejian A, Gehring K, Wing SS, Sonenberg N (2006) Poly(A) binding protein (PABP) homeostasis is mediated by the stability of its inhibitor, Paip2. *EMBO J.* **25**: 1934-44

Zeng W, Wharton KA, Mack JA, Wang K, Gadbaw M, Suyama K, Klein PS, Scott MP (2000) naked cuticle encodes an inducible antagonist of Wnt signalling. *Nature* **403**: 789-95

Zhan T, Rindtorff N, Boutros M (2017) Wnt signaling in cancer. *Oncogene* **36**: 1461-73

Zhang L, Gao X, Wen J, Ning Y, Chen YG (2006) Dapper 1 antagonizes Wnt signaling by promoting dishevelled degradation. *JBC* **281**: 8607-12

Zhang T, Cronshaw J, Kanu N, Snijders AP, Behrens A (2014) UBR5-mediated ubiquitination of ATMIN is required for ionizing radiation-induced ATM signaling and function. *PNAS* **111**: 12091-96

Zhang X, Shaw A, Bates PA, Newman RH, Gowen B, Orlova E, Gorman MA, Kondo H, Dokurno P *et al.* (2000) Structure of the AAA ATPase p97. *Mol. Cell* **6**: 1473-84

Zhang Y, Appleton BA, Wiesmann C, Lau T, Costa M, Hannoush RN, Sidhu SS (2009) Inhibition of Wnt signaling by Dishevelled PDZ peptides. *Nat. Chem. Biol.* **5**: 217-9

Zhang Y, Liu S, Mickanin C, Feng Y, Charlat O, Michaud GA, Schirle M, Shi X, Hild M, Bauer A *et al*. (2011) RNF146 is a poly(ADP-ribose)-directed E3 ligase that regulates Axin degradation and Wnt signalling. *Nat. Cell Biol.* **13**: 623-29

Zheng N, Shabek N (2017) Ubiquitin ligases: structure, function and regulation. *Ann. Rev. Biochem.* **86**: 129-57

Zhou HJ, Wang J, Yao B, Wong S, Djakovic S, Kumar B, Rice J, Valle E, Soriano F, Menon MK *et al*. (2015) Discovery of a first-in-class, potent, selective, and orally bioavailable inhibitor of the p97 AAA ATPase (CB-5083). *J. Med. Chem.* **58**: 9480-97

Appendix 1 CRISPR/Cas9 genome editing

Single-guide RNAs used for CRISPR/Cas9 genome editing

Cell Line	Gene	Exon Targeted	gRNA sequence
HEK293T/ HCT116	*UBR5*	6	(G)CTGGAGCTCGAGATTCCCGC
HEK293T	*HUWE1*	5	GGACCGCTTCGATGGAATAC
HEK293T	*TRIP12*	3	(G)CTGACTCCGTGAACCGCCAG
HEK293T	*HECTD1*	3	(G)TATCTGCGGAATGTACCCGA
HEK293T	*UBE3C*	4	GCTACCTTGTCACAGTCCGG
HEK293T	*XIAP*	2	(G)TATCAGACACCATATACCCG
HEK293T	*CTNNB1*	3	GAAAAGCGGCTGTTAGTCAC
HEK293T	*SQSTM1*	3	(G)CGCTACACAAGTCGTAGTCT
HEK293T	*NBR1*	6	GTGGGGCTTCATCAACGACA
HEK293T	*ATG5*	2	(G)AACTTGTTTCACGCTATATC
HEK293T	*CYLD*	2	(G)CAGGACAGCCCACGTCTATT
HEK293T	*N4BP1*	1	(G)CGGCTAGGCTCACGCCAAAC

Genotyping primers for CRISPR/Cas9 genome editing

Gene	Exon		Primer sequence
UBR5	6	Fwd	GATTGAGCCCGGGAGTTTTG
		Rev	TCCATCTTCATCATCCCGGC
		Seq	TGAGGCAGGAGGATCACTTC
HUWE1	5	Fwd	GCAGATCAAAACATGGAACATTGG
		Rev	CTCTATGGAACTGTACAGATGCCG
		Seq	GTATGACAATGAACTACAGC
TRIP12	3	Fwd	AAGCTGCAGTTCATCATCTGCT
		Rev	TTGCTAATTTGGCCTGTAATCCAGAA
		Seq	GCGCAGTGCTAGTCCAGACT
HECTD1	3	Fwd	GACTACAGGTGCCTGTCACC
		Rev	ACTACCAGGAACTGAAGTGCAC
		Seq	ATATGATTTCTTTCACTACAG
UBE3C	4	Fwd	GAAGAAAGGCGAAGGTTGAAAAATGC
		Rev	CACATCACCACATAGGTAACCTCTC
		Seq	CTACAATTCAACTGTGAGCA
XIAP	2	Fwd	AAACTTGTGTACCTGCAGACA
		Rev	CCGTGCTTCATAATCTGCCA
		Seq	CTTTTGCTAATTTTCCAAGTGG
SQSTM1	3	Fwd	GACAATGGCCATGTCCTACG
		Rev	GGAAGGTGAAACACGGACAC
		Seq	AGTCCATGTTCACTCTAG
NBR1	6	Fwd	AAGAGACAGGCTGCAGTGAG
		Rev	CTGCACTGCAGGATCCTCTG
		Seq	GTTGTTGGATTTAATAAAGC
ATG5	2	Fwd	GCAGTAGACTCTTCTGGGC
		Rev	CCTTCTTTATGCTTATCTGTG
		Seq	GCAATGAATATTACTGGC
CYLD	2	Fwd	TGGACACCACGTTGCTGA
		Rev	CCAAAGAATATTCCGGAGACTGT
		Seq	CAATGAGTTCAGGCTTATG
N4BP1	1	Fwd	AAAGGGGCGGAGGGGTTC
		Rev	GAGACCCGGACCGATCGA
		Seq	TGGCGGGATGGTATAG

Appendix 2 RT-qPCR

Primer pairs used for RT-qPCR analysis of endogenous gene expression

Gene		Primer sequence
PMM1	Fwd	CTCCTAGTGGCACTGGCTTC
	Rev	GCAGGCTAGATCTCGT ACCG
NKD1	Fwd	GCTGAGCGTGTCTCTCAACA
	Rev	AGGAGTGGATCGGGAGACAG
AXIN2	Fwd	CTGGTGCAAAGACATAGCCA
	Rev	GTCCAGCAAAACTCTGAGGG
SP5	Fwd	TCGGACATAGGGACCCAGTT
	Rev	CTGACGGTGGGAACGGTTTA

Appendix 3 – Bioinformatic analysis of histidine-rich domains

Proteins from *H. sapiens* genome containing HRDs

Protein	HRD length	Histidine residues	HRD sequence
ERC2	13	12	HHHYHHHHHHHHH
AXIN1	12	9	HHHRHVHHHVHH
SORBS2	13	12	HHHHHHHHHHHRH
CBL	11	8	HHHHHHHLSPH
IQSEC2	13	11	HHHHHHHHHGHSH
USP34	15	13	HHHHHHHHHHHHDGH
NKD2	19	16	HEHHHHHEHHHHHHHHHFH
NKD1	15	12	HEHHHHHEHHHHYHH
SYNGAP1	10	10	HHHHHHHHHH
RHOBTB2	20	12	HPEDHQGHSDQHHHHHHHHH
EPB41L4B	14	9	HHHQHQHQHQHQHH
SHANK1	23	14	HHHPPHHHHHHAPPPQPHHHHAH
DLGAP3	19	14	HTSHHHHHHHHHHHHQSRH
CPEB4	15	9	HHPHHPHFQHHHSQH
BEAN1	15	12	HRHRHHRHHHHHHHH
SIAH3	29	19	HPHHLSHHHCHHRHHHHLRHHAHPHHLHH
CACNA1A	13	11	HRQHHHHHHHHHH
CACNA1G	15	12	HHLVHHHHHHHHHYH
CACNA1H	24	14	HTASVHHLVYHHHHHHHHHHYHFSH
SLC39A6	23	15	HHHHDYHHILHHHHHQNHHPHSH
PRRT1	9	8	HHHHHHHYH
VGLL3	20	15	HHHPHAHMHHRHRHHHHHHH
CBX4	23	17	HPPSHHPHPHPHHHHHHHHHHHH
CCNT1	25	13	HKEKHKTHPSNHHHHHNHHSHKHSH
MAF	13	10	HHHHHHAAGHHHH
ONECUT2	17	14	HHPHPHHHPHHHHHHHH
HAND1	16	10	HHHHHHHPHPAHPMLH
POU3F3	25	15	HHHHHHHHAHPHPPHPHHAQGPPHH
YY1	16	13	HGHAGHHHHHHHHHHH
OTX1	27	18	HHHHHPHAHHPLSQSSGHHHHHHHHHH
HOXA1	10	10	HHHHHHHHHH
MEOX2	17	15	HHRGHHHHHHHHHHHHH
FOXG1	25	18	HHASHGHHNSHHPQHHHHHHHHHHH
POU4F1	9	9	HHHHHHHHH
POU4F2	15	13	HHHHHHHHHHHHQPH
FOXF2	14	10	HAHPHHHHHHHVPH
DYRK1A	21	17	HHHHGNSSHHHHHHHHHHHHH
FAM76B	21	15	HHPKHHHHHHHHHHRHSSSHH
FOXB2	27	21	HLHPHHHHHPHHHHHHHAAAHHHHHHH
TAF2	12	9	HSDHHHHHHHEH
VGLL2	24	11	HGHLHQGATEPWHHAHPHHAHPHH
ARID1B	24	19	HQQHHHHHHAHHHHHHAHHLHHHH
MAFA	25	19	HHHGAHHAAHHHHAAHHHHHHHHHH
AUTS2	12	9	HDYSHHHHHHHH

Protein	HRD length	Histidine residues	HRD sequence
NR4A3	18	15	HHHHHHHHHHHHHHHQQQH
GATA6	10	10	HHHHHHHHHH
CDX2	12	9	HPHHHPHHHPHH
FOXC2	10	8	HHHQHHGHHH
GSX2	16	12	HAHHHHHPPQHHHHHH
PRDM13	12	11	HHHHHHAHHHHH
CHD8	16	14	HHHHHHPHPHHHHHHH
BMP2K	8	8	HHHHHHHH
FAM120C	11	8	HHHPAHHFHHH
ONECUT1	15	14	HHHHHHHHHHHPHHH
ZNF281	8	8	HHHHHHHH
MAFB	14	11	HHHHHHHHPHPHHA
ZIC3	11	11	HHHHHHHHHHH
ZIC2	9	9	HHHHHHHHH
TSC22D1	23	15	HPHHLHHHHQIHHGHHLQHGHHH
SKOR2	21	15	HSAQTHPHHHHHPHHHHHHHH
RNF111	16	11	HGHHFQHHHHHHHTPH
NUFIP2	40	23	HHHSHHHPHHHPQQQQQQPHHHHHYYFY NHSHNHHHHHHH
NLK	28	18	HHHHHHHHLPHLPPPHLHHHHHPQHHLH
FOXA2	11	8	HHHSHHHHQPH
NCAN	19	13	HRMRRHHHHHQHHHQHHHH
HRG	145	47	HHHPHKPHEHGPPPPPDERDHSHGPPLPQ GPPPLLPMSCSSCQHATFGTNGAQRHSHN NNSSDLHPHKHHSHEQHPHGHHPHAHHP HEHDTHRQHPHGHHPHGHHPHGHHPHGH HPHGHHPHCHDFQDYGPCDPPPHNQGHC CHG
SEPP1	14	9	HYHHEHHHNHGHQH
BTBD11	10	8	HHHHHHHALH
HRCT1	43	23	HHHRHPGHVSHVPNVGLHHHHHPRHTPH HLHHHHHPHRHHPRH
PRICKLE3	13	10	HHHHNHHHHHNRH
C21orf58	8	8	HHHHHHHH
SKIDA1	30	20	HHHHHHHHHHHHHHHHRAQPPQQSHHPPH HH
RBM33	13	9	HPPQHQHHHHHHH
LRCH1	16	12	HPLHHPHHHHHHHQHH